ABSTRACT

Title of Dissertation: DYNAMICS OF METABOLIC GASES IN GROUNDWATER AND THE VADOSE ZONE OF SOILS ON DELMARVA

Rebecca Jane Fox, Doctor of Philosophy, 2011

Dissertation Directed by: Dr. Thomas R. Fisher

Professor of Biological Oceanography

Denitrification removes nitrogen from watersheds under reducing conditions, but N_2O and CH_4, both greenhouse gases, can also be produced. The overarching hypothesis of my thesis was that hydric environments accumulate N_2O and CH_4 in groundwater and the vadose zone. To test the hypothesis, groundwater samples were taken monthly during 2007-2009 at 64 piezometers in 10 wetlands for analysis of excess N_2, N_2O, CH_4, and CO_2. Vadose zone gas and groundwater samples were taken during 2008-2010 at two riparian buffers and a hydrologically restored wetland.

The hydrology of the 10 locations was complex. A hydrologic connection across a transect was determined at one location where NO_3^- significantly decreased, excess N_2 significantly increased, and moderate concentrations of N_2O and CH_4 accumulated. Within these 10 locations, three N_2O and four CH_4 hot spots were identified, and hot

moments accounted for a large percentage of total accumulated N_2O and CH_4. I found evidence of CH_4 ebullition, the production of CH_4 bubbles in the vadose zone that strip other dissolved gases. The locations that accumulated the most dissolved CH_4 and N_2O were natural wetlands and riparian areas, respectively.

I measured both positive and negative excess N_2 concentrations in the vadose zone. Flux estimates ranged from -600 to 880 kg N ha^{-1} yr^{-1}, which brackets missing N estimates at the watershed scale. These concentrations were calculated using N_2/Ar, and both gases are affected by physical processes. These calculated excess N_2 profiles could have been produced through either biological and/or physical mechanisms, and these processes currently cannot be distinguished. Less than 1% of the missing N on the transect scale, measured as the difference in N concentration between two piezometers, was accounted for by calculated diffusional fluxes from groundwater to the vadose zone.

The primary mechanism transporting gases from the vadose zone to the atmosphere was diffusion, but convection transported 20% of the calculated median CO_2 yearly flux. Increased production of N_2O and CO_2 was observed in the vadose zone after rainfall events. Overall, large concentrations of N_2O, CH_4, CO_2, and excess N_2 accumulated in the groundwater and vadose zone of these locations, supporting the overarching hypothesis.

DYNAMICS OF METABOLIC GASES IN GROUNDWATER AND THE VADOSE ZONE OF SOILS ON DELMARVA

By

Rebecca Jane Fox

Dissertation submitted to the Faculty of the Graduate School of the
University of Maryland, College Park in partial fulfillment
of the requirements for the degree of
Doctor of Philosophy
2011

Advisory Committee
Dr. Thomas R. Fisher
Dr. Jeffrey C. Cornwell
Dr. Thomas E. Jordan
Dr. Todd M. Kana
Dr. Sujay S. Kaushal
Dr. Raymond R. Weil
Dr. Brian A. Needelman, Dean's Representative

© Copyright by

Rebecca J. Fox

2011

ACKNOWLEDGEMENTS

Although I am the titled author of the thesis, it would not have been possible without the support, encouragement, and input from my family, lab group, committee, Horn Point friends, and local Cambridge friends. My grandma told me as I was trying to decide on whether I should go straight through and get my Ph.D. that I had told her my freshmen year of college that I was going to be Doctor Fox and she had thought that would be lovely. It does have a nice ring!

I would not have learned so much nor had so much fun collecting and analyzing my data if I had not been a member of an amazing lab group. Tom has taught me so much over the past six years. He read over seemingly endless drafts of this thesis and spent hours with me puzzling over the soil physics that became a major part of this project. Tom was always there to help me when I needed help, and I really do appreciate all of the time and patience he has given me. Anne and I have spent hours doing field work and probably more hours generally gossiping. She has listened to me gripe, helped me in the lab, and generally been an amazing friend. I am not sure what I am going to do in my future career without her!

I have had a very supportive committee, although I am not sure why they didn't stop me trying to directly measure denitrification in soils. Although it isn't solved, I have made some progress, and this would not have been possible without the expertise of Todd Kana. I really did not know much about mass specs when I proposed to create a new mass spec method, and I really lucked out that Todd could figure it out! He also broadened my musical education through playing some good music in the lab. My other

committee members Jeff Cornwell, Tom Jordan, Ray Weil, and Sujay Kaushal have also been a great support and wealth of knowledge. I am also very grateful to Brian Needleman for agreeing to be my dean's representative at the last minute.

Horn Point is a great place to work with an amazing community. So many people influenced my time here as both friends and colleagues. Mike Owens spent a lot of time with me figuring out the GC-ECD, solving problems, interpreting data, and pulling me through a few minor dramatic moments. Jack Seabreeze helped me construct my membrane chambers, and generally helped construct many things for the various projects I have been involved in. Jeff Cornwell and Judy O'Neil both let me use their GC's, and I spent many hours in both of their labs. Much of the work that goes on at Horn Point would not be possible without the help of the business office and maintenance. I would not have had as much fun if it was not for my friends, Desmond Johns, Maggie Sexton, Chris Kelly, Ben Fertig, Britt Burtner, Renee Gruber, Cindy Palinkas, Angie Hengst, Erin Markin, and Jane Thomas.

As part of two different USDA projects and an NSF project I have been fortunate to work with many great scientists. Judy Denver and Scott Ator both made significant contributions to this thesis, and I would have incorrectly interpreted my data without their help. Tom Jordan has really helped as a collaborator by always promptly giving me feedback, and we have had many interesting discussions and likely will have many on the "missing N"!

This most definitely would not have been possible without my husband, Rob. Not only did I write this thesis this year, I also decided that I was going to try to qualify for

the half ironman world championships (which I missed by 1 place!). From mid-January through June I was tired and cranky from training, and brain dead from writing, so generally not a very fun person to be around. Rob allowed me to do this by doing the majority of housework, cooking meals, and not being mad when I was never home! Rob has listened to me, encouraged me, and supported me from near and far (he deployed to Iraq in 2007) for the past ten years and I am really fortunate to have him in my life.

I have the greatest family; we are the type of family that actually likes to spend time together. My parents and my sister Jenny have always supported and encouraged me in whatever I was doing. However, whatever I was doing it was made clear that I was expected to do my best because why else would you do it! Also, if I ever started something, I had to finish it. This has really shaped who I am and made me pretty successful at the things I care most about (modesty not being one of them), but it has also made me ridiculously competitive! Not a bad thing, most of the time.

I was also fortunate to make some amazing friends in the Cambridge community through both teaching and coaching swimming and competing in triathlons. I am part of a group of ladies that started working out together to share our skills and knowledge to become better triathletes. These relationships have morphed into some amazing friendships. It is the first time I have ever been in a popular "clique" and it is with ladies who range in age from 28 to 58! There are few people in the world that I would get up at 4:30 AM for to discuss a book while spinning on a bike so they can get to work on time!

Triathlon has kept me balanced both physically (I really like to eat a lot!) and emotionally through my graduate career. I started triathlons because I swam in college

and it was the next logical step. I really believe that swimming has partially made me who I am today. It taught me to prioritize my life, give everything I had to whatever I was doing, and to manage my time efficiently. It also allowed me to connect to some of the most important people in my life.

I really cannot express enough how much I appreciate all of the support I have received through all of these people and Horn Point in general. My research was supported by the Horn Point Education committee, the National Science Foundation, the USDA CEAP wetlands project, the Washington D.C. Explorers Club, and the University of Maryland Summer Fellowship program. Thank you!

TABLE OF CONTENTS

LIST OF TABLES

Chapter 2

Chapter 3

Chapter 4

LIST OF FIGURES

Chapter 1

Chapter 2

Chapter 3

Chapter 4

Chapter 5

CHAPTER 1:

INTRODUCTION

The original intent of this research was to investigate N_2O concentrations in groundwater in relation to the "missing nitrogen" on a watershed scale. At the transect scale, I wanted to examine N_2O concentrations as a result of denitrification and potentially nitrification in wetlands intended to mitigate NO_3^- in agricultural settings. My research was a small part of two larger projects that were searching for the "missing N" at the watershed scale and were attempting to evaluate the ability of wetlands in agricultural settings to reduce N. These two projects are related as some of the "missing N" is likely denitrified in wetlands receiving agricultural water. I also wanted to examine CH_4 as well as CO_2 concentrations to give a broader view of alternate electron acceptors in these low O_2 environments.

The missing N

The nitrogen budget of most watersheds is unbalanced. Stream N export typically accounts for 10-30% of the net anthropogenic N inputs, or NANI, and the remainder of the budget is missing (Jordan and Weller 1996, Howarth et al. 1996, Boyer et al. 2002). The "missing N" is thought to be stored in biomass, soil, or groundwater within the watershed, or completely lost from the watershed as N_2 and N_2O through denitrification. Both of these processes are difficult to measure on a watershed scale. Van Breemen et al. (2002) estimated that for 16 large watersheds in the northeastern US, denitrification determined by difference was responsible for approximately 50% of N losses, while river export accounted for 20%, food export accounted for 6%, wood export accounted for 5%, and soil storage accounted for 16% (estimated).

Prior to major anthropogenic influences on the nitrogen cycle, the rate of N fixation and N loss to the atmosphere was approximately in balance (Galloway et al. 1995). Reactive N (usually organic N, NH_4^+, NO_2^-, and NO_3^-) is anthropogenically produced through energy production, fertilizer production, and leguminous crops. Reactive N has increased substantially since pre-industrial times, and the balance between N fixation and N loss to the atmosphere has been disrupted (Galloway et al. 1995). With the invention of the Haber-Bosch process in the early 1900's, first gunpowder and later fertilizer usage increased substantially. The use of inorganic fertilizer increased crop outputs, and excess fertilizer was often applied with the intention of producing higher crop yields under ideal growing conditions (Fisher et al. 2006). The unused fertilizer N is leached through the soil to groundwater after conversion to NO_3^- through nitrification. Inorganic fertilizer applied to agricultural fields is a large source of N in agriculturally dominated watersheds. Once in groundwater, NO_3^- will either be denitrified, further transformed, or remain unaltered on its sometimes lengthy passage (decades) to a surface water body. Many researchers have shown a strong positive correlation between N inputs (Boyer et al. 2002) or N concentrations in stream flow (Jordan 1997, Lee et al. 2001) and the fraction of land in agriculture within a basin, especially when agriculture exceeds 60% of land use (Fisher et al. 2006, 2010). The residence time of groundwater can be long, but in the Choptank basin where this research took place, the residence time is relatively short, ranging between <1 to 20 years. Food import and export also affect watershed budgets by decoupling production and consumption and thereby transferring N across great distances (Jordan and Weller 1996).

The increase in reactive N in watersheds since preindustrial times has likely increased both storage within the watershed and denitrification of N.

Balancing watershed budgets is important in order to understand the watershed system and for the purpose of making informed management decisions. In agricultural watersheds, N is either lost as N_2 or N_2O through denitrification or stored within the watershed soil or biomass N. If denitrification accounts for the majority of the "missing N," the N will be completely lost from the watershed and will not detrimentally affect downstream water quality. If the N is stored within the watershed, the N can still be transformed to an active and highly soluble form such as NO_3^-. Under these conditions, the N can further travel through the watershed and negatively contribute to downstream water quality. The movement and storage of reactive N as it passes though the earth's atmosphere, hydrosphere, and biosphere and causes change is known as the nitrogen cascade (Galloway et al. 2005). The only pathway out of the nitrogen cascade is the reduction of reactive N to N_2, and the storage of N is just a delay in the eventual progress of the nitrogen cascade (Galloway et al. 2005).

Fertilizer use and other anthropogenic activities have increased nutrient loading to Chesapeake Bay (Kemp et al. 2005) where this research took place. High concentrations of nitrate (NO_3^-) in groundwater entering the tributaries of the Chesapeake Bay accelerate eutrophication, increase the occurrence of algal blooms (Andersen et al 2002), decrease the abundance of submerged aquatic vegetation (Kemp et al. 1983), create more turbid waters, and generally decrease water quality (Kemp et al. 2005, Fisher et al. 2006). There is a great need to reduce the concentration of NO_3^- leaving agricultural fields in order to improve water quality within the Chesapeake Bay. Finding the locations of areas with

high denitrification rates will allow the protection of these areas, and will provide information on the types of environments reducing N that can potentially be protected or restored. Finding these high N reduction areas will reduce the magnitude of the "missing N" and potentially reduce N losses to surface waters.

Wetlands and NO_3^- reduction

Wetlands as defined by the US EPA section 404 of the Clean Water Act are "areas that are inundated or saturated by surface or ground water at a frequency and duration sufficient to support, and that under normal circumstances do support, a prevalence of vegetation typically adapted for life in saturated soil conditions. Wetlands generally include swamps, marshes, bogs, and similar areas (United States Environmental Protection Agency 2011)." As these areas are often water-saturated, oxygen is typically limiting in wetland environments below the first few surface centimeters (Brady and Weil 2002). This allows the reduction of N in groundwater if contact is made between the high N groundwater and the wetland, but natural wetlands often only receive N through atmospheric deposition. Redox within wetlands can often be low enough for iron, sulfur, and CO_2 or acetate reduction (methanogenesis, Brady and Weil 2002), and wetlands are a large source of CH_4 to the natural global budget (Isermann 1994). Wetlands that are able to intercept agricultural N will likely be N sinks because wetlands are typically not carbon limited and often operate under reduced conditions. If restored wetlands are built in such a way as to have the hydrological and chemical characteristics of natural wetlands and also intercept N-rich groundwater, N reductions in groundwater will likely occur.

Historically, the goal of most farming practices, especially in low lying areas prone to water saturation, was to guide the water out of the soil and into ditches as fast as possible in order to create soils suitable for crops. These ditched areas are referred to as prior converted croplands (PCC). These drainage ditches create a fast-track route for water and nutrients to enter surface waters. The federal Conservation Reserve Enhancement Program (CREP) pays volunteer farmers to convert their low-productivity arable land into conservation practices, including riparian buffers, which are intended to slow the movement of nitrogen species and increase denitrification. With the current understanding of the important roles wetlands play in water quality, habitat, and organism diversity, wetland restoration has been on the rise. Wetlands are often restored to increase and diversify habitat for native animals, as well as to increase water quality by reducing NO_3^- and sediment runoff. This study examined natural wetlands, hydrologically restored wetlands, riparian buffers, controlled drainage ditches, and PCC's with poorly drained areas within them (referred to here as wet spots). The restored wetlands are considered hydrologically restored as only the hydrology of the locations were restored, not necessarily the wetland functions.

Riparian areas along streams and next to drainage ditches can serve to reduce NO_3^-, either through denitrification or uptake by vegetation (Lowrance et al., 1984 b). Riparian buffers have been shown to decrease groundwater NO_3^- concentrations (Lowrance et al., 1984 a, Peterjohn and Correll, 1984, Pinay et al. 1993) and denitrify NO_3^- in surface soils (Pinay et al. 1993). However, riparian areas only work to reduce agricultural N if the groundwater is intercepted by the riparian area. In certain settings, the groundwater has been reported to subduct below the penetration depth of the riparian

zone resulting in little NO_3^- reduction (Lowrance et al., 1997). Riparian areas can also result in fluxes of N_2O to the atmosphere, and high dissolved concentrations of N_2O have been measured in groundwater (Groffman et al. 1998). Understanding the extent of denitrification in these managed areas would allow the most effective placement of these practices within watersheds and could potentially account for a portion of the missing N.

Controlled drainage structures are intended to flood ditches and slow the release of water downstream by restricting flow out of the ditch until the water level in the ditch is great enough to surpass the restriction. Denitrification is expected to be increased in flooded ditch areas because the water is backed up under the field, thereby allowing the water table to reach higher C regions near the root zone. Dukes et al. (2003), however, found that the installation of a controlled drainage structure did not result in an increase in water level between the flooded and unflooded study locations because the unflooded location was randomly installed in a ditch with a shallow impermeable layer, while the flooded site had much more permeable soils. These authors did observe reduced NO_3^- concentrations in the flooded ditch, but did not attribute the loss of NO_3^- to increased denitrification due to the controlled drainage structure as there was no relationship between water table depth and NO_3^- concentration at the ditch edge. In other situations, this practice has been shown to reduce the average NO_3^- concentration (Fisher et al. 2010) and the annual N transport in drainage outflow; however, Evans et al. (1991) indicated that this trend was mostly due to the reduced flow downstream. Controlled drainage structures could also increase the concentration of N_2O in groundwater (saturated zone) and the vadose zone (unsaturated zone). Kliewer and Gilliam (1995) observed increased N_2O production and denitrification under experimental conditions intended to simulate

flooded drainage ditches versus treatments exposed to lower water table levels. However, the percentage of gaseous emissions emerging as N_2O remained stable at ~ 2 % of the denitrification products for all treatments. More recently, Woli et al. (2010) showed a large reduction in tile flow and tile N exported in a controlled drainage location (17 kg N ha^{-1} yr^{-1}) versus a free drainage location (57.2 Kg N ha^{-1} yr^{-1}).

Restored wetlands have been shown to reduce N in some circumstances (e.g., Woltemade and Woodward 2008) and to have limited effect in others (e.g., Orr et al. 2007). Bruland et al. (2006) showed that created and restored wetlands had lower variability in terms of potential denitrification and denitrification related soil properties than natural wetlands. Peralta et al. (2010) found significant differences between bacterial community structure and potential denitrification between natural and restored wetlands, indicating that the restoration project had not been successful in terms of restoring denitrification function to the wetlands. This indicates that restored and created wetlands may not be as capable of reducing N as natural wetlands because wetland restoration does not always initially restore all wetland services. Wetlands are often restored for many different purposes including habitat creation, agricultural nutrient mitigation, and wastewater treatment. Wetlands restored for one specific purpose, e.g., waterfowl, may not function to reduce agricultural N. In order to successfully restore wetlands for agricultural nutrient mitigation, the denitrifying function of wetlands must be restored, and the wetlands must intercept the N-rich water.

Promoting wetland restoration to mitigate agricultural N loading appears to be a partial solution to the problem of excess N loading resulting in accelerated eutrophication. However, a potential problem with this approach could be the inadvertent

production of the greenhouse gases N_2O and CH_4, which are by-products of non-oxygenic respiration in hydric environments or soils experiencing long periods of saturation that inhibit the diffusion of oxygen into the soil, creating reduced conditions (Brady and Weil 2002).

Denitrification

As denitrification has the ability to reduce N in agriculturally influenced wetlands and riparian zones (e.g., Fisher et al. 2010), the process of denitrification is responsible for at least a portion of the missing N. Denitrification is the reduction of NO_3^- to N_2 through the intermediate and sometimes terminal products of NO_2^-, NO, and N_2O (Knowles 1982). Denitrification is typically a heterotrophic process that requires a labile carbon source, NO_3^-, and relatively low levels of O_2. Denitrification is performed by a diverse group of microorganisms that are able to utilize NO_3^- as a respiratory electron acceptor in the absence of oxygen (Knowles 1982). Most of these bacteria are able to reduce NO_3^- completely to N_2, but some only possess the enzymes to complete part of the process (Knowles 1982). Typically, NO_3^- reduction has been associated with denitrification, but other NO_3^- reduction processes can occur including dissimilatory nitrate reduction to ammonium (DNRA), chemoautotrophic denitrification which can be coupled to either sulfur or iron oxidation, and anammox (Mulder et al. 1995, Jetten 2001, Burgin and Hamilton 2007). A benefit to anammox is that it removes NO_3^- from the environment as N_2 without producing N_2O. More recently, evidence of anaerobic methane oxidation coupled to denitrification (AOM-D) has also been observed in lab soil

cores, but not in the field (Raghoebarsing et al. 2006). While all of these processes can potentially contribute to excess N_2 gas in groundwater, denitrification is the most well studied (e.g., Groffman et al. 2006). In this thesis, I will therefore refer to "denitrification", while acknowledging here that other processes may also contribute to NO_3^- loss and N_2 production.

Detecting denitrification requires a sensitive, high precision method to measure N_2. Membrane inlet mass spectrometry (MIMS) provides a method for directly measuring the N_2 concentration within a water sample. This approach directly introduces a water sample through a semi-permeable membrane into a quadrapole mass spectrometer (QMS), which allows the measurement of the N_2/Ar ratio (Kana et al. 1994). The membrane inlet permits introduction of the dissolved gases from the water sample directly to the mass spectrometer, eliminating the necessity for sample preparation.

Conversely, acquiring direct *in situ* measurements of soil denitrification is a challenging problem due to the 78% background of N_2 in the atmosphere. To measure a small increase in soil N_2 from denitrification above the large background N_2 requires sensitive instrumentation and precise techniques. Groffman et al. (2006) reviewed current denitrification techniques; all of the current methods used for measuring soil denitrification have advantages and disadvantages. However, without these methods we would not have the current understanding of the controls on denitrification or the large range of measurements through diverse environments.

In general, warm and wet conditions increase denitrification rates. It has been observed that above a threshold of 60% water-filled pore space (WFPS), as is commonly observed in hydric soils, there are higher rates of denitrification compared to lower %WFPS (De Klein and Van Logtestijn 1996; Dobbie and Smith 2001; Ruser et al. 2006). De Klein and Van Logtesijn (1996) proposed that this threshold is actually field capacity for a given soil. Higher %WFPS decreases oxygen availability by reducing diffusion and higher temperatures increase respiration, creating more hypoxic conditions which are more conducive to higher rates of denitrification (Leffekaar 1986). Increased denitrification has also been observed to occur with higher levels of available organic carbon if sufficient NO_3^- is present (Weier et al. 1993).

Denitrification can occur in many different settings within a watershed. Soils are a major location of denitrification, and Seitzinger et al. (2006) calculated denitrification within global terrestrial soils to be approximately 33% of the newly fixed plus recycled terrestrial N (124 Tg N/yr). Globally, under natural vegetation, Houlton and Bai (2009) estimated that ~ 28 Tg of N was lost annually via denitrification. Agricultural soils specifically have a high tendency to reduce NO_3^- because they hold large concentrations of NO_3^-. Denitrification in agricultural soils was estimated at 66 Tg N/yr (Seitzinger et al. 2006), accounting for the majority of soil based denitrification.

Denitrification in streams and rivers can account for a fraction of the missing N. High spatial variability exists within and between river networks, but Seitzinger et al. (2006) estimated that 35 Tg N yr^{-1} are denitrified, accounting for 13% of all terrestrial N sources. Due to the high surface to volume ratio of low order streams, headwater streams tend to have great control over the chemistry of a watershed (Peterson et al. 2000). As

stream NO_3^- concentrations increase, denitrification has been shown to increase, but denitrification efficiency declines (Mulholland et al. 2008). Nitrogen discharge from a watershed has been correlated with net anthropogenic inputs of N to watersheds (Jordan et al. 1997); therefore, watersheds with high anthropogenic N inputs to headwater streams have low denitrification efficiency and export high concentrations of N downstream.

The occurrence of denitrification within groundwater can be temporally and spatially heterogeneous due to carbon limitation and high oxygen concentrations. As a result, many investigators have emphasized the hot spot and hot moment nature of denitrification throughout different systems (Parkin 1987, McClain et al. 2003, Harms and Grimm 2008). In addition, organic carbon content typically decreases with increasing depth below ground, and lower denitrification rates have been correlated with this decrease in organic carbon with depth (Brettar and Höfle 2002). The occurrence of denitrification in groundwater can be limited by an organic carbon source (e.g., Bradley et al. 1992) or by O_2 that stimulates aerobic pathways. Even when denitrification is favored, some of the N_2 produced may be lost from groundwater to the vadose zone via diffusion (Fig. 1.1) and then move to the atmosphere via diffusion or convective flushing of the vadose zone. The excess N_2 produced by denitrification may also remain dissolved in the groundwater until intersecting with a surface water body, with the eventual fate of diffusing to the atmosphere. Measuring groundwater denitrification is possible through different methods, but due to the spatial heterogeneity of denitrification, and multiple gas loss pathways, extrapolating point measurements to an entire watershed is difficult.

N_2O

Denitrification is more complex than just reducing NO_3^- to N_2, and areas intended to increase N_2 loss could also have N_2O loss. N_2O is a greenhouse gas with a global warming potential of 298 over 100 years (IPCC 2007), and N_2O also has the capacity to contribute to the removal of stratospheric ozone (Crutzen 1981). Agriculture is the major contributor of anthropogenic N_2O, accounting for 36.5% of the yearly anthropogenic emissions (Isermann 1994). N_2O is rising at approximately 0.26% yr^{-1} and reached an atmospheric concentration of 319 ppb in 2005 (IPCC 2007).

Nitrous oxide can be generated by several processes within the N cycle. The major source of N_2O is from denitrification and to a lesser extent nitrification, although nitrification is sometimes the major process (e.g., Ambus 1998). The source of N_2O is mostly controlled by the percent water filled pore space (%WFPS) in soils. At lower %WFPS (more air than water in soils) nitrification is the primary source of N_2O because nitrification is strictly an aerobic process. At higher %WFPS (>60%, more water than air in soils), which produce more reduced conditions, the major source of N_2O is from denitrification (Khalil and Baggs 2005). A larger accumulation of N_2O is expected from denitrification at high %WFPS, and a larger accumulation of N_2O would be expected at intermediate %WFPS from nitrification. Both nitrification and denitrification can occur simultaneously as anoxic microsites can occur within a mostly aerobic soil column (Azam et al. 2002).

Nitrous oxide is an essential reduction step in the process of denitrification that can be further reduced to N_2. The dominant end product of denitrification is typically N_2, but some studies have found N_2O to be the major end product (e.g., Mathieu et al. 2006,

Ruser et al. 2006). High concentrations of N_2O could potentially occur in environments where high levels of NO_3^- exist. Both NO_3^- and N_2O are possible electron acceptors for denitrifying bacteria, but NO_3^- is preferentially used because of the higher energy yield (Blackmer and Bremner 1978). Environments with >60% WFPS and high concentrations of NO_3^- (e.g., hydric environments in agricultural settings) would be expected to produce high fluxes of N_2O (Dobbie and Smith 2001; Ruser et al. 2006). A caveat is that % WFPS values closer to saturation have been associated with a larger conversion of N_2O to N_2. Nitrous oxide reductase is inhibited by oxygen to a greater extent than the other denitrification enzymes, resulting in an accumulation of N_2O at %WFPS high enough to allow denitrification, but with sufficient oxygen to inhibit nitrous oxide reductase to complete the reduction to N_2 (Otte et al. 1996). Environments high in available organic carbon are expected to produce low levels of N_2O as these conditions have been found to increase the conversion of N_2O to N_2 (Weier et al. 1993, Mathieu et al. 2006). This suggests that NO_3^--rich, carbon-poor areas deeper in the soil column might be important sources of N_2O production.

Denitrification “hot spots” can exist and are associated with anoxic microsites and patchy organic carbon (Parkin 1987). N_2O production has also been shown to occur under specific conditions that when reached produce hot moments. Large fluxes of N_2O have been observed after fertilizer addition (Khalil et al. 2002, Dobbie and Smith 2001, Dobbie and Smith 2003), rewetting of soil cores (Ruser et al. 2006), and natural rain events (Dobbie and Smith 2001, Dobbie and Smith 2003). Increased fluxes have also been observed after freeze thaw events (Koponen 2004, Teepe et al. 2001). N_2O production tends to occur in pulses after ideal conditions have been met (Xiong et al.

2006). Agricultural hydric environments are expected to be denitrification-derived N_2O hotspots.

Methanogenesis, methane oxidation, and CH_4 production and consumption

Conditions conducive to denitrification might also be suitable for methanogenesis, the reduction of CO_2 or acetate to CH_4. This process is the lowest redox reaction, resulting in the least energy production per unit organic C, and it occurs after all other electron acceptors have been exhausted. Management practices intended to increase denitrification could also potentially increase CH_4 fluxes to the atmosphere.

Methane is the most abundant hydrocarbon in the atmosphere and is released by both natural and anthropogenic sources. CH_4 is a greenhouse gas with a global warming potential of 25 over 100 years (IPCC 2007). The atmospheric concentration of CH_4 has increased since pre-industrial times, but the concentration leveled off (Dlugokencky et al. 2003) in 1996 through 2006, and then increased in 2007 and 2008 (Rigby et al. 2008, Dlugokencky et al. 2009). The average atmospheric concentration over both hemispheres in 2005 was 1,774 ppb (IPCC 2007).

Approximately 1/3 of global CH_4 emissions are due to natural sources such as wetlands, oceans, freshwater, CH_4 hydrates, termites, and undomesticated ruminants. Agricultural activities comprise 42% of the global CH_4 budget (Isermann 1994). Rice paddies, domesticated ruminants, animal wastes, and biomass burning are the primary agricultural emitters of CH_4 (Isermann 1994, Mosier et al. 1998).

Unsaturated soils can function as CH_4 sinks through methane oxidation to CO_2 (Mosier et al. 1998). Two forms of CH_4 oxidation have been recognized in soils: high affinity oxidation and low affinity oxidation (Le Mer and Rogers 2001). High affinity oxidation occurs at lower CH_4 concentrations close to atmospheric (<12 ppm) and low affinity oxidation occurs at much higher CH_4 concentrations (>40 ppm, Le Mer and Rogers 2001). CH_4 produced at depth in soils or sediments can be oxidized at shallower, aerobic depths through CH_4 oxidation (Conrad and Rothfuss 1991), and variations in CH_4 flux from the soil surface are the net result of methanogens producing CH_4 and methanotrophs consuming CH_4. Dunfield et al. (1995) found soil water content to be negatively correlated with the CH_4 oxidation rate. Increasing the water content of a soil to induce denitrification could create hotspot locations of CH_4 production and reduce CH_4 oxidation, increasing the net flux to the atmosphere.

N_2O, CH_4, and CO_2 transfer mechanisms

Once N_2O, CH_4, and CO_2 are produced in groundwater or the vadose zone, they can move away from their original site of production through diffusion or convection. Diffusion is considered to be the primary mechanism of gas flux from soils (Jury and Horton 2004). The rate of gaseous diffusion depends on the strength of the concentration gradient, which is produced in response to the production or consumption of a gas, and the diffusivity coefficient of that specific gas. Diffusion in free air is a relatively fast process in comparison to diffusion in water. Diffusion in an air or water filled tortuous environment, such as soil or sediment, is much slower than diffusion in the free

atmosphere or water column, and corrections for porosity and tortuosity are routinely made to the free air diffusion coefficients to estimate *in situ* soil diffusion (e.g., Moldrup et al. 2000A, 2000B).

Convection is the bulk movement of soil air caused by total gas pressure gradients (Jury and Horton 2004). Physical mechanisms known to cause convection are wind, barometric pressure changes, temperature fluctuation, and infiltrating water due to precipitation (Jury and Horton 2004). Fluxes out of the soil due to convection are generally considered to be low compared to diffusion, but there is the potential for large convective fluxes if soil gas concentrations are high (Clough et al. 2005).

Objectives

This research addresses questions pertaining to the concentrations of N_2O, CH_4 and CO_2 in the groundwater and the vadose zone of soils. I will also examine the transport mechanisms of these gases from groundwater, through the vadose zone, and across the soil surface to the atmosphere. Groundwater concentrations of excess N_2, N_2O, CH_4, CO_2, Ar, O_2, NO_3^-, and NH_4^+ were monitored monthly from 2007 through 2009 within groundwater piezometers. These piezometers were installed as transects across hydrologically restored wetlands, riparian areas, PCCs, and natural wetlands. The vadose zone gas concentrations of excess N_2, N_2O, CO_2, and CH_4 were examined from the end of 2008 through 2010 using nested equilibration chambers at depths from 0.25 to 1.5 m (Silver et al. 1999).

Wetlands within agricultural settings have the potential to account for the missing N at the watershed scale through denitrification of agricultural N. If these locations are denitrifying NO_3^-, they are also potentially accumulating N_2O in groundwater and the vadose zone. CH_4 is produced through methanogenesis when all other terminal electron acceptors are reduced, and these wetlands may also accumulate large concentrations of CH_4. N_2O and CH_4 have been shown to be produced during short periods of time known as "hot moments" or in small areas of high production in comparison to the surrounding area, known as "hotspots" (McClain et al. 2003). Once denitrification occurs in groundwater, the excess N_2 and N_2O either remain dissolved within the groundwater, or diffuse into the vadose zone (Fig. 1-1). Denitrification and N_2O production and consumption can also occur in the vadose zone, and once in the vadose zone these gases are either transported to the atmosphere though diffusion or convection. I have examined each of these processes and will attempt to answer the following hypotheses.

Research questions and hypotheses

Agricultural hydric environments, managed or natural, need to be evaluated from a greenhouse gas perspective. Conditions conducive to denitrification are also suitable for the production of N_2O and CH_4. I hypothesize that agricultural hydric environments will accumulate large concentrations of N_2O and CH_4 in groundwater and the vadose zone. Although only N_2O and CH_4 fluxes from the soil surface will be atmospherically significant, my PhD research primarily focused on N_2O and CH_4 concentrations in the

unconfined groundwater and vadose zone to understand the dynamics of the production, consumption, and transport of N_2O and CH_4 within the soil.

Chapter 2

Hypothesis 1 - Concentration gradients of N_2O and CH_4 exist in groundwater both horizontally and vertically.

Hypothesis 2 - Hot spots and hot moments will account for a large percentage of N_2O and CH_4 accumulation.

Hypothesis 3 - Soil conditions created by agricultural management practices, such as flow-controlled drainage ditches, riparian areas, and hydrologically restored wetlands will promote the reduction of NO_3^- to N_2 over the width of the buffer, wetland, or ditch bank while promoting the accumulation of N_2O and CH_4 from incomplete denitrification and methanogenesis.

Chapter 3

Hypothesis 4 - High dissolved concentrations of N_2 and N_2O within groundwater will fuel a diffusive loss of N_2 and N_2O into the vadose zone and these diffusive losses will account for the “missing N” in groundwater at the transect scale.

Hypothesis 5 - The diffused N_2 and N_2O will be detectable as vadose zone concentration profiles that we will be able to use to estimate a diffusive flux of N_2 and N_2O from the soil surface.

Chapter 4

Hypothesis 6 - Diffusion will be the dominant process driving fluxes of N_2, CO_2 and CH_4 out of the vadose zone and into the atmosphere, but convection due to rainfall and barometric pressure changes will be an important but smaller flux mechanism.

Hypothesis 7 - Increased concentrations of N_2O, CO_2, and CH_4 will occur in the vadose zone soil profile after rainfall events.

Chapter 5

Synthesis

References

Ambus, P. 1998. Nitrous oxide production by denitrification and nitrification in a temperate forest, grassland and agricultural soils. European Journal of Soil Science. 49(3):495-302.

Anderson, D.M., P.M. Glibert, J.M. Burkholder. 2002. Harmful algal blooms and eutrophication: Nutrient sources, composition, and consequences. Estuaries 25(4B):704-726.

Azam, F., C. Muller, A.Weiske, G. Benckiser, J.C.G. Ottow. 2002. Nitrification and denitrification as sources of atmospheric nitrous oxide- role of oxidizable carbon and applied nitrogen. 35(1):54-61.

Blackmer, A.M., J.M. Bremner. 1978. Inhibitory effect of nitrate on reduction of N_2O to N_2 by soil microorganisms. Soil Biology and Biogeochemistry. 10(3)187-191.

Boyer, E.W., C.L. Goodale, N.A. Jaworki, R.W. Howarth. 2002. Anthropogenic nitrogen sources and relationships to riverine nitrogen export in the northeastern U.S.A. Biogeochemistry. 57/58:137-169.

Bradley, P.M., M. Fernandez, F.H. Chapelle. 1992. Carbon limitation of denitrification rates in an anaerobic groundwater system. Environmental Science and Technology. 26(12):2377-2381.

Brady, N.C., R.R. Weil. 2002. The nature and properties of soils. Upper Saddle River, NJ. Prentice Hall.

Brettar, I., M.G. Höfle. 2002. Close correlation between the nitrate elimination rate by denitrification and the organic matter content in hardwood forest soils of the Upper Rhine floodplain (France). Wetlands. 22(2):214-224.

Bruland, G.W., C.J. Richardson, S.C. Whalen. 2006. Spatial variability of denitrification potential and related soil properties in created, restored, and paired natural wetlands. Wetlands. 26(4):1042-1056.

Burgin, A.J., S.K. Hamilton. 2007. Have we overemphazised the role of denitrification in aquatic ecosystems? A review of nitrate removal pathways. Frontiers in Ecology and the Environment. 5(2):89-96.

Clough, T.J., R.R. Sherlock, D.E. Rolson. 2005. A review of the movement and fate of N_2O in the subsoil. Nutrient Cycling in Agroecosystems. 72:3-11.

Conrad, R., F. Rothfuss. 1991. Methane oxidation in the soil surface layer of a flooded rice field and the effect of ammonium. Biology and Fertility of Soils. 12(1):28-32. DOI: 10.1007/BF00369384.

Crutzen, P.J., 1981. Atmospheric chemical processes of the oxides of nitrogen, including N_2O. In Delwiche,C.C.(ed.). Denitrification, Nitrification, and Atmospheric Nitrous Oxide. Wiley, New York, pp.17-44.

De Klein, C.A.M., R.S.P. Van Logtestijn. 1996. Denitrification in grassland soils in the Netherlands in relation to irrigation, N-application rate, soil water content and soil temperature. Soil Biology & Biochemistry 28(2):231-237.

Dlugokencky, E.J., L. Bruhwiler, W.C. White, L.K. Emmons, P.C. Novelli, S.A. Montzka, K.A. Masarie, P.M. Lang, A.M. Crotwell, J.B. Miller, L.V. Gatti. 2009. Observational constraints on recent increases in the atmospheric CH_4

burden. Geophysical Research Letters. 36, L18803, DOI:10.1029/2009GL039780.

Dlugokencky, E.J., S. Houweling, L. Bruhwiler, K.A. Masarie, P.M. Lang, J.B. Miller, P.P. Tans. 2003. Atmospheric methane levels off: Temporary pause or a new steady-state? Geophysical Research Letters, 30(19), doi:10.1029/2003GL018126,2003.

Dobbie, K.E., K.A. Smith. 2001. The effects of temperature, water-filled pore space and land use on N_2O emission from an imperfectly drained gleysol. European Journal of Soil Science. 52(4):667-673.

Dobbie, K.E., K.A. Smith. 2003. Nitrous oxide emission factors for agricultural soils in Great Britain: The impact of soil water-filled pore space and other controlling variables. Global Change Biology. 9(2):204-218.

Dukes, M.D., R.O. Evans, J.W. Gilliam, S.H. Kunickis. 2003. Interactive effects of controlled drainage and riparian buffers on shallow groundwater quality. Journal of Irrigation and Drainage Engineering. 129(2):82-92. DOI: 10.1061/(ASCE)0733-9437(2003)129:2(82).

Dunfield, P.F., E. Topp, C. Archambault, R. Knowles. 1995. Effect of nitrogen fertilizers and moisture content on CH_4 and N_2O fluxes in a humisol: Measurements in the field and intact soil cores. Biogeochemistry. 29:199-222.

Evans, R.O., J.W. Gilliam, R.W Skaggs. 1991. Controlled drainage management guidelines for improving drainage water quality. Cooperative Extension Service, North Carolina State University Publication No. AG-443: 16pp.

Fisher, T. R., J. A. Benitez, K.-Y. Lee, A. J. Sutton. 2006. History of land cover change and biogeochemical impacts in the Choptank River basin in the mid-Atlantic region of the US. International Journal of Remote Sensing. 27:3683-3703.

Fisher, T.R., T.E. Jordan, K.W. Staver, A.B. Gustafson, A.I. Koskelo, R.J. Fox, A.J. Sutton, T. Kana, K.A. Beckert, J.P. Stone, G.W. McCarty, M.W. Lang. 2010. The Choptank Basin in transition intensifying agriculture, slow urbanization, and estuarine eutrophication. In Kennish M.J., Paerl H.W.(ed.). Coastal Lagoons Critical Habitats of Environmental Change, CRC Press, pp 135-165.

Galloway, J.N., J.D. Aber, J.W. Erisman, S.P. Seitzinger, R.W. Howarth, E.B. Cowling, B.J. Cosby. 2005. The nitrogen cascade. Bioscience. 53(4):341-356.

Galloway, J.N., W.H. Schlesigner, H. Levy II, A. Michaels, J.L. Schnoor. 1995. Nitrogen fixation: Anthropogenic enhancement-environmental response. Global biogeochemical cycles. 9(2):235-252.

Groffman, P.M., A.J. Gold, P. Jacinthe. 1998. Nitrous oxide production in riparian zones and groundwater. Nutrient Cycling in Agroecosystems. 52:179-186.

Groffman, P.M., M.A. Altabet, J.K. Bohlke, K. Butterbach-Bahl, M.B. David, M.K. Firestone, A.E. Giblin, T.M. Kana, L.P. Nielsen, M.A. Voytek. 2006. Methods for measuring denitrification: Diverse approaches to a difficult problem. Ecological Applications. 16(6):2091-2122.

Harms, T.K., N.B. Grimm. 2008. Hot spots and hot moments of carbon and nitrogen dynamics in a semiarid riparian zone. Journal of Geophysical Research-Biogeosciences. 113:1-14.

Houlton, B.Z., E. Bai. 2009. Imprint of denitrifying bacteria on the global terrestrial biosphere. Preceedings of the National Academy of Sciences. 106(51):21713-21716.

Howarth, R.W., G. Billen, D. Swaney, A. Townsend, N. Jaworski, K. Lajtha, J.A. Downing, R. Elmgren, N. Caraco, T. Jordan, F. Berendse, J. Freney, V. Kudeyardov, P. Murdoch, Z. Zhao-Liang. 1996. Regional nitrogen budgets and riverine N & P fluxes for the drainages to the North Atlantic Ocean: natural and human influences. Biogeochemistry. 35(1):75-139.

IPCC (Intergovernmental Panel on Climate Change). 2007. Climate change 2007-The physical science basis. Contribution of working group I to the forth assessment report of the IPCC. Cambridge University Press, Cambridge.

Isermann, K., 1994. Agriculture's share in the emission of trace gases affecting the climate and some cause-oriented proposals for sufficiently reducing this share. Environmental Pollution. 83(1-2):95-111.

Jetten, M.S.M. 2001. New pathways for ammonia conversion in soil and aquatic systems. Plant and Soil. 230(1):9-19.

Jordan, T.E., D. W. Weller. 1996. Human contributions to terrestrial nitrogen flux. BioScience 46(9):655-664.

Jordan, T.E., D.L. Correll, D.E. Weller. 1997. Effects of agriculture of discharges of nutrients from coastal plain watersheds of Chesapeake Bay. Journal of Environmental Quality. 26(3):836-848.

Jury, W.A., R. Horton. 2004. Soil Physics. 6th ed. Hoboken. Wiley.

Kana, T.M., C. Darkangelo, M.D. Hunt, J.B. Oldham, G.E. Bennett, J.C. Cornwell. 1994. Membrane inlet mass spectrometer for rapid high-precision determination of N_2, O_2 and Ar in environmental water samples. Analytical Chemistry. 66(23):4166-4170.

Kemp, W.M., R.R. Twilley, J.C. Stevenson, W.R. Boynton, J.C. Means. 1983. The decline of submerged vascular plants in upper Chesapeake Bay- summary of results concerning possible causes. Marine Technology Society Journal. 17(2):78-89.

Kemp, W.M., W.R. Boynton, J.E. Adolf, D.F. Boesch, W.C. Boicourt, G. Brush, J.C. Cornwell, T.R. Fisher, P.M. Glibert, J.D. Hagy, L.W. Harding, E.D. Houde, D.G. Kimmel, W.D. Miller, R.I.E. Newell, M.R. Roman, E.M. Smith, J.C. Stevenson. 2005. Eutrophication of Chesapeake Bay: Historical trends and ecological interactions. Marine Ecology Progress Series. 303:1-29.

Khalil, M.I., A.B. Rosenani, O.Van Cleemput, C.I. Fauziah, J. Shamshuddin. 2002. Nitrous oxide emissions from the humid tropics under maize-groundnut rotation. Journal of Environmental Quality. 31(4):1071-1078.

Khalil, M.I., E.M. Baggs. 2005. CH_4 oxidation and N_2O emissions at varied soil water-filled pore spaces and headspace CH_4 concentrations. Soil Biology and Biochemistry. 37:1785-1794.

Kliewer, B.A., J.W. Gilliam. 1995. Water table management effects on denitrification and nitrous oxide evolution. Soil Science Society of America. 59(6):1694-1701.

Knowles, R. 1982. Denitrification. Microbiological Reviews. 46(1):43 -70.

Koponen, H.T., L. Flöjt, P.J. Martikainen, 2004. Nitrous oxide emissions from agricultural soils at low temperatures: A laboratory microcosm study. Soil Biology and Biogeochemistry. 36(5):757-766.

Le Mer, J., P. Roger. 2001. Production, oxidation, emission and consumption of methane by soils: A review. European Journal of Soil Biology. 37:25-50.

Lee, K., T.R. Fisher, E. Rochelle-Newall. 2001. Modeling the hydrochemistry of the Choptank River basin using GWLF and Arc/Info: 2. Model validation and application. Biogeochemistry. 56:311-348.

Leffekaar, P.A. 1986. Dynamics of partial anaerobiosis in a model soil in respect to denitrification. Soil Science, 128, 110-120.

Lowrance, R.R., R.L. Todd, L.E. Asmussen. 1984 a. Nutrient cycling in an agricultural watershed: I. Phreatic movement. Journal of Environmental Quality. 13(1):22-27.

Lowrance, R.R., R. Todd, J. Fail Jr., O. Hendrickson Jr., R. Leonard, L. Asmussen. 1984 b. Riparian forests as nutrient filters in agricultural watersheds. BioScience. 34(6):374-377.

Lowrance, R.R, L.S. Altier, J.D. Newbold, R.R. Schnabel, P.M. Groffman, J.M. Denver, D.L. Correll, J.W. Gilliam, J.L. Robinson, R.B. Brinsfield, K.W. Staver, W. Lucas, A.H. Todd. 1997. Water quality functions of riparian forest buffers in Chesapeake Bay watersheds. Environmental Management. 21(5):687-712.

Mathieu, O., J. Lévêque, C. Hénault, M.-J. Milloux, F. Bizouard, F. Andreux. 2006. Emissions and spatial variability of N_2O, N_2 and nitrous oxide mole fraction at

the field scale, revealed with ^{15}N isotopic techniques. Soil Biology and Biogeochemistry. 38(5):941-951.

McClain, M.E., E.W. Boyer, C.L. Dent, S.E. Gergel, N.B. Grimm, P.M. Groffman, S.C. Hart, J.W. Harvey, C.A. Johnson, E. Mayorga, W.H. McDowell, G. Pinay. 2003. Biogeochemical hot spots and hot moments at the interface of terrestrial and aquatic ecosystems. Ecosystems. 6:301-312.

Moldrup, P., T. Olesen, J. Gamst, P. Schjønning, T. Yamaguchi, D.E. Rolston. 2000 A. Predicting the gas diffusion coefficient in repacted soil: Water-induced linear reduction model. Soil Society of America Journal. 64:1588-1594.

Moldrup, P., T. Olesen, J. Gamst, P. Schjønning, T. Yamaguchi, D.E. Rolston. 2000B. Predicting the gas diffusion coefficient in undistrubed soil from soil water characteristics. Soil Society of America Journal. 64:94-100.

Mosier, A.R., J.M. Duxbury, J.R. Freney, O. Heinemeyer, K. Minami, D.E. Johnson. 1998. Mitigating agricultural emissions of methane. Climate Change. 40(1):30-80.

Mulder, A., A.A. Vandergraaf, L.A. Robertson, J.G Kuenen. 1995. Anaerobic ammonium oxidation discovered in a denitrifying fluidized-bed reactor. FEMS Microbiology Ecology. 16(3):177-183.

Mulholland, P.J., A.M. Helton, G.C. Poole, R.O. Hall Jr, S.K. Hamilton, B.J. Peterson, J.L. Tank, L.R. Ashkenas, L.W. Cooper, C.N. Dahm, W.K. Dodds, S.E.G. Findlay, S.V. Gregory, N.B. Grimm, S.L. Johnson, W.H. McDowell, J.L. Meyer, H.M. Valett, J.R. Webster, C.P. Arango, J.J. Beaulieu, M.J. Bernot, A.J. Burgin, C.L. Crenshaw, L.T. Johnson, B.R. Niederlehner, J.M.

O'Brien, J.D. Potter, R.W. Sheibley, D.J. Sobota, S.M. Thomas. 2008. Stream denitrification across biomes and its response to anthropogenic nitrate loading. Nature. 452(7184): 202-205.

Orr, C.H., E.H. Stanley, K.A. Wilson, J.C. Finlay. 2007. Effects of restoration and reflooding on soil denitrification in a leveed Midwestern floodplain. Ecological Applications. 17(8):2365-2376.

Otte, S., N.G. Grobben, L.A. Robertson, M.S.M Jetten, J.G. Kuenen. 1996. Nitrous oxide production by *Alcaligenes faecalis* under transient and dynamic aerobic and anaerobic conditions. Applied and Environmental Microbiology. 62(7):2421-2426.

Parkin, T.B. 1987. Soil microsites as a source of denitrification variability. Soil Science Society of America. 51:1194-1199.

Peralta, A.L., J.W. Matthews, A.D. Kent. 2010. Microbial community structure and denitrification in a wetland mitigation bank. Applied and Environmental Microbiology. 76(13):4207-4215. DOI: 10.1128/AEM.02977-09.

Peterjohn, W.T., D.L. Correll. 1984. Nutrient dynamics in an agricultural watershed: Observations on the role of a riparian forest. Ecology. 65(5):1466-1475.

Peterson, B.J., W.M. Wollheim, P.J. Mulholland, J.R. Webster, J.L. Meyer, J.L. Tank, E. Marti, W.B. Bowden. H.M. Valett, A.E. Hershey, W.H. McDowell, W.K. Dodds, S.K. Hamilton, S. Gregory, D.D. Morrall. 2001. Control of nitrogen export from watersheds by headwater streams. Science. 292(5514):86-90.

Pinay, G., L. Roques, A. Fabre. 1993. Spatial and temporal patterns of denitrification in a riparian forest. The Journal of Applied Ecology. 30(4):581-591.

Raghoebarsing, A.A., A. Pol, K.T. Van de Pas-Schoonen, A.J.P. Smolders, K.F. Ettwig, W.I.C. Rijpstra, S. Schouten, J.S.S. Damste, H.M.M. Op den Camp, M.S.M. Jetten, M. Strous. 2006. A microbial consortium couples anaerobic methane oxidation to denitrification. Nature. 440:918-921. DOI:10.1038/nature04617.

Rigby, M., R.G. Prinn, P.J. Frazer, P.G. Simmonds, R.L. Langenfeld, J. Huang, D.M. Cunnold, L.P. Steele, P.B. Krummel, R.F. Weiss, S. O'Doherty, P.K. Salameh, H.J. Wang, C.M. Harth, J. Mühle, L.W. Porter. 2008. Renewed growth of atmospheric methane. Geophysical Research Letters. 35, L22805, doi:10.1029/2008GL036037.

Ruser, R., H. Flessa, R. Russow, G. Schmidt, F. Buegger, J.C. Munch. 2006. Emissions of N_2O, N_2 and CO_2 from soil fertilized with nitrate: Effect of compaction, soil moisture and rewetting. Soil Biology and Biochemistry. 38:263-274.

Seitzinger, S., J.A. Harrison, J.K. Bohlke, A.G. Bouwman, R. Lowrance, B. Peterson, C. Tobias, G. Van Drecht. 2006. Denitrification across landscapes and waterscapes: A synthesis. Ecological Applications. 16(6):2064-2090.

Silver, W.L., A.E. Lugo, M. Keller. 1999. Soil oxygen availability and biogeochemistry along rainfall and topographic gradients in upland wet tropical forest soils. Biogeochemistry. 44:301-328.

Teepe, R., R. Brumme, F. Beese, 2001. Nitrous oxide emissions from soil during freezing and thawing periods. Soil Biology and Biogeochemistry 33(9):1269-1275.

United States Environmental Protection Agency. 2011. Clean water act, section 404. Retrieved: July 15th, 2011 from http://water.epa.gov/lawsregs/guidance/wetlands/sec404.cfm.

Van Breemen, N., E.W. Boyer, C.L. Goodale, N.A. Jaworki, K. Paustian, S.P. Seitzinger, K. Lajtha, B. Mayer, D. Van Dam, R.W. Howarth, K.J. Nadelhoffer, M. Eve, G. Billen. 2002. Where did all the nitrogen go? Fate of nitrogen inputs to large watersheds in the northeastern U.S.A. Biogeochemistry. 57/57:267-293.

Weier, K.L., J.W. Doran, J.F. Power, D.T. Walters. 1993. Denitrification and the dinitrogen/nitrous oxide ratio as affected by soil water, available carbon, and nitrate. Soil Science Society of America Journal 57(1):66-72.

Woli, K.P., M.B. David, R.A. Cooke, G.F. McIsaac, C.A. Mitchell. 2010. Nitrogen balance in and export from agricultural fields associated with controlled drainage systems and denitrifying bioreactors. Ecological Engineering. 36:1558-1566. DOI:10.1016/j.ecoleng.2010.04.024.

Woltemade, C.J., J. Woodward. 2008. Nitrate removal in a restored spring-fed wetland, Pennsylvania, USA. Journal of the American Water Resources Association. 44(1):222-234. DOI: 10.1111/j.1752-1688.2007.00149.x.

Xiong, Z., Y. Xie, G. Xing, Z.Zhu, C. Butenhoff. 2006. Measurements of nitrous oxide emissions from vegetable production in China. Atmospheric Environment. 40(12):2225-2234.

Figure 1.1 – Excess N_2 dissolved in groundwater can either remain dissolved in groundwater and be transported down the hydraulic gradient, or it can diffuse into the vadose zone. Diffusion into the vadose zone is hypothesized to be the source of the missing N on the transect scale (hypothesis 4)

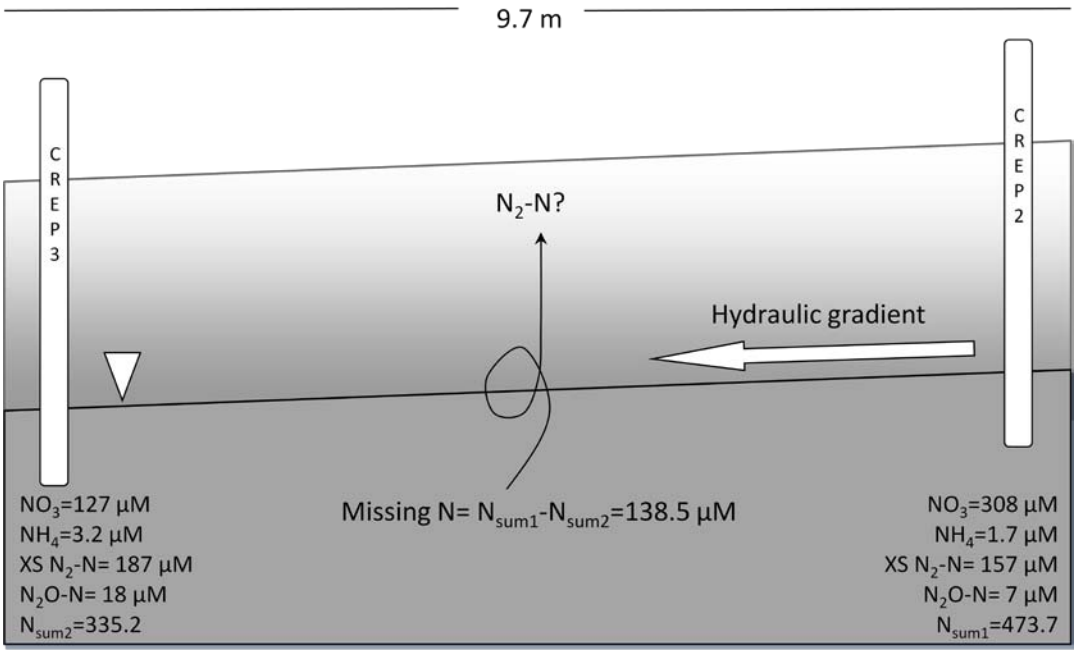

CHAPTER 2:

TEMPORAL AND SPATIAL VARIABILITY OF DISSOLVED N2O AND CH4 IN GROUNDWATER OF THE CHOPTANK BASIN

Abstract

Wetlands, either restored or natural, are areas that can potentially reduce agricultural nitrogen (N). Wetlands intended to reduce agricultural N may also produce the greenhouse gases N_2O and CH_4 which have high global warming potentials, 298 and 25, respectively. To understand the role of wetlands as sources of greenhouse gases, I studied the concentrations of dissolved N_2O and CH_4 in groundwater on the Delmarva Peninsula. Piezometer transects were installed across 10 locations, but I was only able to conclusively determine that the groundwater flowed across the transect at 1 of the 10 sites. This location was a prior converted cropland (PCC) with a wet spot within the field which was able to reduce NO_3^- from ~ 1 mM to 16 µM. Moderate levels of CH_4 (2.1 µM) and N_2O (0.6 µM) accumulated in separate piezometers along this transect.

In other locations, I documented evidence of CH_4 ebullition in the shallow groundwater of the Choptank. Ebullition is the formation and release of CH_4 bubbles to the vadose zone or atmosphere above. The CH_4 bubbles stripped the concentration of N_2 and Ar, and often made it impossible to determine the occurrence and rate of denitrification when CH_4 concentrations were greater than 20 µM.

Spatial and temporal variability was observed both within piezometer transects and between the different sites. Hot moments accounted for an average of 39% and 49% of the produced N_2O and CH_4 at individual piezometers in 9.8 and 10.7% of the time, respectively. Two N_2O and three CH_4 hot spots were identified out of the 64 piezometers. This chapter illustrates the temporal and spatial variation of both N_2O and CH_4 accumulation. It also shows the complexity of groundwater flow paths and the difficulty in making the assumption of groundwater flow down a topographic gradient.

Introduction

Nitrous oxide (N_2O) and methane (CH_4) are both potent greenhouse gases with global warming potentials of 298 and 25 over 100 years, respectively (IPCC 2007). N_2O also has the capacity to contribute to the removal of stratospheric ozone (Crutzen 1981). Both N_2O and CH_4 are produced and consumed naturally, but both cycles have been altered by anthropogenic processes. The atmospheric N_2O concentration is rising at approximately 0.26% yr^{-1} and reached an atmospheric concentration of 319 ppb in 2005 (IPCC 2007). The atmospheric concentration of CH_4 has increased since pre-industrial times, but the concentration leveled off (Dlugokencky et al. 2003) in 1996 through 2006, and then increased in 2007 and 2008 (Rigby et al. 2008, Dlugokencky et al. 2009). The average atmospheric concentration over both hemispheres in 2005 was 1,774 ppb (IPCC 2007). Soils are the largest contributor to the global N_2O budget, accounting for 67.5% of the globally produced N_2O, and agricultural soils alone account for 27% of the budget (Isermann 1994). In contrast, natural sources, including wetlands, account for 33% of the global CH_4 budget. Agricultural practices, mostly rice paddies, domesticated ruminants, and biomass burning, account for 42% of the budget (Isermann 1994).

Natural N_2O production can occur through the heterotrophic process of denitrification. Denitrification is the reduction of NO_3^- to N_2 through the intermediate and sometimes terminal steps of NO_2, NO, and N_2O (Knowles 1982). Denitrification typically requires conditions of low oxygen, a labile carbon source, and denitrifying bacteria, but chemolithotrophic denitrification is also possible (e.g., Shao et al. 2010). Denitrification can produce low excess N_2/ N_2O ratios for a number of reasons including high concentrations of NO_3^- (Blackmer and Bremner 1978), low pH (Blackmer and

Bremner 1978, Martikainen & Deboer 1993), and levels of oxygen (O_2) that limit nitrous oxide reductase but not nitric oxide reductase (Otte et al. 1996). Many researchers have looked for consistent excess N_2/N_2O ratios in different environments, but consistent ratios have not been found.

Other N transformations also result in N_2O production. Nitrification, the oxidation of NH_4^+ to NO_3^-, can also be a dominant process that produces N_2O (e.g., Ruser et al. 2006). Nitrification requires oxic conditions and NH_4^+, and can be either autotrophic or heterotrophic (Wrage et al. 2001), both of which can produce N_2O (e.g., Cai et al 2010). Nitrifier denitrification is a pathway of nitrification that also produces N_2O (Poth and Focht 1985, Wrage et al. 2001). Nitrifier denitrification is the oxidation of NH_3 to NO_2, followed by the reduction of the produced NO_2 to N_2O and N_2. NO_3^- is not produced. This process is not coupled nitrification/denitrification because both nitrifiers and denitrifiers carry out the coupled process whereas only nitrifiers carry out nitrifier denitrification (Wrage et al. 2001). I will not distinguish between the sources that produced the N_2O concentrations reported in this manuscript, but other gases such as excess N_2, a measure of denitrification, and O_2 will allow insight into the production source.

Denitrification and nitrification can simultaneously occur (e.g., Abbasi and Adams 2000) either through coupled nitrification/denitrification, or in locally situated anoxic and oxic microsites. In the denitrification reaction, nitrous oxide reductase is inhibited by oxygen to a greater extent than the other denitrification enzymes; therefore N_2O can accumulate at oxygen concentrations high enough to inhibit N_2O reductase, but low enough to allow denitrification to take place. Nitrification requires oxygen, but can

occur under low oxygen conditions (e.g., Goreau et al. 1980), or in soils with up to 60% water filled pore space (e.g., Bateman and Baggs 2005). These conditions could overlap producing both nitrification and denitrification derived N_2O in soils.

Methanogenesis is primarily the reduction of CO_2 (H_2 mediated) or acetate (acetotrophy) to CH_4. Acetotrophy is responsible for approximately two-thirds of CH_4 produced (Jones 1991, Le Mer & Roger, 2001). Other substrates can also be used such as formate, methylated compounds, and primary and secondary alcohols (Le Mer & Roger, 2001). Methanogens carry out the process of methanogenesis, and are members of the domain Archea. This process yields the least energy production per unit C (Megonigal et al. 2005) and usually occurs after all other electron acceptors have been exhausted in perennially or seasonally saturated areas. In contrast, unsaturated soils can function as CH_4 sinks (Mosier et al. 1998) through methane oxidation to CO_2.

Both N_2O and CH_4 can accumulate in the surficial aquifer either directly through production in groundwater, or indirectly through the percolation of water through elevated vadose zone concentrations of N_2O and/or CH_4. Denitrification and methanogenesis can both occur in groundwater, and both processes can occur in soils. Nitrification has also been cited as the major process producing N_2O in groundwater (Ueda et al. 1993). Both N_2O and CH_4 produced in groundwater can be reduced to N_2 (N_2O) or oxidized to CO_2 (CH_4) in the vadose zone. Therefore, high groundwater concentrations of N_2O and CH_4 do not necessarily represent a source to the atmosphere. Either gas dissolved in groundwater can diffuse to the atmosphere if exposed to air in groundwater seeps or streams, which would negatively impact the atmosphere. Groundwater dissolved N_2O concentrations that are derived from the leaching of N into

groundwater are considered indirect N_2O emissions when they emerge in streams or seeps (IPCC 2007).

High spatial variability is often observed for fluxes of CH_4 (Adrian et al. 1994) and N_2O (Goodroad et al. 1984, Mathieu et al. 2006). Both gases also show large temporal variability. Hot spots and hot moments are types of spatial and temporal variability, respectively. A biogeochemical hotspot is a location with high biogeochemical reaction rates in comparison to the surrounding area (McClain et al 2003). Hot moments are short periods of time with increased biogeochemical reaction rates compared to prior time periods (McClain et al. 2003). The hot spot or hot moment scale can be in the range from micro to macro. Many investigators have emphasized the hot spot and hot moment nature of denitrification throughout different systems (Parkin 1987, McClain et al. 2003, Harms and Grimm 2008). Parkin (1987) associated these hot spots with anoxic microsites and patchy organic carbon. The inherently complex structure of soils and the often patchy distribution of organic carbon appear to cause the heterogeneity of the respiratory gases. The large spatial and temporal variability associated with the production of these gases make sampling and extrapolating to a larger land area (e.g., a watershed) difficult.

I have investigated the concentrations of N_2O and CH_4 in the groundwater of the Choptank Basin. I sampled natural wetlands, prior converted croplands (PCC's, former wetlands drained for agriculture), the poorly drained wet spots within PCC's, drainage ditches, hydrologically restored wetlands, and riparian areas. My research was conducted as part of two larger projects in the Choptank Basin, of which my research was only a

small part. Supporting data from the larger projects is presented in order to enhance interpretation of my data.

The Choptank River is located in the Mid-Atlantic coastal plain on the Delmarva Peninsula and is a tributary to the Chesapeake Bay. Historically, the Choptank basin was primarily forested (Fisher et al. 2006), and in 1664 the first Europeans settled in the area. At that time, agriculture by Native Americans comprised < 2% of the land area (Benitez and Fisher 2004). As more people moved into the basin and the population grew, the large primary forests were converted to agricultural land, greatly changing the nitrogen dynamics of the watershed (Fisher et al. 2006). As agriculture further expanded, wetland areas that were naturally inundated with water were ditched and drained. Today, the primary land use in the Choptank basin is agriculture (52%), and forests and wetlands now only comprise 26% and 4% of the land area, respectively (Lee et al. 2001). The basin is drained by hundreds of km of ditches that directly transport N out of the agricultural soils and into surface waters (Bell and Favero 2000). Wetlands account for a small percentage of the watershed, but have the potential ability to reduce the N export downstream by acting as an area of increased denitrification if situated to capture the N. Many areas that were difficult to farm and continuously produced poor crop yields due to water inundation have been allowed to transition back to wetlands, or were converted to riparian areas or hydrologically restored wetlands. Some are still cultivated, and these produce poor crop yields in wet years and increased crop yields in dry years. Creating environments that produce conditions conducive to denitrification has the potential to significantly improve water quality within watersheds, but incomplete denitrification resulting in large N_2O concentrations could be harmful to the atmosphere.

The main hypothesis of this chapter is that concentration gradients of N_2O and CH_4 exist in groundwater both horizontally across transects and between sampling sites and vertically with depth at nested piezometers. I also hypothesize that hot spots and hot moments account for a large percentage of N_2O and CH_4 accumulation. Lastly, I hypothesize that soil conditions created by agricultural management practices, such as flow-controlled drainage ditches, riparian areas, and hydrologically restored wetlands will promote the reduction of NO_3^- to N_2 over the width of the buffer, wetland, or ditch bank while promoting the accumulation of N_2O and CH_4 from incomplete denitrification and methanogenesis. These hypotheses will be tested by evaluating the effectiveness of the wetland management areas in reducing NO_3^- as well as the production of both N_2O and CH_4, measured as concentrations.

Methods

Location

The Choptank River is located on the Delmarva Peninsula on the Maryland coastal plain and is a tributary to the Chesapeake Bay (Fig. 2.1). The Choptank River has experienced accelerated eutrophication due to increased N and P loading from agriculture and increased sewage outflow from a growing population (Lee et al. 2001). The more northerly sampling sites are underlain by the Pensauken Formation, a fluviatile deposit of Late Cretaceous age, and the more southerly Rfarm sampling location is underlain by the Kent Island Formation, an estuarine deposit of the middle-Wisconsin period (Owens and Denny 1979).

Ten locations were sampled for groundwater, and are described briefly in terms of their land use (Table 2.1). AB and BC are natural, forested wetlands. Piezometer transects run from the road edge (0 m) towards a ponded wetland. Neither of these wetlands have N sources other than atmospheric deposition, N fixation, N mineralization, and N remineralization. Other sites have one or more piezometers that are located in natural forested wetlands. BNDS, EFAG, and JLAG are hydrologically restored wetlands with transects that run from an agricultural field through a hydrologically restored wetland. Mfarm and Rfarm are agricultural locations, but the piezometer transects are located within a forested and Conservation Reserve Enhancement Program (CREP) riparian buffer, respectively. These transects run from the field edge (0m) towards a stream (MFarm) or tidal creek (Rfarm). BRFarm, CFarm, and HFarm have piezometers located within agricultural fields that are on corn/soybean crop rotations. The zero point of measurement for these locations is the field edge next to the dominant

drainage ditch for the crop field. BRfarm has piezometers situated in 3 separate land uses; within the agricultural field (BFF1-3), situated on a drainage ditch (BR3-5), and in the adjoining naturally forested wetland (BR1-2). Both CFarm and HFarm have piezometers located within the agricultural field and adjacent to controlled drainage structures. CFarm also has piezometers located on a regular, non-flood controlled ditch. Small areas with poorer drainage are located within these crop fields, and 4 of these "wetspots" are monitored by groundwater piezometers (BFF2, HFF1, HFF3, and CFF4).

The physical descriptions of the 64 piezometers at these sites are given in Table 2.1. Sets of 2 or more nested piezometers are located at 5 of the 10 sites. The ten sites have varying soil characteristics that range from sandy loams to silt loams (Table 2.1). The sampling time period for each piezometer during 2007-2009 is listed on Table 2.1. Samples were acquired monthly from all of the piezometers if sufficient water was present, resulting in >1500 N_2O samples and CH_4 samples.

Groundwater sampling

Groundwater samples were taken from 5.1 cm (2") inner diameter piezometers with 30 cm long sampling screens. The piezometers were installed by hand augering to depths between 0.5 and 5.0 m (Table 2.1). On the day prior to sampling, the depth to the water table was measured using a Solinst® water level meter, and the piezometers were pumped dry using a portable Solinst® Model 410 peristaltic pump. A slightly smaller diameter fishing float was lowered to the bottom of the piezometer to reduce gas exchange between the freshly inflowing groundwater and the atmosphere. The next day the float was removed, and a 5.1 cm (2") Teflon® bailer was slowly lowered to the

bottom of the piezometer to acquire an undisturbed groundwater sample. A one-way ball valve prevented loss of the groundwater when the bailer was removed from the piezometer. A stopcock connected to a 15 cm length of ½ cm teflon tubing was attached to the bottom of the bailer to control flow into 25 mL ground glass tubes with ground glass stoppers. The glass tubes were overflowed from the bottom with sample and immediately capped and submerged in ice water to prevent gas exsolution. A separate sample was taken for nutrients, conductivity and pH, and the temperature of the sample was taken with a VWR digital thermometer (NBS traceable accuracy of ± 0.3 ^{o}C). The groundwater samples were analyzed by MIMS for excess N_2, Ar, and O_2 (Kana et al. 1994), by gas chromatography for N_2O, CH_4, and CO_2, and by automated colorimetric methods for NO_3^-, PO_4, and NH_4^+.

Groundwater analyses

Groundwater samples were analyzed for N_2, O_2, and Ar using the MIMS method (Kana et al. 1994). The concentration of Ar within the sample was assumed to represent physical exchange between air and water at recharge and was used to calculate an effective recharge temperature of the water at the time of infiltration using the solubility formulations of Colt (1984) based on Weiss (1970). The Ar temperature was used to calculate the background N_2 concentration (e.g., Bohlke and Denver 1995, Mookherji et al. 2003), and observed N_2 greater than the background N_2 was considered "excess N_2" due to denitrification.

Dissolved N_2O and CH_4 samples were all analyzed using gas chromatographic techniques. N_2-purged 12 mL Exetainers® were used to equilibrate 8 mL groundwater

samples with a head space of N_2 gas at room temperature. The concentration of N_2O within the exetainer head space was determined on a Shimadzu GC-14B equipped with an electron capture detector (ECD) with a Porapak Q column. CH_4 was determined on a Shimadzu GC-8A equipped with a flame ionization detector (FID) with a HayeSep A column. The dissolved concentration in the original water sample was calculated using groundwater and headspace volumes, and the appropriate solubility data for the measured room temperature (Weiss and Price 1980, Lange 1961). Matheson Tri-Gas standards were used along with a blank and an atmospheric air injection to create a standard curve.

Soil physical properties

The soil physical property of porosity was determined using a time domain reflectometer (TDR) with the Trime®-Pico IPH and Pico-BT. TDR measures the volumetric water content of a soil along a depth profile. When the soil is completely saturated, the measured volumetric water content is equal to porosity, assuming no trapped air within the soil pores.

Hydraulic conductivity was calculated based upon the Hvorslev Slug-Test method (Fetter 2001):

$$K = \frac{r^2 \ln(L_e / R)}{2 L_e t_{37}} \qquad (1)$$

where K is hydraulic conductivity (cm/s), r is the radius of the piezometer casing (cm), R is the radius of the well screen (cm), L_e is the length of the well screen, and t_{37} is the time it takes for the water level to rise or fall to 37% of the initial change. The values of R and r were identical for our piezometer design. The variable t_{37} was calculated from a water level response record which I obtained by either pumping the piezometers dry and

measuring recharge on 1-2 minute time scales or by using the recharge events on the yearly levelogger 30 minute records (Chapter 3). The water table response record was used to calculate t_{37}.

Hot moment and hot spot classification

For quantitative purposes, I defined a hot moment as a month when the N_2O or CH_4 concentration was in the 95th percentile of all the concentration values from that piezometer over all of the months. I did not measure production rates; therefore, I defined a hot spot or hot moment as an increase in concentration instead of a pulse in rate. This definition allowed each piezometer to be treated independently of one another; therefore, piezometers with high median concentrations had much higher concentrations in their hot moments than a piezometer with lower median concentrations.

I have defined a hot spot piezometer as a location where the median concentration of either N_2O or CH_4 in the piezometer is in the 95th percentile of all of the other piezometer median N_2O or CH_4 concentrations for all of the sampling periods. Individual median values from a specific piezometer had to be greater than 5.5 μM N_2O-N and 17.5 μM CH_4, respectively, to qualify as a hot spot. Both of these values are orders of magnitude greater than N_2O or CH_4 at atmospheric saturation.

Statistics

Non-parametric statistical tests were used because neither the N_2O nor CH_4 data was either normally or log-normally distributed (Fig. 2.2A, B). Log transformation failed to improve the normality of the data (Fig. 2.2C, D), and the N_2O data also failed

homogeneity of variance tests. In order to test differences between two groups of non-normally distributed data, the Mann-Whitley-Wilcoxon or Wilcoxon rank-sum test was performed. The Kruskal-Wallis One-Way Analysis of Variance on Ranks was used to determine differences between more than 2 non-normally distributed populations. When a significant difference was determined for the Krustkal-Wallis One-Way ANOVA, a Dunn's test was used for multiple mean comparisons as it allows for unequal sample size. Spearman Rank Correlation was used to test for correlation between N_2O and CH_4, and the other dissolved constituents (NO_3^-, excess N_2-N, $\%O_2$ saturation, and NH_4^+) when the relationship between the dissolved constituents was monotonic. Spearman Rank Correlation is appropriate for non-normal, monotonic relationships (Quinn and Keough 2004). Spearman rank order uses the rank of the data instead of the value, and then calculates the Spearman's Rank correlation coefficient (r_s). Positive r_s values indicate positive agreement among the ranks, while negative r_s values indicates negative agreement. Sampling dates with evidence of CH_4 ebullition (discussed below) were removed from the N_2O correlation analyses.

Collaborator results

In order to interpret the spatial distribution of groundwater biogeochemical properties at the 10 locations, the groundwater hydrology must be understood. We installed piezometers at these sites assuming that groundwater flow paths followed the local topography, and the groundwater hydrology of the sites was assessed using major ion and water level data as a part of the larger Conservation Effects Assessment Project (CEAP) focused on wetlands in the Choptank Basin. The data collected by Judy Denver and Scott Ator at USGS are summarized below and are available in Denver and Ator (2011).

In order to assess the effectiveness of the management practices to reduce NO_3^-, a groundwater connection had to be established between the piezometers within the transects. Originally, I assumed that groundwater under an agricultural field flowed through piezometer 1 and across the management area to the furthest piezometer down the local topographic gradient. With this simplistic approach, the concentration of NO_3^- at the field edge piezometer could be compared to the concentration of NO_3^- and excess N_2 at the furthest piezometer from the field, allowing an evaluation of the effectiveness of the management area. This assumption is often made in many groundwater piezometer studies. Unfortunately, groundwater flow is not always simple, and the complexities of the groundwater flow paths at four of the ten locations will be discussed using both the hydraulic gradient across the transect and the major ion data for each site.

Brfarm

Brfarm represents an example of the groundwater gradient following the topographic gradient (Fig. 2.3A). The ditch functions as intended and pulls groundwater away from the crop field down the topographic gradient. The depth to the aquiclude is shallow (~8 m), and the forested upland on the other side of the ditch has a higher water table which likely slows the flow of groundwater from the farm side of the ditch, extending the groundwater residence time. Major ion data support this conclusion and indicate that the groundwater between the three piezometers was originally affected by agriculture. At this site (Brfarm) we can interpret the piezometer data as points along a single flow path.

JLAG

The general topographic gradient at JLAG is from the field edge through a wetland towards the ditch (Fig. 2.3B). The ditch (~ 2.5 m deep) on the right side of the JLAG panel controls the hydraulic gradient within the wetland, and the water on average flowed from the field towards the ditch. The hydraulic gradient occasionally varied between the wetland piezometers, but JLAG5 was always the lowest point in the piezometer transect. The major ion data indicated that the groundwater flow paths were controlled by local infiltration, and the groundwater chemistry measured in each piezometer represented local infiltration. The flow paths appear to be independent, and this flow pattern does not allow me to interpret the differences in groundwater chemistry as the result of processes occurring between the piezometers.

EFAG

At EFAG the land slopes towards the wetland from both the forest and agricultural field on either side (Fig. 2.3C). The highest topographic locations at EFAG1 and EFFOR1 slope toward the topographic low within the wetland (Fig 2.3C); however, despite the slope, the average hydraulic gradient indicated groundwater flow from the forest towards the agricultural field opposed to the local topographic gradient. The local hydraulic gradient is controlled by the regional topography, and the groundwater is flowing towards a stream off the left hand side of the EFAG panel of Figure 2.3C. Occasionally, over the course of 2008 to 2009 the hydraulic gradient switched direction and flowed from the agricultural field towards the wetland. This was observed from January to February 2009 when EFAG1 was the highest water table elevation of the transect in January and the lowest in February. Local recharge occurred around all of the piezometers, and the inferred, median groundwater flow paths are illustrated from the individual piezometers down the hydraulic gradient (Fig. 2.3C). The groundwater chemistry measured in each piezometer represented local infiltration and spatial patterns cannot be interpreted in terms of biogeochemical processing between piezometers.

BNDS

The topographic and hydraulic gradients at BNDS are from the agricultural field and forest towards the pond (Fig. 2.3D). The flow paths from BNDS 1 and 2 in the agricultural buffer originated around the piezometers through local recharge and then flowed towards the pond. The bottom of the pond was compacted by heavy machinery during pond construction limiting the movement of water between the pond and the

deeper groundwater. The major ion data indicated an agricultural source for the BNDS 1 groundwater but indicated a non agricultural source for the BNDS 2 and 3 groundwater because this groundwater infiltrated through the buffer. Discharge flow paths for the groundwater could not be determined from these data. Deep groundwater sampling showed oxic water impacted by agriculture at depth.

As a connection cannot be established between the piezometers within transects for all but one of the locations, I am unable to evaluate the effectiveness of the management practices to reduce NO_3^-, and I cannot analyze the concentrations within piezometers in terms of gradients except for Brfarm. For the rest of the locations, I can report the concentrations of the dissolved gases within the piezometers, and I can discuss the relationships among the dissolved gases which illustrate the occurrence of denitrification in these locations.

Results

CH_4 ebullition events

CH_4 ebullition events, or the formation and release of CH_4 bubbles, occur in groundwater when CH_4 accumulates to levels of supersaturation (Fig. 2.4). The concentration gradient for N_2, Ar, and N_2O is from the groundwater into the bubbles. This results in the stripping of these gases from groundwater, and these events result in the mass convective transfer of large concentrations of CH_4 and other gases to the vadose zone and/or atmosphere above. CH_4 ebullition must be considered before discussing other gas relationships because it affects the concentrations of all other dissolved gases.

CH_4 ebullition events present a problem in the estimation of the Ar groundwater recharge temperature (Fig. 2.4). In the calculation of excess N_2, the Ar concentration is assumed to be representative of the temperature at which the groundwater infiltrated. A loss of dissolved Ar through CH_4 ebullition results in low Ar concentrations in groundwater and the calculation of unrealistically high Ar recharge temperatures (30-100^{o}C). A high Ar recharge temperature then results in the calculation of unrealistically low background N_2 concentrations; however, as N_2 is less soluble than Ar, relatively more N_2 is stripped, and negative excess N_2 concentrations are calculated. Although negative N_2 values are possible as a result of nitrogen fixation (e.g., Fulweiler et al. 2007), it is unlikely at our sites due to the high DIN (usually 100-500 μM), and the negative excess N_2 values are primarily the result of CH_4 ebullition and gas stripping. For N_2O and N_2 statistical analyses of temporal variability and gas relationships, groundwater samples with recharge values over 22 ^{o}C were not used, but all of the data was used for CH_4 analyses, including N_2 because the majority of the high CH_4 values

were associated with negative excess N_2 values and eliminating these would eliminate all significant CH_4 accumulations. N_2O data points that were potentially influenced by CH_4 ebullition were left in the figures of spatial variability.

An extreme case of CH_4 ebullition stripping of dissolved gases is shown in Figure 2.4. In September 2009 I calculated Ar recharge temperatures of 94^oC with corresponding CH_4 concentration of ~600 μM at EFWET1a (Fig. 2.4). Both EFWET1a and JLAG3a consistently had unrealistically high Ar recharge temperatures (+30 ^oC) and high levels of CH_4 (Table 2.2). For this reason, both of these piezometers have limited excess N_2 and N_2O data that is reliable. Occasionally, other piezometers had unreasonable Ar recharge temperatures, which usually occurred in conjunction with CH_4 values >20 μM, while other locations had no evidence of CH_4 ebullition despite high CH_4 concentrations (e.g., 340 μM CH_4 at EFFOR2 in Dec 09). Evidence of ebullition was observed throughout the year, but the least number of events were observed in the colder months January, February, March, and April. A peak in the number of events was observed in July (Fig. 2.5). Multiple linear regression was performed over the entire data set, and at most 5.4% of the CH_4 concentration could be significantly predicted by $\%O_2$ saturation and pH. As a non-parametric equivalent to multiple linear regression was not found, multiple linear regression was used, even though it is a parametric statistical test.

Relationships between the gases

Denitrification was evidenced in many of our sampling locations as an accumulation of excess N_2. Typically, the wetland or hydric locations in closest proximity to agriculture had high oxygen and NO_3 concentrations and low excess N_2

values (Fig. 2.6). Locations with lower NO_3 concentrations typically had accumulations of excess N_2 and lower O_2 concentrations (Fig. 2.6). The highest excess N_2 concentrations were observed with low NO_3 concentrations and $\%O_2$ values under 20% which suggests that the excess N_2 was produced through denitrification of the agricultural N after O_2 had been consumed (Fig. 2.6). Denitrification of agricultural N is occurring at many of the sampled locations.

Additional evidence of nitrification and denitrification of agricultural nitrogen was observed within the data set. In general, nitrification tends to occur under conditions of higher O_2 (Bremner and Blackmer, 1978). Nitrification also produces NO_3^- as an end product, whereas NO_3^- is consumed in the process of denitrification. Denitrification tends to occur under low O_2 conditions, and N_2 is typically the dominant end product of denitrification. From visual inspection of Figure 2.7, the highest N_2O values were observed in conjunction with the lowest O_2 and NO_3^- values. These relationships suggest that the highest N_2O concentrations were produced by denitrification. These high N_2O values were also measured with moderate excess N_2 concentrations, which suggest incomplete denitrification that halted at N_2O production. Lower N_2O concentrations that were observed with higher O_2 and NO_3^- values suggest a nitrification source, and the lower N_2O values observed in low O_2 and NO_3^- water were likely produced through denitrification. The data suggest that the highest N_2O concentrations were produced through denitrification, while the lower N_2O concentrations produced in water with high O_2 and NO_3^- were likely from nitrification (Fig. 2.7). Multiple linear regression was performed on the entire data set and $\%O_2$ saturation, NO_3^- concentration, pH, and

conductivity were found to be significant variables that predicted 13.5% of the N_2O concentration.

When the data was broken down by site, both significant and non-significant relationships emerged (Table 2.3). Overall, there was a significant, negative relationship between excess N_2-N and NO_3. However, at the sites excess N_2 had significant negative, no significant or non-monotonic relationships with NO_3^-. Excess N_2 and NO_3^- were significantly negatively related at Hfarm, Cfarm, BNDS, and Mfarm, indicative of denitrification. The EFAG relationship was influenced by NO_3^--rich groundwater that had not been denitrified at EFAG1 (high NO_3^-, low excess N_2), groundwater that had undergone denitrification at EFAG2 (moderate NO_3^-, high excess N_2), and then groundwater that infiltrated locally within the wetland or forest with low NO_3^- and low excess N_2 water, producing a non-monotonic relationship over the entire site. Non-significant relationships were found between NO_3^- and excess N_2 at BC, JLAG, AB, and Rfarm. The relationship at Rfarm was marginally significantly positive ($p=0.06$), and BC and JLAG had very low NO_3^- concentrations which could explain the lack of significant relationships.

The relationship between NO_3^- and N_2O-N was significantly positive at JLAG and significantly negative at Mfarm (Fig. 2.8A). Although a positive relationship was observed between NO_3^- and N_2O at JLAG, I do not suspect that this N_2O was produced through nitrification. Instead, the high N_2O values at JLAG were likely produced when higher NO_3^- groundwater reached the wetland, as these high N_2O concentrations appeared in groundwater with less than 10% O_2 saturation. The significantly negative NO_3^- and N_2O relationship observed at Mfarm was likely due to denitrification (Fig. 2.8A). Non-

monotonic relationships were observed and Spearman Rank Correlation was not appropriate at EFAG, Hfarm, Cfarm, Brfarm, and BNDS. The non-monotonic relationship could be caused by production through nitrification and denitrification, or because there were multiple groundwater sources with varying concentrations of NO_3^- at one site, as for excess N_2-N at EFAG. For example, a non-monotonic relationship could be produced if there was high NO_3^- groundwater at the buffer edge and low NO_3^- groundwater resulting from local wetland recharge in the center of the buffer. This would produce high NO_3^- concentrations with little N_2O at the field edge, moderate NO_3^- concentrations with moderate to high N_2O in the buffer closer to the field, and low NO_3^- groundwater with low N_2O away from the agricultural field (e.g., EFAG, see Fig. 2.14 below). This would produce a relationship that had low N_2O concentrations observed with both low and high NO_3^-, and high N_2O concentrations observed with moderate NO_3^-, producing a "U-shaped" non-monotonic pattern.

The only sites where significant relationships were found between excess N_2 and N_2O were Cfarm, EFAG, and Mfarm (Fig. 2.8B). All three sites showed a positive relationship suggesting denitrification (Table 2.3). $\%O_2$ saturation was negatively correlated with N_2O at Cfarm and Mfarm, supporting the conclusion of denitrification at this location. JLAG had a significantly positive relationship between $\%O_2$ saturation and N_2O, but again, all of the high N_2O concentrations were produced in groundwater with lower than 10% O_2 saturation. NH_4^+ data was somewhat limited, but clear relationships between NH_4^+ and N_2O were found at Hfarm and Cfarm, showing a negative and a positive relationship, respectively.

The overall CH_4 data strongly shows that CH_4 concentrations do not accumulate until oxygen and nitrogen electron acceptors have been reduced (Fig. 2.7). A sharp increase in CH_4 concentrations was observed after O_2 was reduced to less than 10% O_2 saturation and NO_3^- was reduced below 25 µM. A few high CH_4 concentration values were observed with higher % O_2 saturation and NO_3^- concentrations, and this CH_4 was likely produced in anoxic microsites within predominantly oxic or NO_3^--rich groundwater. The CH_4 and excess N_2 relationship (Fig. 2.7F) was mostly controlled by the negative excess N_2 values from the CH_4 ebullition events. These negative excess N_2-N values were the result of CH_4 ebullition and are not accurate, but are left in Figure 2.7F because if they were removed all of the high CH_4 values would also be eliminated.

Significant negative relationships between CH_4 and % O_2 saturation and CH_4 and NO_3^- concentration were found at all of the sites except Rfarm (Fig. 2.7). AB produced a non-monotonic relationship between NO_3^- and CH_4, again probably due to mixing of different groundwater sources. Significant relationships between excess N_2 and CH_4 were found at approximately half of the sites (Table 2.3), but the relationships were strongly controlled by the negative excess N_2 calculated values caused by CH_4 ebullition at AB, EFAG, and JLAG, and somewhat controlled by these negative values at Hfarm. Rfarm had a non-significant relationship between excess N_2 and CH_4 due to the lack of substantial CH_4 accumulation at this site (Table 2.2). Figure 2.9 is a clear example of an inverse hyperbolic relationship between NO_3^- and CH_4 at Brfarm.

If the data are segmented into times when the water table is falling (evaporation exceeds rainfall) versus times when the water table is rising (rainfall exceeds evapotranspiration), the strength of the relationships between the gases increases (Fig.

2.10A), decreases (Fig. 2.10B), or is unaltered. The correlation coefficient between excess N_2 and N_2O at CFarm for the falling water table months shown on Figure 2.10A can be compared to the value for the same relationship over the entire sampling period on Table 2.3 to see that the relationship increases when just the falling water table months are examined. The opposite is true for the relationship displayed on Figure 2.10B at EFAG. This analysis indicates that groundwater level does not have a consistent effect on gas and solute relationships in groundwater.

Horizontal spatial variability

The horizontal variability of N_2O and CH_4, as well as excess N_2, NO_3^-, and % O_2 saturation are presented below for four of the ten sites. I have chosen to present JLAG, EFAG, BNDS, and BrFarm because the hydrology was determined by Denver and Ator (2011) and was discussed above.

The wet spot within the PCC on Brfarm is functioning to reduce the majority of NO_3^- that infiltrated in the upland agricultural field before entering the ditch (Fig. 2.11). The median concentration of NO_3^- within the upland agricultural field (BFF1) was ~ 1 mM and decreased to 16 μM at the ditch edge after passing through the wet spot while excess N_2 concentration increased to ~ 300 μM. The median rate of N_2–N accumulation (G_{N2}) in the surface unconfined aquifer between BFF1 and BFF2 was calculated from the flow (Q, $m^3\ d^{-1}$ (m flow path width)$^{-1}$) and difference in the median concentrations between BFF1 and BFF2 (C_{diff}).

$$Q = kA\left(\frac{h_1 - h_2}{L}\right) \quad (2)$$

$$G_{N_2} = Q * C_{diff} \quad (3)$$

where k is the average hydraulic conductivity between BFF1 and BFF2 (0.64 m d^{-1}), A is the cross sectional area of flow (6.75 m^2), h_1 is the median elevation of the water table at BFF1 (m), h_2 is the median elevation of the water table at BFF2 (m), and L is the distance between BFF1 and BFF2 (m). N_2 accumulated at a rate of 5.3 mmol d^{-1} per m width of flow path over the 6.75 m depth of the unconfined aquifer. Although we did not sample the exact same flow path, according to the major ion data and hydraulic gradient, the groundwater flows from BFF1 to BFF3 and has an agricultural chemical composition. The depth to the aquiclude is shallow (~ 7 m below ground), allowing the zone of reduction created by the wet spot to extend to the aquiclude. This in turn, resulted in denitrification through the entire depth of the surface aquifer. The presence of reduced groundwater at depth was confirmed by deeper groundwater sampling (Denver and Ator 2011). CH_4 was highest within the center of the wet spot (BFF2), and N_2O was highest at the ditch edge (BFF3). However, the median concentration of N_2O was not as large as other locations (Fig. 2.11, Table 2.2), and this site was reducing NO_3^- while only producing moderate dissolved concentrations of N_2O and CH_4. The concentration of N_2-N, N_2O-N, and CH_4 emerging into the stream per meter of stream length was calculated by multiplying the flux of groundwater through a 1 m wide section of the surface aquifer (6.75 m^2) between BFF1 and BFF3 by the median concentration of each gas at BFF3 and was 8.0 mmol N_2-N (m stream length)$^{-1}$ d^{-1}, 0.015 mmol N_2O-N (m stream length)$^{-1}$ d^{-1}, and 0.0019 mmol CH_4 (m stream length)$^{-1}d^{-1}$.

The JLAG site (Fig. 2.12) contrasted sharply with BrFarm (Fig. 2.11). The concentration of N_2O and CH_4 varied greatly, but NO_3^- and $\%O_2$ saturation were low

(<25 μM NO_3^- and <20% O_2 saturation, respectively) and varied little (Fig. 2.12). Local infiltration and land use dominated the groundwater flow and chemistry. Efficient denitrification underneath the agricultural field likely produced the high excess N_2 (median: 485 μM N_2-N), low NO_3^- (median: 1.8 μM NO_3^-), and low N_2O concentrations (median 0.5 μM N_2O-N) that were observed at JLAG1 (Fig. 2.12). The excess N_2 concentrations at JLAG1 were the highest concentration observed over all of the sites (Fig. 2.12 and Fig. 2.13). Excess N_2-N concentrations were lower at JLAG2 than at JLAG1 and the concentration of N_2O, O_2, and NO_3^- were higher. The hydraulic conductivity at JLAG2 was large (137 cm day^{-1}, Table 2.1), and the chemical composition of the groundwater was likely influenced by groundwater mixing and the faster flow of local recharge water through this area. JLAG3 and JLAG 3a were installed next to one another within the wetland, but only JLAG3 is displayed on Figure 2.12. The concentration of N_2O was largest within the piezometer transect at JLAG3, and the concentration of CH_4 was largest at JLAG3a (Table 2.2, Fig. 2.12). Unrealistic Ar recharge temperatures and negative excess N_2 concentrations were often calculated at JLAG3a from methane ebullition. At JLAG4, the concentration of CH_4 was high, but NO_3^-, %O_2 saturation, excess N_2, and N_2O, were all low due to the local infiltration of low NO_3^- water. JLAG5 represents the end of a flow path below the ditch, but not necessarily one of the flow paths that I sampled in the upland transect. The water sampled in JLAG5 could also have originated in the area on the other side of the ditch.

The EFAG site slopes from both a crop field and a forest towards a local topographic low in the wetland (Fig. 2.14). Local infiltration was the dominant control on the gas concentrations in groundwater at this location. Unlike the field edge

piezometer JLAG in Figure 2.12, EFAG1 in Figure 2.14 had high $\%O_2$ saturation, high NO_3^-, low excess N_2-N, and low CH_4 concentrations, which was similar to the other field edge piezometers (Mfield, BNDS1, BFF1, CFF1 and CFF3). This more oxidized condition resulted from the infiltration of well-oxygenated water with high dissolved NO_3^- from the agricultural field. N_2O was more variable between the field edge piezometers (EFAG1 and 2), but was moderate at EFAG1 (median: 1.1 µM N_2O-N, Fig. 2.14). Evidence of denitrification was observed at EFAG2 as excess N_2 accumulated to moderate levels (261 µM N_2-N), and N_2O concentrations were high (median: 4.4 µM N_2O-N). Moderate levels of NO_3^- were observed at EFAG2 which could have resulted from the hydraulic gradient switching directions from the dominant forest source to an agricultural source for short periods of time. The concentration of NO_3^- at EFWET1a was often undetectable, and $\%O_2$ saturation was always under 4%. The only significant NO_3^- (310 µM) and N_2O-N (75 µM) concentrations measured were after the wetland recharged after a dry fall in December 2008. The median concentration of CH_4 was the largest of all the piezometers (311 µM) and the highest individual concentration measured was 1014 µM CH_4. The high CH_4 concentrations caused gas stripping, as evidenced by negative calculated excess N_2 values for 15 of the 21 sampling dates (Fig. 2.5). EFFOR2, located on the far side of the wetland, had low NO_3^- (47 µM) and excess N_2-N (43 µM), moderate oxygen (45 % O_2 saturation), and concentrations of N_2O and CH_4 less than 1 µM, except during a two month CH_4 hot moment in November and December 2009 when CH_4 concentrations reached 340 µM. The concentration of all of the dissolved constituents was low at EFFOR1 because the flow path originated within the forest adjacent to the piezometer transect.

BNDS is a hydrologically restored wetland that borders agriculture and a forest (Fig. 2.15). Initially, BNDS appeared to be an example of a hydrologically restored wetland that was functioning to reduce the majority of NO_3^- leaving the agricultural field (Fig. 2.15). The redox potential and NO_3 concentration decreased with distance across the buffer transect as excess N_2-N accumulated. N_2O was highest at BNDS2 halfway across the transect, and CH_4 was highest on the furthest side of the transect at BNDS4 (Fig. 2.15). However, the hydrology, major ion data, and soil structure of this site indicate that the wetland was not intercepting all of the water leaving the agricultural field. The hydraulic gradient did decrease from the field edge to the pond, but the sampled groundwater at BNDS1 and BNDS2/3 were of a different major ion composition. According to the major ion data, the NO_3^- present at BNDS1 was from agriculture, but the low concentrations of dissolved NO_3^- at BNDS2/3 (median: 86 and 36 µM, respectively) were not of agricultural origin, but likely infiltrated locally through the buffer. Excess N_2 did accumulate in BNDS 2/3 from the denitrification of locally infiltrated NO_3 and conditions were conducive for denitrification (median $\%O_2$ saturation: 11.7 and 9.6% respectively). Elevated concentrations of both N_2O and CH_4 were observed at BNDS 2 and 4, respectively. Deep groundwater sampling showed oxic, high NO_3^- groundwater at depth (Denver and Ator 2011), indicating that the flow path sampled by BNDS1 was flowing below the wetland and not being denitrified. The piezometers installed at BNDS were in the surface unconfined aquifer and conditions were conducive for denitrification at this depth. If the agricultural water was diverted through these soils significant denitrification could result.

Land use relationships

It would be convenient to assign an average concentration of N_2O or CH_4 to different land use categories to understand which areas produced high or low concentrations of either gas. The sites were divided into categories based on the landscape features on which they were situated (Fig. 2.16). Great variability existed between the piezometers located at different sites in similar land uses. Nonetheless, some useful conclusions can be made from categorizing the sites.

The natural forests and forested wetlands had low median N_2O concentrations, but large and varied CH_4 concentrations (Fig. 2.16). In order for large concentrations of N_2O to accumulate, an N source must be available. At natural sites, the only sources of N are atmospheric deposition, N fixation, N mineralization, and N remineralization none of which are likely to produce substantial concentrations of N.

The concentrations of CH_4 and N_2O were both low for the cropland piezometer category, but occasional spikes of N_2O-N less than 2.5 μM were observed. Both NO_3^- and O_2 are present at high concentrations at all of the cropland sites except HFF2, where $\%O_2$ saturation levels became lower than 20% in the summer and NO_3^- was below 100 μM for the entire sampling period.

The piezometers within the anthropogenically altered categories (riparian area, ditch or buffer edge, wet spot, and hydrologically restored wetland) had median N_2O concentrations along a spectrum from slightly greater than atmospheric to greater than 18 μM N_2O-N. The riparian area category had the largest median N_2O concentration followed by the ditch or buffer edge category (Fig. 2.16). The hydrologically restored

wetland category had the largest median concentration of CH_4 and the two highest piezometer median CH_4 values of the anthropogenically altered sites.

Hot spots

I defined N_2O and CH_4 hot spots as piezometers that had median concentrations in the 95th percentile of the other sampled piezometer medians (Table 2.4). The 95th percentile value was 5.5 µM N_2O-N and 17.5 µM CH_4. Using these criteria, three N_2O and four CH_4 hot spots were identified. The piezometers were either N_2O or CH_4 hot spots, but not both.

CREP3 was an N_2O hot spot with extremely high N_2O concentrations and moderate excess N_2-N values (Fig. 2.17). The median excess N_2/N_2O ratio at CREP3 for 2007 was 11, which is a low ratio, especially considering the relatively low concentrations of excess N_2-N (median: 187 µM N_2-N). The $\%O_2$ saturation over this time period was 11.3%, which would be conducive for denitrification, not nitrification, because nitrification tends to be responsible for N_2O production under aerobic conditions (Bremner and Blackmer, 1978).

The CH_4 hot spots EFWET1a (Fig. 2.4) and JLAG3a both showed strong evidence of CH_4 ebullition for the majority of sampling dates. JLAG4 had a few sampling dates when CH_4 ebullition was suspected, and BC1 had no evidence of CH_4 ebullition despite the high accumulations of CH_4.

Vertical spatial variability

The concentration of CH_4 varied with depth at the three BC2 piezometers located at 0.64 m, 1.08 m, and 1.55 m (Table 2.2, Fig 2.18). The concentration of CH_4 at this site was generally low except during the summer months when hot moment concentrations were observed at all three depths (Fig. 2.18). The highest CH_4 concentrations were > 100 µM CH_4, and high concentrations were observed at all three piezometers in July-August 2008. 2008 was a relatively dry year (86.8 cm of rain), and the shallower piezometers dried towards the middle of summer and did not flood again until 2009.

Nested piezometers were located within two independent flow paths at JLAG (Fig. 2.19). Typically, the concentration of N_2O was higher at the 2.75 m piezometer (median: 0.27 vs. 0.02 µM N_2O-N), and the concentration of CH_4 was higher at the 0.54 m piezometer (median: 33.3 vs 0.6 µM CH_4). N_2O only peaked once at the shallower piezometer, while CH_4 was more consistently elevated. This pattern is reversed for the deeper piezometer (Fig. 2.19). The piezometer depths were greater than 2 meters apart; therefore, we are unable to resolve what was occurring between the two depths. The shallower piezometer was most likely influenced by infiltrating surface water from the ponded wetland, while the deeper piezometer flow path likely infiltrated further from the ponded wetland closer to the agricultural field. We were unable to consistently measure excess N_2 from the shallower piezometer due to CH_4 gas stripping; therefore, N_2O concentrations were likely underestimated due to gas stripping, potentially accounting for the lower concentration at this piezometer.

Nested piezometers were also installed at BNDS and EFAG. The shallower piezometer, EFWET1a, had large concentrations of CH_4 (median: 311 µM), but generally

low concentrations of N_2O (Table 2.2). One exception was December 2008 when the concentration of N_2O-N accumulated to 75.1 μM N_2O-N. BNDS had high N_2O concentrations at the shallower 0.6 m piezometer for 7 of the 10 sampled months (median: 6.2 μM N_2O-N). The deeper piezometer at 2.26 m had considerably lower concentrations of N_2O (median: 0.14 μM N_2O-N), but a higher median CH_4 concentration (Table 2.2).

The nested piezometers showed different relationships between the shallower and deeper depths. The vertical variation could be visualized within the same flow path or in multiple bordering flow paths. The water that comprises a flow path originates from the same location; therefore, differences in one flow path would be due to differences in carbon and electron acceptor availability within that flow path. Multiple flow paths that run through an area may have infiltrated at different locations with different land uses and soils. Differences observed with depth could be either due to carbon and electron acceptor availability or due to differences in recharge location. BC2 (Fig. 2.18) was an example where a concentration gradient was likely being sampled at all three depths, which showed an increase in CH_4 concentration in August 2008, although the deepest piezometer appeared to be slightly delayed behind the shallower depths. In contrast, the nest at JLAG appeared to be sampling two separate flow paths (Fig. 2.19). The different relationships at the different locations emphasize the spatial variation between sites as well as the vertical variation with depth.

Temporal variability

The temporal variability of N_2O and CH_4 was evident from time series of the data in Figure 2.13. Both gases showed peaks in concentration that lasted for a month to multiple months. I was able to capture significant temporal variability by sampling monthly. Less frequent sampling would have missed the large gas concentration peaks at time scales of ~1 month (Fig. 2.13).

There were no systematic seasonal differences in N_2O concentrations. Median dissolved N_2O concentrations were not significantly different between seasons (Fig. 2.20A). However, if a comparison is made between times when water is predominantly infiltrating into the groundwater (rising water table), versus times when evaporation is greater than infiltration (falling water table, June, July, August and September), the periods with little infiltration had significantly higher N_2O concentrations (Fig 2.20B). There was no significant difference in the dissolved N_2O concentration in 2008 versus 2009 over all piezometers sampled in both years, but there were some differences at individual piezometers (Fig. 2.21).

Unlike N_2O, there were significant seasonal differences in CH_4 concentration (Fig. 2.20). Seasonal median dissolved CH_4 concentrations were significantly higher in summer (June, July and August) than spring (March, April and May) or winter (December, January, and February). Because of the variability, fall (September, October, November) median values were not significantly different than spring, summer, or winter median concentrations (Fig. 2.20C). If a comparison is made between times of rising groundwater (net infiltration into groundwater), as defined above, versus falling groundwater levels (evaporation is greater than infiltration), the periods with no net

infiltration had significantly greater CH_4 concentrations (Fig. 2.20D). Interannually, CH_4 concentrations were not significantly different between 2008 and 2009 for all piezometers but some individual piezometers showed significant variation between 2008 and 2009 (Fig. 2.21).

Hot moments

Hot moments were defined as months when the concentration of N_2O or CH_4 was in the 95th percentile of all concentrations measured at that piezometer (Fig. 2.22, Table 2.2). This definition only identified the highest 5% of concentrations of either N_2O or CH_4, but also always identified a hot moment because there is always a value in the top 5%. This was a consistent approach, but it eliminated concentrations that were adjacent to a hot moment (e.g., Fig. 2.22). The concentration prior to and after the defined hot moment concentrations in Figure 2.22 could have been considered part of the hot moment, but were not classified in this way in order to maintain a consistent classification.

66 N_2O and 77 CH_4 hot moments were observed (Table 2.2). There were 10 instances when both N_2O and CH_4 hot moment concentrations were observed together, but most hot moments occurred independently. N_2O hot moments ranged from 0.086 to 75 μM N_2O-N, and CH_4 hot moments ranged from 0.046-1014 μM CH_4. The hot moment concentrations were observed for at least one month but no longer than 2 months. On average, hot moments occurred for 9.8 and 10.7 %of the sampling time per piezometer for N_2O and CH_4, respectively (Table 2.2). Although these hot moments only occurred for approximately 10% of the time, they accounted for an average of 39.0% and

48.5% of the sum of gas concentrations at individual piezometers for N_2O and CH_4, respectively (Table 2.2). Hot moment concentrations accounted for between 5 and 99.2% of the sum of N_2O gas concentrations, and between 11.1 and 98.3% of CH_4 at individual piezometers.

Discussion

The main hypothesis of this chapter was that concentration gradients of N_2O and CH_4 exist in groundwater both horizontally across transects and vertically with depth at nested piezometers. Connecting the groundwater between piezometers horizontally was difficult, but differences in concentration did exist within transects. These differences were not necessarily concentration gradients as connections between the water sampled in the piezometers was only established at one transect. The horizontal differences in concentration were likely the result of differences in local infiltration location. Vertically with depth, differences in concentration also existed, but it was difficult to establish whether these were concentration gradients or different flow paths. I also hypothesized that hot spots and hot moments would account for a large percent of the yearly N_2O and CH_4 accumulations in groundwater piezometers. Evidence to support this hypothesis was found. Hot moment peaks in concentration were observed in the time series data sets, and accounted for on average 39 and 49% of the total N_2O and CH_4 produced per piezometer but only occurred for ~ 10% of the time. Three N_2O and four CH_4 hot spots were located in the 64 piezometer data set and the concentrations produced in these piezometers were substantial. Lastly, I hypothesized that soil conditions created by agricultural management practices, such as flow-controlled drainage ditches, riparian areas, and hydrologically restored wetlands would promote the reduction of NO_3^- to N_2 over the width of the buffer, wetland, or ditch bank while promoting the accumulation of N_2O and CH_4 from incomplete denitrification and methanogenesis. This was observed at one of the sampling locations where NO_3^- was reduced from ~ 1 mM to 16 μM over the transect width. Moderate levels of CH_4 (2.1 μM) and N_2O (0.6 μM) accumulated in

separate piezometers along this transect. At the other locations, evidence of denitrification was observed as elevated levels of excess N_2-N.

CH_4 ebullition

CH_4 ebullition events transfer large concentrations of CH_4 to the vadose zone or directly to the atmosphere. These events can be considered hot moment convective transfer mechanisms because prior to these events the slow process of diffusion would be the dominant mechanism transporting CH_4 out of groundwater. Ebullition only occurs when the concentration of CH_4 has become supersaturated, causing bubble formation and the flux of CH_4 and other stripped dissolved gases out of groundwater. I found evidence of CH_4 ebullition in the form of Ar concentrations lower than would be expected in equilibrium with air at typical groundwater recharge values (~5-15^oC). These low Ar concentrations precluded the calculation of realistic recharge temperatures (>22^oC).

As described above, the ebullition of CH_4 causes the stripping of N_2, Ar, and likely N_2O. Mookherji et al. (2003) and Fortuin and Willemsen (2005) also reported CH_4 bubble formation in groundwater that caused the exsolution or ebullition of N_2 and Ar. Prior to this research, Blicher-Mathiesen et al. (1998) reported the degassing of N_2 by using Ar as a physical tracer of degassing. Fortuin and Willemsen (2005) also reported that under lower hydrostatic pressures, less methanogenesis was required to produce conditions that would allow ebullition than at higher hydrostatic pressures. This is the reason that CH_4 ebullition is observed most frequently in summer and fall (Fig. 2.5), when groundwater temperatures are highest and water levels are lowest (Fisher et al.

2010). However, I did find evidence of CH_4 ebullition throughout the year, but the lowest occurrence of ebullition was observed in January through April (Fig. 2.5).

The production and ebullition of CH_4 in groundwater strips the water of dissolved gas, and eliminates the history of what happened to the groundwater as it moved through the wetland. CH_4 ebullition and gas stripping is a limitation to measuring denitrification using the N_2/Ar ratio. Reliable excess N_2 values cannot be acquired from piezometers that have evidence of CH_4 gas stripping, without additional conservative gas tracers. It is easy to detect large ebullition events that produced unrealistically high Ar recharge temperatures, but small changes in the Ar recharge temperature may not be noticed. Sampling after the groundwater is recovering from an ebullition event could also potentially produce unreliable excess N_2 values.

Evaluation of wetlands as landscape NO_3 sinks through denitrification

In order to assess the ability of the wetlands to reduce NO_3^- and produce N_2O and CH_4, a groundwater connection across the wetland had to be established. Denver and Ator (2011) were able to establish a hydrologic connection at Brfarm. The wet spot at Brfarm was able to reduce NO_3^- because the depth of the surface aquifer was shallow, and the groundwater on the forested wetland side of the ditch was higher than on the agricultural side of the ditch. This groundwater imbalance reduced the flow of water out of the agricultural side of the ditch and may have increased the groundwater residence time. This location reduced NO_3^- throughout the entire soil column because the reduced zone created by the wet spot at BFF2 was extended through the entire depth of the surface aquifer. This was determined by deeper groundwater sampling (Denver and Ator

2011). If the surface aquifer had been deeper, a portion of the groundwater might have flowed underneath the zone of reduction, maintaining an elevated NO_3^- concentration. Denitrification reduced NO_3^- to N_2 at BrFarm, and moderate concentrations of dissolved N_2O accumulated. I measured considerably higher values of both N_2O and CH_4 at other locations (Table 2.2).

More complex groundwater flow paths were observed at JLAG, EFAG, and BNDS. Without knowledge of the hydrology or the soil characteristics of the locations, EFAG and BNDS appeared to be reducing most of the high NO_3^- groundwater leaving the agricultural field to N_2 across the wetland widths. From the hydraulic gradient at EFAG, it was determined that the dominant hydraulic gradient sloped from the forest and wetland towards the agricultural field. For short time periods, the hydraulic gradient switched directions allowing mixing of the reduced wetland groundwater with the high NO_3 agricultural groundwater. This resulted in denitrification of some agricultural NO_3^-. However, for the majority of the sampling period the agricultural groundwater was not intercepted by the wetland. At BNDS, the hydraulic gradient flowed along the topographic gradient from the agricultural field towards the wetland. However, the history of the construction of the wetland, information gathered from deep groundwater sampling, and major ion data provided information to interpret more accurate flow paths. From this data, we were able to determine that infiltration occurred locally around the piezometers and the groundwater flowed towards the base of the pond, but interaction between the pond and groundwater was limited due to compaction of the pond bed during construction. High NO_3^- groundwater was observed at depth (Denver and Ator 2011);

therefore, this wetland location does not appear to be functioning to reduce the majority of NO_3^- exiting the agricultural field.

Understanding the hydrology of a study location is an important aspect of correctly assessing the groundwater chemistry of an area. This study would have concluded that these wetlands were working to reduce the majority of agricultural NO_3^- leaving an agricultural field when in fact the wetlands were not always intercepting the agricultural groundwater. Excess N_2 was measured at all of these wetlands however, and oxygen concentrations were reduced providing conditions conducive for denitrification. If the majority of the groundwater had been channeled through these shallow wetland sediments, significant denitrification would likely have occurred. This emphasizes the importance of having major ion and hydrology data to understand the movement of groundwater in a location.

The complexity of groundwater flow underlines the fact that wetlands cannot be constructed randomly to reduce N loss from agricultural fields. Riparian areas have been observed to function to reduce N only when the groundwater is captured by the riparian buffer (Lowrance et al., 1984 a, b). Riparian buffers have been studied where the groundwater flowed underneath the riparian area and entered surface waters without passing through a reduced environment (Lowrance et al., 1997). Similar observations can be made for some of our hydrologically restored wetlands. The wetland at EFAG, for example is topographically lower than the agricultural field, and it could be assumed that the groundwater would flow down the topographic gradient. But in fact, the groundwater predominantly flowed from the wetland towards the agricultural field and towards another nearby stream (Tuckahoe Creek). If wetlands are installed to reduce N, for

greatest efficiency they should be installed in a location where the groundwater from the agricultural field will pass through the reduced zone created by the wetland. The direction of the hydraulic slope could be obtained simply with relatively little work by installing mini-piezometers in the prospective wetland and measuring the depth to the water table periodically for a year. The hydraulic slope could then be determined if the elevation of the piezometers was known. Understanding the direction of groundwater flow would ensure that the wetland had the potential to intercept the N-rich groundwater, especially if the depth to the surface aquifer was shallow.

Spatial and temporal variability; hot spots and hot moments

Spatial variation was seen within transects, both horizontally and vertically, among sites, and among categories of sites (Fig. 2.11-2.16). The spatial variability of both N_2O and CH_4 production or flux has been reported by many researchers (e.g., Goodroad et al. 1984, Goodroad and Keeney 1985, Adrian et al. 1994, Breuer et al. 2000, Mathieu et al. 2006, Yao et al. 2010). The complex structure of soils inherently causes spatial variability due to the heterogeneous accumulation of carbon, and the formation of microsites.

The spatial variation observed on the transect scale was a result of the location through which the groundwater infiltrated into the soil and became groundwater. Groundwater flow paths that originated under agricultural fields had large concentrations of NO_3^- and could acquire large concentrations of excess N_2 if the flow path went through an area conducive to denitrification (e.g., JLAG 1, Fig. 2.12). Groundwater flow paths that originated within wetlands typically had low NO_3^- concentrations, low O_2, and

elevated CH_4 concentrations (e.g., JLAG 4, Fig. 2.12 & 2.13). Without understanding the groundwater flow paths, this spatial variation appeared to be due to an exhaustion of the different electron acceptors as the groundwater flowed through the wetland, but it was actually a function of where the water infiltrated.

Variation in the concentration of N_2O and CH_4 between similar land use sites was also great (Fig. 2.16). Potentially, some of this variation was due to the lack of spatial coverage at each location. One transect of piezometers was installed at each location without replication. If more transects were installed, the median N_2O or CH_4 concentration within land use categories may have been more similar because within the single piezometer transect, individual piezometers could have been installed in hot or cold spots. A greater number of piezometers might have given more representative concentrations for the entire area.

Hot spots are defined as locations where the median groundwater concentration was in the 95^{th} percentile of all other median piezometer values. This quantitatively assigned the hot spot classification to a non-parametric data set, but only allowed a few hot spots to be defined. It was difficult to establish a means of quantitatively assigning the hot spot or hot moment classification to the data set. Defining them in terms of percentiles limited the number of hot spots or hot moments to a few values due to the nature of percentiles. It also insured that hot moments or hot spots would be assigned because there would be a value within the 95^{th} percentile. Although this method had its flaws, I decided it was better than arbitrarily assigning the hot spot and hot moment classification.

Hot spot locations produced large concentrations of N_2O or CH_4, and missing these locations would have resulted in an underestimation of N_2O or CH_4 concentrations. It is difficult to sample hot spot locations without sampling a large area, which requires time, money, and land owner permission. Spatial variation is often more difficult to fit into denitrification models because of the lack of high resolution spatial approximations of denitrification (Groffman et al. 2009).

The large concentrations of N_2O and CH_4 that accumulate in groundwater do not necessarily flux to the atmosphere. CREP 3 is an example of a hot spot location with large concentrations of dissolved N_2O (Fig. 2.17). This N_2O can undergo three fates 1) further reduction to N_2 in groundwater, 2) transport into the vadose zone where it can either move across the soil surface or be reduced to N_2, or 3) be carried with the groundwater as N_2O to a surface water body where it can either diffuse from the water surface or be further reduced to N_2 in the stream sediments. N_2O that reaches the atmosphere through streams or surface water bodies is considered an indirect N_2O emission because the flux occurs far from the source. The hot spot locations may not contribute large concentrations of N_2O through the soil to the atmosphere, but large indirect N_2O emissions are possible. Bowden and Bormann (1986) measured the concentration of N_2O dissolved in water emerging from seeps, and they indicated that the dissolved N_2O emerging in the seep was both temporally and spatially removed from the actual production of the N_2O. Determining whether large fluxes of N_2O and CH_4 are released at surface water locations receiving hot spot groundwater concentrations would fill in a portion of the watershed N_2O and CH_4 budget.

Temporal variability existed within individual piezometers, and this variability is evident from data plotted as a time series (Fig. 2.13). There was no significant difference between the concentrations of N_2O-N dissolved in groundwater between the seasons, but CH_4 concentrations were significantly higher in the summer than the winter or spring. Fall CH_4 concentrations were variable and not significantly different compared to any other season. The dissolved concentrations of N_2O and CH_4 were higher across all sites when the water table was falling in June, July, August, and September than it was in the other months. In the months when the water table was falling, the temperatures were considerably warmer resulting in increased microbial respiration. In the remaining months of the year when the water table was rising, dilution of the groundwater by infiltrating water occurs and groundwater temperatures were lower. The infiltrating water was also potentially introducing oxygen into previously hypoxic water, halting or slowing the production of N_2O through denitrification and CH_4 through methanogenesis.

Hot moments produced large concentrations of N_2O and CH_4 in a short period of time. Hot moment fluxes of N_2O have been reported after rainfall (e.g., Dobbie and Smith 2003), fertilizer application (e.g., Dobbie & Smith, 2003, Meng et al 2005), or freeze-thaw events (e.g., Goodroad et al. 1984, Papen & Butterbach-Bahl 1999, Teppe et al. 2001, Koponen et al. 2004). As hot moments only last for short periods of time, they are difficult to sample without spending significant time and resources on a frequent sampling strategy. Catching these hot moments is extremely important in order to accurately estimate the total N_2O or CH_4 concentration that accumulated at each piezometer. Although I did capture what I defined to be hot moments, I am unable to determine if I sampled the exact peak in concentration. I could have sampled prior to or

after the actual highest concentrations. Although some hot moments lasted for a few months (e.g., Fig. 2.9), I could have also completely missed the peak concentrations because other peaks only lasted for a month (Fig. 2.6). I captured significant variation in N_2O and CH_4 concentrations with a one month sampling strategy and more frequent sampling may not have produced that much more information for the amount of time required to acquire and process the samples.

I have shown that large spatial and temporal variations exist within a site and among sites. In groundwater sampling, a decision has to be made whether to sample over a large spatial distance and resolve the larger scale spatial variability, or sample more frequently over a smaller spatial distance and resolve greater temporal variability. My monthly sampling strategy seemed adequate to capture most temporal changes in CH_4 and N_2O over a yearly time span. Spatially, the area over which I was sampling was large, but only one transect of piezometers was located at each site. This approach was useful to see the large variation in concentration at different locations over a large area and sampling period.

Conclusions

Groundwater flow paths are often complicated. The assumption that groundwater flowed along the topographic gradient from a high elevation to a low elevation was often an invalid assumption (or was not studied). The Choptank basin located on the Delmarva Peninsula is barely above sea level (<30 m asl), and there is very minor topography, potentially creating these unusual flow paths. For further groundwater studies, a greater attempt to understand the local hydrology should be undertaken prior to piezometer installation.

CH_4 ebullition presents a problem when trying to estimate denitrification because it strips the dissolved concentrations of both N_2 and Ar. The CH_4 bubbles also transfer large concentrations of CH_4 from the groundwater to the vadose zone, and this process is most likely to occur in summer months.

At Brfarm, the dissolved concentration of NO_3^- was reduced significantly after passing through a wet spot within a prior converted cropland (from 1mM to 16 µM). However, only moderate levels of CH_4 (2.1 µM) and N_2O (0.6 µM N_2O-N) were present in this piezometer transect. Excess N_2, produced through denitrification, was measured in most of the agriculturally affected piezometers, indicating that denitrification is a commonly occurring process in soils. Relationships were determined between the gases, and the highest N_2O concentrations observed were likely produced by denitrification. The lower concentrations could have been produced by both denitrification (low NO_3^-, low O_2) and nitrification (high NO_3^-, high O_2). When the piezometers were broken into land use categories, the median N_2O and CH_4 concentrations varied considerably within the categories; however, forests and forested wetlands had the lowest median N_2O due to

lack of N sources and the highest median CH_4. In contrast crop fields had very low N_2O and CH_4, whereas groundwater in anthropogenically disturbed landscape features had highly variable and intermediate CH_4 and the highest N_2O.

Temporal and spatial variability was observed within and between all of the locations. Hot moment peaks in concentration were observed in the time series data sets, and accounted for on average 39 and 49% of the total N_2O and CH_4 produced per piezometer but only occurred for ~ 10% of the time. Hot spot locations accumulated large concentrations of N_2O or CH_4, but not both. Three N_2O and four CH_4 hot spots were located in the 64 piezometer data set.

References

Abbasi, M.K., W.A. Adams. 2000. Estimation of simultaneous nitrification and denitrification in grassland soil associated with urea-N using ^{15}N and nitrification inhibitor. Biology and Fertility of Soils. 31:38-44.

Adrian, N.R., J.A. Robinson, J.M. Suflita. 1994. Spatial variability in biodegradation rates as evidenced by methane production from an aquifer. Applied and Environmental Microbiology. 60(10):3632-3639.

Bateman, E.J., E.M. Baggs. 2005. Contribution of nitrification and denitrification to N_2O emissions from soils at different water-filled pore space. Biology and Fertility of Soils. 41:379-388. DOI: 10.1007/s00374-005-0858-3.

Bell, W.H., Favero P. 2000. Moving water. A report to the Chesapeake Bay Cabinet by the Public Drainage Task Force. Contribution No. 2000-1. Center for the Environment and Society, Washington College. http://www.dnr.state.md.us/Bay/tribstrat/public_drainage_report.pdf.

Benitez, J.A., T.R. Fisher. 2004. Historical land-cover conversion (1665-1820) in the Choptank watershed, Eastern United States. Ecosystems. 7:219-232.

Blackmer, A.M., J.M. Bremner, 1978. Inhibitory effect of nitrate on reduction of N_2O to N_2 by soil microorganisms. Soil Biology and Biogeochemistry. 10(3)187-191.

Blicher-Mathiesen, G., G.W. McCarty, L.P. Nielsen. 1998. Denitrification and degassing in groundwater estimated from dissolved dinitrogen and argon. Journal of Hydrology. 208:16-24.

Bohlke, J.K., J.M. Denver. 1995. Combined use of groundwater dating, chemical, and isotopic analyses to resolve the history and fate of nitrate contamination in two agricultural watersheds, Atlantic coastal plain, Maryland. Water Resources Research. 31(9):2319-2339.

Bowden, W.B., F.H. Bormann. 1986. Transport and loss of nitrous oxide in soil water after forest clear-cutting. Science. 233:867-869.

Bremner, J.M., A.M. Blackmer. 1978. Nitrous oxide: Emission from soils during nitrification of fertilizer nitrogen. Science. 199:295-296.

Breuer, L., H. Papen, K. Butterbach-Bahl. 2000. N_2O emission from tropical forest soils of Australia. Journal of Geophysical Research. 105(D21):26,353-26,357.

Cai, Y., D. Weixin, X. Zhang, H. Yu, L. Wang. 2010. Contribution of heterotrophic nitrification to nitrous oxide production in a long-term N-fertilized arable black soil. Communications in Soil Science and Plant Analysis. 41:2264-2278, DOI: 10.1080/00103624.2010.507833.

Colt, J. 1984. Computation of dissolved gas concentrations in water as functions of temperature, salinity, and pressure. Bethesda, MD: American Fisheries Society.

Crutzen, P.J., 1981. Atmospheric chemical processes of the oxides of nitrogen, including N_2O. In Delwiche, C.C. (ed.). Denitrification, Nitrification, and Atmospheric Nitrous Oxide. Wiley, New York, pp.17-44.

Denver, J.M., S.W. Ator. 2011. Nitrogen fate and transport through upland depressional wetlands along an alternation gradient in an agricultural landscape, upper Choptank Watershed, Maryland. In Prep.

Dlugokencky, E.J., L. Bruhwiler, W.C. White, L.K. Emmons, P.C. Novelli, S.A. Montzka, K.A. Masarie, P.M. Lang, A.M. Crotwell, J.B. Miller, L.V. Gatti. 2009. Observational constraints on recent increases in the atmospheric CH_4 burden. Geophysical Research Letters. 36, L18803. DOI:10.1029/2009GL039780.

Dlugokencky, E.J., S. Houweling, L. Bruhwiler, K.A. Masarie, P.M. Lang, J.B. Miller, P.P. Tans. 2003. Atmospheric methane levels off: Temporary pause or a new steady-state? Geophysical Research Letters, 30 (19). doi:10.1029/2003GL018126,2003.

Dobbie, K.E., K.A. Smith. 2003. Nitrous oxide emission factors for agricultural soils in Great Britain: The impact of soil water-filled pore space and other controlling variables. Global Change Biology. 9:204-218.

Fetter, C.W. 2001. Applied Hydrogeology. Upper Saddle River, NJ: Prentice-Hall, Inc.

Fisher, T.R., J.A. Benitez, K. Lee, A.J. Sutton. 2006. History of land cover change and biogeochemical impacts in the Choptank River basin in the mid-Atlantic region of the US. International Journal of Remote Sensing. 27(17):3683-3703.

Fortuin, N.P.M., A. Willemsen. 2005. Exsolution of nitrogen and argon by methanogenesis in Dutch ground water. Journal of Hydrology. 301:1-13. DOI:10.1016/j.jhydrol.2004.06.018.

Fulweiler, R.W., S.W. Nixon, B.A. Buckley, S.L. Granger. 2007. Reversal of the net dinitrogen gas flux in coastal marine sediments. Nature. 448:180-182.

Goodroad, L.L., D.R. Keeney, L.A. Peterson. 1984. Nitrous oxide emissions from agricultural soils in Wisconsin. Journal of Environmental Quality. 13(4):557-561.

Goodroad, L.L., D.R. Keeney. 1985. Site of nitrous oxide production in field soils. Biological Fertility of Soils. 1:3-7.

Goreau, T.J., W.A. Kaplan, S.C. Wofsy, M.B. McElroy, F.W. Valois, S.W. Watson. 1980. Production of NO_2^- and N_2O by nitrifying bacteria at reduced concentrations of oxygen. Applied and Environmental Microbiology. 40(3):526-532.

Groffman, P.M., K. Butterbach-Bahl, R.W. Fulweiler, A.J. Gold, J.L. Morse, E.K. Stander, C. Tague, C. Tonitto, P. Vidon. 2009. Challenges to incorporating spatially and temporally explicit phenomena (hotspots and hot moments) in denitrification models. Biogeochemistry. 93:49-77. DOI 10.1007/s10533-008-9277-5.

Harms, T. K., and N. B. Grimm. 2008. Hot spots and hot moments of carbon and nitrogen dynamics in a semiarid riparian zone. Journal of Geophysical Research. 113:1-14. G01020. DOI:10.1029/2007JG000588.

IPCC (Intergovernmental Panel on Climate Change), 2007. Climate change 2007-The physical science basis. Contribution of working group I to the forth assessment report of the IPCC. Cambridge University Press, Cambridge.

Isermann, K., 1994. Agriculture's share in the emission of trace gases affecting the climate and some cause-oriented proposals for sufficiently reducing this share. Environmental Pollution. 83(1-2):95-111.

Jones, W.J. 1991. Diversity and physiology of methanogens. In Rogers J.E., W.B. Whitman (ed.). Microbial Production and consumption of greenhouse gases: Methane, nitrogen oxides, and halomethanes. American Society for Microbiology, pp.39-55.

Kana, T.M., C. Darkangelo, M.D. Hunt, J.B. Oldham, G.E. Bennett, J.C. Cornwell. 1994. Membrane inlet mass spectrometer for rapid high-precision determination of N_2, O_2 and Ar in environmental water samples. Analytical Chemistry. 66(23):4166-4170.

Knowles, R. 1982. Denitrification. Microbiological Reviews. 46(1):43-70.

Koponen, H.T., L.Flöjt, P.J. Martikainen. 2004. Nitrous oxide emissions from agricultural soils at low temperatures: A laboratory microcosm study. Soil Biology and Biochemistry. 36:757-766.

Lange, N.A., 1961. Handbook of Chemistry and Physics. New York, NY: McGraw-Hill Book Company, Inc.

Le Mer, J., P. Roger. 2001. Production, oxidation, emission and consumption of methane by soils: A review. European Journal of Soil Biology. 37:25-50.

Lee, K., T.R. Fisher, E. Rochelle-Newall. 2001. Modeling the hydrochemistry of the Choptank River basin using GWLF and Arc/Info: 2. Model validation and application. Biogeochemistry. 56:311-348.

Lowrance, R.R., R.L. Todd, L.E. Asmussen. 1984 a. Nutrient cycling in an agricultural watershed: I. Phreatic movement. Journal of Environmental Quality. 13(1):22-27.

Lowrance, R.R., Todd, J. Fail, O. Hendrickson Jr., R. Leonard, L. Asmussen. 1984 b. Riparian forests as nutrient filters in agricultural watersheds. BioScience. 34(6):374-377.

Lowrance, R.R, L.S. Altier, J.D. Newbold, R.R. Schnabel, P.M. Groffman, J.M. Denver, D.L. Correll, J.W. Gilliam, J.L. Robinson, R.B. Brinsfield, K.W. Staver, W. Lucas, A.H. Todd. 1997. Water quality functions of riparian forest buffers in Chesapeake Bay watersheds. Environmental Management. 21(5):687-712.

Martikainen, P.J., W.De Boer. 1993. Nitrous oxide production and nitrification in acidic soil from a Dutch coniferous forest. Soil Biology and Biogeochemistry. 25(3):343-347.

Mathieu, O., J. Lévêque, C. Hénault, M.-J. Milloux, F. Bizouard, F. Andreux. 2006. Emissions and spatial variability of N_2O, N_2 and nitrous oxide mole fraction at the field scale, revealed with ^{15}N isotopic techniques. Soil Biology and Biogeochemistry. 38(5):941-951.

McClain, M.E., E.W. Boyer, C.L. Dent, S.E. Gergel, N.B. Grimm, P.M. Groffman, S.C. Hart, J.W. Harvey, C.A. Johnston, E. Mayorga, W.H. McDowell, G. Pinay. 2003. Biogeochemical hot spots and hot moments at the interface of terrestrial and aquatic ecosystems. Ecosystems. 6:301-312.

Megonigal, J.P., M.E. Hines, P.T. Visscher. 2005. Anaerobic metabolism: Linkages to trace gases and aerobic processes. In Schlesinger W.H. (ed). Biogeochemistry. Elsevier, pp 317-424.

Meng, L., W. Ding, Z. Cai. 2005. Long-term application of organic manure and nitrogen fertilizer on N_2O emissions, soil quality and crop production in a sandy loam soil. Soil Biology & Biochemistry. 37:2037-2045.

Mookherji, S., G.W. McCarty, J.T. Angier. 2003. Dissolved gas analysis for assessing the fate of nitrate in wetlands. Journal of the American Water Resources Association. 39(2):381-387.

Mosier, A.R., J.M. Duxbury, J.R. Freney, O.Heinemeyer, K. Minami, D.E. Johnson. 1998. Mitigating agricultural emissions of methane. Climate Change. 40(1):30-80.

Otte, S., N.G. Grobben, L.A. Robertson, M.S.M Jetten, J.G. Kuenen. 1996. Nitrous oxide production by *Alcaligenes faecalis* under transient and dynamic aerobic and anaerobic conditions. Applied and Environmental Microbiology. 62(7):2421-2426.

Owens, J.P., and C.S. Denny. 1979. Upper Cenozoic deposits of the central Delmarva Peninsula, Maryland and Delaware. US Geological Survey Professional Paper 1067-A.

Papen, H., K. Butterbach-Bahl. 1999. A 3-year continuous record of nitrogen trace gas fluxes from untreated and limed soil of a N-saturated spruce and beech forest ecosystem in Germany, 1 N_2O emissions. Journal of Geophysical Research. 104(D15):18,487-18,503.

Parkin, T.B. 1987. Soil microsites as a source of denitrification variability. Soil Science Society of America Journal. 51(5):1194-1199.

Poth, M., D.D. Focht. 1985. ^{15}N kinetic analysis of N_2O production by *Nitrosomonas europaea* and examination of nitrifier denitrification. 1985. Applied and Environmental Microbiology. 49(5):1134-1141.

Quinn, G.P., M.J. Keough. 2002. Experimental design and data analysis for biologists. Cambridge University Press. Cambridge, U.K.

Rigby, M., R.G. Prinn, P.J. Frazer, P.G. Simmonds, R.L. Langenfeld, J. Huang, D.M. Cunnold, L.P. Steele, P.B. Krummel, R.F. Weiss, S. O'Doherty, P.K. Salameh, H.J. Wang, C.M. Harth, J. Mühle, L.W. Porter. 2008. Renewed growth of atmospheric methane. Geophysical Research Letters. 35, L22805. DOI:10.1029/2008GL036037.

Ruser, R., H. Flessa, R. Russow, G. Schmidt, F. Buegger, J.C. Munch. 2006. Emissions of N_2O, N_2 and CO_2 from soil fertilized with nitrate: Effect of compaction, soil moisture and rewetting. Soil Biology and Biochemistry. 38:263-274.

Shao, M, T. Zhang, H.H. Fang. 2010. Sulfur-driven autotrophic denitrification: Diversity, biochemistry, and engineering applications. Applied Microbiology and Biotechnology. 88:1027-1042, DOI:10.1007/s00253-010-2847-1.

Soil Survey Staff, Natural Resources Conservation Service, United States Department of Agriculture. Web Soil Survey. Available online at http://websoilsurvey.nrcs.usda.gov/ accessed [07/01/2011].

Teepe, R., R. Brumme, F. Beese. 2001. Nitrous oxide emissions from soil during freezing and thawing periods. Soil Biology and Biochemistry. 33:1269-1275.

Ueda, S., N. Ogura, T. Yoshinari. 1993. Accumulation of nitrous oxide in aerobic groundwaters. Water Research. 27(12):1787-1792.

Weiss, R.F. 1970. The solubility of nitrogen, oxygen and argon in water and seawater. Deep Sea Research and Oceanographic Abstracts. 17(4):721-735.

Weiss, R.F., B.A. Price. 1980. Nitrous oxide solubility in water and seawater. Marine Chemistry. 8:347-359.

Wrage, N., G.L. Velthof, M.L. van Beusichem, O. Oenema. 2001. Role of nitrifier denitrification in the production of nitrous oxide. Soil Biology and Biochemistry. 33(12-13):1723-1732.

Yao, Z., B. Wolf, W. Chen, K. Butterbach-Bahl, N. Brüggemann, M. Wiesmeier, M. Dannenmann, B. Blank, X. Zheng. 2010. Spatial variability of N_2O, CH_4 and CO_2 fluxes within the Xilin River catchment of Inner Mongolia, China: A soil core study. Plant and Soil. 331:341-359. DOI 10.1007/s11104-009-0257-x.

Table 2.1 – Land use and the physical properties of the soils surrounding the piezometers. Nested piezometers are identified with a letter after the number (e.g; AB1 and AB1a are at different depths, 3.2 and 0.9 m, at the same location). The hydraulic conductivity and porosity (Φ) were measured at select piezometers and selected depths via TDR. The soil data was acquired through the Soil Survey Staff, Natural Resources Conservation Service, United States Department of Agriculture (2011).

location	Landuse	Piezo-meter ID	distance from edge, m	depth, m mid-screen	Sampling period	Hydraulic conductivity k, cm day-1	Φ m^3/m^3	Φ measured at depth	Soil
AB	wetland	AB1	40.56	3.19	2008	215 ±72			Hammonton-Fallsington-Corsica complex
natural	wetland (shallow)	AB1a	40.56	0.91	2008				Hammonton-Fallsington-Corsica complex
wetland	wetland edge	AB2	35.21	2.26	2008	506 ±53	35.4 ± 1.5	100 cm	Hammonton-Fallsington-Corsica complex
	upland (deep)	AB3	25.82	1.97	2008				Hammonton-Fallsington-Corsica complex
BC	upland (deep)	BC4	39.05	2.20	2009				Ingleside Sandy Loam
natural	upland (shallow)	BC4a	39.05	1.21	2009				Ingleside Sandy Loam
wetland	lower upland (deep)	BC3	48.60	1.95	2009				Hammonton-Fallsington-Corsica complex
	lower upland (shallow)	BC3a	48.60	1.35	2009				Hammonton-Fallsington-Corsica complex
	upper wetland (deep)	BC2	57.52	1.55	2008				Hammonton-Fallsington-Corsica complex
	upper wetland (mid)	BC2a	57.52	1.08	2008				Hammonton-Fallsington-Corsica complex
	upper wetland (shallow)	BC2b	57.52	0.64	2008				Hammonton-Fallsington-Corsica complex
	wetland (deep)	BC1	67.20	1.47	2008	0.65 ± 0.03			Hammonton-Fallsington-Corsica complex
BNDS	field edge	BNDS1	5.25	2.47	2009	75.6 ± 2.4	31.3 ± 1.2	200 cm	Hambrook Sandy Loam
restored	agricultural grass buffer	BNDS2	22.72	2.45	2008	24.3 ± 0.6	38.4 ± 0.0	200 cm	Corsica Mucky Loam
wetland	wetland/pond	BNDS3	38.80	2.26	2009				Corsica Mucky Loam
	wetland/pond	BNDS3a	38.80	0.60	2009				Corsica Mucky Loam
	forest grass buffer, wetlands	BNDS4	83.14	2.27	2008				Corsica Mucky Loam
BRFarm	forested stream bank, wetlands	BR2	-1.62	3.55	2008				Woodston Sandy Loam
natural forest	forested stream bed, wetlands	BR1	0.92	2.75	2008	2303 ± 28			Woodston Sandy Loam
next to	forested stream bed (shallow), wetlands	BR1a	0.92	0.79	2008				Woodston Sandy Loam
agricultural	forest edge, wetlands	BR3	9.04	2.02	2009				Woodston Sandy Loam
field	ditch bordering agricultural field and forested wetland	BR4	5.86	0.58	2009				Woodston Sandy Loam
	field edge	BR5	2.86	1.87	2009				Woodston Sandy Loam
	field ridge	BFF1	84.24	1.60	2009	81.1 ± 2.6	36.7 ± 0.4	175 cm	Ingleside Sandy Loam
	field wetland/wetspot	BFF2	14.67	2.26	2008	46.2 ± 2.1	32.0 ± 0.2	120 cm	Hammonton-Fallsington-Corsica complex
	field wetland edge near ditch	BFF3	-4.50	1.08	2008				Hammonton-Fallsington-Corsica complex
Cfarm	upland edge of flooded ditch	CFD1 **	0.00	1.60	2007-2009	0.24 ± 0.01			Hurlock Sandy Loam
agricultural	waters edge of flooded ditch	CFD2 **	1.85	0.82	2007-2009	3.95 ± 0.9			Hurlock Sandy Loam
field	upland edge of non flooded ditch	CFC1 *	0.00	2.84	2007-2009	1.42 ± 0.2			Ingleside Sandy Loam
	waters edge of non flooded ditch	CFC2 *	2.00	1.15	2007-2009	12.9 ± 0.9			Ingleside Sandy Loam
	upland edge of ditch	CFD3	0.00	1.45	2007				Hammonton Sandy Loam
	waters edge of ditch	CFD4	2.00	1.15	2007				Hammonton Sandy Loam
	field ridge	CFF1	-88.65	2.78	2009				Ingleside Sandy Loam
	mid-field	CFF2	-36.65	1.82	2009				Ingleside Sandy Loam
	field ridge	CFF3	-105.20	3.18	2008-2009				Ingleside Sandy Loam
	mid-field/wetspot	CFF4	-56.70	1.94	2008-2009				Hurlock Sandy Loam
	upland edge of flooded ditch	CFCD1 **	0.00	3.80	2007				Ingleside Sandy Loam
	waters edge of flooded ditch	CFCD2 **	2.00	2.28	2007				Ingleside Sandy Loam
	upland edge of non flooded ditch	CFCC1 *	0.00	2.27	2007				Ingleside Sandy Loam
	waters edge of non flooded ditch	CFCC2 *	2.00	1.44	2007				Ingleside Sandy Loam
EFAG	field edge	EFAG1	0.90	2.69	2008-2009				Ingleside Sandy Loam
restored	agricultural grass buffer	EFAG2	28.80	2.61	2008-2009	34.6 ± 1.2	34.5 ± 1.3	150 cm	Hurlock Sandy Loam
wetland	wetland	EFWET	54.20	4.59	2008-2009				Hurlock Sandy Loam
	wetland (shallow)	EFWET1a	54.20	0.63	2008-2009	23.8 ± 1.4			Hurlock Sandy Loam
	forest grass buffer	EFFOR2	89.45	2.49	2008-2009				Hurlock Sandy Loam
	forest edge	EFFOR1	124.65	3.40	2008				Ingleside Sandy Loam
Hfarm	field edge of flooded ditch	HFD1	4.00	1.19	2007-2009	8.1 ± 0.3			Lenni Silt Loam
Agricultural	flooded ditch edge	HFD2	5.74	0.85	2007-2009				Lenni Silt Loam
field	topographic low in field/wetspot	HFF1	-60.31	0.81	2007-2009	21.6 ± 6.5			Lenni Silt Loam
	topographic ridge in field	HFF2	n/a	3.17	2008				Woodston Sandy Loam
	low (old stream bed) in field/wetspot	HFF3	n/a	1.69	2008				Lenni Silt Loam
	field edge/wetspot	HFF4	n/a	1.77	2008				Lenni Silt Loam
JLAG	field edge	JLAG1	3.05	2.54	2008-2009	29.1 ± 0.4	34.5 ± 0.6	175 cm	Hammonton-Fallsington-Corsica complex
restored	agricultural grass buffer	JLAG2	16.45	2.31	2008-2009	137 ± 6.3	46.8 ± 4.4	150 cm	Hammonton-Fallsington-Corsica complex
wetland	wetland	JLAG3	30.95	2.75	2008-2009				Hammonton-Fallsington-Corsica complex
	wetland (shallow)	JLAG3a	30.95	0.54	2008-2009				Hammonton-Fallsington-Corsica complex
	wetland-ditch buffer	JLAG4	105.90	1.33	2008-2009				Hammonton-Fallsington-Corsica complex
	ditch	JLAG5	120.60	0.97	2008-2009				Hammonton-Fallsington-Corsica complex
Mfarm	Field edge/riparian edge	Mfield	7.02	3.22	2007				Ingleside Sandy Loam
forest	riparian area	Mmid	34.20	1.51	2007	3.1 ± 0.2	26.0 ± 0.2	100 cm	Ingleside Sandy Loam
riparian area	riparian edge/stream edge	Mstream	52.87	1.51	2007	3370.00			Ingleside Sandy Loam
Rfarm	Field edge/riparian edge	CREP-1	1.96	2.32	2007	30.5 ± 1.2	33.9 ± 2.6	150 cm	Keyport Silt Loam
grass/shrub	riparian area	CREP-3	11.69	2.10	2007	70.9 ± 8.8	27.90	100 cm	Keyport Silt Loam
riparian area	riparian area closest to tidal estuary	CREP-4	21.72	2.07	2007				Keyport Silt Loam

**Piezometer situated above a drainage control structure on a flooded ditch

*Piezometer situated below a drainage control structure on a free flowing ditch

Table 2.2 – The N_2O and CH_4 chemical properties of the piezometers. The median concentration of both N_2O and CH_4, the number of hot moments per piezometer, the percentage of the total N_2O or CH_4 concentration accounted for by the hot moments, and the percent of time that the hot moments were occurring are displayed. The bolded values are hot spot piezometers with high concentrations of CH_4 or N_2O.

location	Landuse	Piezo-meter ID	Median N_2O -N, µM	# N_2O samples	N_2O # hot moments	% of N_2O accounted for by hot moments	N_2O % of time accounted for by hot moments	Median CH_4, µM	# CH_4 samples	CH_4 # hot moments	% of CH_4 accounted for by hot moments	CH_4 % of time accounted for by hot moments
AB	wetland	AB1	Not sampled	n/a	n/a	n/a	n/a	0.95	12	1	16.0%	8.33%
natural	wetland (shallow)	AB1a	Not sampled	n/a	n/a	n/a	n/a	3.30	7	1	55.8%	14.29%
wetland	wetland edge	AB2	Not sampled	n/a	n/a	n/a	n/a	1.15	12	1	20.5%	8.33%
	upland (deep)	AB3	Not sampled	n/a	n/a	n/a	n/a	0.16	12	1	18.3%	8.33%
BC	upland (deep)	BC4	0.02	11	1	33.6%	9.09%	0.05	11	1	67.5%	9.09%
natural	upland (shallow)	BC4a	Not sampled	n/a	n/a	n/a	n/a	0.05	6	1	71.3%	16.67%
wetland	lower upland (deep)	BC3	Not sampled	n/a	n/a	n/a	n/a	11.66	12	1	78.1%	8.33%
	lower upland (shallow)	BC3a	Not sampled	n/a	n/a	n/a	n/a	0.39	9	1	32.5%	11.11%
	upper wetland (deep)	BC2	0.01	12	1	62.4%	8.33%	1.98	12	1	34.6%	8.33%
	upper wetland (mid)	BC2a	Not sampled	n/a	n/a	n/a	n/a	4.35	9	1	54.4%	11.11%
	upper wetland (shallow)	BC2b	Not sampled	n/a	n/a	n/a	n/a	2.18	8	1	61.9%	12.50%
	wetland (deep)	BC1	Not sampled	n/a	n/a	n/a	n/a	**21.43**	10	1	31.7%	10.00%
BNDS	field edge	BNDS1	0.12	12	1	30.7%	8.33%	0.04	11	1	44.3%	9.09%
restored	agricultural grass buffer	BNDS2	0.90	12	1	15.4%	8.33%	0.03	12	1	58.4%	8.33%
wetland	wetland/pond	BNDS3	0.14	12	1	30.9%	8.33%	1.02	12	1	25.7%	8.33%
	wetland/pond	BNDS3a	**6.21**	9	1	20.4%	11.11%	0.14	8	1	63.1%	12.50%
	forest grass buffer, wetlands	BNDS4	0.01	12	1	69.5%	8.33%	6.49	12	1	59.3%	8.33%
BRFarm	forested stream bank, wetlands	BR2	Not sampled	n/a	n/a	n/a	n/a	6.08	12	1	11.1%	8.33%
natural forest	forested stream bed, wetlands	BR1	Not sampled	n/a	n/a	n/a	n/a	6.43	12	1	11.5%	8.33%
next to	forested stream bed (shallow), wetlands	BR1a	Not sampled	n/a	n/a	n/a	n/a	0.23	8	1	29.2%	12.50%
agricultural	forest edge, wetlands	BR3	0.01	12	1	30.5%	8.33%	2.11	12	1	11.6%	8.33%
field	ditch bordering agricultural field and forested wetland	BR4	0.84	11	1	45.4%	9.09%	0.19	12	1	43.5%	8.33%
	field edge	BR5	0.04	12	1	29.7%	8.33%	0.04	12	1	22.3%	8.33%
	field ridge	BFF1	0.12	11	1	33.6%	9.09%	0.02	11	1	35.1%	9.09%
	field wetland/wetspot	BFF2	0.01	12	1	53.1%	8.33%	2.13	12	1	15.7%	8.33%
	field wetland edge near ditch	BFF3	0.58	8	1	33.1%	12.50%	0.07	8	1	24.9%	12.50%
Cfarm	upland edge of flooded ditch	CFD1 **	2.59	27	2	26.6%	7.41%	0.04	25	2	83.4%	8.00%
agricultural	waters edge of flooded ditch	CFD2 **	2.91	35	2	23.8%	5.71%	0.15	34	2	69.7%	5.88%
field	upland edge of non flooded ditch	CFC1 *	1.16	29	2	25.8%	6.90%	0.03	28	2	45.7%	7.14%
	waters edge of non flooded ditch	CFC2 *	1.42	30	2	22.4%	6.67%	0.05	29	2	67.9%	6.90%
	upland edge of ditch	CFD3	0.09	5	1	0.0%	20.00%	0.29	4	1	94.7%	25.00%
	waters edge of ditch	CFD4	0.09	10	1	32.1%	10.00%	3.50	10	1	84.2%	10.00%
	field ridge	CFF1	0.08	9	1	59.9%	11.11%	0.03	8	1	90.9%	12.50%
	mid-field	CFF2	0.65	8	2	67.7%	25.00%	0.01	9	1	66.4%	11.11%
	field ridge	CFF3	0.44	23	2	25.2%	8.70%	0.02	22	2	38.9%	9.09%
	mid-field/wetspot	CFF4	2.97	15	1	18.3%	6.67%	0.08	16	1	43.2%	6.25%
	upland edge of flooded ditch	CFCD1 **	1.46	12	1	27.9%	8.33%	0.06	10	1	35.5%	10.00%
	waters edge of flooded ditch	CFCD2 **	0.54	12	1	43.6%	8.33%	0.06	9	1	32.3%	11.11%
	upland edge of non flooded ditch	CFCC1 *	0.09	4	1	93.6%	25.00%	0.05	2	n/a	n/a	n/a
	waters edge of non flooded ditch	CFCC2 *	2.24	11	1	31.0%	9.09%	0.22	9	1	83.8%	11.11%
EFAG	field edge	EFAG1	1.09	24	2	16.7%	8.33%	0.01	24	2	25.3%	8.33%
restored	agricultural grass buffer	EFAG2	4.41	24	2	22.1%	8.33%	0.19	24	2	44.2%	8.33%
wetland	wetland	EFWET	aquiclude	2	n/a	n/a	n/a	aquiclude	2	n/a	n/a	n/a
	wetland (shallow)	EFWET1a	0.01	20	1	98.4%	5.00%	**310.55**	19	1	15.5%	5.26%
	forest grass buffer	EFFOR2	0.16	24	2	20.6%	8.33%	0.18	24	2	98.3%	8.33%
	forest edge	EFFOR1	0.02	12	1	35.3%	8.33%	0.13	12	1	19.7%	8.33%
Hfarm	field edge of flooded ditch	HFD1	0.51	36	2	44.8%	5.56%	0.07	32	2	74.6%	6.25%
Agricultural	flooded ditch edge	HFD2	0.34	35	2	51.9%	5.71%	1.16	32	2	44.5%	6.25%
field	topographic low in field/wetspot	HFF1	0.59	27	2	57.8%	7.41%	0.06	23	2	67.8%	8.70%
	topographic ridge in field	HFF2	0.01	6	1	0.0%	16.67%	0.06	5	1	65.4%	20.00%
	low (old stream bed) in field/wetspot	HFF3	0.08	12	1	31.1%	8.33%	0.49	11	1	48.3%	9.09%
	field edge/wetspot	HFF4	slowrecharge	2	n/a	n/a	n/a	slowrecharge	2	n/a	n/a	n/a
JLAG	field edge	JLAG1	0.05	23	2	44.8%	8.70%	0.04	22	2	54.6%	9.09%
restored	agricultural grass buffer	JLAG2	0.13	24	2	28.8%	8.33%	0.23	24	2	56.2%	8.33%
wetland	wetland	JLAG3	0.27	24	2	43.0%	8.33%	0.56	24	2	77.7%	8.33%
	wetland (shallow)	JLAG3a	0.01	18	1	77.4%	5.56%	**33.32**	18	1	30.5%	5.56%
	wetland-ditch buffer	JLAG4	0.01	23	2	48.4%	8.70%	**17.82**	23	2	27.6%	8.70%
	ditch	JLAG5	0.16	23	2	45.7%	8.70%	0.16	22	2	82.8%	9.09%
Mfarm	Field edge/riparian edge	Mfield	0.16	7	1	57.9%	14.29%	0.02	4	1	51.3%	25.00%
forest	riparian area	Mmid	0.90	12	1	13.8%	8.33%	0.03	10	1	34.8%	10.00%
riparian area	riparian edge/stream edge	Mstream	2.38	12	1	24.3%	8.33%	0.07	10	1	70.9%	10.00%
Rfarm	Field edge/riparian edge	CREP-1	**6.98**	7	1	36.1%	14.29%	0.13	4	1	54.3%	25.00%
grass/shrub	riparian area	CREP-3	**18.11**	8	1	25.7%	12.50%	0.15	5	1	31.7%	20.00%
riparian area	riparian area closest to tidal estuary	CREP-4	0.09	6	1	99.2%	16.67%	0.31	3	1	n/a	33.33%

**Piezometer situated above a drainage control structure on a flooded ditch
*Piezometer situated below a drainage control structure on a free flowing ditch

Table 2.3- Site specific Spearman Rank Correlation statistics for both N_2O and CH_4. Relationships that were not possible due to a lack of data are denoted with n/a and relationships that were not monotonic, and therefore not appropriate for Spearman Rank Correlation are designated as NM. Significant relationships are designated with bold text in a gray box. In this table excess N_2-N is shorted to N_2.

	NO_3 vs N_2	NO_3 vs N_2O	N_2 vs N_2O	$\%O_2$ vs N_2O	NH_4 vs N_2O	$\%O_2$ vs CH_4	NO_3 vs CH_4	N_2 vs CH_4
All data	**r_s=-0.267 p<0.001**	**NM**	**NM**	**NM**	r_s=0.00641 p=0.875	**r_s=-0.656 p<0.001**	**r_s=-0.608 p<0.001**	**NM**
Hfarm	**r_s=-0.335 p<0.001**	**NM**	**NM**	r_s=-0.0823 p=0.381	**r_s=-0.408 p<0.001**	**r_s=-0.522 p<0.001**	**r_s=-0.496 p<0.001**	r_s=0.124 p=0.206
Cfarm	**r_s=-0.581 p<0.001**	**NM**	**r_s=0.348 p<0.001**	**r_s=-0.387 p<0.001**	**r_s=0.267 p=0.00176**	**r_s=-0.550 p<0.001**	**r_s=-0.486 p<0.001**	**NM**
EFAG	**NM**	**NM**	**r_s=0.529 p<0.001**	r_s=-0.0685 p=0.523	r_s=0.169 p=0.114	**r_s=-0.773 p<0.001**	**r_s=-0.716 p<0.001**	r_s=-0.164 p=0.0944
BC	r_s=0.145 p=0.219	r_s=0.305 p=0.0702	**NM**	**NM**	r_s=-0.0614 p=0.721	**r_s=-0.732 p<0.001**	**r_s=-0.399 p<0.001**	**r_s=0.279 p=0.0143**
Brfarm	**NM**	**NM**	r_s=0.126 p=0.303	**NM**	r_s=-0.208 p=0.0885	**r_s=-0.723 p<0.001**	**r_s=-0.779 p<0.001**	**NM**
JLAG	r_s=-0.0613 p=0.486	**r_s=0.724 p<0.001**	**NM**	**r_s=0.199 p=0.0266**	r_s=0.0926 p=0.304	**r_s=-0.425 p<0.001**	**r_s=-0.215 p=0.0129**	**r_s=-0.457 p<0.001**
BNDS	**r_s=-0.630 p<0.001**	**NM**	r_s=-0.0917 p=0.508	r_s=0.267 p=0.0514	r_s=0.0563 p=0.685	**r_s=-0.534 p<0.001**	**r_s=-0.680 p<0.001**	**r_s=0.549 p<0.001**
AB	r_s=0.0102 p=0.647	n/a	n/a	n/a	n/a	**r_s=-0.563 p<0.001**	**NM**	**r_s=-0.364 p=0.0166**
Rfarm	r_s=0.414 p=0.0609	r_s=0.413 p=0.0618	r_s=0.354 p=0.113	r_s=-0.315 p=0.16	n/a	r_s=-0.203 p=0.513	r_s=-0.529 p=0.0705	r_s=-0.322 p=0.295
Mfarm	**r_s=-0.829 p<0.001**	**r_s=-0.661 p<0.001**	**r_s=0.615 p<0.001**	**r_s=-0.659 p<0.001**	n/a	**r_s=-0.437 p=0.0329**	**r_s=-0.547 p=0.00584**	**r_s=0.496 p=0.0140**

Table 2.4 – The hotspot piezometers for the data set. Hot spots were defined as a location where the median CH_4 or N_2O concentration of a piezometer was in the 95th percentile of all of the sampled piezometer median concentrations.

N_2O hot spot piezometer	**median >5.49 µM N_2O-N**	**CH_4 hot spot piezometer**	**median > 17.51 µM CH_4**
BNDS3a	6.21	BC1	21.43
CREP1	6.98	EFWET1a	310.55
CREP3	18.11	JLAG3a	33.32
		JLAG4	17.82

Figure 2.1- The Choptank watershed is located in the Mid-Atlantic region within the Chesapeake Bay watershed. All of the sampling locations are in the upper Choptank watershed except RFarm, which is located in the Little Choptank watershed closer to the mouth of the Choptank River.

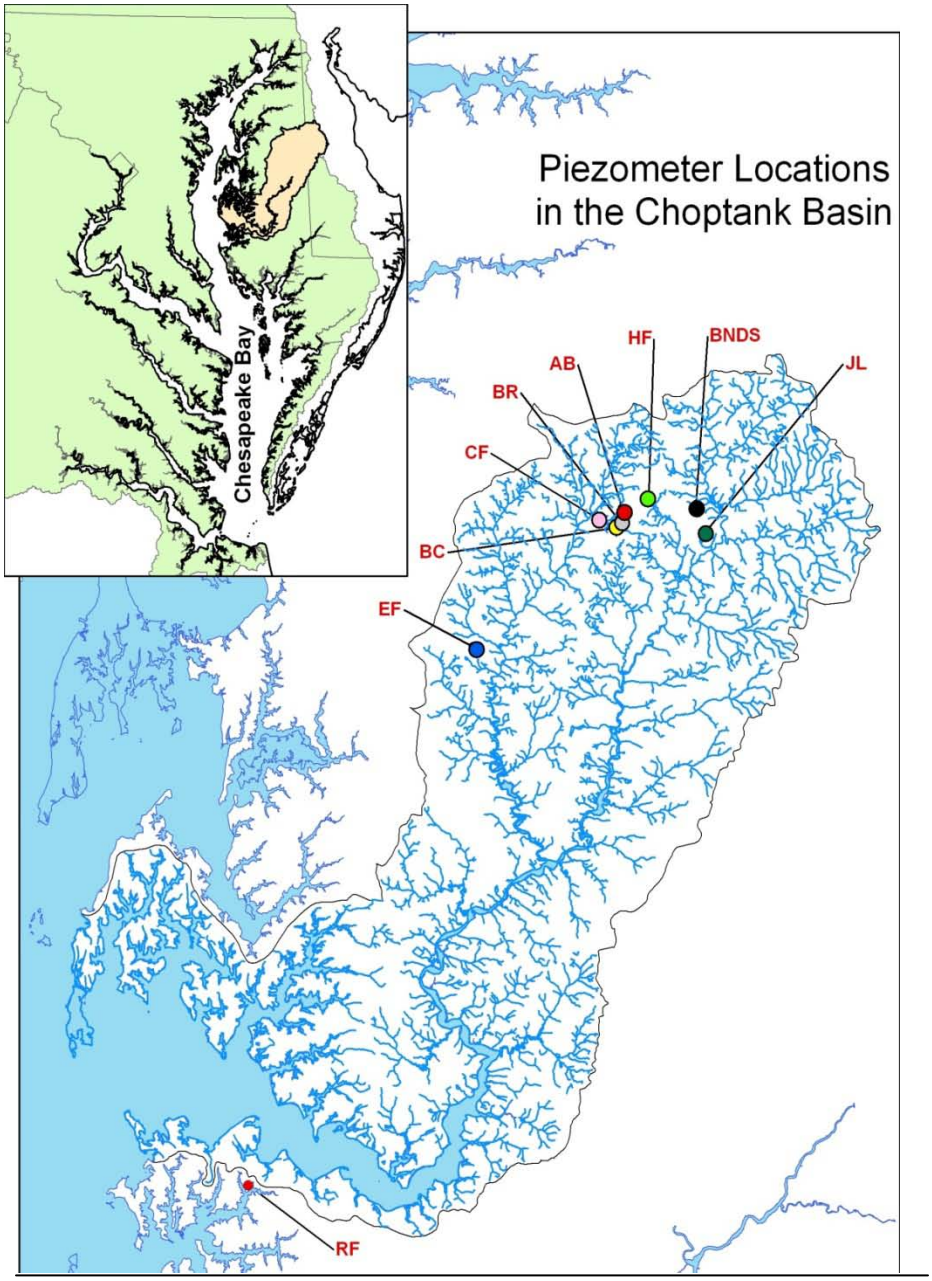

Figure 2.2- The distribution of the N_2O and CH_4 data sets before log transformation (**A,B**) and after log transformation (**C,D**).

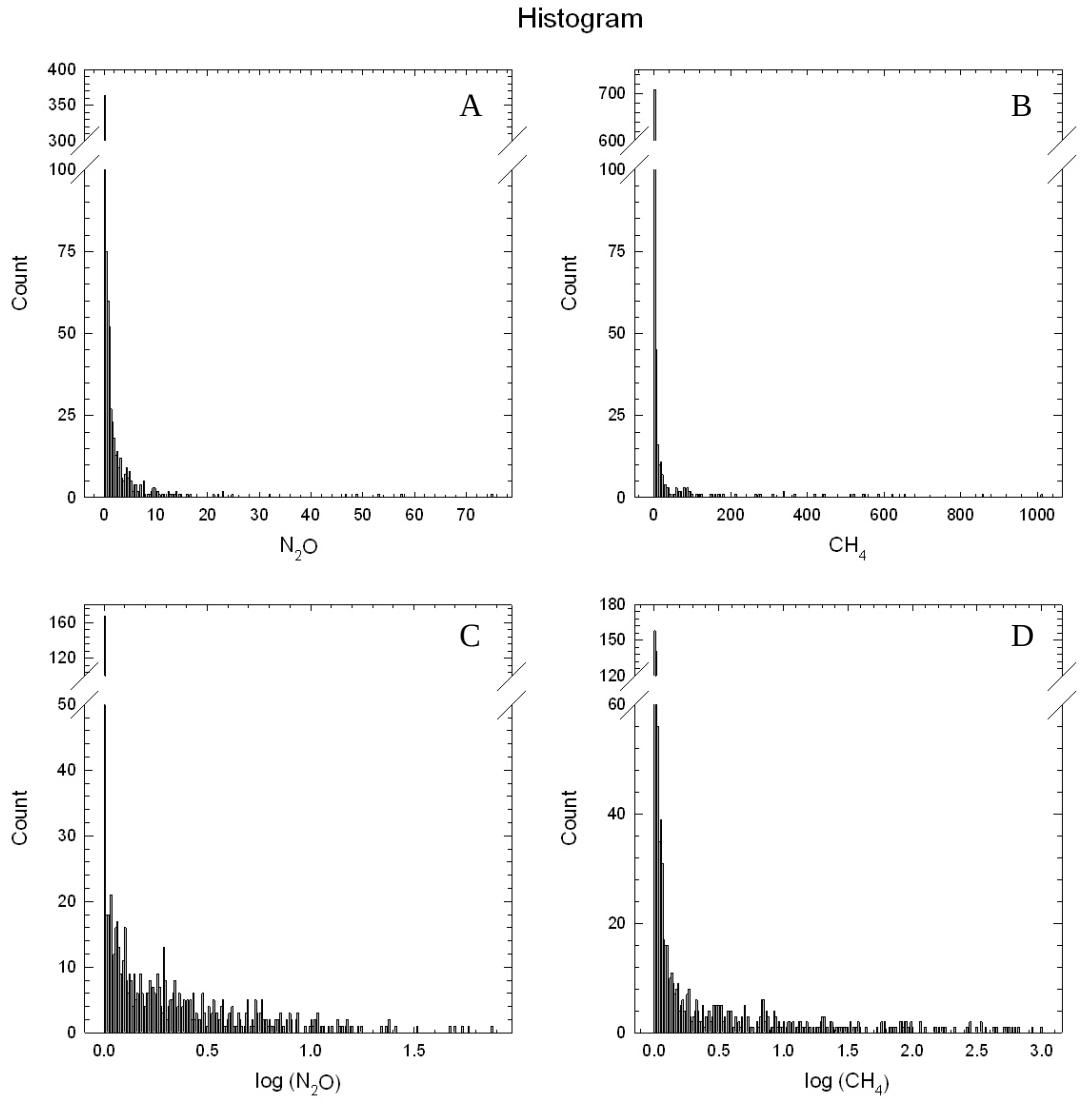

Figure 2.3 – The groundwater flow paths for the sites **A**) BrFarm, **B**) JLAG, **C**) EFAG, and **D**) BNDS. Streamtubes are illustrated from the point of infiltration and in the direction for which the groundwater predominantly flows. The minimum, median, and maximum values for depths of the water tables for each individual piezometer are displayed as a black dotted, straight, and white dotted lines, respectively.

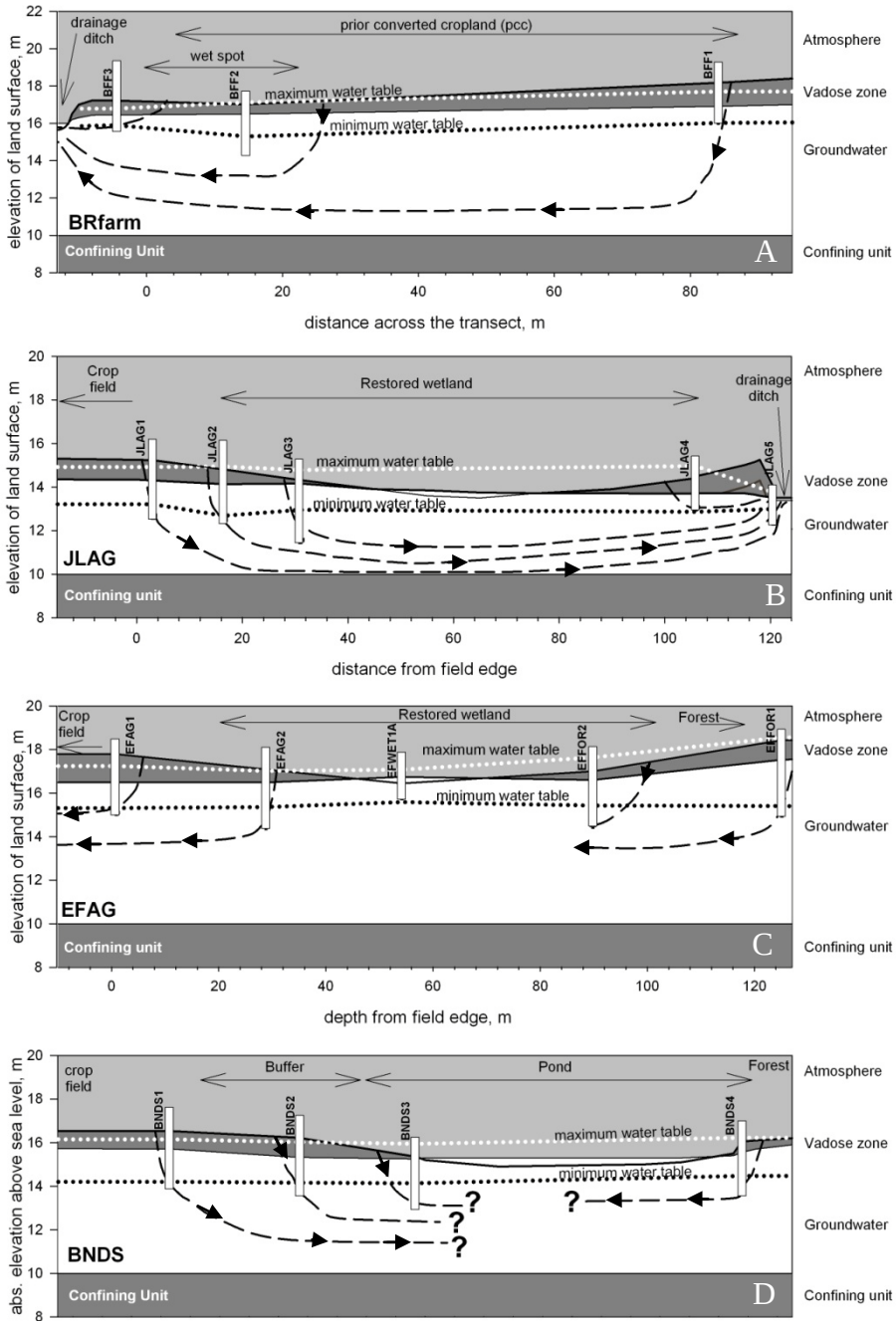

Figure 2.4 – An example of a CH_4 hotspot where large concentrations of CH_4 accumulated causing CH_4 ebullition and stripping of other gases. Removal of Ar and N_2 leads to the calculation of high Ar recharge temperature values and negative excess N_2 values.

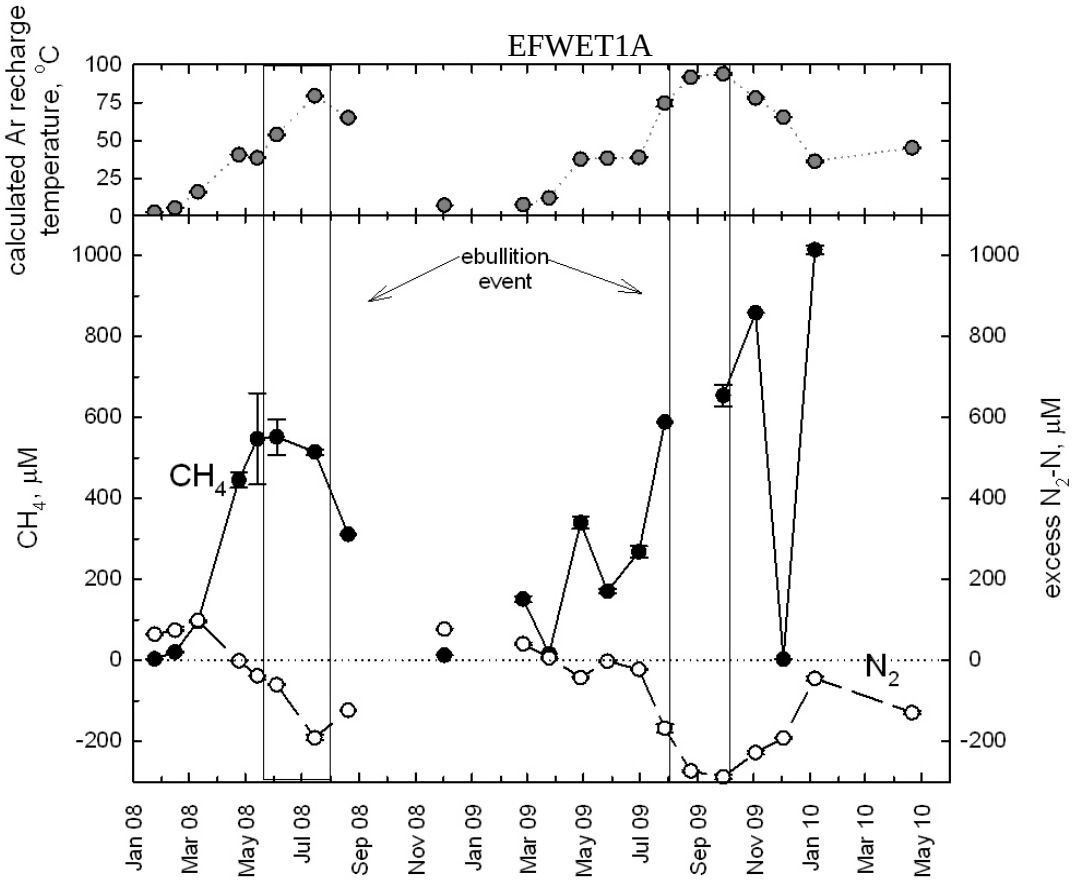

Figure 2.5 – The seasonal distribution of the evidence for CH_4 ebullition events, documented as unusually high Ar recharge temperatures (>22^{o}C), and/or negative excess N_2-N concentrations, in conjuncture with CH_4 concentrations >20 µM.

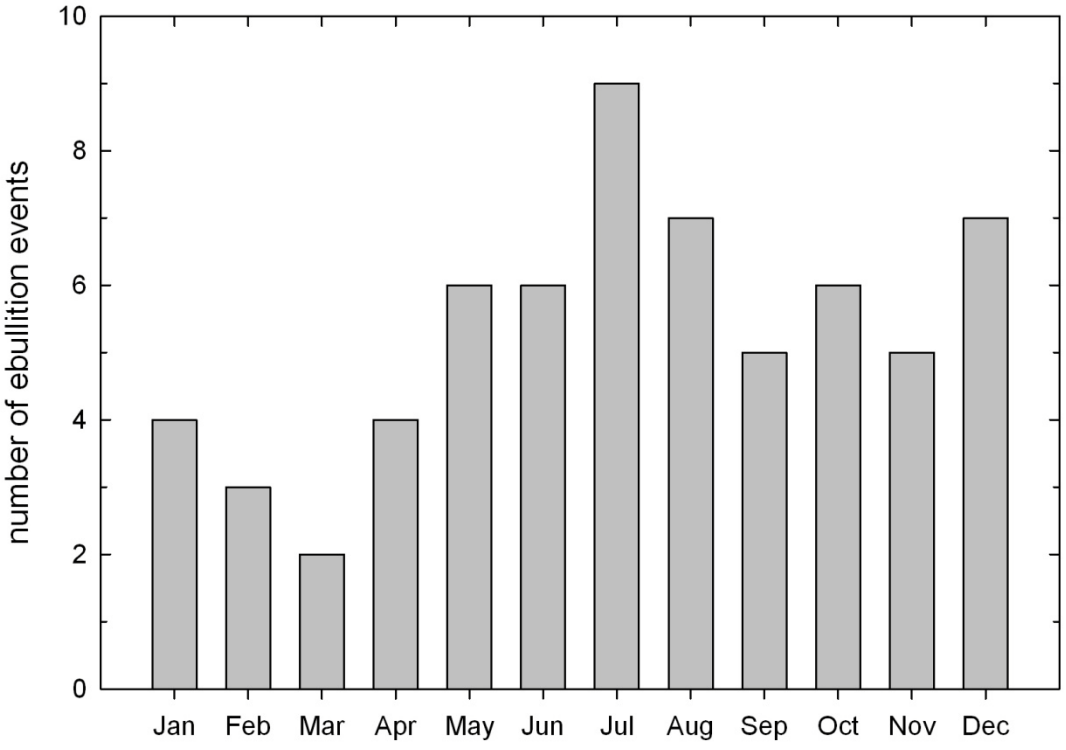

Figure 2.6 – The median concentrations of NO_3 and excess N_2-N (left panel) and $\%O_2$ saturation (right panel) for each individual piezometer for 2008

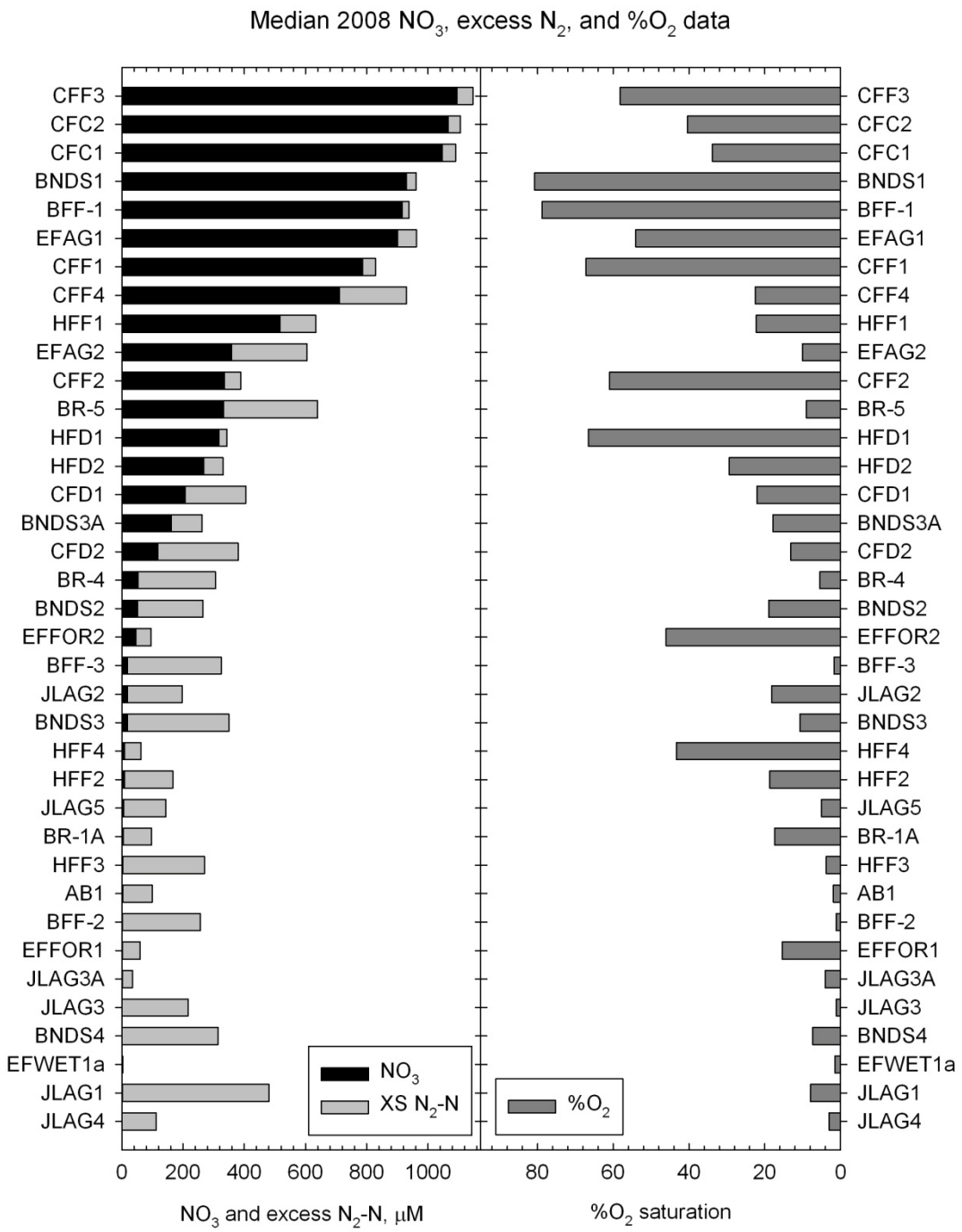

Figure 2.7 – Relationships over the entire data set between **A**) $\%O_2$ and N_2O, **B**) $\%O_2$ saturation and CH_4, **C**) NO_3^- and N_2O, **D**) NO_3^- and CH_4, **E**) excess N_2 and N_2O, **F**) excess N_2 and CH_4, **G**) NO_3^- and excess N_2, and **F**) N_2O and CH_4.

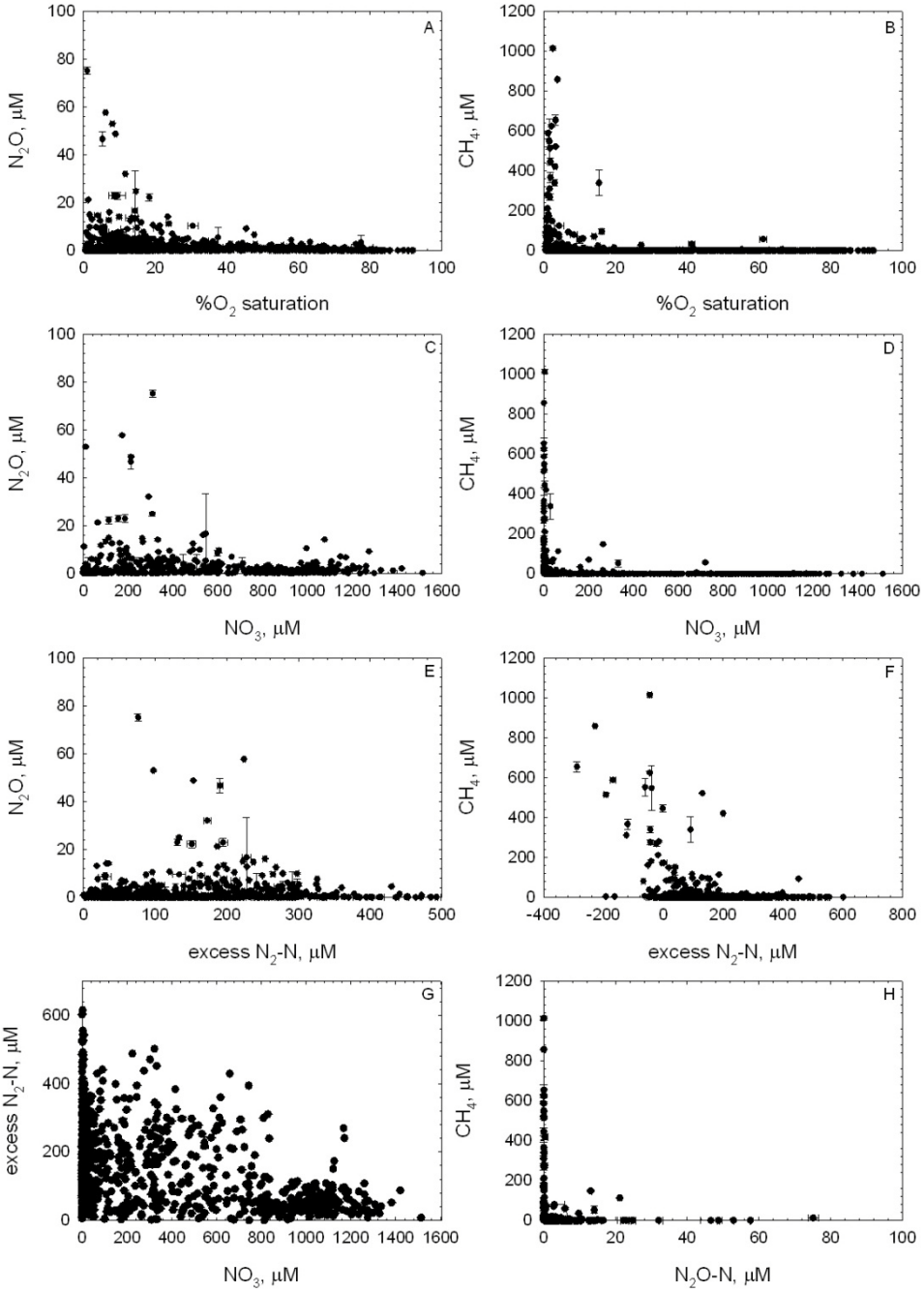

Figure 2.8 – A site specific example of significant relationships between **A**) NO_3^- and N_2O and **B**) excess N_2 and N_2O. The Spearman Rank correlation statistics are displayed in each figure.

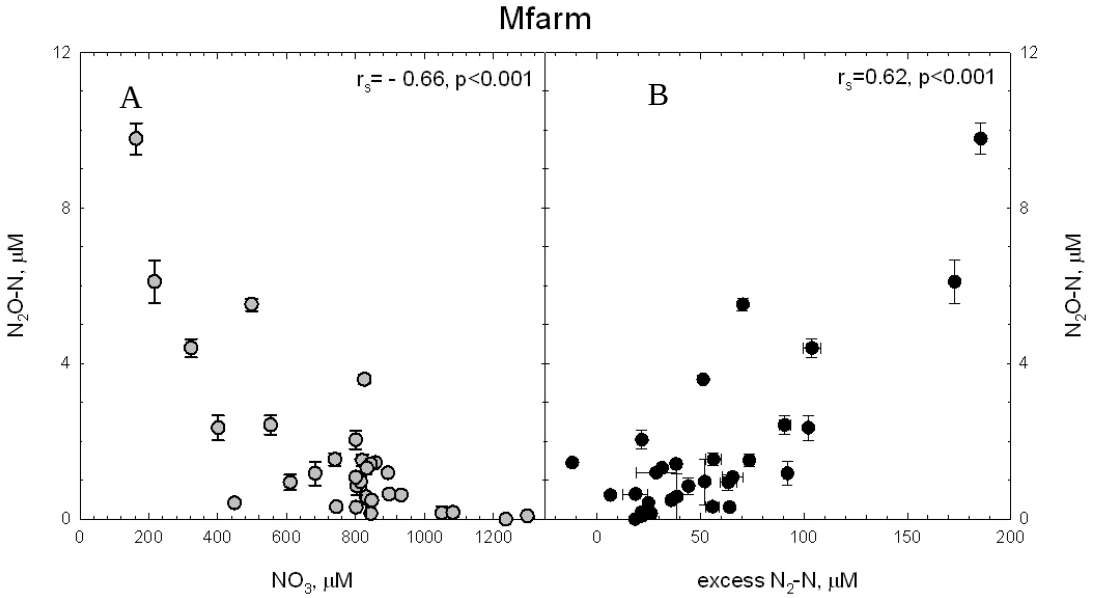

Figure 2.9- By selecting an individual site, a clear relationship between dissolved gas concentrations becomes apparent. NO_3^- concentrations below 50 μM allow CH_4 concentrations to increase. The highest CH_4 values are not observed until after NO_3^- has been reduced to <1 μM. At this site, CH_4 concentrations are relatively low in comparison to the higher values observed in the entire data set.

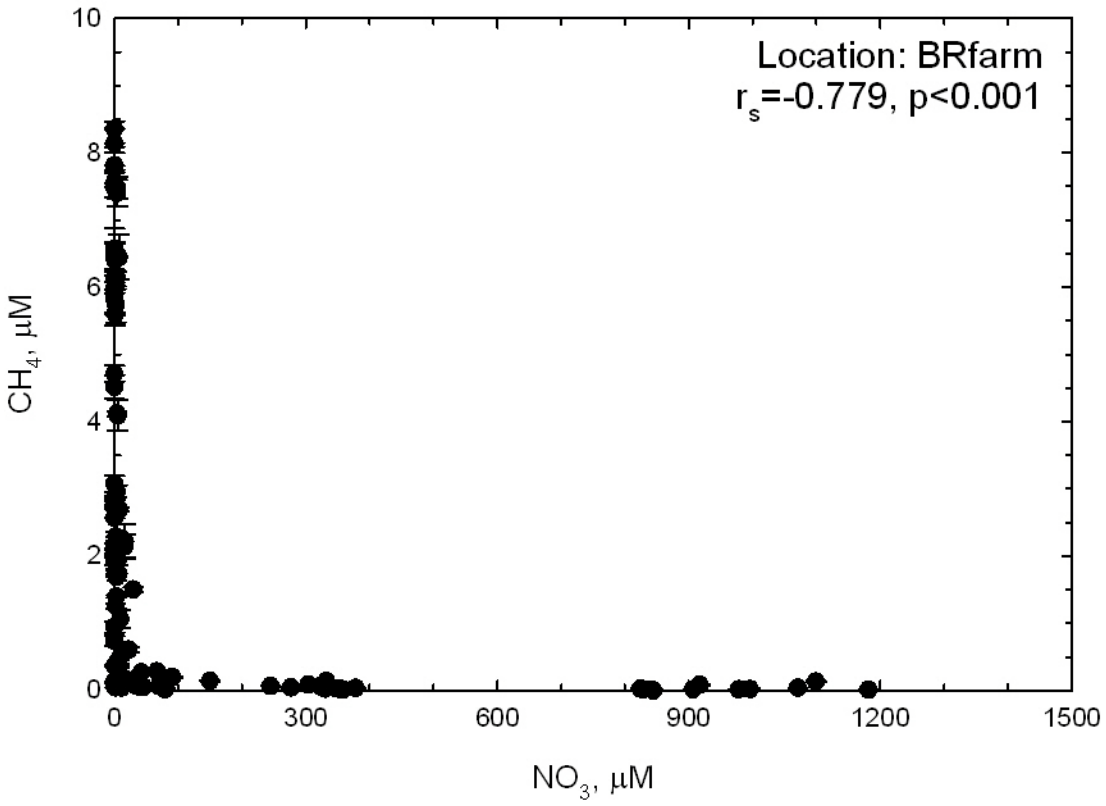

Fig. 2.10 – **A**) An example at CFarm where the strength of a relationship increased from r_s=0.35 to r_s=0.56 when just examining the falling water table concentrations and **B**) an example at EFAG where the strength of the relationships decreased (from r_s=0.53 to r_s=0.44) when just examining the falling water table concentrations. The Spearman Rank correlation statistics can be compared to Table 2.3.

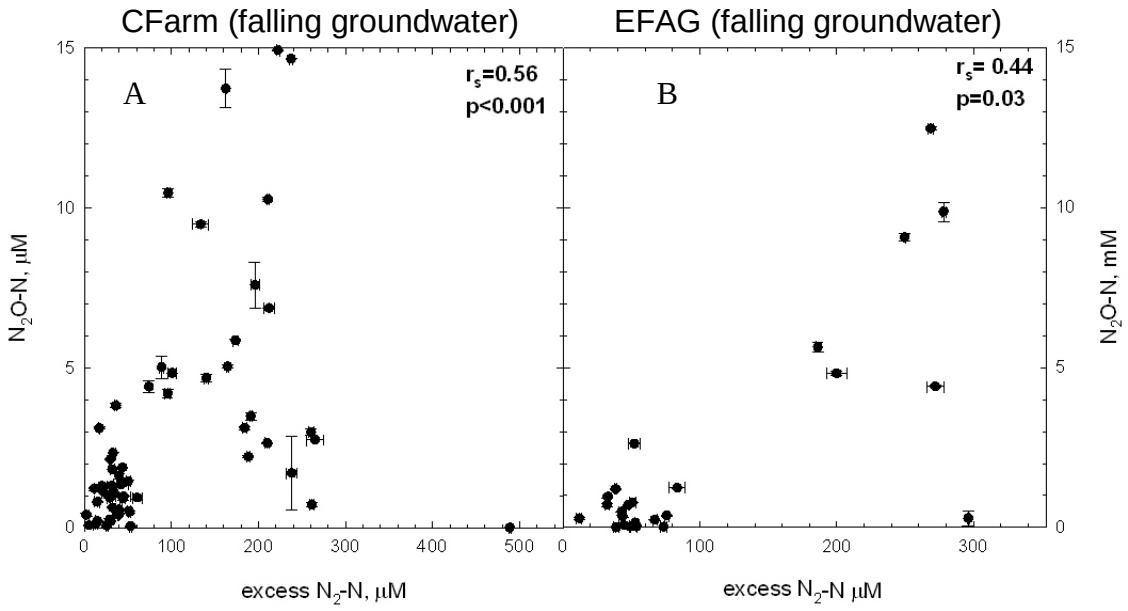

Figure 2.11 - The topography and median groundwater table drawn horizontally to scale for BrFarm (vertically exaggerated 3:1). Groundwater flow is from right to left towards the drainage ditch. The concentrations of NO_3^-, excess N_2-N, $\%O_2$ saturation, N_2O and CH_4 are displayed on the lower panels. The dashed line is the maximum and minimum concentrations at each piezometer.

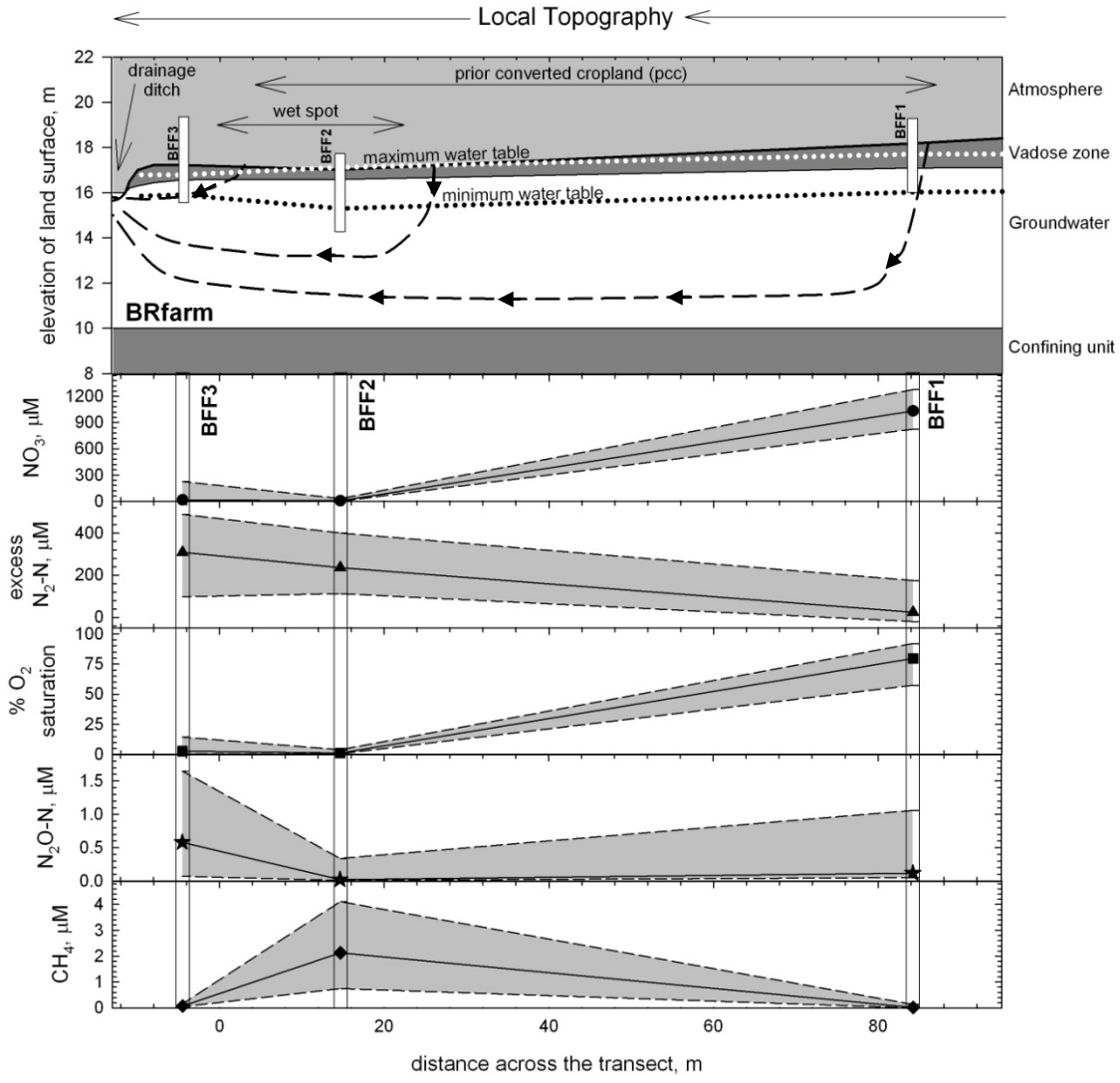

Figure 2.12 – The topography and median groundwater table drawn horizontally to scale for JLAG (vertical exaggeration is 4:1). The concentrations of NO_3^-, excess N_2-N, $\%O_2$ saturation, N_2O and CH_4 are displayed on the lower panels. The maximum and minimum concentration at each piezometer is shown as the dash marks.

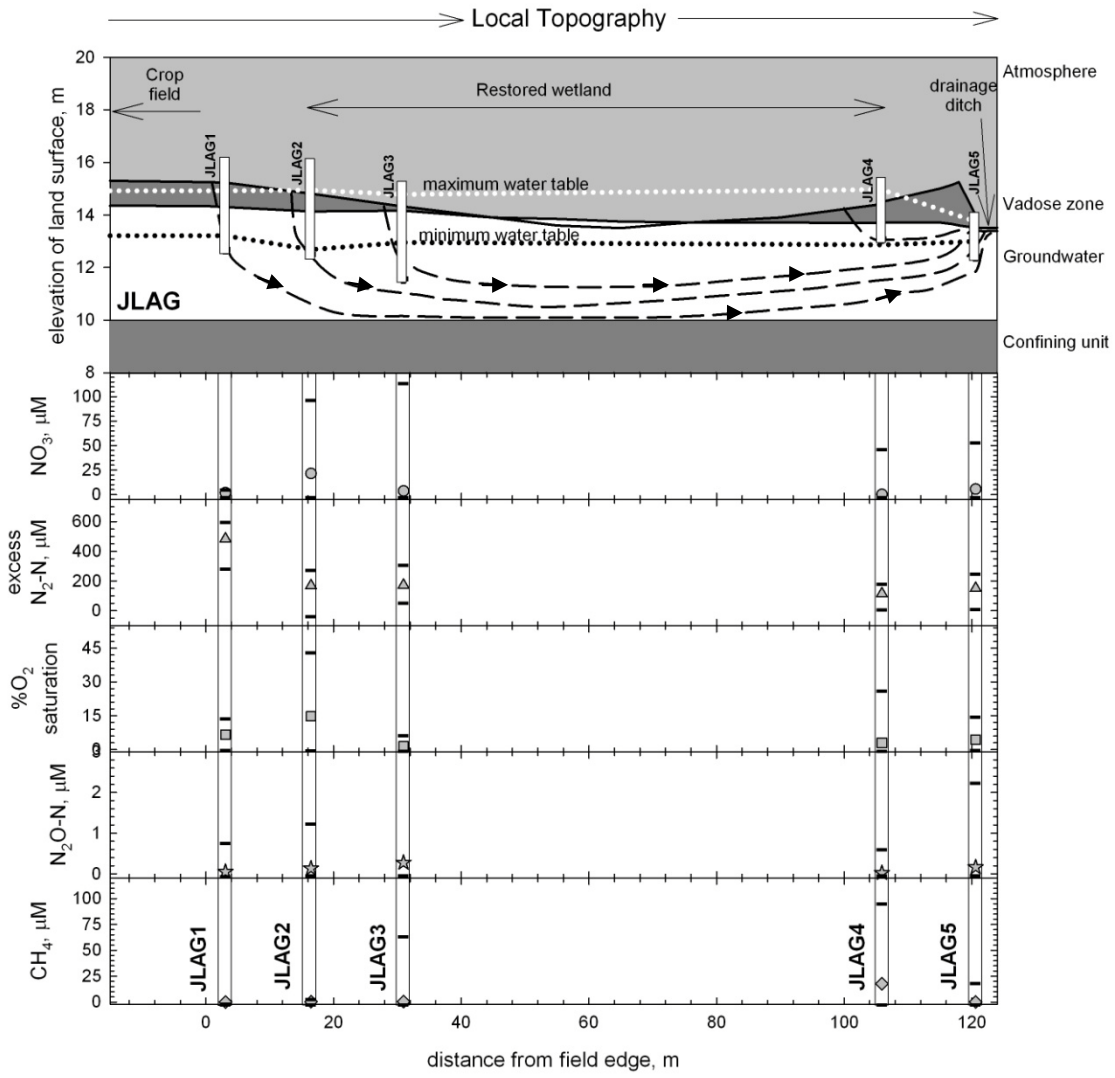

Figure 2.13 – An example of temporal and spatial variability within a piezometer transect. Hot moments can be observed as the highest peak concentrations. The agricultural field is on the left hand side of the graph at distance 0. Data from JLAG-3a is not presented in this figure.

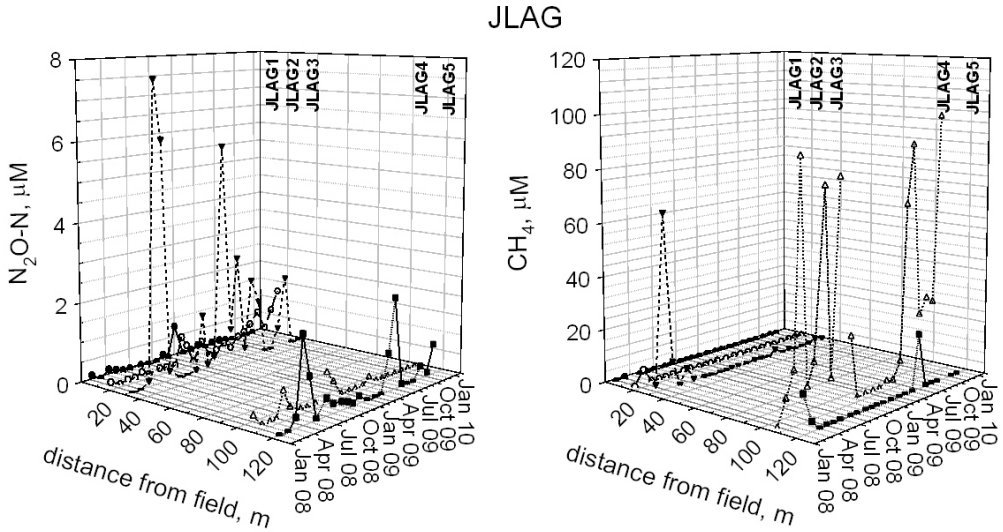

Figure 2.14 – The topography and median groundwater table drawn horizontally to scale for EFAG. The concentrations of NO_3^-, excess N_2-N, $\%O_2$ saturation, N_2O and CH_4 are displayed on the lower panels. The maximum and minimum concentration at each piezometer is shown as the dash marks.

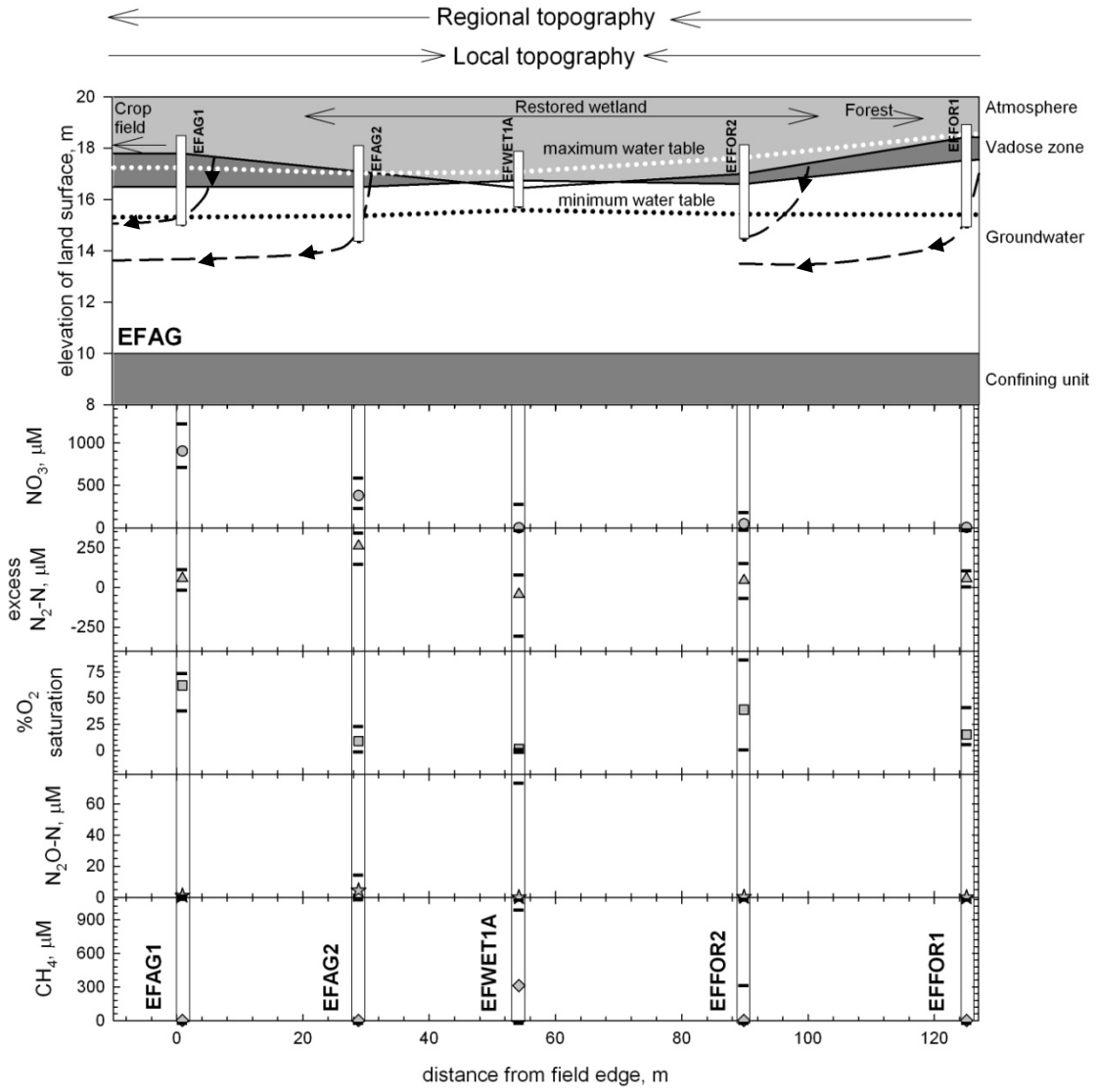

Figure 2.15- The topography and median groundwater table drawn horizontally to scale for BNDS. The concentrations of NO_3^-, excess N_2-N, $\%O_2$ saturation, N_2O and CH_4 are displayed on the lower panels. The maximum and minimum concentration at each piezometer is shown as the dash marks.

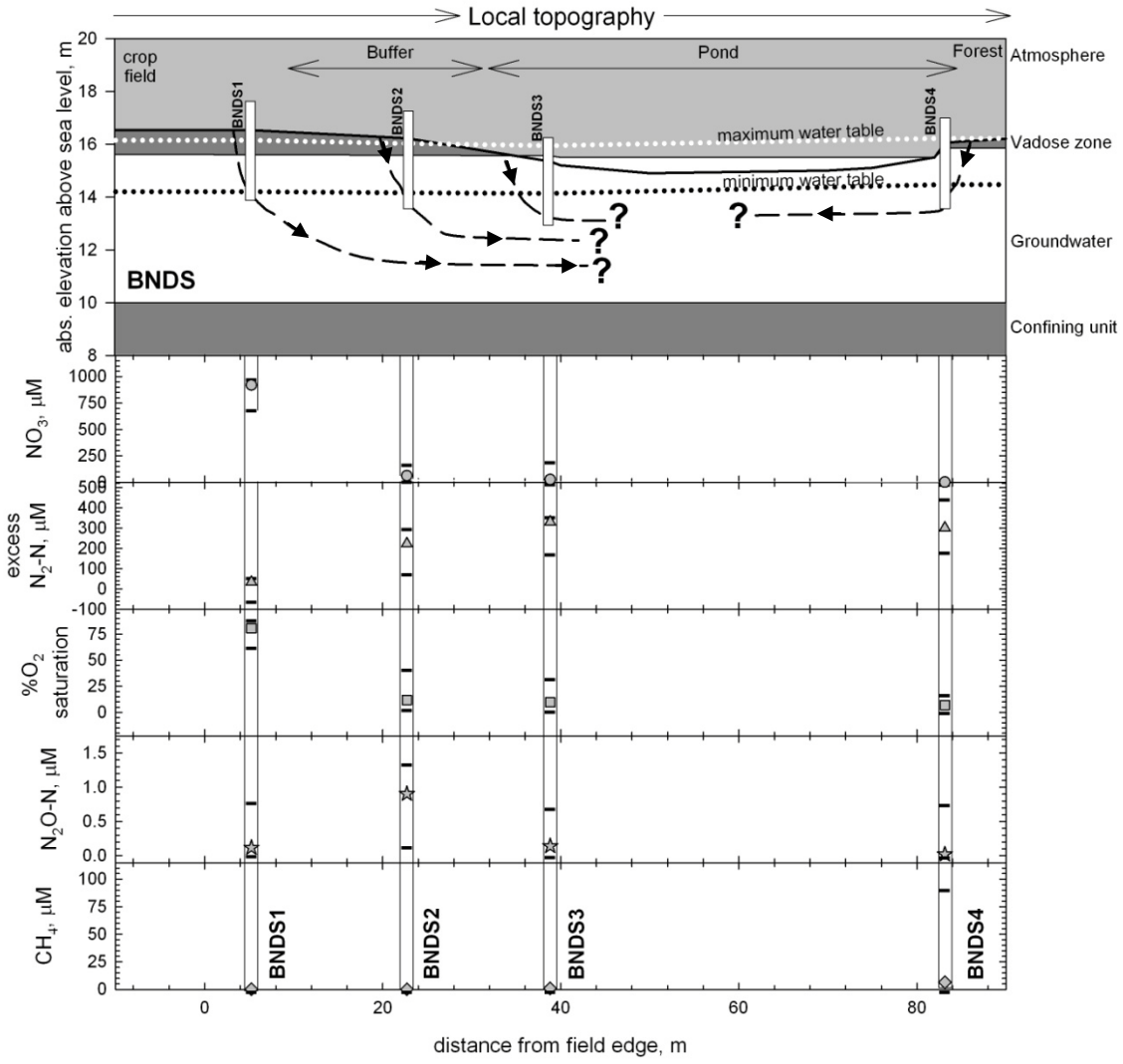

Figure 2.16- Spatial variability between the individual piezometers and between land use categories of piezometers. The median values for each different category are given and there is a scale change at 1 µM CH_4 and 7 µM N_2O. N_2O for the forested sites were all very low, <0.1 µM.

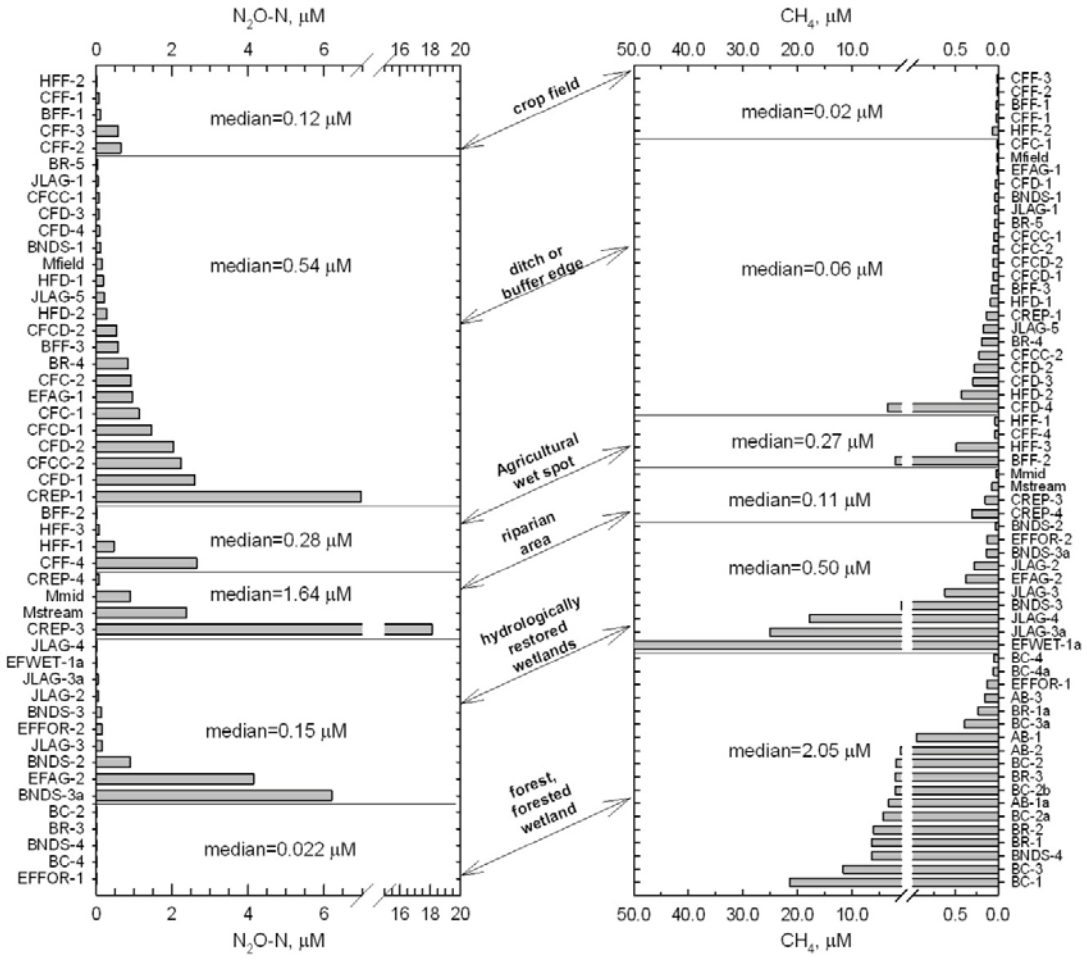

Figure 2.17- An example of a N_2O hot spot at CREP3. The N_2O hot spot threshold is a 5.5 µM N_2O-N and is displayed as the dotted horizontal line.

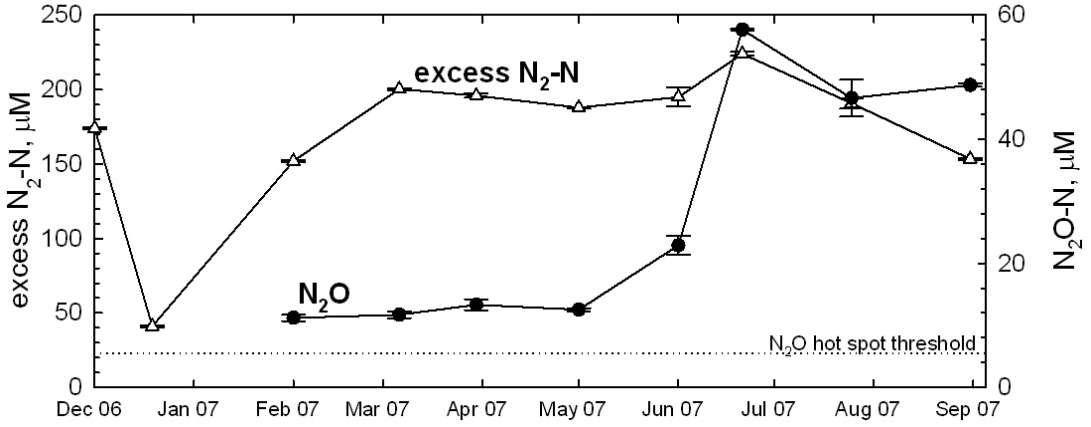

Figure 2.18 – An example of the concentrations of CH_4 throughout 2008 at one of the piezometer nests in the data set. Hot moment concentrations are circled.

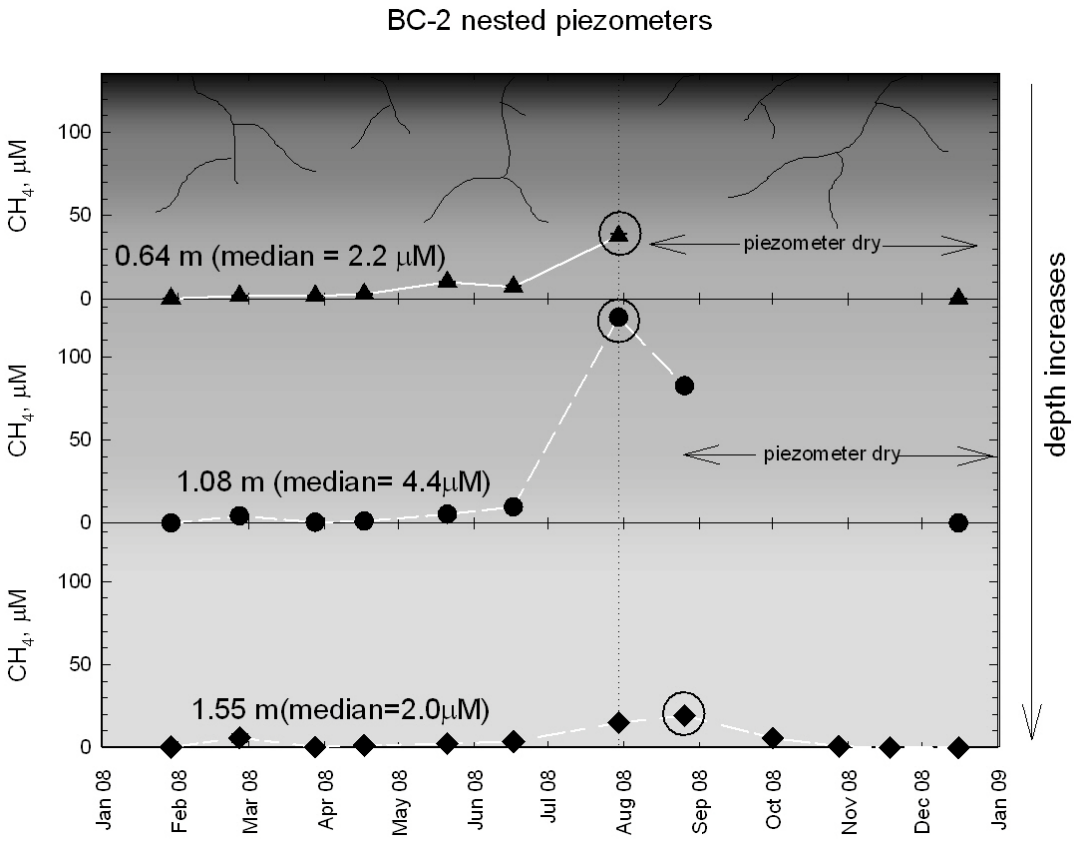

Figure 2.19 –An example of a time series of N_2O and CH_4 concentrations at the JLAG piezometer nest. Hot moment concentrations are indicated as circled values. Each time series graph is positioned vertically at the depth of the piezometer.

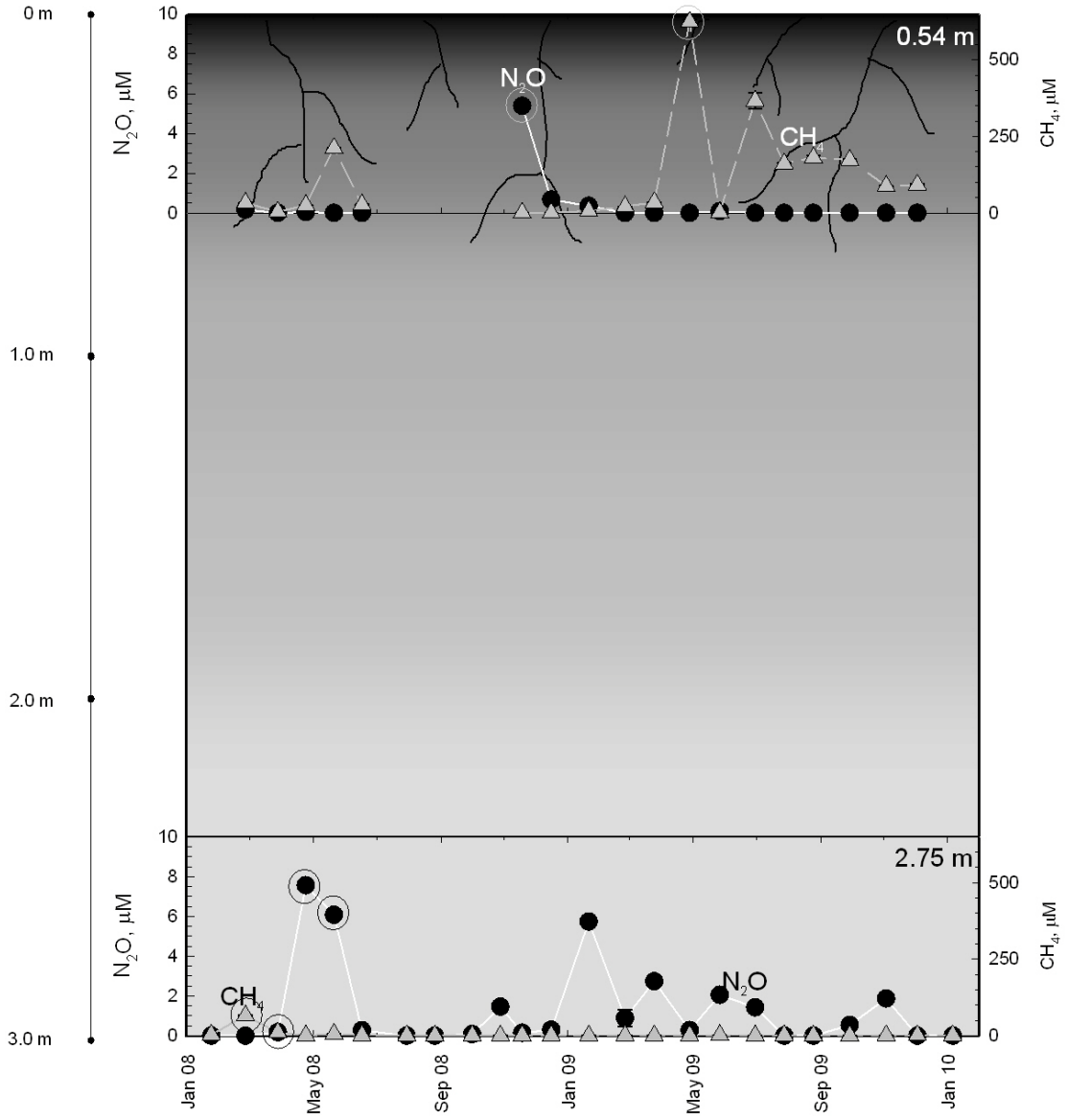

Figure 2.20 – The temporal variability for **A**) N_2O by season, **B**) N_2O for rising or falling water tables, **C**) CH_4 by season, and **D**) CH_4 for rising or falling water tables. The different letters indicate significantly different median values.

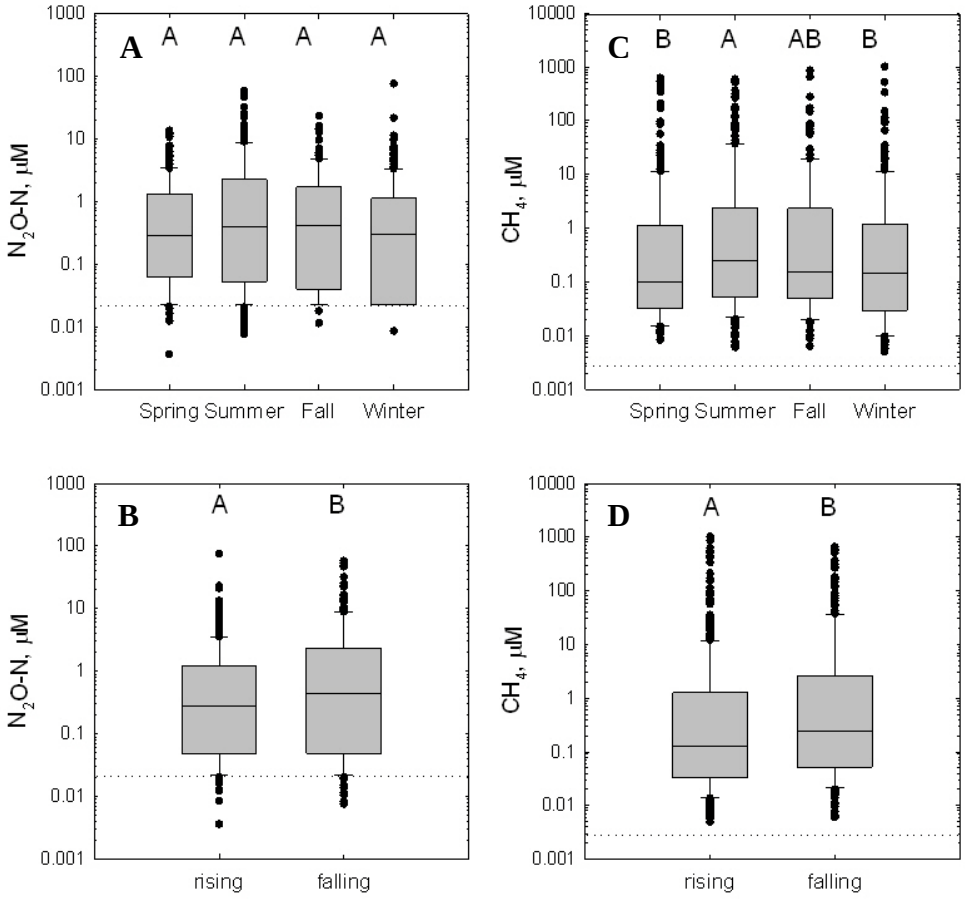

Figure 2.21 – An inter-annual comparison of the piezometers sampled in both 2008 (gray) and 2009 (white). The stars indicate statistically significant differences; the gray stars indicate that the 2008 value was significantly greater, and the white stars indicate that the 2009 value was significantly greater.

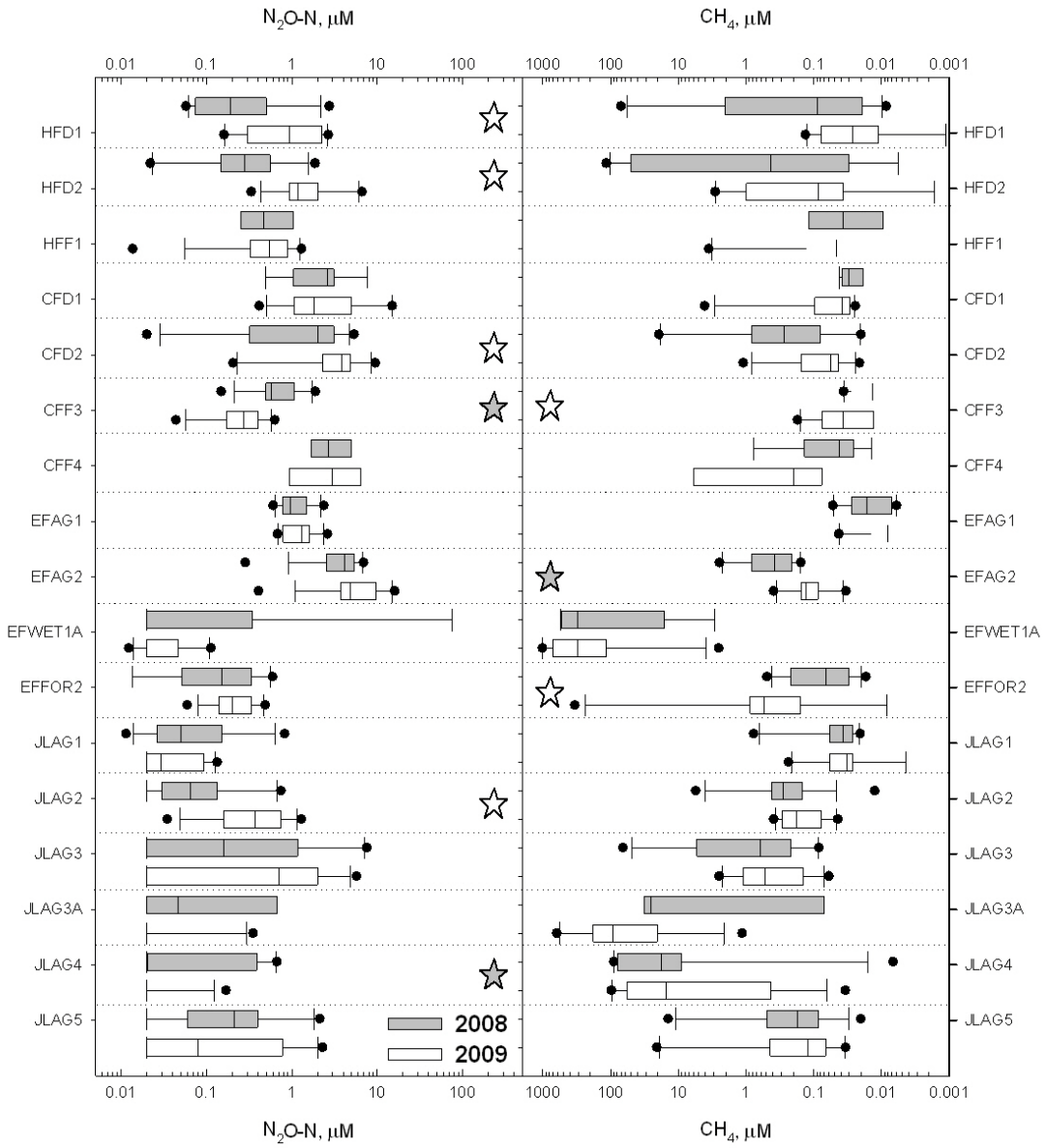

Figure 2.22 – An example of a hot moment, which was quantitatively defined as a time period during which the dissolved N_2O or CH_4 concentration was ranked in the 95th percentile of all values from that individual piezometer.

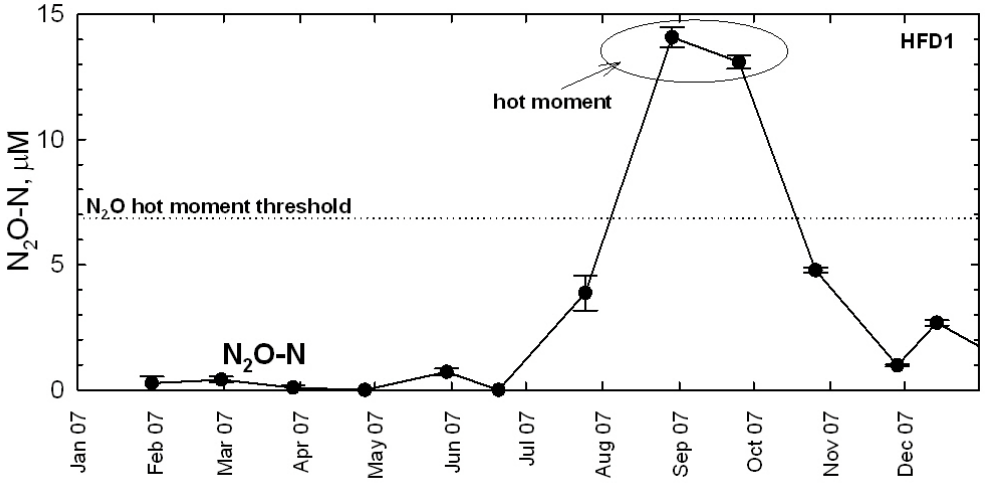

CHAPTER 3:

DIFFUSIONAL FLUXES OF EXCESS N_2, N_2O, AND CO_2 ACROSS THE WATER TABLE AND SOIL SURFACE IN AN AGRICULTURAL RIPARIAN BUFFER

Abstract:

Watershed nitrogen (N) budgets are usually imbalanced, and a large portion of the N is missing. The "missing N" is either stored within the watershed in soil, biomass, or groundwater, or lost as N_2 or N_2O via denitrification. Both storage and denitrification are difficult to measure directly because of the large background concentrations of N stored in watersheds and N_2 present in air. However, we can measure dissolved N_2 in groundwater in excess of atmospheric backgrounds using MIMS. To address the missing N at a smaller spatial scale, I used a piezometer transect at a site in the Little Choptank Basin (Mid-Atlantic region of USA) where I have observed that a portion of the NO_3^- and excess N_2 dissolved in groundwater is unaccounted for at a mid piezometer within the horizontal hydraulic gradient. I hypothesized that this missing N (138.5 μM N) on the transect scale can be accounted for as a vertical diffusive loss across the water table, and that I can measure the resulting excess N_2 diffusional gradient. Using a new method for measuring excess N_2 in gas, I further hypothesized that I can estimate the flux of excess N_2 from the soil surface

The missing N at the transect scale was estimated from the calculated transit time of the groundwater between the piezometers and the calculated diffusive flux estimates from groundwater into the vadose zone. The transit time and diffusive flux rates indicate that only 0.1 to 0.5% of the horizontal N decrease can be accounted for by vertical diffusion. Therefore, my calculations indicate that the missing N on the transect scale cannot be accounted for as a diffusional loss across the water table.

I measured excess N_2 in the gas phase directly using a new *in situ* method that measures the N_2/Ar ratio in a gas sample in comparison to the atmospheric ratio with a

precision of 0.05%. The groundwater and vadose zone profiles of excess N_2 and N_2O showed the largest partial pressures in groundwater, and the partial pressures decreased approaching the soil surface. The CO_2 profiles also showed a peak in the soil 1 m below the surface, but not always in groundwater. The calculated fluxes of CO_2 from the vadose zone to the atmosphere ranged from 10.9 to 180 mmol CO_2-C m^{-2} day^{-1}, the excess N_2-N fluxes ranged from -11.9 to 17.3 mmol N_2-N m^{-2} $day^{-1,}$ and the N_2O fluxes ranged from -0.0003 to 0.0019 mmol N_2O-N m^{-2} day^{-1}. However, in the calculation of excess N_2, I assumed that Ar was constant. There are many physical mechanisms that can potentially affect the concentration of Ar and N_2, including temperature-mediated solubility changes. I currently cannot distinguish between the effects of biological and physical processes on N_2/Ar, but the addition of other noble gas measurements might solve this problem. Although our flux estimates span a large range, that range includes excess N_2 fluxes sufficient to explain the missing N on the watershed scale. This is the first attempt at directly measuring excess N_2 *in situ* in the vadose zone, and my results represent an improvement over our current ability to make direct excess N_2 measurements in the vadose zone.

Introduction:

The nitrogen budget of most watersheds is unbalanced. Stream N export typically accounts for 10-30% of the net anthropogenic N inputs, or NANI, and the remainder of the budget is missing (Jordan and Weller 1996, Howarth et al. 1996, Schaefer and Alber 2007). The "missing N" is thought to be stored in the biomass, soil, or groundwater within the watershed, or completely lost from the watershed as N_2 and N_2O through denitrification. Both of these processes are difficult to measure on a watershed scale.

Denitrification is a major process that removes inorganic nitrogen (N) from aquatic and terrestrial systems. Denitrification is the reduction of nitrate (NO_3^-) to dinitrogen gas (N_2) through the intermediate and sometimes terminal products of nitrite (NO_2^-), nitric oxide (NO), and nitrous oxide (N_2O, Knowles 1982). The direct measurement of a small increase in N_2 from denitrification over the 78% background concentration of N_2 in air has been viewed as a difficult problem. N_2 can be directly measured in water using membrane inlet mass spectrometry (MIMS, Kana et al. 1994) with high precision (0.05% coefficient of variation, %CV), but the background concentration of N_2 in water at 20^oC is 531.4 µmol L water^{-1}, while in air the background N_2 at 20^oC is much greater, 32,480 µmol L air^{-1}.

N_2O is an intermediate and sometimes terminal end product of denitrification. Besides being a potent greenhouse gas with a global warming potential of 298 over 100 years (IPCC 2007), N_2O has the ability to destroy stratospheric ozone (Crutzen 1981). N_2O can also be produced through nitrification, and can be denitrified in soils after production and converted to N_2. The removal of watershed N through complete

denitrification to N_2 is an attractive process for N-enriched watersheds, but incomplete denitrification that stops at N_2O has negative atmospheric implications.

Outside of the major urban centers, the major source of N in watersheds is fertilizer applied to agricultural fields and lawns (e.g., Bohlke and Denver 1995, Fisher et al. 2010). Regardless of the form in which fertilizer is applied, most of the N not consumed by crops during the growing season is oxidized to NO_3^- in soils during fall and winter (Staver and Brinsfield 1998). Because NO_3^- is highly soluble, it is easily leached through the soil by rain infiltrating to groundwater. As a result, concentrations of NO_3^- in groundwater under agricultural fields and fertilized lawns typically range over 0.2-2 mM (Staver and Brinsfield 1998, Fisher et al. 2010). In addition to NO_3^-, concentrations of excess N_2 dissolved in groundwater in agricultural areas can range from 0-500 μM N_2-N (Fisher et al. 2010), and N_2O concentrations range from negligible to ~70 μM N_2O-N (Chapter 2) which implies significant amounts of denitrification. These data suggest that denitrification or other biological processes producing excess N_2 (e.g., anammox and anaerobic oxidation of methane; Mulder et al. 1995, Jetten 2001, Raghoebarsing et al. 2006, Burgin and Hamilton 2007) may be responsible for some of the missing N at the watershed scale. Here I will use the term "denitrification." although I acknowledge that other biological processes may produce excess N_2.

The concept of missing N applies to spatial scales smaller than the watershed scale. In previous research, it has been shown that the amount of N in groundwater from a piezometer at a higher hydraulic elevation cannot be completely accounted for by the concentrations of NO_3^- and excess N_2 at subsequent piezometers down a hydraulic slope on a scale of 10-100 m (Fisher et al. 2010). The missing N on the transect scale may be

converted to another form of N, such as NH_4^+, utilized by plants, or denitrified and lost from groundwater into the vadose zone as N_2 or N_2O. Here I will test the hypothesis that the high dissolved concentrations of excess N_2 and N_2O within groundwater fuel a diffusive loss of excess N_2 and N_2O into the vadose zone and that these diffusive losses will account for the "missing N" in groundwater at the transect scale. Second, I hypothesize that I will be able to detect the diffused excess N_2 and N_2O within vadose zone concentration profiles and that I will be able to estimate a diffusive flux of excess N_2 and N_2O from the soil surface. To test these hypotheses, I measured vertical profiles of excess N_2, N_2O, and CO_2, and I estimated the diffusive fluxes from groundwater into the vadose zone and from the vadose zone to the atmosphere within a riparian buffer of an agricultural field.

Research was conducted in the Little Choptank watershed which is situated within the Chesapeake Bay watershed on the Maryland coastal plain (Fig. 3.1). The Chesapeake Bay and its tributaries have experienced increased nutrient inputs from agriculture and urban development that have led to accelerated eutrophication, hypoxia (Kemp et al. 2005), and harmful algal blooms (Anderson et al. 2008). Reducing the concentration of NO_3^- in surface waters is important if we want to minimize further damage and restore the Chesapeake Bay and its tributaries to a less nutrient-rich, healthier state. Understanding the location and rates of denitrification is necessary to protect and restore areas that could reduce the concentrations of NO_3^- entering surface waters, in addition to providing a better understanding of watershed N budgets.

Methods:

Location

The research was conducted on the Mid-Atlantic coastal plain on the Maryland portion of the Delmarva Peninsula (Fig. 3.1). The region is underlain by the Kent Island Formation, an estuarine deposit of the middle-Wisconsin period (Owens and Denny, 1979), and the soils are mostly Keyport silt loam, a moderately well-drained soil (Soil Survey Staff, Natural Resources Conservation Service, United States Department of Agriculture, 2011). The study site is an 11 year old USDA Conservation Reserve Enhancement Program (CREP) agricultural buffer that lies adjacent to a crop field and a tidal creek of the Little Choptank River. The agricultural field is planted in a corn/soybean crop rotation, which is typical for the Delmarva Peninsula (Staver and Brinsfield, 2001), and the farm practices include fertilizer application rates of 50-150 kg N ha^{-1} yr^{-1} under no-till agriculture.

Groundwater sampling

Groundwater samples were taken from 5.1 cm (2") inner diameter piezometers with 30 cm long sampling screens. Originally, a transect of piezometers from the agricultural field (CREP1) to the far buffer edge (CREP3) were installed in 2004 at depths of ~2 m (Sutton et al. 2010). In the current study, CREP1 at the agricultural field edge, and CREP3 in the mid buffer were used. In the fall of 2008, two additional piezometers were hand augered in the vicinity of CREP3 (2.1 m to mid screen) to add sampling depths of 3.1 m (CREP3-3.0) and 3.9 m (CREP3-4.0). These CREP3

piezometers are a nested set within a 2 m radius sampling groundwater at 2.1, 3.1, and 3.9 m depths.

Groundwater samples were taken from the piezometers between December 2008 and September 2010. On the day prior to sampling, the depth to the water table was measured in each piezometer using a Solinst® Model 101 mini water level meter, and the piezometers were pumped dry using a portable Solinst® Model 410 peristaltic pump. A fishing float with a 5 cm diameter was lowered to the bottom of the piezometer to reduce gas exchange between the freshly inflowing groundwater and the atmosphere. On the next day, the float was removed, and a 5.1 cm (2") Teflon® bailer was slowly lowered to the bottom of the piezometer to acquire an undisturbed groundwater sample. A one-way ball valve prevented loss of the groundwater when the bailer was removed from the piezometer. A stopcock connected to a 15 cm length of 2mm id diameter Teflon ® tubing was attached to the bottom of the bailer to control flow into 25 mL ground glass tubes with ground glass stoppers. The tubes were overflowed from the bottom with sample and immediately capped and submerged in ice water to prevent gas exsolution. A separate sample was taken for nutrients, conductivity, and pH, and the temperature of the sample was taken with a VWR digital thermometer (NBS traceable accuracy of ± 0.3 ^{o}C). The groundwater samples were analyzed for excess N_2, Ar, and O_2 by MIMS; N_2O, CH_4, and CO_2 by gas chromatography; and by automated colorimetric methods for NO_3^-, PO_4 and NH_4^+. Analytical details are given below.

Groundwater analyses

Groundwater samples were analyzed for excess N_2, O_2, and Ar using the MIMS method (Kana et al. 1994). The concentration of Ar within the sample was assumed to represent physical exchange between air and water at recharge and was used to calculate an effective recharge temperature of the water at the time of infiltration using the solubility formulations of Colt (1984) based on Weiss (1970). The Ar recharge temperature was used to calculate the background N_2 concentration (e.g., Bohlke and Denver 1995, Mookherji et al. 2003), and observed N_2 greater than the background N_2 was considered "excess N_2" due to denitrification. The excess N_2 data reported here were not corrected for excess air, although we are now evaluating excess air with measurements of other noble gases.

N_2O and CO_2

Dissolved and gaseous phase N_2O and CO_2 samples were analyzed using gas chromatographic techniques. For N_2O groundwater analysis, 8 mL of groundwater was injected into N_2-purged 12 mL Exetainers® that were vented to maintain atmospheric pressure. For CO_2 groundwater analysis, 4 mL of groundwater was injected into an N_2-purged 12 mL Exetainers® that was vented to maintain atmospheric pressure and then the vent was removed and 1 mL of 1N H_2SO_4 was added (Stainton 1973). Both N_2O and CO_2 Exetainers® were shaken vigorously for 2 minutes to allow complete equilibration between the headspace and groundwater sample. The concentrations of N_2O and CO_2 within the exetainer head spaces were determined on a Shimadzu GC-14B equipped with both an electron capture detector (ECD, N_2O) with a Porapak Q column and a thermal

conductivity detector (TCD, CO_2) with a 80/100 Hayesep Q column. The dissolved concentration in the original water sample was calculated using groundwater and headspace volumes, and the appropriate solubility data for the measured room temperature and pressure (Weiss and Price 1980). The vadose zone samples were directly injected into the GC from the gas-filled exetainers® acquired from the vadose zone in the field (see below). Matheson Tri-Gas standards were used along with a blank and an atmospheric air injection to create a standard curve for N_2O. Standard concentrations of $NaHCO_3$ solution were used for the dissolved CO_2 standards. For CO_2 in groundwater, a second subsample was equilibrated with air and then injected into an N_2-purged exetainer ® vial as above to measure background CO_2. The difference between the two measurements is referred to as "excess CO_2".

Water level monitoring

Half hourly groundwater level and temperature data were recorded at the 2.1 m piezometer beginning in 2005 using a Solinst® model 3001 levelogger® Silver. Recorded pressure was corrected for barometric pressure variations using a separate Solinst® Barologger® record. The corrected water pressure was equivalent to the water height within the piezometer which was converted to the water table depth below ground using the fixed depth of the logger at the bottom of the piezometer.

Vadose zone sampling

Vadose zone gas samples were acquired using equilibration chambers. These are inverted 50 mL centrifuge tubes connected to a section of 3.2 mm (1/8") copper tubing

and to a three-way stopcock (Silver et al. 1999). The equilibration chambers were installed in the CREP buffer near the piezometer nest. Two replicate rows of equilibration chambers were installed in August 2008 (transect A) and November 2008 (transect B) at 0.25, 0.5, 0.75, 1.0, and 1.5 m. Samplers were inserted into the ground by hand augering a 3.8 cm (1.5") borehole, and the hole was backfilled with approximately the same soil strata in the appropriate order. We allowed 2-4 weeks for re-equilibration of soil gases and settling of the soil before sampling.

To sample the equilibration chambers, 60 mL of gas was first pulled out of the samplers to flush the copper tubing after attaching a 60 mL syringe to the stopcock, and then 16 ml of gas sample was transferred to over-pressurize 12 mL pre-evacuated exetainers®. Triplicate samples were taken for each depth. Field air was used as the standard on each sampling date and treated the same as the sampling tubes. The samples were analyzed within three days of collection for excess N_2, Ar, N_2O, CH_4, and CO_2 (analytical details below).

Vadose zone analytical methods

A new capillary inlet system was created as part of a novel analytical technique to introduce vadose zone gas (0.6 mL) directly into a quadrapole mass spectrometer (QMS). The criteria required in the creation of this method were a small injection volume (<1 mL) and high precision to measure small changes in the large background N_2 concentration. This was accomplished using a 90 cm length of SGE © fused silica capillary tubing attached to a Swagelok ® reducing union which served as a sample reservoir (Fig. 3.2). The reducing union was partially filled with epoxy to reduce the

internal inlet volume to 0.6 mL. An Exetainer® septa sealed the reducing union from the atmosphere and allowed injection of sample gases into the inlet system. A valved 2-stage rotary vane pump was used to evacuate the previous sample from the inlet system. The capillary tube coming from the inlet was thermally stabilized at 50 ^{o}C using a water bath. On the vacuum side, the sample passed across 600^{o}C copper to eliminate O_2 followed by a liquid nitrogen cryotrap which eliminated CO_2 and water vapor prior to entering the QMS.

Variations in the CO_2 and O_2 partial pressure were tested to determine whether variations in either gas had a significant effect on the measured N_2/Ar ratio. A gas tank with 99% N_2 and 1% Ar and either a UPC CO_2 or O_2 tank were connected to flow controllers to achieve a range of CO_2 and O_2 partial pressures against a constant N_2/Ar ratio. Without either the copper furnace or the liquid nitrogen cryotrap in line, O_2 and CO_2 significantly deflected the N_2/Ar ratio. The cryo trap and the copper furnace eliminated significant effects of O_2 and CO_2 on the N_2/Ar ratio (Fig. 3.3 A, B), and no further corrections were made. All data except those from December 3rd, 2008 were analyzed using both a cryo trap and a copper furnace, and the December 3rd data were corrected in order to account for the effects of both CO_2 and O_2.

The QMS monitored the peaks at 14, 28, 32, 40, and 44. The N_2/Ar ratio was used in the determination of excess N_2, and the 32 and 44 peaks were monitored to ensure the elimination of all O_2 and CO_2 from the sampling stream. The 14 peak (N^+) was used to measure N_2 gas to avoid potential interference from trace amounts of CO_2 which generates the fragment CO^+, which has the same mass to charge ratio (m/e) as N_2^+. Only the 14/40 (N^+/Ar^+) ratio was used to determine an excess or deficit of N_2 to eliminate any

possible error caused by an over or under injection of individual gas samples. The instrument was calibrated using injections of field air which were collected in the same manner as the samples.

To calculate excess N_2, a two-sided t-test was done between the soil sample gas tubes and the standard field air tubes. Samples that were not significantly different than the standard field air tubes were reported as zero excess N_2. The precision of the method was determined from the % CV from all samples which averaged 0.05%. Excess N_2-N values were reported in terms of partial pressure (mmHg) to account for the differences in the background concentrations of N_2 in vadose zone gas and in groundwater solution.

Concentration gradients and diffusional flux estimates

Concentration gradients cause diffusive exchanges between the atmosphere and the vadose zone, or the groundwater and the vadose zone. Positive concentration gradients were defined as concentrations that increase with depth, resulting in a net upward flux from the groundwater to the vadose zone or from the vadose zone to the atmosphere. Negative gradients were defined as the opposite: concentrations that were highest at the surface and decreased with depth resulting in a net downward flux into the vadose zone or groundwater. The concentration gradient, $\delta C/\delta z$ (mmol m^{-4}), was calculated as

$$\frac{\partial C}{\partial z} = \frac{C_2 - C_1}{z_2 - z_1} \qquad (1)$$

where C is the gas concentration (mmol m^{-3}), z is the depth in meters, C_1 is the shallower concentration, C_2 is the deeper concentration, z_1 is the shallower depth, and z_2 is the

deeper depth. The atmospheric concentration and the concentration at the shallowest equilibration chamber were used to calculate the concentration gradients from the soil to the atmosphere. Gradients between groundwater and the vadose zone were calculated using the partial pressure of the respective gas at the shallowest piezometer and the deepest unflooded equilibration chamber. The concentration gradients from groundwater to the vadose zone were converted from units of mmHg d^{-1} to μmol L^{-1} day^{-1} using the following conversions that have units of mmol m^{-3} $mmHg^{-1}$

$$N_2\text{-N conversion}=0.4723+0.912*e^{(-0.0385*\text{temperature})} \quad (2)$$

$$N_2O\text{-N conversion} =0.0146+0.0635*e^{(-0.0503*\text{temperature})} \quad (3)$$

$$CO_2 \text{ conversion} =181.65+821.47*e^{(-0.04538*\text{temperature})} \quad (4)$$

These conversions are the equations fit to the solubility data of Colt (1980, N_2), Weiss & Price (1980, N_2O), and Lange (1961, CO_2) divided by the fraction of the gas in the head space of the solubility experiments in mmHg (air, N_2=593.41 mmHg, pure N_2O= 760 mmHg, atmospheric air, CO_2=0.266 mmHg).

Excess N_2-N and N_2O-N diffusional fluxes from the soil to the atmosphere and from groundwater into the vadose zone were calculated using Fick's first law of diffusion.

$$F_d = -D_s \frac{\delta C}{\delta z} \quad (5)$$

where F_d is equal to the diffusional flux (μmol m^{-2} d^{-1}), D_s is a tortuosity-corrected diffusion coefficient (m^2 day^{-1}), and $\delta C/\delta z$ is the concentration gradient (mmol m^{-4}). The gaseous diffusion coefficients of N_2, N_2O, and CO_2 in air were obtained from Massman (1998) and were corrected for temperature, pressure, porosity, and tortousity according to

the Buckingham-Burdine-Campbell model for gas diffusivity in undisturbed soil (Moldrup et al. 1999):

$$\frac{D_s}{D_0} = \phi^2 \left(\frac{\varepsilon}{\phi} \right)^{2+\frac{3}{b}} \quad (6)$$

where D_s is the gas diffusion coefficient in soil ($m^2\ d^{-1}$), D_0 is the diffusion coefficient in the free atmosphere, Φ is total porosity (m^3 void volume m^{-3} soil), and ε is the volumetric air content m^3 air m^{-3} soil. Values for the Campbell soil-water retention parameter (b) were taken from Clapp and Hornberger (1978). N_2 diffusion coefficients in water were obtained from Wise and Houghton (1966), and a regression of temperature versus N_2O diffusion coefficient values was formed using compiled literature values (Hamborg et al. 2008, Heincke and Kaupenjohann 1999). The CO_2 diffusion coefficients were obtained from Maharajh and Walkley (1972). The aqueous diffusion coefficients in groundwater were corrected for tortuosity (Popovičová and Brusseau, 1997):

$$\frac{D_{GW}}{D_0} = \phi^{-\frac{2}{3}} \quad (7)$$

where D_{gw} is the diffusion coefficient in groundwater ($m^2\ d^{-1}$), D_0 is the diffusion coefficient in free water, and Φ is the porosity ($m^3\ m^{-3}$).

Soil water content (θ, m^3 water m^{-3}soil; θ=Φ-ε); data were collected using time domain reflectometry (TDR) with the Trime®-Pico IPH and Pico-BT. This instrument provided both porosity (Φ) and volumetric water content (θ) for the July, August, and September 2010 water content values. Prior to these dates water content was estimated. Surface air temperature and pressure was obtained from the CBOS weather station at the Horn Point Laboratory, Cambridge, MD (http://hpl.cbos.org/download.php).

Results:

Water table depth and temperature

2009 and 2010 were very different years in terms of rainfall (Fig. 3.4 A,B). 2009 was an unusually wet year receiving 114.4 cm of rainfall, and 2010 was a drier than average year, receiving 87.1 cm of rainfall. Over the past six years, the average amount of rainfall per year was 97.9 cm, and the long term average is 110 cm y^{-1} (Lee et al. 2001). Rainfall is not seasonal in the Mid-Atlantic U.S.A.; precipitation events are relatively evenly distributed throughout the year (Fig. 3.4A, B, Fisher et al. 2010).

The depth to the water table varied in response to the rainfall in 2009 and 2010 (Fig. 3.4C). As 2009 was an unusually wet year, the average depth to the water table was only 0.43 m while in 2010 the average depth to the water table was 1.04 m. In 2009, the water table fluctuated considerably in the summer months as a result of multiple infiltration events (Fig. 3.4C), which is not typical, and is not seen in 2010 (Fig. 3.4C). The rapid rise in groundwater level in the fall typically occurs within a month time frame in October to November, which is evident in the 2010 data. The water table intersected the soil surface in both 2009 and 2010, but the water table remained closer to the soil surface in fall 2009 and winter of 2010 than in fall 2010.

Groundwater temperature followed a seasonal cycle similar to but delayed compared to the seasonal atmospheric temperature cycle in the Mid-Atlantic (Fig. 3.4D). Although 2009 was significantly wetter than 2010, the seasonal temperature cycle was maintained, and the average temperatures were almost exactly the same, 13.62^{o}C and 13.65^{o}C for 2009 and 2010, respectively (Fig. 3.4D). The groundwater temperature

variability was slightly greater in 2010, with temperatures ranging between 7.1 and 19.8 ^{o}C in 2009 and between 6.67 and 20.24^{o}C in 2010.

Gas Profiles

The excess N_2, N_2O, and CO_2 data are presented in order of addressing the hypotheses. First, the combined measured gas profiles in the vadose zone and groundwater are presented showing that we can measure excess N_2 profiles as well as N_2O and CO_2 profiles in the vadose zone. Second, calculated diffusional fluxes of excess N_2, N_2O, and CO_2 out of the groundwater and into the vadose zone are presented to answer whether these fluxes can account for the missing N on the transect scale. Lastly, estimated diffusional fluxes of excess N_2, N_2O, and CO_2 from the soil surface are presented based on the measured vadose zone gas profiles.

We were able to detect excess N_2 concentrations in the vadose zone and construct gas profiles from groundwater into the vadose zone (Fig. 3.5A). These profiles are expressed in partial pressure units of mmHg to standardize the units between the gas dissolved in water and the gas present in the vadose zone. Excess N_2 partial pressure was highest in groundwater at 2-3 m depth below ground and decreased towards the soil surface (Fig. 3.5A). Within the vadose zone, the partial pressure of excess N_2-N was positive (excess N_2 present relative to atmospheric air), negative (a deficit of N_2 relative to atmospheric air) or zero (no significant excess or deficit in N_2, Fig. 3.6A). However, excess N_2 in the vadose zone was always less than the partial pressure of excess N_2 dissolved in groundwater (Fig. 3.5A). The vadose zone profiles of excess N_2-N showed evidence of excess N_2 production in the vadose zone (Fig. 3.6A). An example of this is

June 2010 when a mid vadose zone maximum was observed at 1.0 m (Fig. 3.6A). The large negative excess N_2 values observed at 1.0 and 1.5 m for July 2009 are likely the result of soil and/or groundwater physical processes that are discussed below.

The partial pressure of N_2O was large in groundwater, and decreased towards the soil surface (Fig. 3.5B). The concentration of N_2O was always highest in groundwater at the 3.1 m piezometer and decreased upwards approaching the water table. The highest N_2O concentration in the vadose zone profile was typically seen at the deepest equilibration chamber, but production of N_2O in the vadose zone was inferred from the convex gas profiles (Fig 3.6B). Production of N_2O appeared to occur in the vadose zone (Fig. 3.6B), but the largest partial pressure of N_2O was always observed in groundwater (Fig. 3.5B).

The partial pressure of CO_2 increased with depth below the soil surface (Fig. 3.5C). The peak in CO_2 concentration was always seen at or below 1.0 m, but the peak concentration was not always observed in groundwater (Fig. 3.5C). More accumulation of CO_2 was observed in the vadose zone profiles than either the excess N_2 or N_2O vadose zone profiles (Fig. 3.6C). The largest measured CO_2 value (3160 μmoles CO_2 L^{-1} air) shown in Figure 3.6 C was taken in June 2010 at the 1 m sampler. This value was equivalent to 7.1 vol % of the soil gas and coincided with the large excess N_2 (600 μmoles N_2 L^{-1} air) and N_2O (0.2 μmoles N_2O L^{-1} air) values measured at that depth on the same date.

O_2 concentrations generally decreased with depth through the vadose zone and into the groundwater (Fig. 3.5D). In the vadose zone in December 2008, O_2 was near atmospheric values and decreased with depth. Vadose zone O_2 measurements are only

available for December 2008 before O_2 was trapped out of the sampling stream. CREP3-4 had higher concentrations of O_2 at 3.9 m (88 mmHg for Dec. 08, and ranged from 70-110 µM O_2 over the sampling period 2008-2010) than the shallower two piezometers (10.6 mmHg for Dec. 08, 10-50 µM O_2 over the sampling period 2008-2010), likely because it was sampling a flow path that originated further into the agricultural field (Fig. 3.5D).

The ratio of N_2O/excess N_2 concentrations increased downward from the soil surface (Fig. 3.7). The N_2O/excess N_2 concentration ratios in groundwater were high, greater than the typical 0.01 to 0.05 observed at our other sites (Fisher et al. 2010). The N_2O/excess N_2 concentration ratio in the vadose zone was considerably smaller because the concentration of N_2O was typically small while the concentration of excess N_2 was often large in both the positive and negative directions. Ratios when the excess N_2 concentration was zero were not used in Figure 3.7.

The dissolved NO_3^- in groundwater was moderate at this site (50-210 µM NO_3^--N, Fig. 3.8). At other agricultural locations in the Choptank, groundwater NO_3^- ranges over 200-1000 µM (Fisher et al. 2010). The concentration was consistently between 100 and 200 µM NO_3^--N at the 3.9 m piezometer, and temporally varied most at the shallowest 2.1 m piezometer. NO_3^- concentrations in the soil water of the vadose zone were not measured.

Calculated diffusional flux of excess N_2, N_2O, and CO_2 from groundwater into the vadose zone

Groundwater concentrations of NO_3^-, excess N_2, and N_2O were measured monthly in 2006 (NO_3^- and excess N_2) and 2007 (N_2O). These data are used as the concentration data to estimate the missing N on the transect scale. The 2008-2010 data were not used because the data were not collected monthly. The median concentration of NO_3^- was higher at CREP2 than at CREP3, which was located on the hydraulic gradient below CREP2 (Fig. 3.9). The observed hydraulic gradient slopes from CREP2 to CREP3 (Sutton et al. 2010), and the piezometers are less than 10 m apart. We therefore assumed that the groundwater generally flowed from CREP2 to CREP3. The median concentrations of NO_3^-, NH_4^+, excess N_2-N, and N_2O-N at CREP2 and CREP3 were used to estimate N_{sum1} and N_{sum2} (Fig. 3.9). If all of the measured NO_3^-, NH_4^+, excess N_2-N, and N_2O-N at CREP2 (N_{sum1}) were detected down the hydraulic slope at CREP3 as either NO_3^-, NH_4, excess N_2-N, or N_2O-N, then we would estimate no loss of N to the vadose zone between the two piezometers. However, the median values at CREP2 and 3 indicated that only 71% of the N_{sum1} at CREP2 appeared at CREP3 as N_{sum2}, and that there was a median missing N of 138.5 µM N at CREP3. The missing N was potentially lost as N_2 or N_2O to the vadose zone via diffusion, diluted by local infiltration of low concentration N water, or consumed or transformed by other microbial or plant processes (Fig. 3.9).

The estimated excess N_2 and N_2O diffusional fluxes from the shallowest sampled groundwater piezometer to the deepest sampled vadose zone equilibration chamber from December 2008 through August 2010 are presented in Table 3.1. The missing N can be

converted from a missing concentration (138.5 µM N) to a diffusional flux that would need to occur between CREP2 and CREP3 (9.73 m apart) to account for the missing N. The diffusional flux required to create the missing N can be calculated by knowing the travel time and the vertical diffusion distance. The travel time can be calculated from the average hydraulic conductivity (0.51 m day^{-1}, Chapter 2) and was 19.2 days. The median distance over which the diffusion took place was 0.88 m, which was the difference between the shallowest piezometer (2.1 m) and the median depth to the water table in 2007 (1.2 m). The diffusional flux that would need to occur to produce a loss of N of 138.5 µM N between CREP2 and 3 would be 6,348 µmol m^{-2} d^{-1}. The calculated excess N_2-N fluxes from groundwater to the vadose zone ranged between 4.4 and 24 µmol m^{-2} d^{-1} and the calculated N_2O-N fluxes from groundwater to the vadose zone ranged between 0.2 and 1.4 µmol m^{-2} d^{-1} (Table 3.1). Together, these excess N_2-N and N_2O-N calculated fluxes only account for between 0.07 and 0.4 % of the flux that would be required to create a missing N of 138.5 µM. Therefore, the missing N between the two piezometers cannot be the result of a diffusional flux from groundwater to the vadose zone (Fig. 3.9), and the data do not support the hypothesis.

The alternative hypothesis was that some of the missing N at the transect scale was accounted for by plant uptake and/or dilution of low N infiltrating water. Peterjohn and Correll (1984) estimated N vegetative uptake within their riparian buffer to be 77 kg N ha^{-1} yr^{-1} or 1510 µmol N m^{-2} d^{-1}. N vegetative uptake at this rate between CREP2 and CREP3 could account for 24% of the missing N (6,348 µmol m^{-2} d^{-1}) on the transect scale.

Plant uptake appears to potentially be able to account for 24% of the missing N and dilution has the potential to account for the remaining missing N on the transect scale. In 2010, the cumulative increase in water table height due to infiltration events was 4.5 m (Fig. 3.4c). Corrected for porosity and an assumed yearly average %WFPS of 50% in the vadose zone, this water table height increase translates to 0.57 m^3 water m^{-2} land area. The median water table depth above the bottom of the piezometer at CREP3 was 0.88 m, or a porosity corrected water depth of 0.22 m or 0.22 m^3 water m^{-2} land area. As a maximum estimate, only 28% of the nitrogen from CREP2 would reach CREP3 if all of the infiltration mixed into the median porosity corrected water depth at CREP3. In contrast, I observed 71% of the N_{sum1} of CREP2 at CREP3 as N_{sum2}. Dilution by local recharge clearly has the potential to explain the missing N.

The N_2O/excess N_2 ratio is often used to understand the efficiency of denitrification. Locations efficient in denitrification are considered to have the majority of the denitrification product accumulating as excess N_2, while inefficient sites have large accumulations of N_2O. The N_2O/excess N_2 ratio of the calculated fluxes over the water table ranged from 0.02 to 0.21 (Table 3.1). This site often had a high dissolved N_2O/excess N_2 ratio, ranging from 0.02-0.26, but in the previous 2007 sampling period it was as high as 0.54 (Chapter 3). The majority of our other sites had dissolved N_2O/excess N_2 ratios in the range of 0.01 to 0.05 (Chapter 2).

The diffusive flux of excess CO_2 across the water table was high, but not always from groundwater to the vadose zone (Table 3.1). Sometimes the excess CO_2 concentration in the vadose zone exceeded the dissolved CO_2 concentration and caused a diffusive flux from the vadose zone into groundwater (Table 3.1). The flux into

groundwater was observed in June, July, and August, but not all of the dates within these months showed diffusional fluxes into groundwater. The fluxes across the water table ranged from -1730 to 1015 μmol m^2 day^{-1} (Table 3.1). Occasionally, a negative flux was observed within one transect, and a positive flux was observed in the other transect (e.g., August 6th 2009, Table 3.1). This variability illustrates the heterogeneity observed within soils even just meters apart and emphasizes the need for replication.

Calculated diffusional fluxes from the soil surface

Fickian diffusion was also used to estimate the flux of excess N_2, N_2O, and CO_2 from the soil surface. Concentration gradients were calculated from the shallowest equilibration chamber to the atmosphere, and are displayed in Table 3.2. The excess N_2-N concentration gradients ranged from -384 to +586 mmole N m^{-4}. The N_2O-N concentration gradients ranged from -0.01 to +0.88 mmole N m^{-4}, and the CO_2 concentration gradients ranged from +1100 to +7770 mmole m^{-4}. Large concentration gradients did not always translate into large fluxes from the soil surface because the diffusivity coefficient used in the calculation of diffusion can be greatly decreased by small volumetric air contents (equation 6).

The calculated diffusional fluxes of CO_2 from the soil surface were always positive, while both positive and negative excess N_2 and N_2O diffusional fluxes were calculated (Table 3.2). The calculated fluxes of CO_2 ranged from 10.9 to 180 mmol CO_2-C m^{-2} day^{-1}, the N_2O fluxes ranged from -0.0003 to 0.0019 mmol N_2O-N m^{-2} day^{-1}, and the excess N_2-N fluxes ranged from -11.9 to 17.3 mmol N_2-N m^{-2} day^{-1}.

The calculated fluxes from the soil surface were similar or considerably larger than the calculated fluxes from groundwater into the vadose zone. The N_2O flux estimates from groundwater into the vadose zone were bracketed within the range of N_2O fluxes from the soil surface, but the median flux from the soil surface (3 μ mol m^{-2} d^{-2}) was greater than the median flux from groundwater (0.64 μ mol m^{-2} d^{-2}). The calculated flux of excess N_2 from the soil surface (-12 to +17 mmol N_2-N m^{-2} d^{-1}, Table 3.2) was three orders of magnitude greater than the calculated flux from groundwater into the vadose zone (4-23 μmol N_2-N m^{-2} d^{-1}, Table 3.1). The highest flux of N_2-N from groundwater into the vadose zone was only 0.13% of the calculated highest flux from the soil surface. Note that Table 3.1 is expressed in units of μmol m^{-2} day^{-1} and Table 3.2 is expressed in units of mmol m^{-2} day^{-1}. The CO_2 flux estimates from the soil surface were always positive, while the CO_2 flux estimates were often into groundwater in the summer months. The highest calculated flux of CO_2 from groundwater into the vadose zone was only 0.4% of the highest CO_2 calculated flux from the soil surface.

This imbalance of gas flux across the water table and soil surface can be due to several reasons. (1) There is a smaller diffusivity coefficient for the groundwater to the vadose zone calculations because diffusion is much slower in a water-filled tortuous environment than a gas-filled tortuous environment. (2) The new vadose zone excess N_2 method may only be able to measure high concentrations of excess N_2; therefore, we are only capturing high concentrations in the vadose zone that result in the calculation of large flux estimates from the soil surface. (3) Production of N_2 and CO_2 in the vadose zone must be occurring to maintain this high flux from the soil surface. (4) Physical

processes enhance or decrease the N_2/Ar ratio in the vadose zone (discussed below). (5) The measurement error is large.

Discussion

The diffusive loss of excess N_2 and N_2O across the water table can only account for a small fraction of the N lost horizontally between two piezometers separated by 10 m (Table 3.1, Fig. 3.9). Other processes, such as plant uptake and dilution by local recharge, are likely to be responsible for the bulk of the missing N on the transect scale. Although the diffusive fluxes are small, they represent a transfer of N from groundwater to the vadose zone. Once excess N_2 and N_2O diffuses into or is produced in the vadose zone, it can be measured as excess N_2 and N_2O in the gas phase of the vertical profiles (Fig. 3.5), using the new method for excess N_2 described above. These profiles can be used to estimate the flux of excess N_2 and N_2O from the soil surface to the atmosphere (Table 3.2). The profiles, fluxes, and the accuracy of these fluxes are evaluated below in comparison to other values in the literature.

Gas profiles

The excess N_2 and N_2O gas profiles are dominated by the large dissolved excess N_2 and N_2O concentrations in groundwater (Fig. 3.5 A,B). The partial pressure of excess N_2 was moderate in comparison to other sites that I have investigated on the Delmarva Peninsula (Fisher et al. 2010), but were still large. The partial pressure of N_2O at all three piezometers is very large compared to other sites (Fisher et al. 2010, Chapter 2); the concentrations reported here are among the highest that I have observed on the Delmarva Peninsula. There is evidence of production of excess N_2 and N_2O within the vadose zone, but the largest partial pressures were observed in groundwater. We have shown that

there was substantial excess N_2 and N_2O accumulation in the groundwater flow paths under this riparian area that borders an agricultural field.

The high concentrations of N_2O observed in groundwater (4.2 to 38.4 μM N_2O-N) did not translate into large concentrations in the vadose zone (Fig. 3.5B & 3.6B). Once N_2O has diffused from groundwater into the vadose zone, the N_2O can be absorbed into the vadose soil water where it can be further reduced to N_2. Clough et al. (1999) showed that N_2O injected at depth could be denitrified further to N_2 after passage through the subsoil. Therefore, the low concentrations of N_2O in the upper soil horizon could be the result of further reduction of N_2O to N_2 upon its journey towards the soil surface through the more oxic, upper soil horizons (Fig. 3.5D).

The CO_2 profiles were controlled by the concentration of CO_2 below 1 m in the soil column. However, the highest concentrations were not always observed in groundwater. Large concentrations of excess CO_2 were observed in the soil profile (0.5-2mM), with considerable variability observed in the vadose zone (Fig. 3.6C). Concentrations of CO_2 in the vadose zone increased to levels greater than dissolved in groundwater in the summer months likely due to increased respiration in the vadose zone (Fig. 3.5C). We have shown that substantial concentrations of CO_2 accumulate in groundwater and the deeper vadose zone depths (1-3 mM).

The ratio of N_2O/excess N_2 is very high in groundwater at this site (0.05-0.25). N_2O was either an important end product of denitrification as well as N_2, or the N_2O accumulated through nitrification. The concentration of O_2 is quite low at the three nested piezometers (Fig. 3.5D); therefore, the N_2O is likely produced through denitrification as nitrification is an aerobic process. N_2O is favored as the denitrification

end product at O_2 levels that are low enough, but not optimal, for denitrification. N_2O reductase is limited by moderate O_2 concentrations more than the other reduction enzymes (Otte et al. 1996); therefore, at the upper O_2 denitrification limit, N_2O can build to high concentrations. Although the groundwater N_2O/excess N_2 ratio was high (0.02 to 0.26), other researchers have reported situations where N_2O was the dominant denitrification end product in soils (Mathieu et al. 2006, Ruser et al. 2006). Similarly, high N_2O accumulations have been observed to accumulate in hypoxic and suboxic ocean waters because oxygen concentrations are sufficiently low for either denitrification or nitrification derived N_2O production (Codispoti and Christensen 1985, Codispoti 2010).

In contrast with groundwater, the N_2O/excess N_2 ratio in the vadose zone was often quite low (<0.02) due to large excess N_2 and low N_2O concentrations (Fig. 3.7). Although the excess N_2-N concentrations in the vadose zone were large, we observed large partial pressures of excess N_2 in groundwater. If the dissolved N_2O that diffused into the vadose zone was reduced to N_2 within the vadose zone, then this is another source that is potentially fueling the excess N_2 profile.

Missing N on the transect scale

We were unable to account for all of the missing N on the transect scale through diffusion of N_2 out of groundwater and into the vadose zone. Diffusion in water is a slow process, and soils have a low porosity (20-40%) and are highly tortuous; therefore, a low flux across the water table is not surprising. The additional missing N is potentially taken up by plants or diluted by the local infiltration of water with low N concentrations through the buffer (Fig. 3.9). My calculations indicated that plant uptake could account

for approximately 24% of the missing N and that dilution by local groundwater recharge with low N has sufficient magnitude to explain the remaining missing N on the transect scale. Another possible explanation is that our assumption that the groundwater that flowed from CREP2 could be sampled later at CREP3 is invalid. Groundwater flow paths can be complex (e.g., Chapter 2), but it is generally thought that they flow in curved flow paths from the point of infiltration to the point of emergence in a surface water body. It is possible that we sampled two completely different flow paths. However, I lacked major ion data at this site to test this idea. Although we could only account for between 0.1 and 0.53 % of the missing N at the transect scale by diffusion, we were able to detect differences in the vadose zone concentrations of excess N_2 that were caused by a diffusive flux from groundwater and/or by production of excess N_2 within the vadose zone.

Flux evaluation

The N_2O and CO_2 flux estimates to the atmosphere represent the flux driven by the elevated concentrations at the 0.25 m vadose zone sampler. However, fluxes of N_2O and CO_2 from above the 0.25 m equilibration chamber were not captured in this study, and our estimated N_2O fluxes are within the low end of N_2O-N fluxes summarized by Eichner (1990). The concentration of N_2O within the vadose zone was low, but other researchers have reported large fluxes of N_2O that originated from the top 5 cm of soil (e.g., Breuer et al. 2000).

The CO_2 flux estimates were large, but within the range of values reported by other investigators. Pacific et al. (2008) reported CO_2 surface flux values from a riparian

area and adjacent hillslope in Montana to range from approximately 170 to 780 mmol m^{-2} day^{-1} over the months June through August, which is the same time that we sampled. Mander et al. (2008) reported a similar range of CO_2 fluxes for riparian buffers, ranging from median site values of 50-66 mmol m^{-2} day^{-1} for the gray alder sites and a median value of 480 mmol m^{-2} day^{-1} from the black alder riparian location with a lowered water table. I believe that our N_2O and CO_2 flux estimates compare well with other reported values and represent actual fluxes of N_2O and CO_2 from the soil surface. As part of my post doctorial research I will use chamber methods to evaluate whether the calculated N_2O and CO_2 fluxes to the atmosphere are reasonable and within range of what I would calculate from the soil surface based upon the measured soil gas concentration on that day.

I was able to calculate the flux of excess N_2 from the soil surface using the excess N_2 vadose zone profiles. The range of flux estimates was from -12 to 17 mmoles N_2-N m^{-2} day^{-1} (Table 3.2). If no additional excess N_2-N was produced in the vadose zone and the dissolved N_2 in groundwater was the only source of N_2, then between 3.5 and 6.7 µmol N_2-N m^{-2} day^{-1} would have diffused over the soil surface. The concentration gradient is calculated from CREP3 in groundwater directly to the atmosphere. The resulting flux estimates are 1000 times lower than the calculated flux estimates from the soil surface (-12 to 17 mmoles N_2-N) which suggests that production in the vadose zone is a large source of excess N_2-N.

It is important to evaluate whether these computed flux estimates represent an actual flux of excess N_2 across the soil surface or whether these apparent excess N_2 fluxes are influenced by other processes. Although the positive flux estimates are large, they do

fall within the range of values reported by other researchers (e.g., Lindau et al. 1990). Mander et al. (2008) reported N_2-N fluxes from riparian alder stands to range from 360 to 1,200 kg ha^{-1} yr^{-1} which are similar to our positive excess N_2-N values (-610 to 880 Kg N ha^{-1} yr^{-1}, Table 3.2). I only measured the concentration of excess N_2 in the vadose zone in the months when the vadose zone was present. Therefore, I have few flux estimates for late fall, winter, or early spring when the vadose zone was small (Fig. 3.4C). At this time lower excess N_2 flux values might occur, or at least a lower soil diffusivity coefficient would be calculated due to the cooler temperatures and increased soil volumetric water content. I was also only able to detect moderate to large excess N_2 concentrations; therefore, low excess N_2 flux estimates were missed.

The negative excess N_2-N fluxes are more difficult to explain from a biological perspective (Table 3.2). Fulweiler et al. (2007) measured nitrogen fixation as a negative change in the N_2/Ar ratio in estuarine sediments; however, given the large amounts of NH_4^+, NO_2^-, and NO_3^- at the agricultural site investigated here, nitrogen fixation is not likely to be the cause of the negative ratio changes, especially at the greater depths. We do not believe that the negative excess N_2-N values and flux estimates represent an actual flux of excess N_2 into the soil, but instead are the result of the physical processes described below that are associated with temperature changes that occur in soils and groundwater (Fig. 3.4). However, the positive excess N_2-N values could be measuring an actual excess N_2 flux, but our estimates might be enhanced or reduced by soil physical processes.

Currently, the flux of excess N_2 from the soil surface can be constrained only to within -12 to 17 mmoles N_2-N m^{-2} day^{-1} by directly measuring excess N_2 concentration

gradients in the vadose zone and calculating a diffusional flux from the soil surface. In comparison to typical crop field fertilization rates of 50-150 kg N ha^{-1} yr^{-1}, the calculated soil flux rates are up to six times greater (-610 to 880 Kg N ha^{-1} yr^{-1}, Table 3.2). This excess N_2 range is quite large, but it is the first attempt at directly measuring the excess N_2 concentration within the vadose zone of soils *in situ*. If the assumption is made that the largest calculated soil surface flux of 881 Kg N ha^{-1} yr^{-1} (Table 3.2) is due to biological nitrogen reduction within riparian buffers, this flux scaled to riparian areas in the nearby German Branch watershed within the Choptank Basin could account for as much as 26% of the missing N within that watershed (Fisher et al. in prep). This calculation assumes a constant 10 m buffer width along the entire German Branch stream network and also does not take into account additional N reduction in areas other than riparian areas. If areas other than riparian areas were added into this calculation we could account for more of the missing N within this watershed. Although the calculated fluxes are likely affected by both biological and physical processes, similar magnitude fluxes could account for the missing N at the watershed scale.

Processes influencing vadose zone N_2 and Ar composition

I calculated the concentration of excess N_2 assuming that the Ar concentration remained at the atmospheric concentration in the vadose zone. Unfortunately, the concentrations of N_2 and Ar are affected by physical processes in addition to biology, but these physical effects can potentially be accounted for. We discuss below the biological and physical mechanisms that affect the concentrations of N_2 and Ar in the vadose zone. The calculated magnitude of each physical process can be found in Table 3.3.

There are multiple N_2 source and loss terms in the vadose zone (Table 3.3). These include the biological processes of denitrification, anammox, and nitrogen fixation, and the physical processes of solubility-driven diffusion, bubble formation and dissolution (excess air), CH_4 ebullition events, and evaporation. The concentration of Ar can also vary but only due to physical processes. These groups of processes influencing gas concentration are discussed below.

Biological processes

Denitrification and nitrogen fixation may contribute significantly to changes in the vadose zone N_2/Ar ratio (Table 3.3). We measured the N_2/Ar ratio to calculate excess N_2 concentrations, which were assumed to be the end product of denitrification. Ideally, any increase in the N_2/Ar ratio would be due to biological processes that produced excess N_2. In contrast, nitrogen fixation could cause a deficit in N_2 gas, and ideally, any decrease in the N_2/Ar ratio would be assumed to be due to this process. Unfortunately, the soil physical system is complex, and changes in soil properties have the potential to affect the N_2/Ar ratio as well.

Solubility driven changes

Physical processes influencing dissolved gases in groundwater can be a source of both N_2 and Ar to the vadose zone (Table 3.3). Groundwater recharge following rain events primarily occurs during the cooler months in the Mid-Atlantic region (Fig. 3.4). Infiltrating water acquires its dissolved gas concentrations from the atmosphere as rainfall or from the soil gases as it percolates through the soil to the water table to

become groundwater. Seasonal changes in groundwater, soil, and air temperature cause higher gas solubility in water when it is cooler (winter) and lower solubility when it is warmer (summer). Furthermore, N_2 is less soluble than Ar in water, and the negative effect of increasing temperature on Ar solubility is slightly stronger than on N_2 solubility. This results in a small, nearly linear, increasing temperature effect on the N_2/Ar ratio in equilibrium with air of almost 0.2%/^{o}C (Fig. 3.10). In contrast to seasonal changes in dissolved N_2/Ar, atmospheric N_2/Ar is constant at 83.6. Therefore, infiltrating rain will bring seasonally varying amounts of N_2 and Ar gas to groundwater.

Groundwater has long residence times, and heat conduction through the soil causes seasonal changes in groundwater temperature (Fig. 3.4D). Increasing groundwater temperature in the spring causes the supersaturation of both N_2 and Ar, but the increasing temperature effect has a greater effect in Ar partial pressure due to its relatively lower solubility in warmer water. Due to the higher partial pressure increase, more Ar will diffuse out of the cold groundwater as it warms than N_2, resulting in an increased N_2/Ar in groundwater and a decreased vadose zone N_2/Ar ratio (Table 3.3). Conversely, warm groundwater cooling in fall and winter will preferentially absorb Ar from the soil gases, lowering the N_2/Ar in groundwater and enhancing the vadose zone N_2/Ar ratio.

Infiltration events in the fall and winter may also change N_2/Ar. This process in the fall is potentially less likely to affect the N_2/Ar ratio within the vadose zone if we make the assumption that the infiltrating water is in equilibrium with the atmosphere during its fall to the earth. If the air temperature is similar to the groundwater temperature, then little effect from infiltrating water is likely as the solubility differences

will be negligible. If the air temperature is cooler than the groundwater temperature, the infiltrating water could decrease the N_2/Ar ratio.

The following example is provided to quantify the effect of changing groundwater temperature. If the temperature of infiltrating groundwater in winter is 7°C (see Fig. 3.12) and at equilibrium with the atmosphere, the concentrations in the recharging groundwater will be 692.9 μmole N_2 L^{-1} water and 18.53 μmole Ar L^{-1} water (Fig. 3.12A). I will call this water "groundwater parcel 1" (GW1) as it moves along the groundwater flow path indicated by arrows (Fig. 3.12). Throughout the spring as the groundwater gradually warms (Fig. 3.12B), the concentrations of N_2 and Ar could potentially remain at the equilibrium concentrations of 7°C if there was some hydrostatic pressure from overlying groundwater and limited exposure to the vadose zone (Fig. 3.12B). The calculated groundwater Ar recharge temperatures at the study location ranged from 6-17 °C with a median value of 12°C. By spring, the groundwater warms to 12 °C (Fig. 3.12B) and now has concentrations greater than would be present in equilibrium with air at the warmer *in situ* temperature of 12°C (Fig. 3.12B). When evapotranspiration increases in summer, groundwater levels fall and temperature increases to 19°C (Fig. 3.4), allowing groundwater parcel GW1 from the previous winter to interact with the vadose zone (Fig. 3.12C). At this point, the gases dissolved in excess of equilibrium will diffuse from groundwater into the vadose zone. A maximal change due to solubility-driven differences is illustrated in Figure 3.12C by assuming isolation of the groundwater from the vadose zone until a summer sampling. This diffusional flux of N_2 and Ar out of groundwater and into the vadose zone due to temperature driven solubility changes would not be associated with a biological process, but could be

detectable in the N_2/Ar ratio and could be mistakenly assigned to a biological process. For the example given in Figure 3.12, if 1 m^3 of groundwater which recharged at 7^oC comes into equilibration with 1 m^3 of gas in the vadose zone at 19^oC, the solubility driven changes would result in net increases of 151.8 μM N_2-N and 4.34 μM Ar in the vadose zone, reducing the N_2/Ar ratio by 0.64%, which is easily detectable by our 0.05% precision. This calculation assumed that all of the equilibrium excess N_2 and Ar diffused into the vadose zone at once, and it illustrates the largest possible solubility driven effect. This example is not realistic, but does demonstrate the maximum effect solubility differences could have on the ratio. The solubility mechanism described could explain the negative N_2/Ar values that result in an apparent N_2 depletion observed in both July and August and could also explain why the N_2 depletion increased with depth as the sampling approached groundwater (Fig. 3.5A). Similarly, the positive excess N_2 values seen in December and October could be partially due to the reverse effect, a flux of N_2 and Ar from the vadose zone redissolving into the cooling groundwater.

Excess air and air entrapment

Another physical process that could result in an apparent excess of N_2 in both groundwater and the vadose zone is air entrapment. Frequent fluctuations in the water table such as those shown in the summer of 2009 or both winters in Figure 3.4C, can lead to air entrapment within the soil matrix below the water table. Entrapped air has been measured to be as much as 10% of the soil bulk volume (Faybishenko 1995 and citations within). Entrapped air bubbles within quasi-saturated soils, or soils with entrapped air, could result in higher proportions of dissolved excess air within groundwater. The

hydrostatic pressure of the rising water table can partially or completely collapse entrapped air bubbles. With such a large potential volume of entrapped air, it is unlikely that all of the air bubbles would be completely dissolved, as the hydrostatic pressure would not be sufficient (Aeschbach-Hertig et al. 2008).

Aeschbach-Hertig et al. (2000, 2008) have proposed a closed-system equilibration (CE) model that allows for partial dissolution of gases from the entrapped air due to the hydrostatic pressure upon the bubble.

$$c_{iw} = c_{iw}^{eq}\left(\frac{1+AH_i}{1+FAH_i}\right) \tag{8}$$

$$F = \frac{B}{A} \tag{9}$$

where C_{iw} is the concentration of gas i in water, C_{eq}^{iw} is the concentration of gas i in air-equilibrated water, A is equal to the initial volume of air (V_a) in the entrapped bubble divided by the volume of initially air-equilibrated water (V_b), B (V_b/V_w) is the final volume of the bubble after partial or complete collapse over the volume of water (V_w), F is the CE-model fractionation parameter which is the ratio of the final to the initial bubble volumes, and H_i is the Henry's constant. The Henry's constants were obtained from Benson and Krause (1976) and converted to the dimensionless form necessary for the calculation (Sander 1999). The model was developed for noble gases, which are only affected by physical processes, unlike nitrogen gas. Therefore, we used this model to calculate background N_2. The ratio of N_2/Ar dissolved in water increases no matter how large the bubble, how much of the bubble is dissolved, or what the temperature is (Fig. 3.10). As a bubble is forced into solution, more N_2 would be forced to dissolve above

equilibrium than Ar. Excess air will cause a stronger N_2 gradient out of groundwater relative to an Ar gradient, thereby increasing the N_2/Ar ratio in the vadose zone. The partially collapsed, entrapped air bubble would undergo the opposite effect, and the N_2/Ar ratio within the air bubble would decrease. When the water table dropped and the bubbles were reintroduced into the vadose zone, the soil gas N_2/Ar ratio could decrease if sufficient trapped air was present.

Ingram et al. (2007) have shown that there is a significant relationship between mean annual water table fluctuations and the % of Ne present over saturation from excess air

$$\% \Delta Ne = [(Ne_{[sample]}/Ne_{[air\ equilibrium]}) - 1] \times 100\% \quad (10)$$

Neon is often used to quantify the contribution of excess air in groundwater because of its relatively high abundance in groundwater, lack of a radiogenic component (e.g., He), and relative insensitivity to equilibrium temperature (Andrews 1991). Multiple noble gas tracers allow multiple estimates of groundwater recharge temperature, but these estimates will be different if excess air is present because the ratio of the gas solubility is different from the gas volume ratios in air (Wilson and McNeill 1997). Models have been developed to determine the corrected groundwater recharge temperature from multiple noble gas measurements and to determine the amount of excess air entrained in a groundwater sample (e.g; Aeschbach-Hertig et al. 2000). The largest water table fluctuation observed at our research site in 2007 was ~ 2.5 m, which corresponds to a % ΔNe of 50% based on Ingram et al (2007). In 2009, the water table did not decrease more than 1.5 m below the surface, and mostly remained within 0.5 m of the surface or less

(Fig. 3.4a). This fluctuation would result in a % ΔNe value of less than 10%. These estimates indicate that the physical process of excess air dissolution could potentially influence the N_2/Ar ratio in the vadose zone, and further noble gas sampling is needed to estimate the effect of excess air on accumulated N_2 and Ar in the groundwater of this site.

Degassing events

Methane ebullition and the subsequent stripping of N_2 and Ar has been documented to occur in groundwater when methane concentrations are high (Mookherji et al. 2003, Fortuin and Willemsen 2005, Chapter 2). Blicher-Mathiesen et al. (1998) have also reported ebullition of N_2 that resulted in Ar stripping. We have documented evidence for CH_4 ebullition at other sites on the Delmarva Peninsula (Fisher et al. 2010, Chapter 2), but we have not observed CH_4 ebullition events at the site described here. Bubbles caused by CH_4 supersaturation will strip both N_2 and Ar from groundwater. As N_2 is less soluble than Ar, N_2 concentrations in groundwater will be stripped more than Ar. When the gas bubbles reach the vadose zone, relatively more N_2 than Ar will be released potentially increasing the N_2/Ar ratio.

Evaporation and wicking

Evaporation and the subsequent wicking of replacement water from a deeper depth could also cause a decrease in the N_2/Ar ratio. In the summer, surface soils are warmer than deeper soils due to solar radiation warming the soil surface. Evaporation of

water occurs from the soil surface, and replacement water from a deeper depth is wicked up via capillary action. If deeper soil water in equilibrium with cooler temperatures is pulled to a shallower depth that is warmer, the gas that diffuses out of the deeper water will be relatively enriched in Ar, which will cause a decrease in the N_2/Ar ratio. As an example, assume that all of the water from the top 5 cm of soil with a porosity of 0.38 m^3 m^{-3} with a % WFPS of 6.75%, is evaporated and that an equivalent amount of water wicks up from deeper depths to replace the evaporated water. If the temperature at the shallower depth (5 cm) is 28 ^oC and at the deeper depth (30 cm) the temperature is 22 ^oC with a %WFPS of 11%, then we could have a decrease in the N_2/Ar ratio of 0.04%. Although this is a small decrease, this could potentially be detected as a negative 14/40 ratio.

Atmospheric flushing

A potential criticism for using excess N_2 to measure denitrification directly in the gas phase is that excess N_2 would not build to a detectable level before the profile was flushed to the atmosphere. Flushing of the vadose zone can occur through infiltration events or atmospheric pressure changes (Chapter 4). Soil texture and structure greatly influence the connectivity between the soil and the free atmosphere, and therefore the flushing time of the vadose zone. Sandier soils have a higher connectivity than fine textured soils (Paul 2007) such as those on the farm on which the measurements were made. 2009 was a very wet year, and not only was there very little vadose zone, there was also a lot of infiltration-induced flushing. We have been able to measure changes in

the 14/40 ratio in the gas phase of the vadose zone, and, therefore the flushing of the vadose zone appears to be slower than the processes changing the gas composition.

Conclusions

I was able to calculate fluxes of excess N_2 from the soil surface using the excess N_2 profile measured directly in the vadose zone of soils. We calculated the excess N_2 concentration by directly measuring the N_2/Ar ratio in the vadose zone and the reported measurements are the first reported direct *in situ* N_2/Ar measurements in the vadose zone. N_2 can be affected by both biological and physical processes, whereas Ar can only be affected by physical processes. We calculated diffusive fluxes of excess N_2 from the soil surface in the range of -12 to 17 mmoles N_2-N m^{-2} day^{-1}. The N_2O and CO_2 flux estimates were in the range of values measured by other researchers. I believe that the negative fluxes are the result of the physical processes outlined above, and that the positive fluxes are potentially measuring a net flux of excess N_2 out of the soil surface, although these fluxes could be enhanced or reduced by soil physical processes. Currently it is not possible to separate the physical and biological processes affecting the N_2/Ar ratio in the vadose zone, but I hope to estimate the soil physical processes in future research by adding additional noble gas measurements (e.g., neon, krypton, xenon) to separate the biological and physical processes. The N_2 and Ar concentrations will be corrected for some of the physical effects mentioned above by creating an appropriate model for the vadose zone using the noble gases. Also, the Ar concentration can be measured more precisely with the noble gas method which would eliminate the necessity for the assumption that the Ar concentration was at the atmospheric concentration. If we can account for the physical processes using noble gas measurements, this method could be used to estimate the flux of excess N_2 from the soil surface which would help find the "missing N" on the watershed scale.

References

Aeschbach-Hertig, W., F. Peeters, U. Beyerle, and R. Kipfer. 2000. Palaeotemperature reconstruction from noble gases in groundwater taking into account equilibration with entrapped air. Nature. 405:1040-1044.

Aeschbach-Hertig, W., H. El-Gamal, M. Wieser, L. Palcsu. 2008. Modeling excess air and degassing in groundwater by equilibrium partitioning with a gas phase. Water Resources Research. 44:1-12.

Anderson, D.M., J.M. Burkholder, M.P. Cochlan, P.M. Glibert, C.J. Gobler, C.A. Heil, R.M. Kudela, M.L. Parsons, J.E.J. Rensel, D.W. Townsend, V.L. Trainer, G.A. Vargo. 2008. Harmful algal blooms and eutrophication: Examining linkages from selected coastal regions of the United States. Harmful Algae. 8:39-53.

Andrews, J.N. 1991. Noble gases and radioelements in groundwater. In Downing R.A., Wilkinson W.B. (ed.). Applied Groundwater Hydrology, Oxford University Press, pp 243-265.

Benson, B.B., D. Krause, Jr. 1976. Empirical laws for dilute aqueous solutions of nonpolar gases. The Journal of Chemical Physics. 64(2):689-709.

Blicher-Mathiesen, G.W. McCarty, L.P. Nielsen. 1998. Denitrification and degassing in groundwater estimated from dissolved dinitrogen and argon. Journal of Hydrology. 208:16-24.

Bohlke, J.K., J.M. Denver. 1995. Combined use of groundwater dating, chemical, and isotopic analyses to resolve the history and fate of nitrate contamination in

two agricultural watersheds, Atlantic coastal plain, Maryland. Water Resources Research. 31(9):2319-2339.

Burgin, A.J., S.K. Hamilton. 2007. Have we overemphasized the role of denitrification in aquatic ecosystems? A review of nitrate removal pathways. Frontiers in Ecology and the Environment. 5(2):89-96.

Breuer, L., H. Papen, K. Butterbach-Bahl. 2000. N_2O emission from tropical forest soils of Australia. Journal of Geophysical Research. 105(D21):26,353-26,357.

Clapp, R.B., G.M. Hornberger. 1978. Empirical equations for some soil hydraulic properties. Water Resources Research. 14(4):601-604.

Clough, T.J., S.C. Jarvis, E.R. Dixon, R.J. Stevens, R.J. Laughlin, D.J. Hatch. 1999. Carbon induced subsoil denitrification of ^{15}N-labelled nitrate in 1 m deep soil columns. Soil Biology and Biochemistry. 31:31-41.

Codispoti, L.A., J.P. Christensen. 1985. Nitrification, denitrification and nitrous oxide cycling in the eastern tropical South Pacific Ocean. Marine Chemistry. 16:277-300.

Codispoti, L.A., 2010. Interesting times for marine N_2O. Science. 327:1339-1340.

Colt, J. 1984. Computation of dissolved gas concentrations in water as functions of temperature, salinity, and pressure. Bethesda, MD: American Fisheries Society.

Crutzen, P.J., 1981. Atmospheric chemical processes of the oxides of nitrogen, including N_2O. In Delwiche,C.C.(ed.). Denitrification, Nitrification, and Atmospheric Nitrous Oxide. Wiley, pp.17-44.

Eichner, M.J. 1990. Nitrous oxide emissions from fertilized soils: Summary of available data. Journal of Environmental Quality. 19:272-280.

Faybishenko, B.A. 1995. Hydraulic behavior of quasi-saturated soils in the presence of entrapped air: Laboratory experiments. Water Resources Research. 31:2421-2435.

Fisher, T.R., T.E. Jordan, K.W. Staver, A.B. Gustafson, A.I. Koskelo, R.J. Fox, A.J. Sutton, T. Kana, K.A. Beckert, J.P. Stone, G.W. McCarty, M.W. Lang. 2010. The Choptank Basin in transition intensifying agriculture, slow urbanization, and estuarine eutrophication. In Kennish M.J., Paerl H.W (ed.). Coastal Lagoons Critical Habitats of Environmental Change, CRC Press, pp 135-165.

Fisher, T.R., R.J. Fox, A.B. Gustafson, T.E. Jordan, K.W. Staver, M. Fogel, M. Altabet, T. Kana. In prep. The search for the missing N.

Fortuin, N.P.M., A. Willemsen. 2005. Exsolution of nitrogen and argon by methanogenesis in Dutch groundwater. Journal of Hydrology. 301:1-13.

Fulweiler, R.W., S.W. Nixon, B.A. Buckley, S.L. Granger. 2007. Reversal of the net dinitrogen gas flux in coastal marine sediments. Nature. 448:180-182.

Hamborg, E.S, P.W.J. Derks, S.R.A. Kersten, J.P.M. Niederer, G.F. Verstegg. 2008. Diffusion coefficients of N_2O in aqueous piperazine solutions using the Taylor Dispersion technique from (293 to 333) K and (0.3 to 1.4) $mol \cdot dm^{-3}$. Journal of Chemical Engineering Data. 53:1462-1466.

Heincke, M., M. Kaupenjohann. 1999. Effects of soil solution on the dynamics of N_2O emissions: A review. Nutrient Cycling in Agroecosystems. 55:133-157.

Howarth, R.W., G. Billen, D. Swaney, A. Townsend, N. Jaworski, K. Lajtha, J.A. Downing, R. Elmgren, N. Caraco, T. Jordan, F. Berendse, J. Freney, V. Kudeyardov, P. Murdoch, Z. Zhao-Liang. 1996. Regional nitrogen budgets and riverine N & P fluxes for the drainages to the North Atlantic Ocean: Natural and human influences. Biogeochemistry. 35(1):75-139.

Ingram, R.G.S., K.M. Hiscock, P.F. Dennis. 2007. Noble gas excess air applied to distinguish groundwater recharge conditions. Environmental Science Technology. 41:1949-1955.

IPCC (Intergovernmental Panel on Climate Change), 2007. Climate change 2007-The physical science basis. Contribution of working group I to the forth assessment report of the IPCC. Cambridge University Press, Cambridge.

Jetten, M.S.M. 2001. New pathways for ammonia conversion in soil and aquatic systems. Plant and Soil. 230(1):9-19.

Jordan, T.E., D. W. Weller. 1996. Human contributions to terrestrial nitrogen flux. BioScience 46(9):655-664.

Kana, T.M., C. Darkangelo, M.D. Hunt, J.B. Oldham, G.E. Bennett, J.C. Cornwell. 1994. Membrane inlet mass spectrometer for rapid high-precision determination of N_2, O_2 and Ar in environmental water samples. Analytical Chemistry. 66(23):4166-4170.

Kemp, W.M., W.R. Boynton, J.E. Adolf, D.F. Boesch, W.C. Boicourt, G. Brush, J.C. Cornwell, T.R. Fisher, P.M. Glibert, J.D. Hagy, L.W. Harding, E.D. Houde, D.G. Kimmel, W.D. Miller, R.I.E. Newell, M.R. Roman, E.M. Smith, J.C.

Stevenson. 2005. Eutrophication of Chesapeake Bay: Historical trends and ecological interactions. Marine Ecology Progress Series. 303:1-29.

Knowles, R. 1982. Denitrification. Microbiological Reviews. 46(1):43-70

Lange, N.A., 1961. Handbook of Chemistry and Physics. New York, NY, McGraw-Hill Book Company, Inc.

Lee, K., T.R. Fisher, E. Rochelle-Newall. 2001. Modeling the hydrochemistry of the Choptank River basin using GWLF and Arc/Info: 2. Model validation and application. Biogeochemistry. 56:311-348.

Lindau, C.W., W.H. Patrick Jr., R.D. Delaune, K.R. Reddy. 1990. Rate of accumulation and emission of N_2, N_2O and CH_4 from a flooded rice soil. Plant and Soil. 129:269-276.

Maharajh, D.M., J. Walkley. 1973. The temperature dependence of the diffusion coefficients of Ar, CO_2, CH_4, CH_3Cl, CH_3Br, and $CHCl_2F$ in water. Canadian Journal of Chemistry. 51:944-952.

Mander, Ü., K. Lõhmus, S. Teiter, V. Uri, J. Augustin. 2008. Gaseous nitrogen and carbon fluxes in riparian alder stands. Boreal Environment Research. 13:231-241.

Massman, W.J. 1998. A review of the molecular diffusivities of H_2O, CO_2, CH_4, O_3, SO_2, NH_3, N_2O, NO, and NO_2 in air, O_2 and N_2 near STP. Atmospheric Environment. 32(6):1111-1127.

Mathieu, O., J. Lévêque, C. Hénault, M.-J. Milloux, F. Bizouard, F. Andreux. 2006. Emissions and spatial variability of N_2O, N_2 and nitrous oxide mole fraction at

the field scale, revealed with ^{15}N isotopic techniques. Soil Biology and Biogeochemistry. 38(5):941-951.

Moldrup, P., T. Olesen, T. Yamaguchi, P. Schjonning, and D. Rolston. 1999. Modeling diffusion and reaction in soils: IX. The Buckingham-Burdine-Campbell equation for gas diffusivity in undisturbed soil. Soil Science. 164:542-551.

Mookherji, S., G.W. McCarty, J.T. Angier. 2003. Dissolved gas analysis for assessing the fate of nitrate in wetlands. Journal of the American Water Resources Association. 39(2):381-387.

Mulder, A., A.A. Vandergraaf, L.A. Robertson, J.G Kuenen. 1995. Anaerobic ammonium oxidation discovered in a denitrifying fluidized-bed reactor. FEMS Microbiology Ecology 16(3):177-183.

Otte, S., N.G. Grobben, L.A. Robertson, M.S.M Jetten, J.G. Kuenen. 1996. Nitrous oxide production by *Alcaligenes faecalis* under transient and dynamic aerobic and anaerobic conditions. Applied and Environmental Microbiology. 62(7):2421-2426.

Owens, J.P., and C.S. Denny. 1979. Upper Cenozoic deposits of the central Delmarva Peninsula, Maryland and Delaware. US Geological Survey Professional Paper 1067-A.

Pacific, V.J., B.L. McGlynn, D.A. Riveros-Iregui, D.L. Welsch, H.E. Epstein. 2008. Variability in soil respiration across riparian-hillslope transitions. Biogeochemistry. 91:51-70.

Paul, E.A. (ed), 2007. Soil Microbiology, Ecology, and Biochemistry, Academic Press, pp 532.

Peterjohn, W.T., D.L. Correll. 1984. Nutrient dynamics in an agricultural watershed: Observations on the role of a riparian forest. Ecology. 65(5):1466-1475.

Popovičová, J., M.L. Brusseau. 1997. Dispersion and transport of gas-phase contaminants in dry porous media: Effects of heterogeneity and gas velocity. Journal of Contaminant Hydrology. 28:157-169.

Raghoebarsing, A.A., A.Pol, K.T. Van de Pas-Schoonen, A.J.P. Smolders, K.F. Ettwig, W.I.C. Rijpstra, S. Schouten, J.S.S. Damste, H.M.M. Op den Camp, M.S.M. Jetten, M. Strous. 2006. A microbial consortium couples anaerobic methane oxidation to denitrification. Nature. 440:918-921. DOI:10.1038/nature04617.

Ruser, R., H. Flessa, R. Russow, G. Schmidt, F. Buegger, J.C. Munch. 2006. Emissions of N_2O, N_2 and CO_2 from soil fertilized with nitrate: Effect of compaction, soil moisture and rewetting. Soil Biology and Biochemistry. 38:263-274.

Sander, R. 1999. Compilation of Henry's Law constants for inorganic and organic species of potential importance in environmental chemistry (Version 3) http://www.henrys-law.org

Schaefer, S. C. and M. Alber. 2007. Temperature controls a latitudinal gradient in the proportion of watershed nitrogen exported to coastal ecosystems. Biogeochemistry. 85:333-346.

Silver, W.L., A.E. Lugo, M. Keller. 1999. Soil oxygen availability and biogeochemistry along rainfall and topographic gradients in upland wet tropical forest soils. Biogeochemistry. 44:301-328.

Soil Survey Staff, Natural Resources Conservation Service, United States Department of Agriculture. Web Soil Survey. Available online at http://websoilsurvey.nrcs.usda.gov/ accessed [07/01/2011].

Stainton, M.P. 1973. A syringe gas-stripping procedure for gas-chromatographic determination of dissolved inorganic and organic carbon in fresh water and carbonates in sediments. Journal of Fisheries Research Board of Canada. 30:1441-1445.

Staver, K.W., R.B. Brinsfield. 2001. Agriculture and water quality on the Maryland eastern shore: Where do we go from here? Bioscience 51:859-868.

Staver, K.W., R.B. Brinsfield. 1998. Using cereal grain winter cover crops to reduce groundwater nitrate contamination in the Mid-Atlantic coastal plain. The Journal of Soil and Water Conservation. 53(3):230-240.

Sutton, A.J., T.R. Fisher, A.B. Gustafson. 2010. Effects of restored stream buffers on water quality in non-tidal streams in the Choptank River basin. Water Air and Soil Pollution. 208(1-4):101-118. DOI: 10.1007/s11270-009-0152-3

Weiss, R.F. 1970. The solubility of nitrogen, oxygen and argon in water and seawater. Deep Sea Research and Oceanographic Abstracts. 17(4):721-735.

Weiss, R.F., B.A. Price. 1980. Nitrous oxide solubility in water and seawater. Marine Chemistry. 8:347-359.

Wilson, G.B., G.W. McNeill. 1997. Noble gas recharge temperatures and the excess air component. Applied Geochemistry. 12:747-762.

Wise, D.L., G. Houghton. 1966. The diffusion coefficients of ten slightly soluble gases in water at 10-60^{o}C. Chemical Engineering Science. 21:999-1010.

Table 3.1 – The calculated fluxes of excess N_2-N, N_2O-N, and CO_2 and the ratio of N_2O/excess N_2 fluxes from groundwater into the vadose zone using Fickian diffusion. The diffusion gradients were calculated from the shallowest piezometer to the deepest unflooded equilibration chamber.

	Flux from groundwater to the vadose zone							
	μmol m^{-2} day^{-1}							
	excess N_2-N		**N_2O-N**		**N_2O:N_2**	**N_2O:N_2**	**excess CO_2**	
date	transect A	transect B	transect A	transect B	transect A	transect B	transect A	transect B
12/03/08	6.5	6.5	1.35	1.37	0.21	0.21	92	77
12/15/08			0.53	0.37			431	421
07/24/09	19.7	20.2	0.97	0.97	0.05	0.05	-383	-1033
08/06/09	20.8	19.9	1.02	1.04	0.05	0.05	-372	438
08/13/09	11.4	9.5	0.41	0.34	0.04	0.04	60	268
08/19/09	10.4	8.5	0.42	0.35	0.04	0.04	62	178
09/15/09	6.8	6.8	0.21	0.21	0.03	0.03	433	340
10/06/09	6.7	6.7	0.47	0.47	0.07	0.07	416	255
10/23/09	5.1	4.4	0.30	0.30	0.06	0.07	750	436
06/18/10	23.3	23.4	0.66	0.66	0.03	0.03	-333	-434
08/11/10	11.6	11.4	1.25	1.26	0.11	0.11	-59	-185
08/13/10	15.5	15.7	0.28	0.29	0.02	0.02	-244	-1278
min	4.4		0.21		0.02		-1278	
median	10.9		0.47		0.05		85	
max	23.4		1.37		0.21		750	

Table 3.2 – Calculated diffusional gradients and fluxes of excess N_2-N, N_2O-N, and CO_2 from the soil surface using Fickian diffusion. The diffusion gradients were calculated from the shallowest vadose zone sampler to the atmosphere.

	date	N_2-N	N_2O-N	CO_2-C	N_2-N	N_2O-N	CO_2-C
		gradient, mmole m^{-4}			flux, mmoles m^{-2} day^{-1}		
Equilibration chamber transect A	11/17/08		0.421	1149.5		0.0091	23.8
	12/03/08	309.65	0.877	3978.0	8.31	0.0189	82.5
	12/15/08		0.412	2478.5		0.0096	55.2
	07/24/09	-225.93	0.045	2929.2	-6.99	0.0011	70.0
	08/06/09	-236.92	0.095	5409.5	-7.09	0.0023	125.1
	08/13/09	152.53	0.300	5708.0	4.61	0.0073	133.3
	08/19/09	-127.64	0.239	4839.2	-3.89	0.0058	113.9
	09/15/09	0.00	0.137	5566.1	0.00	0.0033	128.2
	10/06/09	377.11		2857.0	10.99		64.3
	10/23/09	0.00	0.159	3338.4	0.00	0.0037	
	06/18/10	563.33	0.147	1223.4	16.73	0.0035	28.1
	08/11/10	-57.50	0.112	1103.3	-1.80	0.0028	26.7
	08/13/10	80.24	0.161	3303.0	0.34	0.0006	10.9
Equilibration chamber transect B	11/17/08	not installed			not installed		
	12/03/08	116.37	0.868	1924.8	3.12	0.0187	39.9
	12/15/08		0.648	1684.3		0.0150	37.5
	07/24/09	-383.76	0.034	3682.0	-11.87	0.0008	88.0
	08/06/09	0.00	0.173	7771.1	0.00	0.0042	179.7
	08/13/09	0.00	0.383	6414.9	0.00	0.0093	149.8
	08/19/09	-74.71	0.134	6122.0	-2.28	0.0033	144.1
	09/15/09	0.00	0.004	6459.4	0.00	0.0001	148.8
	10/06/09	586.32		5106.5	17.08		114.9
	10/23/09	0.00		3965.6	0.00		89.7
	06/18/10	580.65	0.064	1433.2	17.25	0.0015	32.9
	08/11/10	80.24	-0.011	1354.2	2.52	-0.0003	32.8
	08/13/10	-43.21	0.059	7635.0	-0.19	0.0002	25.3
	min	-383.76	-0.01	1103.27	-11.87	0.000	10.94
	median	0.00	0.15	3682.04	0.00	0.003	76.23
	max	586.32	0.88	7771.10	17.25	0.019	179.73
					flux, Kg ha^{-1} yr^{-1}		
				min	-606.70	-0.01	479.01
				median	0.00	0.17	3339.03
				max	881.42	0.97	7872.16

Table 3.3– Processes that potentially alter the N_2/Ar ratio in the vadose zone and the degree to which the process might affect the ratio expressed as a percent increase or decrease.

Increases in N_2/Ar relative to atmospheric	**Percent increase in the N_2/Ar ratio**	**Decreases in N_2/Ar relative to atmospheric**	**Percent decrease in the N_2/Ar ratio**
Denitrification/ Anammox	0.89% = 563 μM N_2-N	**Nitrogen fixation**	-0.89% = 563 μM N_2-N
Cooling of groundwater in late fall with diffusion of N_2 and Ar into the groundwater	Likely slower process, but same magnitude as warming of GW	**Warming up of GW in spring with diffusion of N_2 and Ar into the vadose zone (Figure 3)**	Recharge at 10°C sampling at 18°C -0.42%
Infiltration of warm groundwater that cools in the vadose zone	Rain=20°C Soil=15°C 0.23%	**Infiltration of cool groundwater that warms in the vadose zone**	Rain=20°C Soil=25°C Δ%WFPS = 25% -0.19%
Complete bubble dissolution – Forces relatively more N_2 than Ar into groundwater When equilibrium starts to form, more N_2 will flux out of the groundwater relative to Ar.	Small effect. 1mL bubble completely dissolved at 25°C results in 22.05 uM excess air.	**The wicking of cooler groundwater with a lower N_2/Ar ratio to the surface soils to replace previously evaporated water.**	15cm = 27°C 30cm=22°C -0.038%
Methane ebullition	Unknown, will depend on the size of the CH_4 bubbles	**Evaporation in the subsurface**	-0.411% (same temps as above)
		Daily salinization of surface soils due to evaporation	Salinity=0.5 -0.01%

Figure 3.1- **A**) The location of the Little Choptank within the Mid-Atlantic region, **B**) the location of the site within the Little Choptank watershed, and **C**) the location of the piezometers with respect to the agricultural field. The buffer is a young forest (<10 m tall) planted in 2000 under the USDA's CREP (Conservation Reserve Enhancement Program)

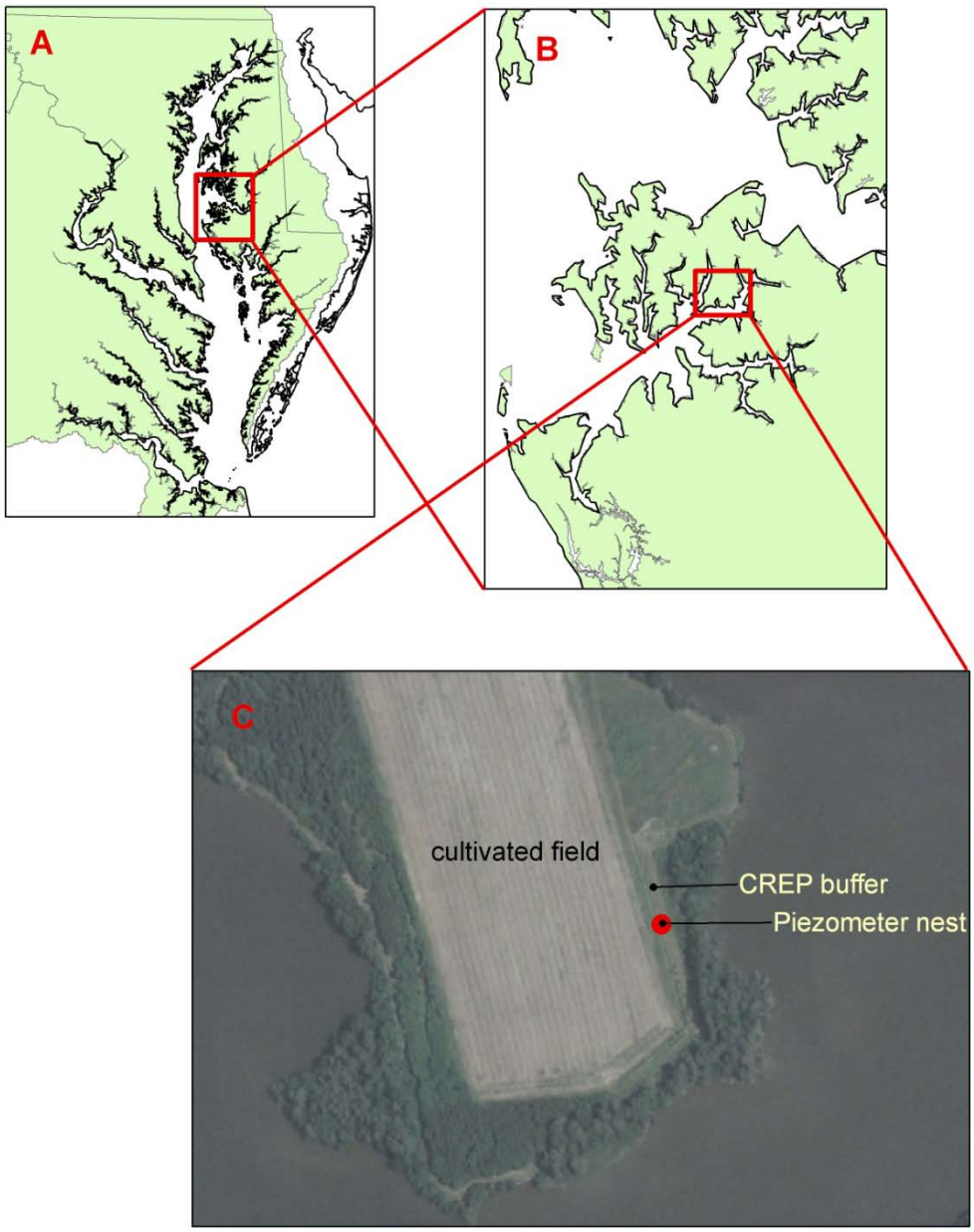

Figure 3.2 – The capillary inlet system. A fused silica capillary tube is connected to a Swagelock reducing union via a pierced Teflon ferrule. The inlet system is sealed off from the atmosphere by a septa and a 2-stage rotary vane pump allows removal of the previous gas sample. The injected sample passes through a hot water bath, a copper furnace to remove O_2, and a liquid nitrogen cryotrap to remove CO_2 and water vapor before entering the mass spectrometer.

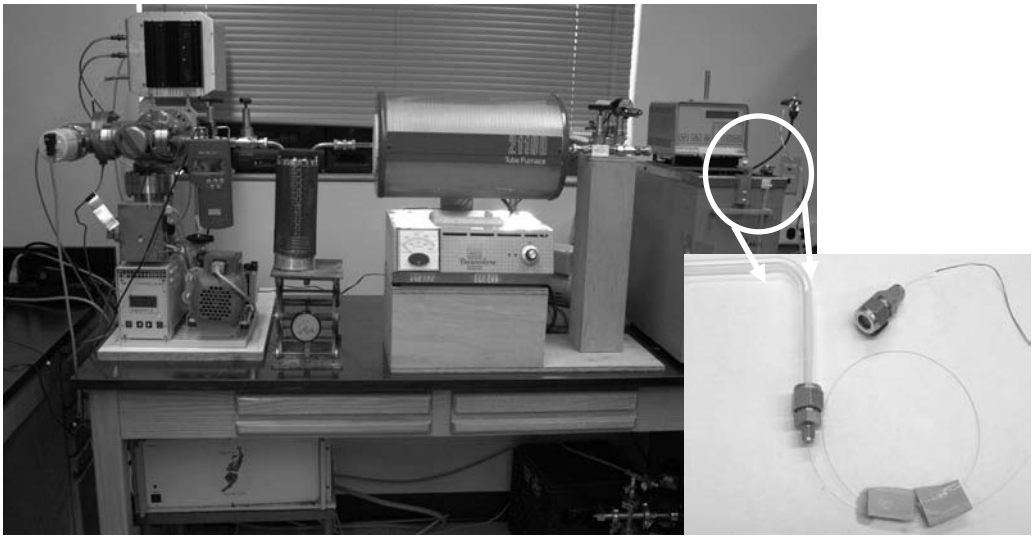

Figure 3.3 - **A)** The effect O_2 has on the 14/40 signal, **B**) the effect CO_2 has on the 14/40 signal, **C)** The effect O_2 has on the 14/40 signal with the copper furnace in line to remove O_2, and **D**) the effect CO_2 has on the 14/40 signal when CO_2 has been removed from the sampling stream by a cryo trap.

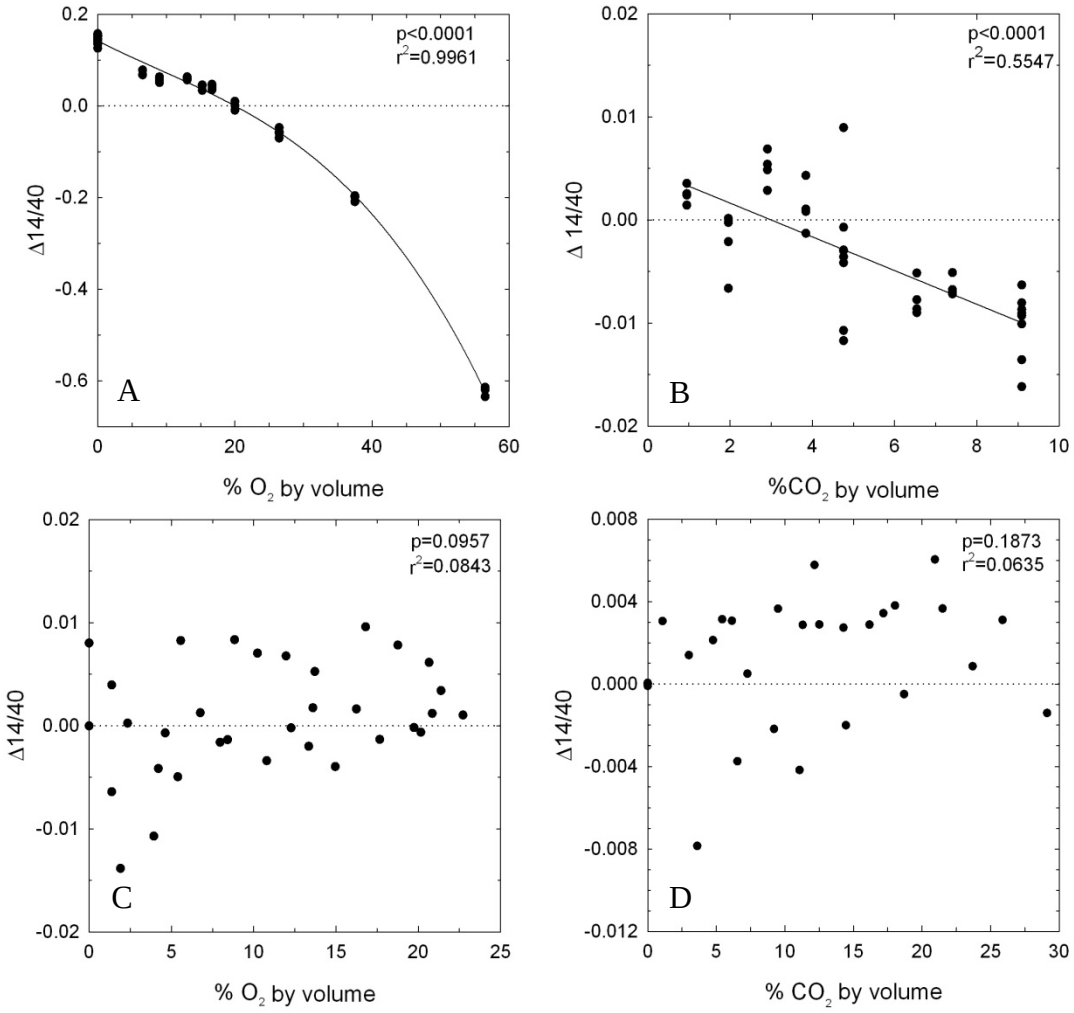

Figure 3.4- The annual rainfall accumulations for 2009 (**A**) and 2010 (**B**) and the seasonal and interannual variations in groundwater depth (**C**) and temperature (**D**)**.** The 2010 rainfall data is missing December 13th through December 31st.

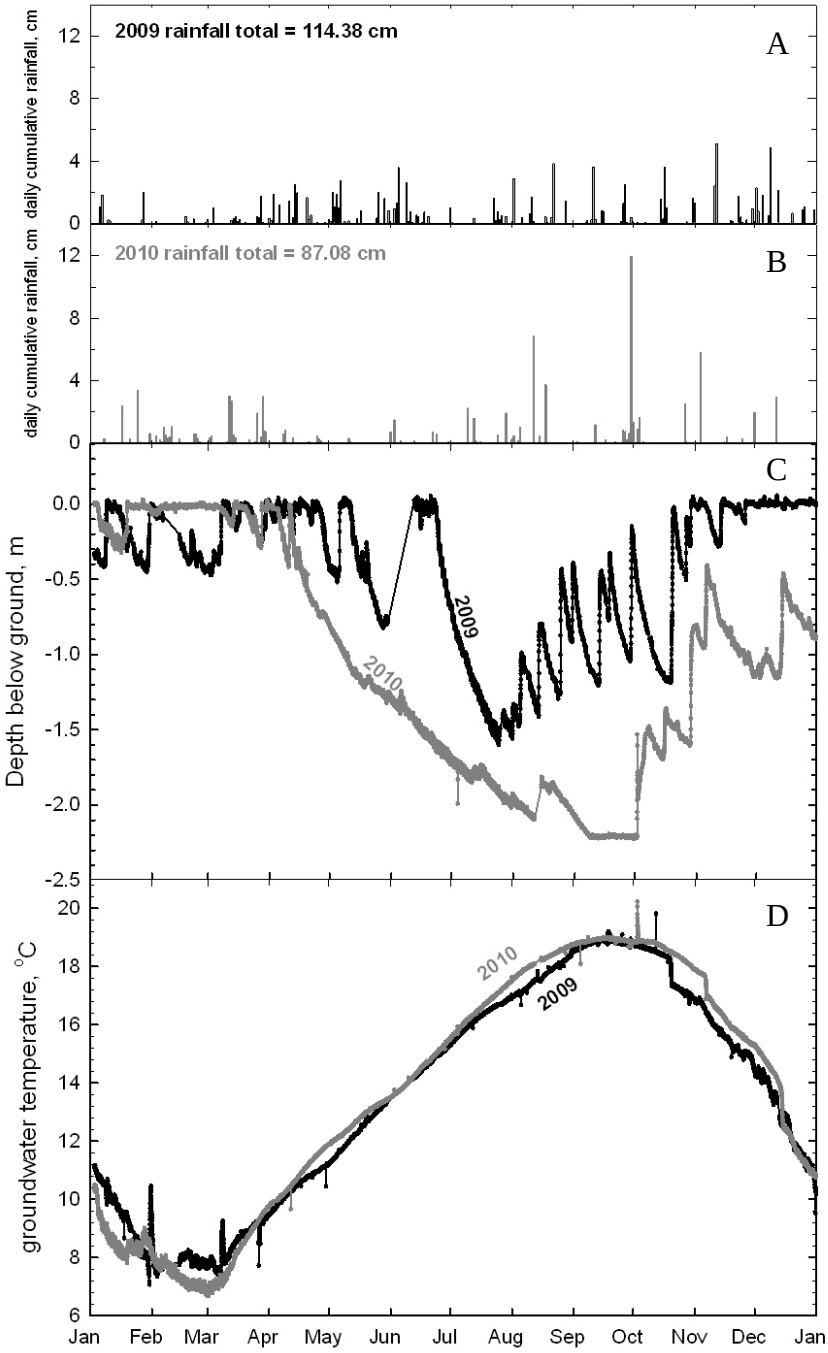

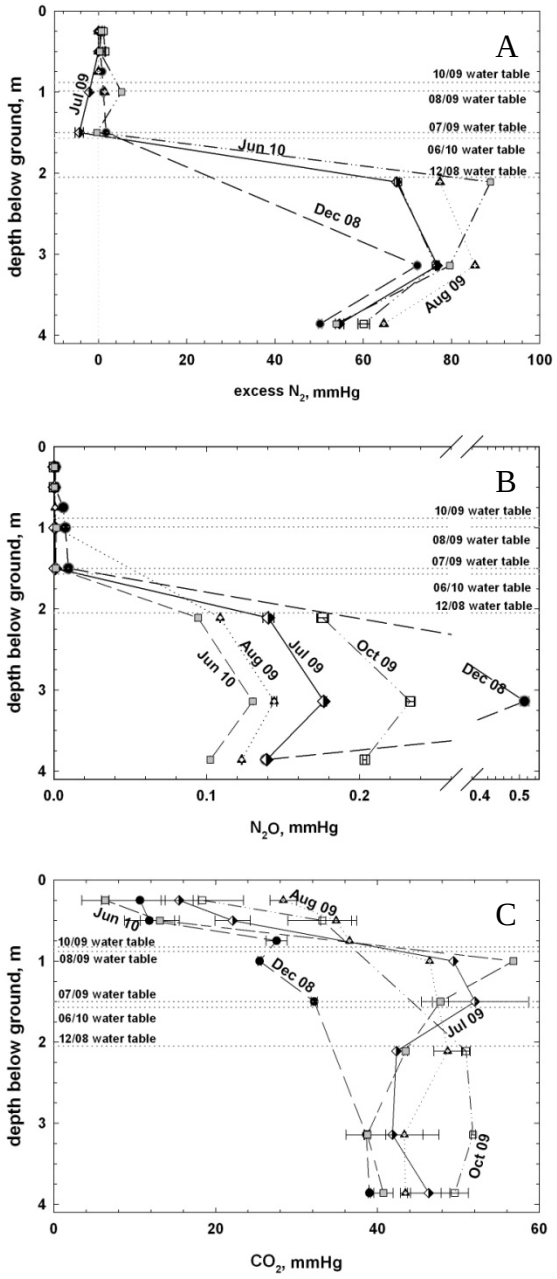

Figure 3.5 – Vertical partial pressure gradients of **A)** excess N_2, **B)** N_2O, **C)** excess CO_2, and **D)** O_2 from the equilibration chambers in a CREP riparian buffer. O_2 partial pressure data was only acquired for December 2008, prior to scrubbing O_2 out of the sample stream

Figure 3.6 – Vadose zone excess N_2-N (**A**), N_2O-N (**B**), and CO_2 (**C**) concentrations.

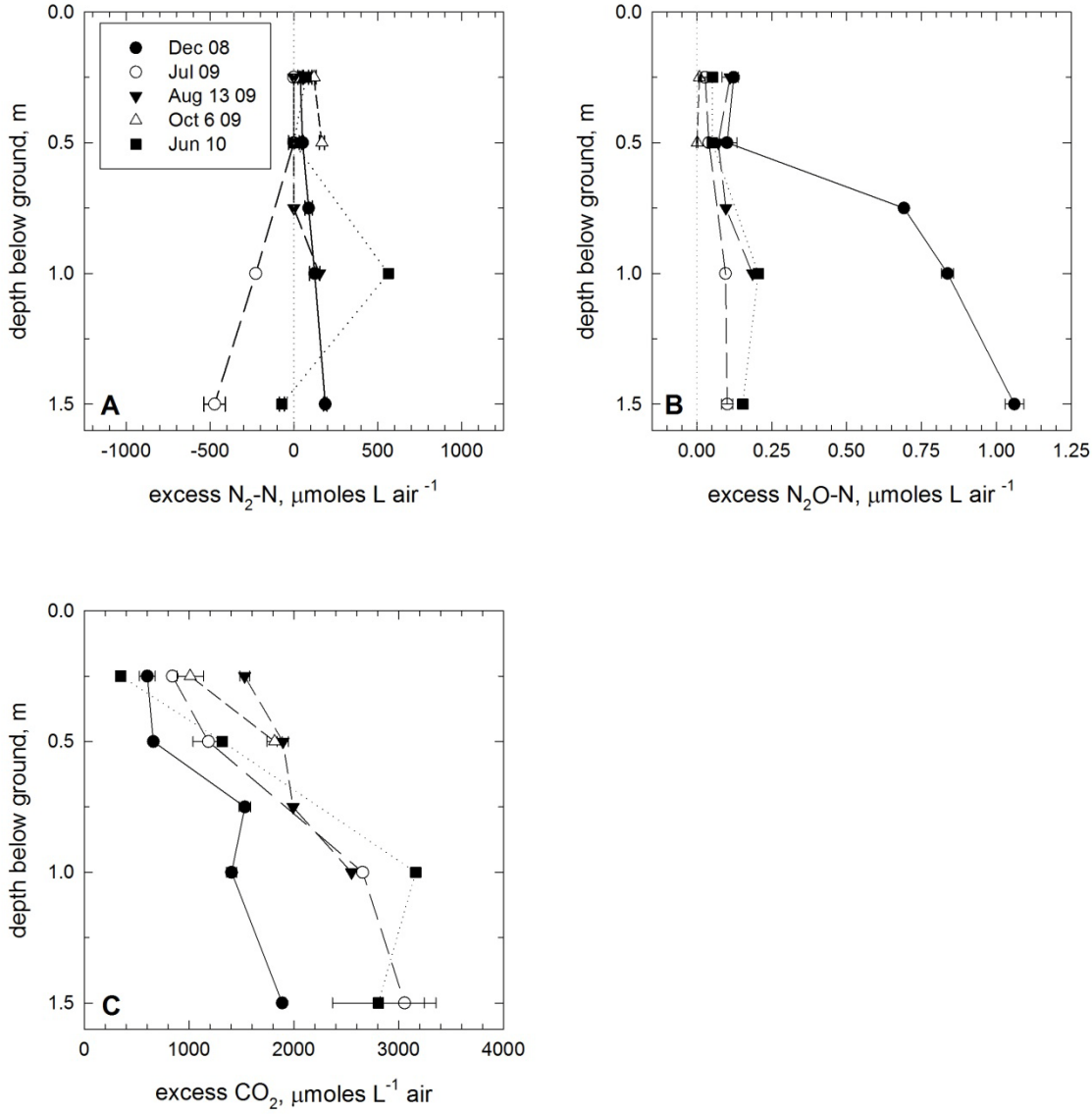

Figure 3.7- The ratio of N_2O-N to excess-N_2-N concentrations in the vadose zone and groundwater. The points at 2.1, 3.1, and 3.9 m are the groundwater values and the points above these depths are vadose zone gas samples.

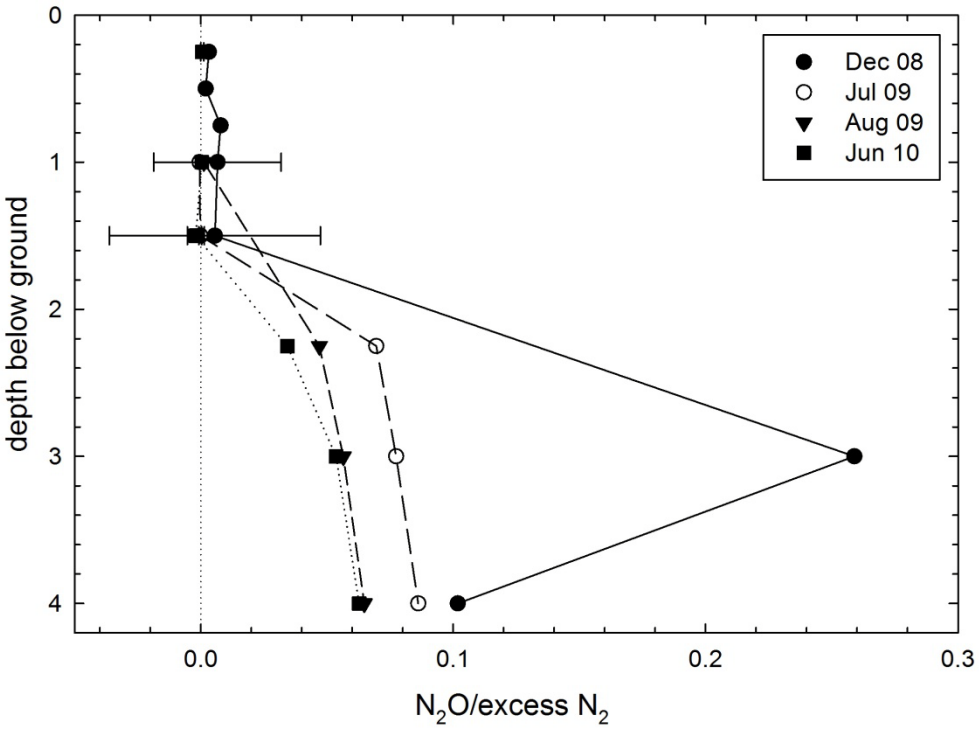

Figure 3.8- The dissolved NO_3^- concentrations in groundwater at the three nested piezometers

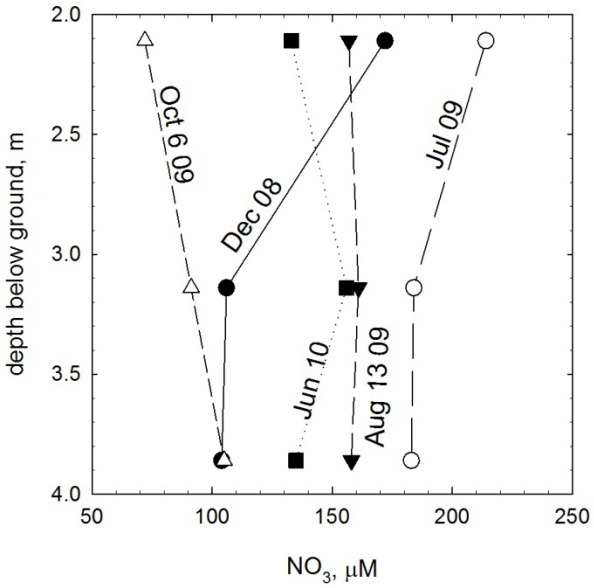

Figure 3.9 - A cross sectional view of the CREP riparian buffer between piezometers CREP2 and CREP3. The missing N on the transect scale is computed from medians of monthly concentration of NO_3, NH_4, excess N_2, and N_2O during 2007. I hypothesized that the missing N is the result of the diffusion of excess N_2 and N_2O from the groundwater into the vadose zone between the two piezometers.

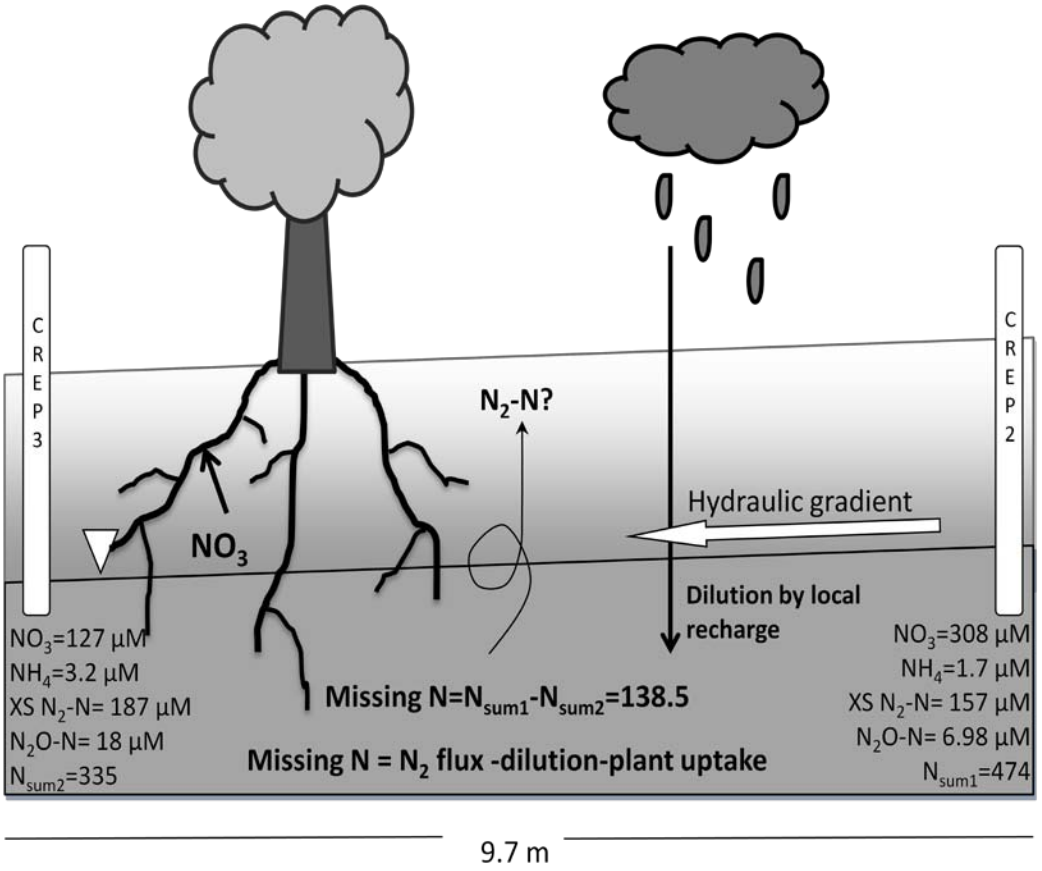

Figure 3.10- The N_2/Ar ratio that results from the total or partial dissolution of an air bubble into 1 L of water calculated using the closed system equilibration model described by Aeschbach-Hertig et al. (2000, 2008), presented here as equations 8 and 9. The effect that just temperature (no bubble dissolution) has on solubility is shown as the bottom data points (stars) connected by the dotted line.

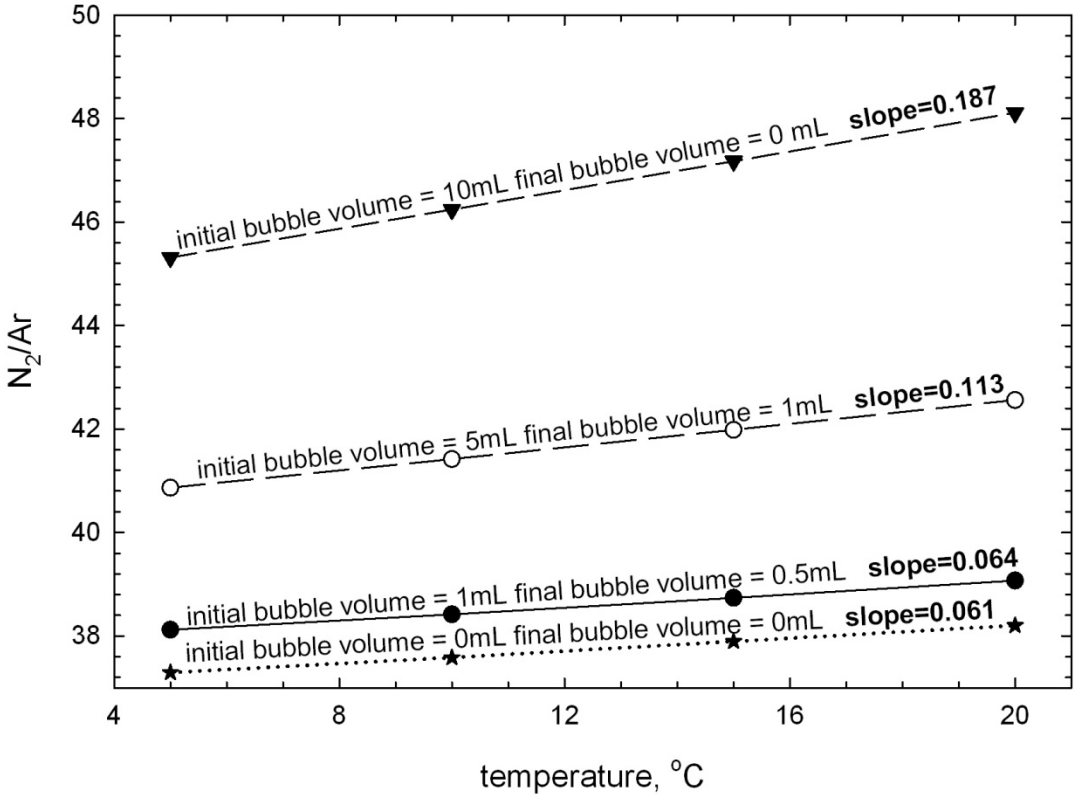

Figure 3.11 –An example of how changes in groundwater temperature affect the N_2/Ar ratio in the vadose zone. As temperatures increase in the spring, N_2 is relatively more soluble than Ar resulting in a relative increase in Ar over N_2 in the vadose zone which decreases the N_2/Ar ratio. The boxes in groundwater show the dissolved concentrations of N_2 and Ar and the N_2/Ar ratio in groundwater. The boxes in the atmosphere with the arrow pointing into the vadose zone show the concentrations in the vadose zone. Panel C shows the concentrations in the vadose zone that will result after the N_2 and Ar above air equilibrium dissolved in groundwater has diffused into the vadose zone with the result of decreasing the N_2/Ar ratio.

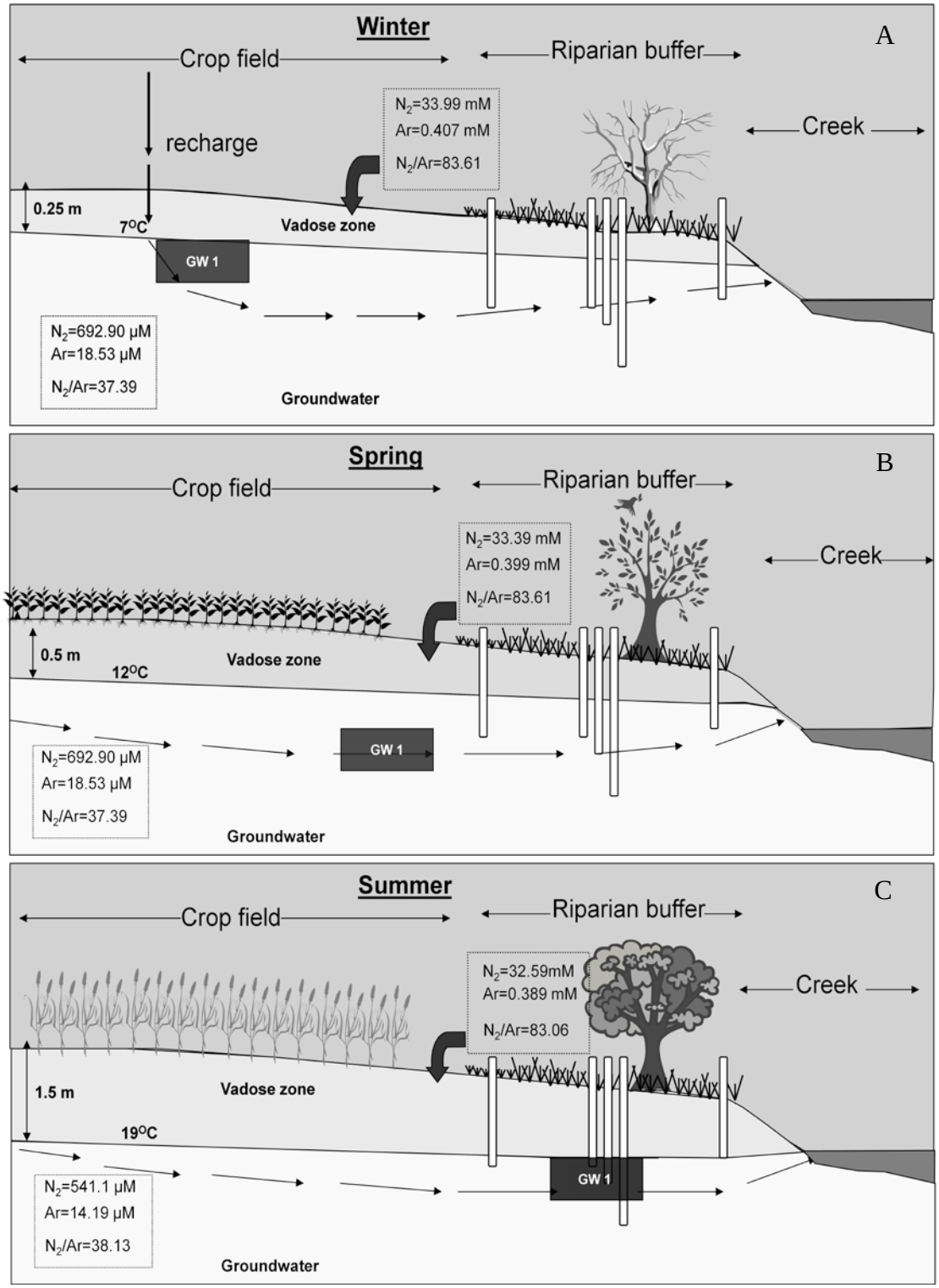
Winter
A
Crop field
Riparian buffer
Creek
recharge
N_2=33.99 mM
Ar=0.407 mM
N_2/Ar=83.61
0.25 m
7°C
Vadose zone
GW 1
N_2=692.90 µM
Ar=18.53 µM
N_2/Ar=37.39
Groundwater
Spring
B
Crop field
Riparian buffer
Creek
N_2=33.39 mM
Ar=0.399 mM
N_2/Ar=83.61
0.5 m
12°C
Vadose zone
GW 1
N_2=692.90 µM
Ar=18.53 µM
N_2/Ar=37.39
Groundwater
Summer
C
Crop field
Riparian buffer
Creek
N_2=32.59mM
Ar=0.389 mM
N_2/Ar=83.06
1.5 m
Vadose zone
19°C
GW 1
N_2=541.1 µM
Ar=14.19 µM
N_2/Ar=38.13
Groundwater

CHAPTER 4:

DIFFUSIONAL AND CONVECTIVE FLUXES OF N_2O, CO_2, AND CH_4 FROM THE SOIL TO THE ATMOSPHERE AND CHANGES IN THE VADOSE ZONE GAS CONCENTRATIONS AFTER RAINFALL EVENTS

Abstract

The greenhouse gases N_2O, CO_2, and CH_4 are respiratory gases produced in both the unsaturated and saturated zone of soils. Once produced, these gases will either be further consumed, or released to the atmosphere via diffusion or convection. To examine the relative importance of these transport processes, measurements were made in the Choptank and Little Choptank Basins in two riparian buffers and one hydrologically restored wetland bordering agriculture. Two transects of equilibration chambers were installed at each location next to a groundwater piezometer. I have calculated the contribution of diffusion and the convective fluxes produced by infiltration of precipitation or decreases in barometric pressure, and I have also measured the soil concentrations of these gases before and after rainfall events.

Diffusion is the dominant mechanism for the transport of these gases to the atmosphere. The yearly, combined diffusional and convective flux of N_2O to the atmosphere ranged from 0.1 to 1.5 Kg N_2O-N ha^{-1} yr^{-1}, which is on the low end of the range of fluxes reported by other researchers, and the median convective N_2O-N flux constituted 5% of the median total yearly flux. The reported N_2O fluxes are only 0.5-2% of the approximate yearly N fertilization rate of 50-150 kg N ha^{-1} yr^{-1} to crop fields. The combined diffusional and convective flux of CH_4-C to the atmosphere ranged over -0.5 to 12.6 Kg CH_4-C ha^{-1} yr^{-1}, and the convective fluxes only accounted for 0.31% of the maximum calculated yearly CH_4 flux. These CH_4 fluxes are on the low end of the range of other reported fluxes. The combined diffusional and convective CO_2 flux to the atmosphere was 643-10,627 Kg CO_2–C ha^{-1} yr^{-1}, and the median convective fluxes accounted for 20% of the annual median calculated CO_2-C flux. These CO_2 flux

estimates are in the middle of the reported range of CO_2 fluxes. The convective flux of CO_2 was larger than either N_2O or CH_4 because there were greater concentrations of excess CO_2 in the soil gas (200-5400 µM) in the upper soil horizon that could be transported via convective mechanisms. The calculated convective CO_2 fluxes from the soil surface were not minor and convective fluxes of high concentration vadose zone gases should be considered in yearly budgets.

Increased concentrations of N_2O and CO_2 were observed after rainfall events, but CH_4 concentrations often remained unaltered or decreased, indicating increased CH_4 oxidation. Precipitation events are predicted to increase with global climate change; therefore, there is the potential for increased production of N_2O and CO_2 and an increased convective flux via precipitation.

Introduction

Gas exchange between soil and the atmosphere

Soils are major contributors to the global budgets of nitrous oxide (N_2O), methane (CH_4), and carbon dioxide (CO_2). All three of these gases are produced naturally as intermediate or end products of microbial respiratory processes, but the natural carbon and nitrogen cycles have been enhanced by anthropogenic emissions. All three of these gases contribute to global climate change as greenhouse gases, and N_2O also contributes to stratospheric ozone depletion (Crutzen et al. 1981). N_2O, CH_4, and CO_2 can be produced within groundwater and/or the vadose zone. Once produced, these gases can be consumed or further transformed in the soil, or are transported from the soil surface to the atmosphere. Positive flux out of the soil or negative flux into the soil occurs through two mechanisms, diffusion or convection.

Diffusion is considered to be the primary mechanism of gas flux from soils (Jury & Horton 2004). The rate of gaseous diffusion depends on the strength of the concentration gradient, which is produced in response to the production or consumption of a gas, and the diffusivity coefficient of that specific gas. Diffusion in free air is a relatively fast process in comparison to diffusion in water. Diffusion in an air or water filled tortuous environment, such as soil or sediment, is much slower than diffusion in the free atmosphere or water column, and corrections for tortuosity and porosity are routinely made to the free air diffusion coefficients to estimate *in situ* soil diffusion (e.g., Moldrup et al. 2000A, 2000B). Diffusion coefficients are calculated for each individual site and date because they vary based on the soil porosity and the gas filled pore space of that soil on that day.

Convection is the bulk movement of soil air caused by total gas pressure gradients (Jury and Horton 2004). Physical mechanisms known to cause convection are wind, barometric pressure changes, temperature fluctuation, and infiltrating water due to precipitation (Jury and Horton 2004). Fluxes out of the soil due to convection are generally considered to be low compared to diffusion, but there is the potential for large convective fluxes if soil gas concentrations are high (Clough et al. 2005).

Each convective mechanism of gas exchange has a different basis. Barometric pressure changes from low to high pressure approximately every week in the Mid-Atlantic where this study took place. Pressure changes can work to both "push" air into the soil when a high pressure system moves into the area, or "pull" air from the soil when a low pressure system moves in. In the Mid-Atlantic, rainfall is distributed evenly throughout the year, but percolation of the rainwater to the water table primarily occurs in the cooler months when evapotranspiration is reduced, unless a major rain event occurs in the summer. Rainfall that percolates into the soil will first displace soil air, but as the wetting front moves through, the pores will be refilled with replacement air (Jury & Horton 2004). Oxygen can also be transported and exchanged with the soil atmosphere from infiltrating water (Jury & Horton 2004).

Gas production processes

Carbon dioxide is primarily produced through aerobic respiration, which is the reduction of O_2 to water and the oxidation of a labile carbon source to CO_2 (Prescott et al. 2002). Aerobic respiration has the highest energy yield of any respiratory process and is favored over the other respiratory processes when O_2 is present. Photosynthesis at the

soil surface consumes CO_2 using light energy to produce glucose (Prescott et al. 2002), and the actual flux of CO_2 to the atmosphere is the net between aerobic respiration and photosynthesis.

Denitrification is the reduction of NO_3^- to N_2 through the intermediate and sometimes terminal products of NO_2^-, NO, and N_2O (Knowles, 1982). Denitrification is typically a heterotrophic process that requires a labile carbon source, NO_3^-, and relatively low levels of O_2. Denitrification can occur after O_2 is reduced if a NO_3^- source is available. Typically, NO_3^- reduction has been associated with denitrification, but other NO_3^- reduction processes can occur, including dissimilatory nitrate reduction to ammonium (DNRA), chemoautotrophic denitrification, which can be coupled to either sulfur or iron oxidation, and anammox (Burgin and Hamilton 2007). A benefit to anammox is that it removes NO_3^- from the environment as N_2 without producing N_2O. More recently, evidence of anaerobic methane oxidation coupled to denitrification (AMO-D) has also been observed in lab soil cores, but not in the field (Raghoebarsing et al. 2006). While there are multiple processes that consume NO_3^- and/or produce excess N_2, in this chapter I will refer to the production of excess N_2 as "denitrification" as it is well documented to occur in soils, while acknowledging here that other processes may also contribute to NO_3^- loss and N_2 production.

Nitrification is an aerobic process that oxidizes NH_3^+ to NO_3^-. Nitrification has the potential to produce N_2O, but it is not an obligate step. Nitrification can be autotrophic as an energy source for fixing carbon, or heterotrophic using labile carbon for carbon and energy; both processes produce N_2O (Wrage et al. 2001). Nitrifier denitrification is a form of nitrification that oxidizes NH_3^+ to NO_2^- followed by the

reduction of that NO_2^- to N_2O and N_2 (Wrage et al. 2001). Coupled nitrification and denitrification can also occur simultaneously, and both potentially produce N_2O.

Methanogenesis is primarily the reduction of CO_2 (H_2 mediated) or acetate to CH_4 (acetotrophy). Acetotrophy is responsible for approximately two-thirds of CH_4 produced (Jones 1991, Le Mer & Roger 2001), and other substrates can be used such as formate, methylated compounds, and primary and secondary alcohols (Le Mer & Roger 2001). Methanogens carry out the process of methanogenesis, and are members of the domain Archea. This process is a redox reaction which results in the least energy production per unit organic C (Megonigal et al. 2005) and it occurs after all other electron acceptors have been exhausted in perennially or seasonally saturated areas. CH_4 can be transported to the atmosphere through diffusion, convection, ebullition (Mookherji et al. 2003, Fortuin and Willemsen 2005, Chapter 2), and through plant aerenchyma (Kutzbach et al. 2004).

Unsaturated soils can function as CH_4 sinks through methane oxidation to CO_2 (Mosier et al. 1998). Two forms of CH_4 oxidation have been recognized in soils, high affinity oxidation and low affinity oxidation (Le Mer and Rogers 2001). High affinity oxidation occurs at lower CH_4 concentrations close to atmospheric (<12 ppm), and low affinity oxidation occurs at much higher CH_4 concentrations (>40 ppm, Le Mer and Rogers 2001). CH_4 produced at depth in soils or sediments can be oxidized at shallower, aerobic depths through CH_4 oxidation (Conrad and Rothfuss 1991), and variations in CH_4 flux from the soil surface are the net result of methanogens producing CH_4 and methanotrophs consuming CH_4.

The fluxes of N_2O, CH_4, and CO_2 have been shown to be temporally and spatially heterogeneous (e.g., Goodroad and Keeney 1985, Adrian et al. 1994, Goodroad et al. 1984, Breuer et al. 2000, Mathieu et al. 2006, Yao et al. 2010). Hot moments are a type of temporal variability and are defined as short periods of time with increased biogeochemical reaction rates compared to longer periods with much lower rates (McClain et al. 2003). These hot moments can occur when ideal conditions for aerobic respiration, nitrification, denitrification, methanogenesis, or methane oxidation, have been reached. Researchers have shown hot moments with increased fluxes of N_2O after rainfall events, both using soil cores (Ruser et al. 2006) and in the field (Dobbie and Smith 2003). These flux measurements are often made within chambers, and therefore provide only the diffusional flux from the surface with little indication of what is occurring below ground. Increased N_2O production has also been observed after soil thawing (Goodroad et al. 1984, Papen & Butterbach-Bahl 1999, Teppe et al. 2001, Koponen et al. 2004) and fertilizer additions (Dobbie & Smith, 2003, Meng et al 2005). Pulses of CO_2 have also been observed after rainfall events (Morell et. al. 2010, Rochette et al. 1991) and after soil disturbance such as tillage (Morell et al. 2010).

The majority of soil N_2O, CO_2, and CH_4 studies look at fluxes from the soil surface using diffusional chambers. Some studies have looked at below ground concentrations of N_2O, CH_4, and CO_2, (e.g., Dunfield et al. 1995), but more recently the majority of studies use chambers or micrometeorological towers. Elmi et al. (2003) found large rates of N_2O production in subsurface soils, suggesting that a significant portion of the N_2O produced would be missed if only surface fluxes were examined. The resulting gas concentrations that accumulate in surface gas chambers will be through

diffusion, and potentially barometric convective fluxes. Micro-meteorological towers measure both convective and diffusive fluxes averaged over small scale heterogeneity, but are expensive.

Two main hypotheses will be addressed in the research reported here. The **first hypothesis** is that diffusion is the dominant process driving fluxes of N_2, CO_2 and CH_4 out of the vadose zone and into the atmosphere at my study sites, but convection due to rainfall and barometric pressure changes is an important but smaller flux mechanism. The **second hypothesis** is that increased concentrations of N_2O, CO_2, and CH_4 occur in the vadose zone soil profile after rainfall events. Other researchers have shown increased flux from the soil surface after rainfall events, but few researchers have looked at below ground concentrations to see where the increased production is occurring. Both hypotheses will be addressed in the Choptank River watershed, located within the Chesapeake Bay basin.

Methods

Location

This study took place on the Delmarva Peninsula of Maryland, within the Mid-Atlantic coastal plain (Fig. 4.1). The groundwater and vadose zone of two riparian areas and one hydrologically restored wetland were investigated on three separate farms (Mfarm, Rfarm, and EFAG). In accordance with USDA policy, we do not identify individual farms. Mfarm and EFAG are located in the upper Choptank Basin, and Rfarm is located just south of the Choptank Basin within the adjacent Little Choptank Basin. The upper Choptank sampling sites are underlain by the Pensauken Formation, a fluviatile deposit of Late Cretaceous age, and Rfarm is underlain by the Kent Island Formation, an estuarine deposit of the middle-Wisconsin period (Owens and Denny, 1979). All three sampling locations border agricultural fields with high NO_3^- in groundwater, and therefore have the potential to produce large concentrations of N_2O and N_2 through denitrification. The characteristics of each site are described below.

Mfarm

The Mfarm site is within a mature forested riparian buffer of approximately 100 m width on both sides of a stream (Fig. 4.2A). A transect of groundwater piezometers was installed across one side of the buffer in 2005, and two vadose zone gas samplers were installed at 0.25 and 0.5 m in August 2009. In 2010, additional samplers were installed next to Mmid, which has a depth of 1.51 m to the center of the piezometer screen to create two transects of vadose zone samplers at depths of 0.25, 0.5, 0.75, and 1.0 m below the soil surface. The hydraulic conductivity at Mmid is 3.09 cm day^{-1}, the

porosity is approximately 0.26 cm^3 cm^{-3} (Chapter 2), and the soil type is Ingleside sandy loam (Soil Survey Staff, Natural Resources Conservation Service, United States Department of Agriculture, 2011). Mfarm is an organic farm that uses a corn/soybean crop rotation.

EFAG

The vadose zone samplers at EFAG are located within a hydrologically restored wetland of ~300 m width adjacent to a crop field (Fig. 4.2B). A transect of 5 piezometers was installed in the saturated zone across the wetland in 2008, and the vadose zone samplers were installed in 2009. Nested piezometers are located at EFWET1 directly within the hydrologically restored wetland at depths of 4.59 and 0.63 m. The vadose zone samplers were installed at 0.25, 0.5, 0.75, and 1.0 m next to EFAG2, which is within the buffer between the agricultural field and ponded wetland (Fig. 4.2B). EFAG2 is 2.61 m deep (to the center of the piezometer screen), has a porosity of 0.345 cm^3 cm^{-3} and has a hydraulic conductivity of 35 cm day^{-1} (Chapter 2). The soil type around EFAG2 is Hurlock Sandy Loam, but the two outer piezometers within the piezometer transect are situated within Ingleside sandy loam (Soil Survey Staff, Natural Resources Conservation Service, United States Department of Agriculture, 2011). The agricultural field next to the hydrologically restored wetland uses a corn/soybean crop rotation.

Rfarm

The sampling location at Rfarm is within a 10 year old Conservation Reserve Enhancement Program (CREP) riparian buffer separating an agricultural field and a tidal

creek (Fig 4.2C). A transect of 3 piezometers was installed within the riparian buffer in 2003 with replicate piezometers at the field and near the tidal creek edge (Sutton et al. 2010). In 2008, two rows of vadose zone samplers were installed at depths of 0.25, 0.5, 0.75, 1.0, and 1.5 m next to CREP3, which has a depth to the center of the piezometer screen of 2.1 m. In 2009, two additional piezometers were installed around CREP3 at depths of 3.1 m (CREP3-3) and 3.9 m (CREP3-4, Fig. 4.2C). The porosity of CREP3 is 0.28 cm^3 cm^{-3}, the hydraulic conductivity is 70.9 cm day^{-1} (Chapter 2), and the soil type is Keyport silt loam (Soil Survey Staff, Natural Resources Conservation Service, United States Department of Agriculture, 2011). Rfarm uses no-till management practices and is on a corn/soybean crop rotation.

Sampling methods

Vadose zone samples were acquired using equilibration chambers (Silver et al. 1999). Equilibration chambers are simple and inexpensive to construct. They are inverted 50 mL centrifuge tubes connected to sections of 3.2 mm (1/8") copper tubing with a three-way stopcock at the opposite end. Connections are sealed with Amazing Goop ® automotive adhesive. Duplicate gas samples were taken at each depth from each chamber, and these samplers are discussed in more detail in Chapter 3. Two transects of equilibration chambers were installed at each location. The depth of the equilibration chambers were randomized at EFAG and Mfarm, but not at Rfarm (Fig. 4.2). Vadose zone and groundwater samples were taken from December 2008 through August 2010 and were analyzed for excess N_2, N_2O, CH_4, and CO_2. Analytical details are given below. Samples were taken on 23 different dates, some of which are also used in Chapter 3.

Groundwater samples were taken from 5.1 cm (2”) inner diameter piezometers with 30 cm long sampling screens. The piezometers were installed by hand augering at 15 cm intervals, and soil logs were recorded to construct soil profiles for each location. Several weeks were allowed for soil settling prior to sampling. On the day prior to sampling, the depth to the water table was measured using a Solinst® water level meter, and the piezometers were pumped dry using a portable Solinst® Model 410 peristaltic pump. A slightly smaller diameter fishing float was lowered to the bottom of the piezometer to reduce gas exchange between the freshly inflowing groundwater and the atmosphere. The next day the float was removed, and a 5.1 cm (2”) Teflon® bailer was slowly lowered to the bottom of the piezometer to acquire an undisturbed groundwater sample. A one-way ball valve prevented loss of the groundwater when the bailer was removed from the piezometer. A stopcock connected to a 15 cm length of ½ cm Teflon® tubing was attached to the bottom of the bailer to control flow into duplicate 25 mL ground glass tubes with ground glass stoppers. The tubes were overflowed from the bottom with sample and immediately capped and submerged in ice water to prevent gas exsolution. A separate sample was taken for nutrients, conductivity, and pH, and the *in situ* temperature of the sample was taken immediately with a VWR digital thermometer (NBS traceable accuracy of ± 0.3 ^{o}C). The groundwater samples were analyzed for excess N_2, Ar, and O_2 by MIMS, and for N_2O, CH_4, and CO_2 by gas chromatography. Automated colorimetric methods were used for NO_3^-, PO_4, and NH_4^+.

Analytical methods

Dissolved and gas phase N_2O, CO_2, and CH_4 samples were analyzed using gas chromatographic techniques. N_2-purged, 12 mL Exetainers® were used to equilibrate 8 mL subsamples of groundwater with a head space of N_2 gas at room temperature for N_2O and CH_4 analyses. For CO_2 groundwater analysis, 4 mL of groundwater was injected into an N_2-purged 12 mL exetainer that was vented to maintain atmospheric pressure. After sample injection, the vent was removed and 1 mL of 1N H_2SO_4 was added (Stainton 1973). The samples were then vigorously shaken for 2 minutes to insure full gas equilibration between the groundwater sample and the N_2 headspace. The concentrations of N_2O and CO_2 within the exetainer head space were determined on a Shimadzu GC-14B equipped with both an electron capture detector (ECD, N_2O) with a Porapak Q column and a thermal conductivity detector (TCD, CO_2) with a 80/100 Hayesep Q column. CH_4 was determined on a Shimadzu GC-8A equipped with a flame ionization detector (FID) with a HayeSep A column. The dissolved concentration in the original water sample was calculated using groundwater and headspace volumes, and the appropriate solubility data for the measured room temperature (Weiss and Price 1980, Lange 1961). The vadose zone samples were directly injected into the GC from pre-evacuated exetainers® (12 mL) overfilled with 15 mL of vadose zone gas. Matheson Tri-Gas standards were used along with a blank and an atmospheric air injection to create a standard curve. Standard concentrations of $NaHCO_3$ solution were used for the dissolved CO_2 standards. For CO_2 in groundwater, an initial sample was run directly for CO_2, and a second subsample was equilibrated with air and then injected into an N_2-purged

exetainer ® vial as above to measure background CO_2 in equilibrium with atmospheric air. The difference between the two measurements is referred to as "excess CO_2".

Groundwater samples were analyzed for N_2, O_2, and Ar using the MIMS method (Kana et al. 1994). The concentration of Ar within the sample was assumed to represent physical exchange between air and water at recharge and was used to calculate an effective recharge temperature of the water at the time of infiltration using the solubility formulations of Colt (1984) based on Weiss (1970). The Ar recharge temperature was used to calculate the background N_2 concentration (e.g., Bohlke and Denver 1995, Mookherji et al. 2003), and observed N_2 greater than the background N_2 was considered "excess N_2" due to denitrification and other biological N_2 production processes.

The concentration of excess N_2 in the vadose zone was determined using the method described in Chapter 3. This method is capable of precisely measuring the 14/40 or N^+/Ar^+ ratio, of a small vadose zone gas volume. The 14 peak is used to measure N_2 gas to avoid potential interference from trace amounts of CO_2, which generates the fragment CO^+, with the same molecular weight as N_2. Only the 14/40 ratio is used to determine an excess or deficit of N_2 to eliminate any possible error caused by an over or under injection of individual gas samples. This method precisely determines the ratio of N_2/Ar, but we do not currently have the ability to measure additional noble gases to determine whether increases or decreases in this ratio are due to biological production or consumption, such as denitrification and nitrogen fixation, or due to confounding physical processes in the soils (see Chapter 3).

The volumetric water content of soil at depths below ground was determined using the Trime ®-Pico IPH and Pico-BT. The Trime-Pico® TDR is a probe that can

measure the water content of the soil around a piezometer or other access tube. Our specific TDR was calibrated for schedule 40 PVC pipe, which is what was used for the majority of our piezometers. The water content of saturated soils was used to determine soil porosity because the volumetric water content is equivalent to the porosity when the soil is saturated, assuming that trapped air bubbles within the soil do not constitute a large volume of the pore space.

Flux calculations

Diffusion

Concentration gradients cause diffusive exchanges between the atmosphere and the vadose zone, or the groundwater and the vadose zone. Positive concentration gradients were defined as concentrations that increase with depth, resulting in a net upward flux from the groundwater to the vadose zone and into the atmosphere. Negative gradients were defined as the opposite: concentrations that were highest at the surface and decreased with depth resulting in a net flux into the vadose zone and/or groundwater. The concentration gradient over depth ($\delta C/\delta z$, mmol m^{-4}) was calculated as

$$\frac{\partial C}{\partial z} = \frac{C_2 - C_1}{z_2 - z_1} \qquad (1)$$

where C_1 is the shallower concentration (mmol m^{-3}), C_2 is the deeper concentration (mmol m^{-3}), z_1 is the shallower depth (m), and z_2 is the deeper depth (m). The units of the concentration gradient are mmol m^{-4} or mmol m^{-3} per m depth. The atmospheric concentration and the concentration at the shallowest equilibration chamber (0.25m) were used to calculate the concentration gradients from the soil to the atmosphere.

Excess N_2-N and N_2O-N diffusional fluxes from the soil surface to the atmosphere were calculated using Fick's first law of diffusion.

$$F_d = -D_0 \frac{\delta C}{\delta z} \quad (2)$$

where F_d is the diffusive flux (μmoles N m^{-2} d^{-1}), and D_o is the gaseous diffusion coefficient in air (m^2 d^{-1}). The gaseous diffusion coefficients of N_2, N_2O, and CO_2 in air were obtained from Massman (1998) and were corrected for temperature, pressure, porosity, and tortousity according to the Buckingham-Burdine-Campbell model for gas diffusivity in undisturbed soil (Moldrup et al. 1999):

$$\frac{D_s}{D_0} = \phi^2 \left(\frac{\varepsilon}{\phi} \right)^{2+\frac{3}{b}} \quad (3)$$

where D_s is the gas diffusion coefficient in soil (m^2 d^{-1}), D_0 is the diffusion coefficient in the free atmosphere (m^2 d^{-1}), Φ is total porosity (m^3 m^{-3}), and ε is the volumetric air content (m^3 m^{-3}). Values for the Campbell soil-water retention parameter (b) were taken from Clapp and Hornberger (1978). Soil water content data were collected using time domain reflectometry (TDR) with the Trime®-Pico IPH and Pico-BT and was used for the July, August, and September 2010 water content values. Prior to these dates water content was estimated from the measured water content profiles. Surface temperature and pressure was obtained from the CBOS weather station at the Horn Point Laboratory, Cambridge, MD (http://hpl.cbos.org/download.php).

Convection due to barometric pressure decrease

Low pressure systems that move into an area after a high pressure system cause convective gas fluxes. Low pressure results in the expansion of the pore space gas, and a

convective loss of gas from the soil to the atmosphere. Samples were not specifically taken on high pressure days, but 10 dates randomly fell on high pressure days that were followed shortly by low pressure systems. The volumetric gas filled pore space was calculated for 25 cm increments for the high pressure system and the low pressure system using the volumetric water content, which was measured using a TDR. We did not acquire the TDR probe until 2010; therefore, estimates of gas filled pore space were made for 7 of the 10 sampling dates based on the measured water content profiles. Measured volumetric water content values were available for June 18th 2010, July 9th 2010, and July 12th 2010. The water (WFPS) or gas filled pore space (GFPS) can be calculated by:

$$\text{Fractional WFPS} = \theta / \Phi \quad (4)$$

$$\text{Fractional GFPS} = 1 - \text{fractional WFPS} \quad (5)$$

where θ is the volumetric water content ($m^3\ m^{-3}$) and Φ is porosity ($m^3\ m^{-3}$). The calculated high pressure volumetric gas filled pore space (Φ_g) at each 0.25 m individual depth increment expands because of the decreased pressure, and the difference between the calculated high and expanded low volumetric gas content (corrected to the new low pressure) is lost to the atmosphere. Although some of these low pressure systems inevitably produced rainfall, I made this calculation strictly based on barometric pressure changes, and calculated changes due to infiltration separately. The volume lost was assumed to occur from the soil surface without mixing from the deeper soil depths, and the lost gas was assumed to have the same concentration as the shallowest, 0.25 m equilibration chamber. These calculations were made for each transect at each location.

These estimates were scaled up to a yearly time scale for 2009 using the groundwater depth record from Rfarm, and the barometric pressure changes from a Solinist barologger located at the Horn Point Laboratory, Cambridge, MD, approximately 8 km from Rfarm. The groundwater depth record was broken into seasons, Winter (Dec.-Feb.), Spring (Mar.-May), Summer (Jun.-Aug.), and Fall (Sep.-Nov.), and the average groundwater depth for each season was determined. The yearly average barometric pressure change between the maximum high pressure and the minimum low pressure was determined for the 33 low pressure events of 2009. Low pressure systems were defined as lower than the 10^{th} percentile of all half hourly barometric pressure recordings taken. If the pressure fell below this 10^{th} percentile, it was defined as a low pressure system. This consistent approach did not consider the effect of small changes in barometric pressure. The volumetric water content of the soil for each season was calculated or inferred, and calculations of flux from the soil surface using the average N_2O, CO_2, and CH_4 concentrations from the 0.25 m equilibration chambers at Rfarm were determined for the average winter, spring, summer, and fall event. The flux calculations were made as described in the previous paragraph as the difference between the previous high pressure volume and the corrected low pressure volume. The difference between the two being the volume lost from the soil surface. Each seasonal N_2O, CO_2, or CH_4 average flux was then multiplied by 8 for spring, summer, and fall, and 9 for winter, which represents the number of low pressure systems almost evenly distributed between the seasons. The spring, summer, fall, and winter fluxes were then totaled to give a yearly convective gas flux due to low pressure systems.

Convection due to rainfall events

The infiltration and percolation of rain water into the soil reduces the volumetric gas filled pore space of the soil, and raises the groundwater level, which causes a loss of gas to the atmosphere. This loss was calculated using the pre-rainfall TDR measured water filled pore space and the post-rainfall TDR measured water filled pore space. Soil gas profiles were taken at 25 cm increments, and the decrease in the volumetric gas content was determined for each increment. The losses from each increment were then summed to get a volumetric gas loss at the surface. The measured N_2O, CH_4, and CO_2 concentrations from the equilibration chamber at 0.25 m depth (transect A and B) were used to calculate a flux from the soil surface through this mechanism. Transfer of the gases from the vadose zone into the infiltrating water was considered negligible. It was again assumed that the gas volume was lost from the top 0.25 m of the soil and that no mixing of soil gases from deeper depth occurred.

The convective fluxes were scaled up to a year using the 2009 rainfall (from the Horn Point weather station, www.cbos.org) and groundwater level record from Rfarm. The previously determined average depth of the vadose zone for each season in 2009, and the same estimated GFPS from the barometric flux calculations were used. An estimated average fraction of air lost from the vadose zone at the soil surface due to infiltrating water was determined based upon 3 measured rainstorms. An estimated loss of the total soil column air volume per average seasonal rainstorm was calculated from the estimated GFPS data and the average fractional loss of air for the three rainstorms. As there was no consistent statistical difference between the number of rainfall events that occurred during each season, the yearly rainstorms were divided evenly between the seasons. It

was assumed that the average concentrations of N_2O, CH_4, and CO_2 at the 0.25 m equilibration chambers were representative of the average yearly concentration at this depth because we have limited spring, fall, and winter data.

Pre and post rainfall sampling

In order to capture the difference between pre- and post-rainfall conditions, samples were taken prior to large rainstorms in 2010. Samples were taken the day of, or the day before, a large rainfall event. Two large rainstorms were captured, and a third attempt was made to capture the rainfall from Hurricane Earl in early September 2010, but no significant precipitation was recorded. Gas and groundwater samples were taken again two to three days after the rainfall event in order to allow the water to fully infiltrate to the subsoils, and allow an incubation time. TDR data was taken before and after the rainstorms, and I had to assume minimal loss due to evapotranspiration between the rainstorm and my sampling. Paired t-tests were run to determine if differences existed between the pre and post rainfall concentrations. The concentration of each respective gas prior to the rainfall event at each depth in each transect was compared to the concentration after the rainfall event to determine if a statistical difference existed.

Results

Diffusive losses

In order to compare the magnitude of groundwater and vadose zone values, concentrations were converted to the partial pressure units of mmHg. If comparisons between groundwater and the vadose zone are not being made, the concentrations are expressed in μM units. At Mfarm and EFAG, the concentration of N_2O was always greater in groundwater than within the vadose zone (Fig. 4.3 A,B). The groundwater concentrations of CO_2 were greater than the vadose zone concentrations for all sampling dates except 7/9/2010 at Mfarm in transect B and 8/25/09 at EFAG where the concentration was greatest at the 0.25 m A depth. The high concentration on this date is responsible for the large calculated flux from the soil surface (Table 4.1). Similarly, at Rfarm, higher concentrations of CO_2 were observed in the vadose zone than in groundwater during the summer months of June, July and August (Chapter 3). The concentrations of CH_4 are very low at all three locations, but the concentration of CH_4 was always greater in groundwater than in the vadose zone for EFAG and Mfarm except for 7/12/10 at Mfarm when the dissolved CH_4 concentration was undetectable (Table 4.1).

The calculated diffusive losses of N_2O and CO_2 from the soil surface at Mfarm and EFAG are positive (Table 4.1). The concentration gradient of N_2O-N ranged from 0.09 to 1.64 mmole m^{-4}, and the diffusional flux of N_2O from the surface ranged from 1 to 29 μmoles m^{-2} day^{-1}. These fluxes are similar to those seen at Rfarm (range -0.3 to 19 μmoles m^{-2} day^{-1}), although slightly higher (Chapter 3). The concentration of CO_2 within the vadose zone was often large, and concentration gradients to the soil surface ranged

from 755-11,200 mmole CO_2 m^{-4} (Table 4.1). The calculated flux of CO_2 from the soil surface ranged from 7.2 to 235 mmoles CO_2 m^{-2} day^{-1}, which is similar to the Rfarm reported concentrations (range 10.9 to 180 mmoles CO_2 m^{-2} day^{-1}, Chapter 3).

The concentration gradient of CH_4 between the atmosphere and the vadose zone was often negative. CH_4 concentrations within the vadose zone were often below atmospheric (Table 4.1), indicating that a small net flux of CH_4 was moving into the soil (-10.2 to -0.4 μmoles m^{-2} day^{-1}). Slightly higher positive fluxes were calculated for August and September 2009 and September 2010 at EFAG, but generally, the concentrations of CH_4 within the vadose zone at these sites were below atmospheric (Table 4.1), indicating net CH_4 consumption. Vadose zone CH_4 concentrations for Rfarm were also low and ranged from 0 to 0.23 μM. Although the accumulated concentrations of CH_4 in the groundwater at these locations were low, dissolved concentrations did accumulate to substantial levels at nearby locations (Chapter 2). For example, a shallow piezometer at EFAG within a ponded wetland produced substantial concentrations of CH_4 in groundwater (median: 311 μM), likely due to its shallow depth in flooded sediment.

The diffusive losses of excess N_2-N to the atmosphere are highly variable. This is likely due to interacting biological and physical processes which affect both the Ar (physical) and N_2 (biological and physical) concentrations, and these processes were discussed in more detail in Chapter 3. The concentration gradient ranged from -585 to 843 mmole m^{-4} which is approximately the same range as the Rfarm gradients reported in Chapter 3 (-383 to 870 mmole m^{-4}). The excess N_2-N fluxes from the soil surface ranged from -28 to 22 mmole m^{-2} day^{-1} or -1200 to 970 kg ha^{-1} yr^{-1}. These estimates cannot be

used to infer denitrification or nitrogen fixation until physical processes, such as temperature mediated exchange with soil water, are accounted for, which is not yet possible (see Chapter 3).

Convection

Barometric convective losses:

Vadose zone gas can be transported from the soil to the atmosphere via convection due to decreases in pressure from a low pressure system moving into the area after a high pressure system. I sampled vadose zone gases during 10 high pressure systems that were followed by a low pressure system (Table 4.2). The changes in pressure from the time I sampled to the lowest low pressure ranged from 2.8 to 10.7 mmHg, and the time range over which this change occurred was 0.3 to 6.4 days. The volume lost from the vadose zone across the soil surface ranged from 0.0004 to 0.073 m^3 m^{-2}, or between 0.34 and 1.32% of the soil column gas volume. In order for a large volume of vadose zone gas to be lost through this mechanism, a large volume of gas had to be present in the surface soils. Soils with high water contents do not have large volumes of gas to lose and therefore will not lose large volumes due to barometric pressure changes. The convective N_2O flux from this mechanism ranged from 0.05 to 1.80 μmol N_2O-N m^{-2} $event^{-1}$ (Table 4.2). In time units, this scales to 0.02 to 2.80 μmol N_2O-N m^{-2} day^{-1}, which is 0.21 to 14.9% of the diffusive flux estimates (Table 4.1). The convective CH_4 flux ranged from 0.08 to 0.66 μmol m^{-2} $event^{-1}$ or 0.01 to 2.3 μmol m^{-2} day^{-1}, which is -52 to 8.9% of diffusive CH_4 estimates (Table 4.1). The convective CO_2

flux ranged from 439 to 7,380 μmol m^{-2} $event^{-1}$ or 240 to 11,500 μmol m^{-2} day^{-1}, (Table 4.2) which is 0.17 to 18.8% of diffusional CO_2 flux estimates (Table 4.1 and 4.2).

In order to compare diffusive and convective fluxes at the yearly time scale, it is necessary to consider the time scales over which these processes operate. Convection at Rfarm in 2009 was calculated using the groundwater depth record, average 0.25 m N_2O, CO_2, and CH_4 gas concentrations, and recorded barometric pressure changes. The average concentrations used to calculate yearly convective loss due to barometric pressure changes (and for infiltration induced convection described below) were 0.064 μM N_2O-N, 0.087 μM CH_4, and 932.4 μM CO_2. Low pressure was defined as the 10th percentile of all hourly barometric pressure measurements from 2009 (Fig. 4.4B). 33 low pressure events met this criterion in 2009, and the average barometric pressure change for these low pressure systems from the previous high was 13.3 mmHg (Fig. 4.4B). Calculations of gas loss for an average event were made per season and then scaled to the entire season (Table 4.3). The total gas volume lost during low pressure events from all four seasons was then combined to give a yearly loss due to barometric pressure changes. These pressure events scaled up to a yearly time scale accounted for 0.0005 kg N_2O-N ha^{-1} yr^{-1}, 0.0007 Kg CH_4-C ha^{-1} yr^{-1}, and 7.3 kg CO_2-C ha^{-1} yr^{-1} (Table 4.3).

Infiltration induced convective losses:

Infiltrating rainwater forces gases from the vadose zone to the atmosphere. There are two mechanisms: (1) decreases in the depth to the water table, and (2) increases in the percent water filled pore space (%WFPS) of the vadose zone. The largest volume of gas lost was from the top of the vadose zone because the surface soil has the largest gas filled

pore space, and therefore the largest volume of gas to lose (Table 4.4). The top 25 cm of soil absorbs rain initially and accounted for 49% and 55% of the gas volume lost from a July 2010 rain event for EFAG and Mfarm, respectively, and 23% from an August 2010 rain event at Rfarm (see Fig. 4.6A, 4.7A, 4.8A). A greater total volume of gas was lost from Rfarm (0.1 m^3 m^{-3}) because the vadose zone was deeper than at EFAG or Mfarm (~0.05 m^3m^{-2}, Table 4.4). TDR measurements were taken 2-3 days after the rain event; therefore, the loss in volume is a minimum estimate as evapotranspiration following the rain could have caused a loss of water from the surface soils. Nevertheless, a large increase in the %WFPS was observed at all three locations (Table 4.4).

Two rainstorms were sampled in July and August, 2010. Both rainstorms produced significant amounts of precipitation, and the precipitation totals were 6.9 cm over 1.5 hours (thunderstorm) and 5.84 cm over ~19 hours, respectively during August and July, 2010. The July rainfall data was taken from a weather station located at Mfarm, but if we had used the Horn Point Laboratory (HPL) weather station data we would have significantly underestimated the amount of precipitation as only 0.79 cm of rainfall was measured at HPL. However, the HPL weather station was used for RFarm because it is located less than 8 km away. Precipitation may have exceeded infiltration for the intense August rain event of 6.9 cm in 1.5 hours, and over land flow may have occurred. The July event occurred over a considerably longer period of time, potentially allowing infiltration to keep pace with precipitation. Samples were taken three days apart for the July event and only two days apart for the August event; therefore, more moisture was likely lost due to evaporative drying from the July sampling than the August sampling.

The convective fluxes due to infiltration were pulses of < 1 day. If expressed on a per day basis, the rates during a fraction of a day were similar to or greater than the diffusional N_2O, CO_2, and CH_4 fluxes (Table 4.1 & 4.4). The calculated convective N_2O fluxes ranged from 3.4 to 5.4 μmole N_2O-N m^{-2} $event^{-1}$, or for comparison, 4.3 to 62.5 μmole N_2O-N m^{-2} day^{-1}. These convective fluxes are similar or slightly greater than the diffusional fluxes accounting for between 38 and 300% of the diffusional N_2O fluxes. The calculated convective CO_2 fluxes ranged from 12.2 to 33.4 mmole m^{-2} $event^{-1}$ or 15.2 to 534 mmole m^{-2} day^{-1}, which is 40 to 112% of the calculated diffusional fluxes. The convective CH_4 fluxes fall within the same range or greater than the positive diffusional fluxes, ranging from 2.5 to 9.7 μmole m^{-2} $event^{-1}$ or 3.1-156 μmole m^{-2} day^{-1} (Table 4.4). The convective fluxes account for between -162 to 305% of the diffusional CH_4 fluxes, although the majority of the calculated diffusional CH_4 fluxes were negative (Table 4.1). Expressing these convective fluxes in per day units is not really relevant because the three sampled rainstorms all lasted less than a day, but it allows rate comparisons between diffusional and convective fluxes.

The convective flux from infiltration was scaled to a yearly time scale using the groundwater depth record, average N_2O, CO_2, and CH_4 gas concentrations at 0.25 m depth, and inferred average seasonal gas-filled pore-space profile. In 2009, rainfall was measured at the Horn Point Laboratory weather station for 144 of the 365 days (Fig. 4.4A & 4.5). The majority of these rainfall events were less than 0.5 cm, but one rainfall measured 5.12 cm (Fig. 4.5). A Kruskal-Wallis one-way ANOVA found that there was a significant difference between the amount of rainfall that fell per season ($p=0.041$), but Dunn's multiple mean comparison test found no significant difference between the

seasons. The median rainfall, excluding precipitation free days, was 0.30 cm day^{-1}. For the three rainstorms sampled in 2010, the average post-rainfall volume of gas-filled, pore space was 51.1 % of the pre-rainfall volume of gas-filled pore space. The post-rainfall gas filled pore space values were estimated assuming that on average, 51.1% of the pre-rainfall gas filled pore space remained in the soil after the rain event. The average convective loss per event was estimated seasonally and then scaled to the entire season (Table 4.5). The total gas volumes lost per season were then added to estimate a yearly convective flux due to infiltration. These calculated convective fluxes due to the infiltration of rainwater scaled up to a year account for 0.02 Kg N_2O-N ha^{-1} yr^{-1}, 0.03 Kg CH_4-C ha^{-1} yr^{-1}, and 323 Kg CO_2-C ha^{-1} yr^{-1} (Table 4.5).

Production after rainfall

The sampled precipitation events altered the concentrations of gases within most of the vadose zone and groundwater profiles sampled in summer 2010. The replicate piezometer transects are displayed separately to illustrate the heterogeneity between locations less than a meter apart (Fig. 4.6-4.8). As discussed above, measureable increases in the soil profile water filled pore space were observed after the rainfall event (Table 4.4, Fig. 4.6-4.8A).

The concentration of both N_2O and CO_2 significantly increased in the vadose zone after rainfall events at most of the depths (Table 4.6, Fig. 4.6-4.8). Moderate (Fig. 4.6C, 4.7 B,C & 4.8C) and large (Fig. 4.6B) increases in N_2O were observed in the vadose zone between the pre- and post-rainfall sampling as well as no significant change (Fig. 4.8B). Similarly, the concentration of CO_2 showed moderate (Fig. 4.6D, Fig. 4.8D), large (Fig.

4.7 D,E, Fig. 4.8E), and no changes (Fig. 4.6E) in the pre- and post-rainfall profile concentrations. The concentration of CH_4, if altered, significantly decreased (Table 4.6, Fig. 4.6 F, Fig. 4.8 F,G). These limited observations show that the dissolved gases in groundwater were not consistently affected by precipitation events. Dissolved N_2O and CO_2 significantly increased, decreased, or showed no significant difference between pre- and post-rainfall, depending on the location (Fig. 4.6-4.8 H, I, J). The concentrations of CH_4 dissolved in groundwater were largely lower than atmospheric at these three sites, and it was difficult to determine a significant change between pre- and post-rainfall.

Stoichiometry

The profiles of N_2O, CH_4, and CO_2 described above are the result of respiratory processes, and CO_2 is produced as a final product through all respiratory processes. If the concentration of excess CO_2 is compared to estimators of the electron acceptors consumed in respiration, in this case excess N_2 and the deficit in oxygen, a slope of 3.4 results (Fig. 4.9). This indicates that for all oxygen and NO_3^- that is consumed, 3.4 times more excess CO_2 is produced. This is greater than the approximate 1:1 stoichiometry expected for respiration. The additional excess CO_2 could be produced by the combined influences of agricultural liming and soil weathering. The concentrations of SO_4^{-2} measured in April 2008 and April 2009 at select piezometers ranged from 22.3 to 840 µM SO_4^{-2}, and the use of SO_4^{-2} as an alternative electron acceptor could account for some of the CO_2 production. The regression line does not cross exactly through the origin because other electron acceptors (e.g., Fe^{+3}, SO_4^{-2}) are likely also producing CO_2.

Discussion

Diffusion vs. convection

On a yearly time scale, the fluxes to the atmosphere via diffusion are much greater than the convective fluxes combined (Fig. 4.10). The convective fluxes due to infiltrating rain transported more N_2O, CH_4, and CO_2 than the convective fluxes due to barometric pressure changes (Fig. 4.10). The total flux of N_2O to the atmosphere from the soil from all three mechanisms is within the range of 0.07 to 1.49 Kg N_2O-N ha^{-1} yr^{-1}, and the median convective fluxes constituted 5 % of the median total yearly N_2O-N flux (Fig. 4.10). The total flux of CH_4 to the atmosphere from the soil from all three mechanisms is within the range of -0.5 to 13 Kg CH_4 ha^{-1} yr^{-1}, and the convective fluxes only accounted for 0.3% of the maximum calculated yearly CH_4 flux. The CO_2 flux from all three mechanisms is 643-10,627 Kg CO_2 ha^{-1} yr^{-1}, and the median convective CO_2 fluxes accounted for approximately 20% of the median calculated yearly CO_2-C flux (Fig. 4.10). These data clearly support hypothesis 1, although a large percent of CO_2 was transported via the convective mechanisms.

On a yearly time scale, the fluxes of N_2O, CO_2, and CH_4 are dominated by diffusional fluxes (Fig. 4.10). It is widely considered that diffusion constitutes the major soil flux process (Jury & Horton, 2004, Heincke & Kaupenjohann 1999, Clough et al. 2005), but a few studies have found convection to be important (Christensen 1985, Ohashi et al. 2007). If large concentrations were to build in the soil prior to a rainstorm when the water table was low and the soil had a low % WFPS, a large volume of high concentration gas could be transported to the atmosphere. However, this flux occurs over

a short time frame, making it difficult for this convective flux to account for a substantial amount of the annual flux.

Concentration & flux comparison

The soil gas concentrations are within the range of reported literature values for N_2O (Heincke & Kaupenjohann, 1999, Dunfield et al. 1995). N_2O concentrations 23,000 times the ambient atmospheric concentration have been reported in soils (Heincke & Kaupenjohann, 1999), but my values were rarely greater than 25 times the ambient concentration of 8.5 nM. The calculated flux values and yearly estimates were also in the range of those reported in the literature by review papers (e.g., Liebig et al. 2005, Heincke and Kaupenjohann, 1999, Munoz et al. 2010) and by other studies, but my rates are relatively low (Table 4.7).

Rfarm is a location with high groundwater N_2O concentrations (Fig. 4.8). The median N_2O concentrations at the three nested piezometers were 7.8, 11.1, and 8.3 μM N_2O-N, for the 2.1, 3.1 and 3.9 m depths, respectively, and concentrations as high as 38.4 μM N_2O-N were measured at the 3.0 m piezometer. This nested set of piezometers has the highest median concentrations of N_2O in groundwater that we have observed on the Delmarva Peninsula.

However, the groundwater N_2O concentrations do not translate into high vadose zone concentrations (Fig. 4.8) or high diffusional fluxes from the soil surface (Table 4.1). A few plausible explanations for the high groundwater N_2O but low vadose zone N_2O concentrations exist. First, I did not frequently measure the groundwater surface concentration of N_2O; therefore, the concentration dissolved in groundwater closer to the

water table could be lower than the concentrations reported at 2.1 m. Second, N_2O can be further reduced to N_2 in the vadose zone (Clough et al. 1999) or can be absorbed into the soil water where it can be further reduced to N_2 (Clough et al. 2005). This disconnects N_2O production rates at depth from N_2O flux from the soil surface (Goodroad & Keeney 1985, Clough et al. 1999). Due to the tortuous nature of soils, the travel time of a molecule of N_2O can be long, and the longer the molecule stays within the vadose zone, the higher the chances that it will be further reduced to N_2.

Small CH_4 sinks were observed in the soils at all three sites. The calculated CH_4 oxidation values are within the range or smaller than those reported by other researchers (Table 4.7). My calculated CH_4 oxidation rates fall on the lowest end of those reported in a review paper by Liebig et al. (2005), and decreased CH_4 oxidation rates in agricultural soils have been reported in the literature (Powlson et al. 1997, Dobbie et al. 1996A, B). The positive concentrations and fluxes observed at EFAG were minor, but within the range reported by other investigators (Lindau et al. 1990, Table 4.7). The consumption or production of CH_4 at these sites was not important, but at EFAG in particular, large CH_4 production in groundwater did occur down the topographic gradient at EFWET1a.

The CO_2 concentrations and fluxes seen within our profiles are similar to those seen by other researchers (e.g., Elberling et al. 2011, Liebig et al. 2005, Pacific et al. 2008, Table 4.7). For instance, the 20 cm measurement values of Pacific et al. (2008) approached 1800 µmol CO_2 L^{-1}, while the median CO_2 value at Rfarm at 25 cm was 850 µM CO_2 but the highest value observed in my data set at 25 cm was 1960 µM CO_2. The groundwater concentrations of CO_2 in the Delmarva locations often exceeded the vadose zone values, but in summer the deepest depths in the vadose zone often had higher

concentrations than groundwater (Chapter 3). The soil and groundwater CO_2 concentrations were large, and the soil CO_2 concentration in August 2010 at the 1.5 m depth at Rfarm represented 12% of the gas composition. The median CO_2 flux observed in this data set (36.5 mmol C m^{-2} d^{-1}) is similar to respiratory CO_2 fluxes from estuarine sediments (annual mean=68 mmol C m^{-2} d^{-1}, Boyton et al. 1980), affirming parallels between terrestrial soil and aquatic sediment biogeochemistry.

Gas fluxes to the atmosphere varied considerably between gases. The positive CH_4 fluxes to the atmosphere were minimal when they did occur, and often minor net CH_4 oxidation occurred (Figs. 4.6-4.8), removing CH_4 from the atmosphere. The CO_2 concentrations and fluxes to the atmosphere were large, but this does not necessarily translate into these areas being large contributors to the global CO_2 budget since CO_2 will also be taken up by plants at the surface for photosynthesis. The actual flux of CO_2 to the atmosphere will be the net between respiration in the soil and photosynthesis at the soil surface. Significant groundwater concentrations of N_2O accumulated at Rfarm and EFAG, but did not translate into large concentrations in the vadose zone. Indirect fluxes of these gases are possible, and groundwater could be transporting large concentrations of N_2O into nearby surface waters.

Convection calculations

A few generalizing assumptions were made in the calculation of infiltration induced convection. Primarily, I assumed that the gas does not mix between depths, and that the gas gradually fluxes out of the soil with the infiltration of rainwater. Although these assumptions are likely often valid, infiltration is not always this simple. In order

for rainfall to infiltrate into the soil, the gas that occupies the pore space needs to be able to flux out of the soil. If a saturated wetting front moved downward within the soil, infiltration could confine the soil air below the infiltrating water, inducing piston pressure, and inhibiting further infiltration (Adrian & Franzini 1966, Wang et al. 1998). In such a situation, vadose zone gas would not escape, and the water would stay above the trapped soil gas. Wang et al. (1998) showed that infiltrating water can trap gas resulting in significantly slower infiltration rates, with occasional gas eruption at the soil surface. This study shows that our assumptions are only valid if the infiltrating water displaced the surface gas gradually from the soil surface. Once vadose zone gas is trapped below rapidly infiltrating water and pressurized, some gas mixing may occur, and the erupting gas bubbles would likely be a mixture of all the trapped depths together.

When air bubbles become trapped under increased hydrostatic pressure, a portion of the trapped air can be forced into solution (Aeschbach-Hertig et al. 2000, 2008). N_2O can also be transferred into the dissolved state through diffusion because N_2O is highly soluble. If the concentration of N_2O was high in the trapped air, the concentration gradient would be from the trapped air into the infiltrating water. Instead of N_2O fluxing from the soil surface, the N_2O could be transferred from the gas phase to the water phase and remain trapped within the soil or further percolate down to groundwater.

Even if vadose zone gas does not get trapped under the infiltrating water, N_2O could still diffuse into the soil water. Water within the vadose zone is a potential sink for N_2O if it is reduced to N_2 (Clough et al. 2005). Large concentrations up to three orders of magnitude above air equilibrium have been reported to accumulate in soil solution (Heincke & Kaupenjohann 1999). High % WFPS can lead to the diffusion of N_2O into

the soil water because it is trapped within the vadose zone, and then the dissolved N_2O can be further reduced to N_2 (Lessard et al. 1996). Infiltrating water could also act to introduce gases into the vadose zone. Both O_2 and CH_4 concentrations were often below atmospheric concentrations in the vadose zone, therefore infiltrating rain in equilibrium with air could introduce both gases into the vadose zone.

The assumptions made in the calculation of barometric pressure-induced losses of soil gas are likely reasonable. Pressure changes tend to occur much more gradually than infiltration events, and without disturbance. The gas is lost because the gas volume gradually increases from the reduction in pressure, and it is likely that little mixing occurs and that the gas is lost from the soil surface. Pressure changes in the soil column have been observed as the result of a change in atmospheric pressure (e.g. Massman and Farrier, 1992, Choi et al. 2002); therefore, the expansion of the entire soil column in my calculations is reasonable. Romell (1922) estimated that no more than 1% of soil aeration could be due to barometric pressure changes, which falls within the range of the estimates I presented. Scenarios can be imagined, however, where large concentrations of N_2O, CH_4, or CO_2 built up within the soil profile before a large pressure change from an elevated high pressure system to a depressed low pressure system. Such a situation might occur in a hurricane or tornado. Category 3 hurricanes are classified to have central pressures of 945-964 mb or 708-723 mmHg, considerably lower than normal barometric air pressure (760 mmHg, Ahrens 2007).

The convective flux calculations were made for either the loss of gas due to infiltration, or a decrease in barometric pressure, not a simultaneous decrease in pressure caused by a storm system that produced precipitation. In such a situation, the soil gas

would be drawn from the soil surface by the decrease in barometric pressure, and then further flushed by the infiltrating precipitation. These calculations also did not take into account the increased production or consumption of soil gases that has been reported by other scientists after rainfall events, but will be discussed below. Convective fluxes of high concentration vadose zone gas can account for a substantial percentage of a yearly flux estimate (e.g., CO_2 in this study). For the low concentration gases, these convective mechanisms do not substantially affect the yearly flux estimates, but over the span of a day or a few hours, these mechanisms could be important, short-term fluxes to the atmosphere.

Surface chambers vs. profile measurements

Instead of using surface chamber-based methods to give a direct flux from the soil surface, concentration profiles were used to examine the concentrations below the soil surface to calculate a diffusion-based flux to the atmosphere. Clough et al (2005) stated that "the fate and movement of N_2O in the subsoil is still poorly quantified" which was a motivation for this research. Both surface chamber-based and profile-calculation methods have their advantages and disadvantages, which are discussed below.

Logistically, the equilibration chambers (referred to in this comparison as vadose zone samplers) and surface flux chambers are different. The vadose zone samplers require some installation time as they need to be hand-augered into the ground and then left to settle for a period of time. The surface flux chambers on the other hand can be set up much faster. Once installed, the vadose zone gas samplers can be sampled in less than 5 minutes per sampler, while surface flux chambers require a longer amount of time to

sample as initial measurements are taken, and then further samples are taken at varying intervals. One surface chamber can be used to make a measurement of flux from the soil surface, while multiple vadose zone samplers are required to acquire a gas profile. In my calculations, however, I only used the shallowest vadose zone samplers to calculate the composition of the gas flux from the soil surface.

However, the diffusion calculations for vadose zone samplers require knowledge of the soil physical processes. The diffusion coefficients were not directly measured, but literature reported, laboratory-measured coefficients in free air were instead corrected for porosity and tortuosity. Tortuosity corrections were based upon literature empirical measurements, which were the only option with our resources, but may not be the best option. The soil surface flux measured in a soil chamber is a direct measurement and does not require a knowledge of the below-ground soil physical properties, although wind effects on boundary layer gradients could potentially be under-estimated. Determining an accurate soil gas flux from the surface using soil concentration profiles is affected by the accuracy of the diffusivity coefficients and the errors and uncertainties involved in measuring the actual gas profile (Rolston et al. 1976).

The shallowest vadose zone samplers installed at all three sites were 0.25 m below the ground. We do not have data from the high C root zone (0-0.25 m), which potentially produced large concentrations of CO_2 and N_2O.. If N_2O, CH_4, or CO_2 hot spots exist at the soil surface, I did not include them in the measurements reported above.

Soil flux chambers have some inherent problems associated with their use. The concentration gradients of gases can be disturbed in the soil by the use of a gas chamber (Davidson et al. 2002), and the installation of unvented chambers has been found to

disturb the initially emerging gas concentrations (Christensen et al. 2011). Chamber mixing is also an issue; chambers without mixing can significantly underestimate the flux out of the soil surface in comparison to well mixed chambers (Christiansen et al. 2011). Pressure differentials within the gas chamber caused by changing temperature or the circulating of gases can cause gases to be sucked out of the soil or pushed into the soil, which can be alleviated by chamber vents (Davidson et al. 2002). Similarly, syringe suction of a closed chamber can create a partial vacuum that the soil gases will alleviate (Bekkue et al. 1995). Even though there are many problems associated with gas chambers, Davidson et al. (2002) stated that "properly designed and deployed chambers provide a reliable means of accurately measuring soil respiration in terrestrial ecosystems."

Pre and post rainfall measurements- hot moments?

Pre and post rainfall sampling was limited to summer and early fall months when there was a substantial vadose zone. This limited the measurements mostly to the summer because the vadose zone on the Delmarva Peninsula largely vanishes in late autumn through spring (Fig. 4.11A). In the summer, rainfall events along with high temperatures have the greatest chance of increasing vadose zone microbial respiratory processes. The increased concentrations of N_2O and CO_2 observed in this study might not have been observed in the winter, as the vadose zone is much smaller, moisture is often not limited, and temperatures are considerably lower (Fig. 4.11B). Nonetheless, the available data support hypothesis 2 concerning the effect of rainfall on vadose zone N_2O and excess N_2 concentrations, but not for CH_4.

Wetting of the soil typically produced an increase in the CO_2 concentrations within the vadose zone, or no significant difference was observed (Fig. 4.6-4.8). Increased fluxes of CO_2 from the soil surface have been observed by other researchers (Rochette et al. 1991, Morell et al. 2010, Mariko et al. 2007). The actual peak of CO_2 production was potentially missed from the locations that showed no significant difference before and after the rainstorms as other researchers have observed increases in CO_2 flux from the soil surface within minutes to hours after rainfall events (Lee et al. 2004, Rochette et al. 1991). The immediate pulse in CO_2 flux has been postulated to occur from rainfall because the organic layer in the surface soil is often below the water potential necessary to allow microbial processes to occur. When it does rain, the organic layer becomes wet, which activates the soil microbes, promoting a flux of CO_2 from the soil surface (Lee et al. 2004). However, other researchers have shown a delay in the peak CO_2 flux after rainfall events (Hao et al. 2010). This slower response could be from rainfall induced translocation of substrate to depth, causing an increased pulse of CO_2 from deeper soil layers (Lee et al. 2004). Increased water content alone could initiate increased soil respiration and decreased diffusion away from the area of production, causing an increase in CO_2 concentrations within the vadose zone as I observed.

Another factor that can influence the amount of CO_2 produced from a rainstorm and the mechanism that produced the pulse is the amount of rainfall received. If a small amount of precipitation reaches the soil surface, increased CO_2 production would only occur in the surface soils (Hao et al. 2010). Larger rainfall events, such as the ones sampled in this study, are more likely to infiltrate to deeper depths and cause increased CO_2 production at depth, which I have shown.

Wetting of the soil sometimes produced an increase in N_2O or produced no significant change in the soil gas concentration (Fig. 4.6-4.8). N_2O surface emissions have been shown to increase with % WFPS (Breuer et al. 2000, Dobbie and Smith 2001, 2003) and to pulse after rainfall events in the field (Breuer et al. 2000, Dobbie and Smith 2003) or experimentally using soil cores (Priemé and Christensen 2001, Ruser et al. 2006). Rainfall could stimulate denitrification if the % WFPS increased substantially, or stimulate nitrification if the soils were very dry, and the % WFPS increased moderately. In laboratory experiments, Khalil and Baggs (2005) and Bateman and Baggs (2005) found N_2O derived from denitrification to be highest from the highest WFPS treatments (75% and 70% WFPS, respectively), and N_2O derived from nitrification to be highest from the moderate WFPS treatments (30-60%). Although most of these experiments measure soil core or chamber headspaces, Goodroad and Keeney (1985) observed an increase in N_2O concentration within the soil profile after rainfall events.

Although pulses in N_2O have been observed to occur immediately after rainfall events, I sampled 2 to 3 days after large storms. This strategy was partially based on the relationship found between increasing N_2O emissions and the amount of rainfall received in the previous three days prior to sampling by Dobbie and Smith (2003). Waiting to sample also allowed the infiltrating rainfall time to percolate into the subsoils.

The observed production of N_2O at my study sites occurred in areas that were not actively receiving agricultural N. However, denitrification of soil NO_3^- is the suspected source of the N_2O. The source of NO_3^- in these soils is residual NO_3^- from years of previous fertilization, N recycling, precipitation, and groundwater that infiltrated locally underneath the nearby agricultural field (Chapter 2). Therefore, areas such as agricultural

fields with a much steadier source of N to the surface soils would likely produce larger fluxes from the soil surface, and respond with a much larger pulse after rainfall events. Increased surface fluxes of N_2O after rainfall events have been seen shortly after fertilization (Sehy et al. 2003), and Dobbie and Smith (2003) found increased N_2O fluxes out of the surface soils with increasing %WFPS if 5 mg NO_3^--N Kg^{-1} was present in the soil. Similarly, events might be seen in the fall due to crop senescence and biomass breakdown and conversion of DON to NH_4^+ and then oxidation of NH_4^+ to NO_3^- through nitrification, potentially producing N_2O. Areas that might produce higher responses to rainfall events are lawns, golf courses, and agricultural fields.

Few significant differences existed in the CH_4 data before and after the rainstorms. When significant differences were observed, gaseous soil CH_4 concentration decreased (Fig. 4.6-4.8). Other studies have found relationships between high % WFPS and reduced CH_4 oxidation (e.g., Castro et al. 1994, van den Pol-van Dasselaar et al. 1998). Studies that have examined the effect of rainfall on CH_4 flux typically report no significant difference between pre- and post-rainfall (e.g., Priemé & Christensen 2001). CH_4 oxidation has been shown to be limited in dry soils (Dobbie and Smith 1996b, van den Pol-van Dasselaar et al. 1998), but the % WFPS of my soils were likely not limiting (~40% WFPS before the rainstorm at 25 cm). Potentially, CH_4 was produced or consumed above our 25 cm sampler in the high organic layers near the soil surface, but we were unable to capture this production or consumption. However, Saari et al. (1998) found negligible microbial CH_4 oxidation in the organic horizon, and found increased oxidation of atmospheric CH_4 when the organic layer was peeled indicating that CH_4 oxidation was occurring in the mineral soil, and oxidation increased because the organic

horizon was restricting the diffusion of CH_4 from the atmosphere into the mineral soil. This study suggests that I captured the majority of CH_4 oxidation with my sampling strategy. CH_4 exchange with infiltrating rainfall could also occur, and in low CH_4 environments rainfall could be a source of CH_4 to the soil.

Conclusions

Diffusion is the dominant mechanism that drives transport of the gases N_2O, CO_2, and CH_4 to the atmosphere. Convective fluxes caused by precipitation events or barometric pressure changes have the ability to affect the short term N_2O, CO_2, or CH_4 flux to the atmosphere, and the convective flux of CO_2 did substantially increase (20%) the CO_2 yearly flux to the atmosphere. The calculated N_2O annual flux estimates fall within the range of reported yearly flux estimates, but my N_2O flux to the atmosphere is not large compared to other sites. Groundwater concentrations of N_2O are substantial, especially at Rfarm, but these concentrations do not translate into large soil N_2O fluxes. Indirect fluxes to the atmosphere via transport in groundwater to surface water bodies are possible (but unmeasured here) and could potentially transport substantial concentrations through this mechanism. The CO_2 flux from the soil surface is large, whereas the fluxes of CH_4 were often slightly negative and into the soil (oxidation of atmospheric CH_4), with occasional small positive fluxes. Increased concentrations of both CO_2 and N_2O were observed in the vadose zone after rainfall events at all three locations, which has been observed by other researchers as an increased pulse of either N_2O or CO_2 from the soil surface, but fewer studies have looked at N_2O and CH_4 below ground concentrations after rainfall events. CH_4 concentrations sometimes decreased after rainfall events, and the literature suggested that CH_4 oxidation would be reduced under increased %WFPS conditions. As global climate change appears to be inevitable, and many areas are predicted to have increased precipitation and longer dry periods, the increased production of these greenhouse gases after rainfall events is important to understand.

References

Adrian, D.D., J.B. Franzini. 1966. Impedance to infiltration by pressure build-up ahead of the wetting front. Journal of Geophysical Research. 71:5858-5862.

Adrian, N.R., J.A. Robinson, J.M. Suflita. 1994. Spatial variability in biodegradation rates as evidenced by methane production from an aquifer. Applied and Environmental Microbiology. 60(10):3632-3639.

Aeschbach-Hertig, W., F. Peeters, U. Beyerle, and R. Kipfer. 2000. Palaeotemperature reconstruction from noble gases in groundwater taking into account equilibration with entrapped air. Nature. 405:1040-1044.

Aeschbach-Hertig, W., H. El-Gamal, M. Wieser, L. Palcsu. 2008. Modeling excess air and degassing in groundwater by equilibrium partitioning with a gas phase. Water Resources Research. 44:1-12.

Ahrens, C.D. 2007. Meterology Today: An introduction to weather, climate, and the environment. 8th ed. Belmont, CA. Thomas Brooks/Cole.

Bateman, E.J., E.M. Baggs. 2005. Contribution of nitrification and denitrification to N_2O emissions from soils at different water-filled pore space. Biology and Fertility of Soils. 41:379-388. DOI: 10.1007/s00374-005-0858-3.

Bekku, Y., H. Koizumi, T. Nakadai, H. Iwaki. 1995. Measurements of soil respiration using closed chamber methods: An IRGA technique. Ecological Research. 10:369-373.

Bohlke, J.K., J.M. Denver. 1995. Combined use of groundwater dating, chemical, and isotopic analyses to resolve the history and fate of nitrate contamination in

two agricultural watersheds, Atlantic coastal plain, Maryland. Water Resources Research. 31(9):2319-2339.

Boynton, W.R., W.M. Kemp, C.G. Osborne. 1980. Nutrient fluxes across the sediment-water interface in the turbid zone of a coastal plain estuary. Estuarine Perspectives. Academic Press, pp. 93-107.

Breuer, L., H. Papen, K. Butterbach-Bahl. 2000. N_2O emission from tropical forest soils of Australia. Journal of Geophysical Research. 105(D21):26,353-26,357.

Burgin, A.J., S.K. Hamilton. 2007. Have we overemphazised the role of denitrification in aquatic ecosystems? A review of nitrate removal pathways. Frontiers in Ecology and the Environment. 5(2):89-96.

Castro, M.S., J.M. Melillo, P.A. Steudler, J.W. Chapman. 1994. Soil moisture as a predictor of methane uptake by temperate forest soils. Canadian Journal of Forestry Research. 24:1805-1810.

Choi, J.W., F.D. Tillman Jr., J.A. Smith. 2002. Relative importance of gas-phase diffusive and advective trichloroethene (TCE) fluxes in the unsaturated zone under natural conditions. Environmental Science and Technology. 36:3157-3164.

Christensen, S. 1985. Denitrification in a sandy loam as influenced by climatic and soil conditions. Tidsskr. Planteavl. 89:351-365.

Christiansen, J.R., J.F.J. Korhonen, R. Juszczak, M. Giebels, M. Pihlatie. 2011. Assessing the effects of chamber placement, manual sampling and headspace mixing on CH_4 fluxes in a laboratory experiment. Plant and Soil. 343:171-185. DOI 10.1007/s11104-010-0701-y.

Clapp, R.B., G.M. Hornberger. 1978. Empirical equations for some soil hydraulic properties. Water Resources Research. 14(4):601-604.

Clough, T.J., S.C. Jarvis, E.R. Dixon, R.J. Stevens, R.J. Laughlin, D.J. Hatch. 1999. Carbon induced subsoil denitrification of ^{15}N-labelled nitrate in 1 m deep soil columns. Soil Biology and Biochemistry. 31:31-41.

Clough, T.J., R.R. Sherlock, D.E. Rolson. 2005. A review of the movement and fate of N_2O in the subsoil. Nutrient Cycling in Agroecosystems. 72:3-11.

Colt, J. 1984. Computation of dissolved gas concentrations in water as functions of temperature, salinity, and pressure. Bethesda, MD: American Fisheries Society.

Conrad, R., F. Rothfuss. 1991. Methane oxidation in the soil surface layer of a flooded rice field and the effect of ammonium. Biology and Fertility of Soils. 12(1):28-32. DOI: 10.1007/BF00369384.

Crutzen, P.J., 1981. Atmospheric chemical processes of the oxides of nitrogen, including N_2O. In Delwiche,C.C.(ed.). Denitrification, Nitrification, and Atmospheric Nitrous Oxide. Wiley, New York, pp.17-44.

Davidson, E.A., K. Savage. L.V. Verchot, R. Navarro. 2002. Minimizing artifacts and biases in chamber-based measurements of soil respiration. Agricultural and Forest Meterology. 113:21-37.

Dobbie, K.E., K.A. Smith, A. Priemé, S. Christensen, A. Degorska, P. Orlanski. 1996A. Effect of land use on the rate of methane uptake by surface soils in northern Europe. Atmospheric Environment. 30(7):1005-1011.

Dobbie, K.E., K.A. Smith. 1996B. Comparison of CH_4 oxidation rates in woodland, arable and set aside soils. Soil biology & biochemistry. 28(10-11):1357-1365.

Dobbie, K.E., K.A. Smith. 2001. The effects of temperature, water-filled pore space and land use on N_2O emissions from an imperfectly drained gleysol. European Journal of Soil Science. 52:667-673.

Dobbie, K.E., K.A. Smith. 2003. Nitrous oxide emission factors for agricultural soils in Great Britain: The impact of soil water-filled pore space and other controlling variables. Global Change Biology. 9:204-218.

Dunfield, P.F., E. Topp, C. Archambault, R. Knowles. 1995. Effect of nitrogen fertilizers and moisture content on CH_4 and N_2O fluxes in a humisol: Measurements in the field and intact soil cores. Biogeochemistry. 29:199-222.

Elberling, B., L. Askaer, C.J. Jørgensen, H.P. Joensen, M. Kühl, R.N. Glud, F.R. Lauritsen. 2011. Linking soil O_2, CO_2, and CH_4 concentrations in a wetland soil: Implications for CO_2 and CH_4 fluxes. 45:3393-3399. dx.doi.org/10.1021/es103540k.

Elmi, A.A., C. Madramootoo, C. Hamel, A. Liu. 2003. Denitrification and nitrous oxide to nitrous oxide plus dinitrogen ratios in the soil profile under three tillage systems. Biology and Fertility of Soils. 38(6):340-348.

Fortuin, N.P.M., A. Willemsen. 2005. Exsolution of nitrogen and argon by methanogenesis in Dutch groundwater. Journal of Hydrology. 301:1-13.

Goodroad, L.L., D.R. Keeney, L.A. Peterson. 1984. Nitrous oxide emissions from agricultural soils in Wisconsin. Journal of Environmental Quality. 13(4):557-561.

Goodroad, L.L., D.R. Keeney. 1985. Site of nitrous oxide production in field soils. Biological Fertility of Soils. 1:3-7.

Hao, Y., Y. Wang, X. Mei, X. Cui. 2010. The response of ecosystem CO_2 exchange to small precipitation pulses over a temperate steppe. Plant Ecology. 209:335-347.

Heincke, M., M. Kaupenjohann. 1999. Effects of soil solution on the dynamics of N_2O emissions: A review. Nutrient Cycling in Agroecosystems. 55:133-157.

Jones W.J. 1991. Diversity and physiology of methanogens. In Rogers J.E., W.B. Whitman (ed). Microbial Production and consumption of greenhouse gases: Methane, nitrogen oxides, and halomethanes. American Society for Microbiology, pp.39-55.

Jury, W.A., R. Horton. 2004. Soil Physics. 6th ed. Hoboken. Wiley.

Kana, T.M., C. Darkangelo, M.D. Hunt, J.B. Oldham, G.E. Bennett, J.C. Cornwell. 1994. Membrane inlet mass spectrometer for rapid high-precision determination of N_2, O_2 and Ar in environmental water samples. Analytical Chemistry. 66(23):4166-4170.

Khalil, M.I., E.M. Baggs. 2005. CH_4 oxidation and N_2O emissions at varied soil water-filled pore spaces and headspace CH_4 concentrations. Soil Biology and Biochemistry. 37:1785-1794.

Knowles, R. 1982. Denitrification. Microbiological Reviews. 46(1):43 -70

Koponen, H.T., L.Flöjt, P.J. Martikainen. 2004. Nitrous oxide emissions from agricultural soils at low temperatures: A laboratory microcosm study. Soil biology and biochemistry. 36:757-766.

Kutzbach, L., D. Wagner, E.M. Pfeiffer. 2004. Effects of micro relief and vegetation on methane emissions from wet polygonal tundra, Lena Delta, Northern Siberia. Biogeochemistry. 69:341-362.

Lange, N.A., 1961. Handbook of Chemistry and Physics. New York, NY. McGraw-Hill Book Company, Inc.

Le Mer, J., P. Roger. 2001. Production, oxidation, emission and consumption of methane by soils: A review. European Journal of soil Biology. 37:25-50.

Lee, X., H.J. Wu, J. Sigler, C. Oishi, T. Siccama. 2004. Rapid and transient responses of soil respiration to rain. Global Change Biology. 10:1017-1026.

Lessard, R., P. Rochette, E.G. Gregorich, E. Pattey, R.L. Desjardins. 1996. Nitrous oxide fluxes from manure-amended soil under maize. Journal of Environmental Quality. 25(6):1371-1377.

Liebig, M.A., J.A. Morgan, J.D. Reeder, B.H. Ellert, H.T. Gollany, G.E. Schuman. 2005. Greenhouse gas contributions and mitigation potential of agricultural practices in northwestern USA and western Canada. Soil & Tillage Research. 83:25-52.

Lindau, C.W., W.H. Patrick, Jr., R.D. Delaune, K.R. Reddy. 1990. Rate of accumulation and emission of N_2, N_2O and CH_4 from a flooded rice soil. Plant and Soil. 129:269-276.

Massman, J., D.F. Farrier. 1992. Effects of atmospheric pressures on gas transport in the vadose zone. Water Resources Research. 28(3):777-791.

Massman, W.J. 1998. A review of the molecular diffusivities of H_2O, CO_2, CH_4, O_3, SO_2, NH_3, N_2O, NO, and NO_2 in air, O_2 and N_2 near STP. Atmospheric Environment. 32(6):1111-1127.

Mathieu, O., J. Lévêque, C. Hénault, M.-J. Milloux, F. Bizouard, F. Andreux. 2006. Emissions and spatial variability of N_2O, N_2 and nitrous oxide mole fraction at the field scale, revealed with ^{15}N isotopic techniques. Soil Biology and Biogeochemistry. 38(5):941-951.

McClain, M.E., E.W. Boyer, C.L. Dent, S.E. Gergel, N.B. Grimm, P.M. Groffman, S.C. Hart, J.W. Harvey, C.A. Johnston, E. Mayorga, W.H. McDowell, G. Pinay. 2003. Biogeochemical hot spots and hot moments at the interface of terrestrial and aquatic ecosystems. Ecosystems. 6:301-312.

Megonigal, J.P., M.E. Hines, P.T. Visscher. 2005. Anaerobic metabolism: Linkages to trace gases and aerobic processes. In Schlesinger W.H. (ed). Biogeochemistry. Elsevier, pp 317-424.

Meng, L., W. Ding, Z. Cai. 2005. Long-term application of organic manure and nitrogen fertilizer on N_2O emissions, soil quality and crop production in a sandy loam soil. Soil Biology & Biochemistry. 37:2037-2045.

Moldrup, P., T. Olesen, J. Gamst, P. Schjønning, T. Yamaguchi, D.E. Rolston. 2000 A. Predicting the gas diffusion coefficient in repacted soil: Water-induced linear reduction model. Soil Society of America Journal. 64:1588-1594.

Moldrup, P., T. Olesen, J. Gamst, P. Schjønning, T. Yamaguchi, D.E. Rolston. 2000B. Predicting the gas diffusion coefficient in undistrubed soil from soil water characteristics. Soil Society of America Journal. 64:94-100.

Moldrup, P., T. Olesen, T. Yamaguchi, P. Schjonning, and D. Rolston. 1999. Modeling diffusion and reaction in soils: IX. The Buckingham-Burdine-Campbell equation for gas diffusivity in undisturbed soil. Soil Science. 164:542-551.

Mookherji, S., G.W. McCarty, J.T. Angier. 2003. Dissolved gas analysis for assessing the fate of nitrate in wetlands. Journal of the American Water Resources Association. 39(2):381-387.

Morell, F.J., J. Álvaro-Fuentes, J. Lampurlanés, C. Cantero-Martínez. 2010. Soil CO_2 fluxes following tillage and rainfall events in a semiarid Mediterranean agroecosystems: Effects of tillage systems and nitrogen fertilization. Agriculture, Ecosystems and Environment. 139:167-173.

Mosier, A.R., J.M. Duxbury, J.R. Freney, O.Heinemeyer, K. Minami, D.E. Johnson. 1998. Mitigating agricultural emissions of methane. Climate Change. 40(1):30-80.

Munoz, C., L. Paulino, C. Monreal, E. Zagal. 2010. Greenhouse gas (CO_2 and N_2O) emissions from soils: A review. Chilean Journal of Agricultural Research. 70(3):485-497.

Ohashi, M., L. Finer, T. Domisch, A.C. Risch, M.F. Jurgensen, P. Niemela. 2006. Seasonal and diurnal CO_2 efflux from red wood ant (*Formica aquilonia*) mounds in boreal coniferous forests. Soil Biology and Biogeochemistry. 39(7):1504-1511. DOI:10.1016/j.soilbio.2006.12.034 .

Owens, J.P., and C.S. Denny. 1979. Upper Cenozoic deposits of the central Delmarva Peninsula, Maryland and Delaware. US Geological Survey Professional Paper 1067-A.

Pacific, V.J., B.L. McGlynn, D.A. Riveros-Iregui, D.L. Welsch, H.E. Epstein. 2008. Variability in soil respiration across riparian-hillslope transitions. Biogeochemistry. 91:51-70.

Papen, H., K. Butterbach-Bahl. 1999. A 3-year continuous record of nitrogen trace gas fluxes from untreated and limed soil of a N-saturated spruce and beech forest ecosystem in Germany, 1 N_2O emissions. Journal of Geophysical Research. 104(D15):18,487-18,503.

Powlson, D.S., K.W.T. Goulding, T.W. Willison, C.P. Webster, B.W. Hütsch. 1997. The effect of agriculture on methane oxidation in soils. Nutrient cycling in agroecosystems. 49:59-70.

Prescott, L.M., J.P Harley, D.A. Klein. 2002. Microbiology. 5th ed. New York. McGraw-Hill.

Priemé, A., S. Christensen. 2001. Natural pertubations, drying-wetting and freezing-thawing cycles, and the emission of nitrous oxide, carbon dioxide and methane from farmed organic soils. Soil Biology and Biochemistry. 33:2083-2091.

Raghoebarsing, A.A., A.Pol, K.T. Van de Pas-Schoonen, A.J.P. Smolders, K.F. Ettwig, W.I.C. Rijpstra, S. Schouten, J.S.S. Damste, H.M.M. Op den Camp, M.S.M. Jetten, M. Strous. 2006. A microbial consortium couples anaerobic

methane oxidation to denitrification. Nature. 440:918-921. DOI:10.1038/nature04617.

Rochette, P., R.L. Desjardins, E. Pattey. 1991. Spatial and temporal variability of soil respiration in agricultural field. Canadian Journal of Soil Science. 71:189-196.

Rolston, D.E., M. Fried, D.A. Goldhamer. 1976. Denitrification measured directly from nitrogen and nitrous oxide gas fluxes. Soil Science Society of America. 40: 259-266.

Romell, L.G. 1922. Luftväxlingen I marken som ekologisk factor. Medd. Statens Skogsfarsoks-anstalt 19:2.

Ruser, R., H. Flessa, R. Russow, G. Schmidt, F. Buegger, J.C. Munch. 2006. Emissions of N_2O, N_2 and CO_2 from soil fertilized with nitrate: Effect of compaction, soil moisture and rewetting. Soil Biology and Biochemistry. 38:263-274.

Saari, A., J. Heiskanen, P.J. Martikainen. 1998. Effect of the organic horizon on methane oxidation and uptake in soil of a boreal Scots pine forest. FEMS Microbiology Ecology. 26:245-255.

Sehy, U., R. Ruser, J.C. Munch. 2003. Nitrous oxide fluxes from maize fields: Relationship to yield, site-specific fertilization, and soil conditions. Agricultural, Ecosystems and the Enviornment. 99:97-111.

Silver, W.L., A.E. Lugo, M. Keller. 1999. Soil oxygen availability and biogeochemistry along rainfall and topographic gradients in upland wet tropical forest soils. Biogeochemistry. 44: 301-328.

Soil Survey Staff, Natural Resources Conservation Service, United States Department of Agriculture. Web Soil Survey. Available online at http://websoilsurvey.nrcs.usda.gov/ accessed [07/01/2011].

Stainton, M.P. 1973. A syringe gas-stripping procedure for gas-chromatographic determination of dissolved inorganic and organic carbon in fresh water and carbonates in sediments. Journal of Fisheries Research Board of Canada. 30:1441-1445.

Sutton, A.J., T.R. Fisher, A.B. Gustafson. 2010. Effects of restored stream buffers on water quality in non-tidal streams in the Choptank River basin. Water Air and Soil Pollution. 208(1-4):101-118. DOI: 10.1007/s11270-009-0152-3.

Teepe, R., R. Brumme, F. Beese. 2001. Nitrous oxide emissions from soil during freezing and thawing periods. Soil Biology and Biochemistry. 33:1269-1275.

Van den Pol-van Dasselaar, A., M.L. van Beusichem, O. Oenema. 1998. Effects of soil moisture content and temperature on methane uptake by grasslands on sandy soils. Plant and Soil. 204:213-222.

Wang, Z., J. Feyen, M.T. Van Genuchten, D.R. Nielsen. 1998. Air entrapment effects on infiltration rates and flow instability. Water Resources Research. 34(2):213-222.

Weiss, R.F. 1970. The solubility of nitrogen, oxygen and argon in water and seawater. Deep Sea Research and Oceanographic Abstracts. 17(4):721-735.

Weiss, R.F., B.A. Price. 1980. Nitrous oxide solubility in water and seawater. Marine Chemistry. 8:347-359.

Wrage, N., G.L. Velthof, M.L. van Beusichem, O. Oenema. 2001. Role of nitrifier denitrification in the production of nitrous oxide. Soil Biology and Biochemistry. 33(12-13):1723-1732.

Yao, Z., B. Wolf, W. Chen, K. Butterbach-Bahl, N. Brüggemann, M. Wiesmeier, M. Dannenmann, B. Blank, X. Zheng. 2010. Spatial variability of N_2O, CH_4 and CO_2 fluxes within the Xilin River catchment of Inner Mongolia, China: A soil core study. Plant Soil. 331:341-359. DOI 10.1007/s11104-009-0257-x.

Table 4.1- Calculated concentration gradients and diffusional fluxes across the soil surface. The concentration gradients were calculated from the shallowest equilibration chamber to the soil surface, and the flux estimates were made using this gradient and a diffusion coefficient, corrected for atmospheric temperature, pressure, tortuosity, and porosity (eq. 2-3).

			Gradient				Flux			
Site	Transect	date	N_2O-N	CH_4	N_2-N	CO_2	N_2O-N	CH_4	N_2-N	CO_2
			mmole m^{-4}				μmoles m^{-2} day^{-1}		mmoles m^{-2} day^{-1}	
Mfarm	A	12/13/2009	1.04	-0.10	-240		7.46	-0.94	-2.14	
	B	12/13/2009	0.15	-0.09	-255	1040	1.04	-0.83	-2.27	7.2
	A	7/9/2010	0.44	-0.04	0	1397	13.31	-1.58	0.00	40.9
	B	7/9/2010	0.15	-0.06	-255	1046	4.71	-2.43	-9.66	30.7
	A	7/12/2010	1.39	-0.10	-336	2086	21.41	-2.12	-6.42	30.8
	B	7/12/2010	0.48	-0.07	-444	1498	7.38	-1.51	-8.48	22.1
	A	9/2/2010	0.21	0.09	0	2756	3.02	1.75	0.00	38.5
	B	9/2/2010	0.16	0.26	-312	1421	2.38	5.21	-5.64	19.8
EFAG	A	8/25/2009	0.59	8.29	-585	11214	12.83	245.63	-15.88	235.1
	B	8/25/2009	1.32	3.83	-228	5804	28.70	113.37	-6.20	121.7
	A	9/29/2009	0.49	0.37	843	9348	10.24	10.50	22.13	189.5
	B	9/29/2009	Flooded				Flooded			
	A	6/18/2010	0.23	-0.11	-65	2360	4.98	-3.22	-1.71	48.4
	B	6/18/2010	0.40	-0.14	112	2290	8.61	-4.01	2.96	46.9
	A	7/9/2010	0.09	-0.20	-48	955	3.28	-10.17	-2.24	34.5
	B	7/9/2010	0.23	0.00	-130	755	8.63	0.18	-6.10	27.3
	A	7/12/2010	0.44	-0.21	-461	3660	1.55	-1.00	-2.03	12.4
	B	7/12/2010	1.64	-0.08	-252	4486	5.79	-0.37	-1.11	15.2
	A	9/2/2010	0.18	0.23	0	2496	13.80	24.74	0.00	188.0
	B	9/2/2010	0.15	0.14	-286	2228	11.61	14.83	-27.90	167.9
min			0.09	-0.21	-585	755	1.04	-10.17	-27.90	7.2
median			0.40	-0.06	-240	2259	7.46	-0.83	-2.24	36.5
max			1.64	8.29	843	11214	28.70	245.63	22.13	235.1
							Kg ha^{-1} yr^{-1}			
						min	0.05	-0.45	-1221.84	313
						median	0.38	-0.04	-98.01	1,598
						max	1.47	10.76	969.10	10,297

Table 4.2- Calculated convective fluxes due to atmospheric pressure changes. Convective fluxes due to changes in pressure were calculated assuming that the volume of soil that expanded due to the pressure change was lost from the soil surface at the concentration measured at the 0.25 m equilibration chamber. Reported fluxes are averages of transect A and B

						μmol m^{-2} $event^{-1}$								μmol m^{-2} d^{-1}							
location	date	mmHg	day	m^3 m^{-2}	volume	N_2O-N		excess N_2-N		CH_4		excess CO_2		N_2O-N		excess N_2-N		CH_4		excess CO_2	
		Δ pressure	Δ time	Δ volume	lost, %	avg	se	avg	se	avg	se	avg	se	avg	se	avg	se	avg	se	avg	se
rfarm	12/3/2008	7.9	0.6	0.0073	1.00	1.80		564.8		0.53		7380		2.80		879.7		0.83	0.00	11496	
	8/6/2009	7.6	3.7	0.0042	0.93	0.19	0.10	0.0	0.0	0.29	0.01	6980	1239	0.05	0.03	0.0	0.0	0.08	0.00	1881	334
	8/13/2009	3.6	6.4	0.0010	0.43	0.11	0.01	0.0	0.0	0.08	0.00	1535	89	0.02	0.00	0.0	0.0	0.01	0.00	240	14
	8/19/2009	3.8	1.3	0.0012	0.46	0.09	0.02	0.0	0.0	0.10	0.01	1672	193	0.07	0.01	0.0	0.0	0.08	0.01	1316	152
	10/6/2009	10.7	0.8	0.0021	1.32			252.9	54.9	0.21	0.01	2125	591			328.1	71.3	0.27	0.02	2757	766
	10/23/2009	8.4	1.0	0.0008	1.09	0.05		0.0	0.0	0.14	0.03	707	60	0.05		0.0	0.0	0.14	0.03	694	59
	6/18/2010	5.6	1.8	0.0040	0.68	0.21	0.04	290.7	290.7	0.22	0.01	1395	105	0.12	0.02	164.2	164.2	0.12	0.00	788	59
EFAG	8/25/2009	2.8	0.3	0.0004	0.34	0.14	0.01	-42.5	18.6	0.66	0.23	896	283	0.49	0.03	-146.7	64.3	2.29	0.80	3091	975
	7/9/2010	4.6	0.9	0.0046	0.55	0.30	0.08	0.0	0.0	0.22	0.12	1047	114	0.35	0.10	0.0	0.0	0.25	0.14	1232	134
mfarm	7/9/2010	3.8	0.8	0.0014	0.47	0.14	0.05	-43.5	43.5	0.08	0.00	439	60	0.18	0.06	-58.0	58.0	0.11	0.00	586	80

Table 4.3– Scaled annual convective flux from the soil surface due to barometric pressure changes from a high pressure system to a low pressure system.

	Average advective flux per event			Average advective flux per season			depth below ground	fractional GFPS
	μmol m^{-2} $event^{-1}$			μmol m^{-2} $season^{-1}$				
	N_2O-N	CH_4	CO_2	N_2O-N	CH_4-C	CO_2-C	m	m^3 m^{-3}
Summer								
Vadose zone depth=0.9m	0.26	0.35	3801	2.08	2.8	30408	0.1	0.75
soil temp 20°C							0.25	0.5
8 low pressure systems							0.5	0.25
							0.75	0.15
Fall								
Vadose zone depth =0.5m	0.11	0.15	1591	0.88	1.2	12728	0.1	0.65
soil temp 14°C							0.25	0.25
8 low pressure systems							0.5	0
Spring								
Vadose zone depth=0.2m	0.054	0.07	781.5	0.432	0.56	6252.1	0.1	0.5
soil temp 12°C								
8 low pressure systems								
Winter								
Vadose zone depth=0.15m	0.023	0.03	340.7	0.207	0.27	3065.9	0.1	0.21
soil temp 5°C								
9 low pressure systems								
yearly flux due to low barometric pressure changes				**3.60**	**4.83**	**52,453**	μmol m^{-2} yr^{-1}	
				0.0005	0.0007	7.3435	kg ha^{-1} yr^{-1}	

Table 4.4- Increases in the fractional, water-filled pore space before (Φ_{wpre}) and after (Φ_{wpost}) the sampled rainfall events. Also shown are the total porosity for each site (Φ), and the estimated fluxes of N_2O, CH_4, and CO_2 from the soil surface. The rainfall totals for the EFAG and Mfarm rainfall event was 5.84 cm measured at Mfarm, and the rainfall accumulation at Rfarm was 6.88cm.

	depth	water	Φ	Φ_w	Φ_w	gas	N_2O		CH_4		CO_2		N_2O		CH_4		CO_2	
location	range	table ↑		pre	post	fluxed	Flux	se	Flux	se	Flux	se	Flux	se	Flux	se	Flux	se
	m	m	$m^3\ m^{-3}$	$m^3\ m^{-3}$	$m^3\ m^{-3}$	$m^3\ m^{-2}$	$\mu mole\ m^{-2}\ event^{-1}$						$\mu mole\ m^{-2}\ d^{-1}$					
EFAG	0-0.25		0.32	0.638	0.304	0.0264												
	0.25-0.5			0.48	0.34	0.011												
	0.5-0.75			0.32	0.33	-0.001												
	0.75-1.0			0.19	0.11	0.007												
	1.0-1.36			0.08	0.00	0.01												
	total	0.1				**0.0534**	3.4	0.9	2.5	1.3	12186	1327	4.3	1.2	3.1	1.7	15,192	1,654
Mfarm	0-0.25		0.30	0.64	0.23	0.030												
	0.25-0.5			0.39	0.22	0.025												
	0.5-0.75			0.03	0.04	-0.001												
	total	0.1				**0.055**	5.4	1.9	3.3	0.1	17612	2404	6.8	2.4	4.1	0.2	21,958	2,997
Rfarm	0-0.25		0.26	0.64	0.28	0.024												
	0.25-0.5			0.56	0.31	0.016												
	0.5-0.75			0.46	0.26	0.015												
	0.75-1.0			0.37	0.09	0.020												
	1.0-1.5			0.22	0.08	0.018												
	1.5-1.8			0.09	0.01	0.006												
	1.8-2.1			0.02	0.00	0.004												
	total	0.3				**0.103**	3.9	1.6	9.7	1.2	33398	3245	62.5	25.5	155.9	19.0	534,369	51,926

Table 4.5- The calculated yearly convective flux of N_2O, CH_4 and CO_2 from the soil surface due to infiltration at Rfarm.

	Average advective flux per event			Average advective flux per season			depth below ground	Pre-GFPS	Post-GFPS
	µmol m^{-2} $event^{-1}$			µmol m^{-2} $events^{-1}$					
	N_2O-N	CH_4	CO_2	N_2O-N	CH_4-C	CO_2-C	m	m^3 m^{-3}	m^3 m^{-3}
Summer									
Vadose zone depth=0.9m	2.12	2.89	30941	76.32	104.04	1,113,876	0.1	0.75	0.54
soil temp 20°C							0.25	0.5	0.25
36 rainstorms							0.5	0.25	0.15
Producing on avg 0.7 cm							0.75	0.15	0
Fall									
Vadose zone depth =0.5m	1.61	2.19	23463	57.96	78.804	844,668	0.1	0.65	0.41
soil temp 14°C							0.25	0.4	0.2
							0.5	0.25	0.1
Spring									
Vadose zone depth=0.2m	0.415	0.57	6050	14.94	20.34	217,800	0.1	0.5	0.255
soil temp 12 °C									
36 rainstorms									
Producing on avg 0.7 cm									
Winter									
Vadose zone depth=0.15m	0.254	0.35	3704	9.144	12.456	133,351	0.1	0.31	0.1
soil temp 5 °C									
36 rainstorms									
Producing on avg 0.7 cm									
yearly flux due to infiltration				**158.36**	**215.64**	**2,309,695**	µmol m^{-2} yr^{-1}		
				0.02	0.03	323.4	kg ha^{-1} yr^{-1}		

Table 4.6- Changes in gas concentrations as a function of depth in the vadose zone in transects A and B, and at the top of the saturated zone after rainfall events. The up arrow indicate that the concentrations increased after the rainfall, the down arrows indicate a decrease in concentration, and ns indicates no significant differences between the before and after concentrations.

location	depth	N_2O		CH_4		CO_2	
	m	A	B	A	B	A	B
Mfarm	0.25	↑	↑	↓	ns	ns	ns
	0.5	↑	↑	↓	ns	↑	ns
	0.75	↑		↓		↑	
	1						
	1.51	ns		ns		ns	
EFAG	0.25	↑	↑	ns	ns	↑	↑
	0.5	↑	↑	ns	ns	↑	↑
	0.75						
	1						
	2.61	↓		ns		↑	
Rfarm	0.25	ns	↑	ns	↓	↑	↑
	0.5	ns	↑	ns	ns	↑	↑
	0.75						
	1	ns		ns		↑	
	1.5	ns	ns	↓	ns	ns	↑
	2.21	↓		dry		dry	
	3.1	↓		↓		ns	
	3.9	↑		ns		ns	

Table 4.7- A review of N_2O, CH_4, and CO_2 flux values reported in the literature

	Flux range	original units	µmol m^{-2} d^{-1}	location	source
N_2O	0.2 to 24.8	ng N_2O-N m^{-2} s^{-1}	1.2 to 153.6	praire, forest, manure-amended, and control sites in	Goodroad & Keeney 1985
	0.5 to 603.5	µg N_2O-N m^{-2} h^{-1}	0.864 to 1,034	Höglwald Forest, Bavaria, Germany	Papen and Butterbach-Bahl, 1999
	>3	g N ha^{-1} d^{-1}	>21.4	Flooded rice soil, Louisiana, USA	Lindau et al. 1990
	-20 to 150	µmol N_2O-N m^{-2} d^{-1}	-20 to 150	Central Agricultural experiment farm, Ottawa, Cananda	Dunfield et al. 1995
	-0.07 to 0.45	mg m^{-2} h^{-1}	-120 to 771.43	boreal forestry-drained peatlands, Finland	Ojanen et al. 2010
	0 to 28.7	µmol m^{-2} d^{-1}	0 to 28.7	riparian/hydrologically restored wetland, MD coastal plain	Fox 2011
yearly N_2O	0.9-6.3	Kg N_2O-N ha^{-1} yr^{-1}		Agricultural soils, Wisconsin, USA	Goodroad et al. 1984
	1.7-27.6	Kg N_2O-N ha^{-1} yr^{-1}		Grasslands & arable sites around Great Britain	Dobbie and Smith 2003
	0.4	Kg N_2O-N ha^{-1} yr^{-1}		riparian/hydrologically restored wetland, MD coastal plain	Fox 2011
CH_4	-0.01 to -3.3	mg CH_4 m^{-2} d^{-1}	-0.625 to -206.3	Forest, woodland & Agriculture	Dobbie et al. 1996 A
	-10 to -25	µmol m^{-2} d^{-1}	-10 to -25	Central Agricultural experiment farm, Ottawa, Cananda	Dunfield et al. 1995
	-0.53 to 24.5	mg m^{-2} h^{-1}	-795 to 36,750	boreal forestry-drained peatlands, Finland	Ojanen et al. 2010
	ND to 33	g ha^{-1} d^{-1}	ND to 206.3	Flooded rice soil, Louisianan, USA	Lindau et al. 1990
	-10.2 to 245.6	µmol m^{-2} d^{-1}	-10.2 to 245.6	riparian/hydrologically restored wetland, MD coastal plain	Fox 2011
CO_2	<<0.1 - 1.3	g CO_2 m^{-2} hr^{-1}	54.5 to 709.1	riparian-hillslope transitions, Rocky Mountains, Montana	Pacific et al. 2008
	-0.03-1.38	g m^{-2} h^{-1}	-16.4 to 753	boreal forestry-drained peatlands, Finland	Ojanen et al. 2010
	7.2 to 235.1	µmol m^{-2} d^{-1}	7.2 to 235.1	riparian/hydrologically restored wetland, MD coastal plain	Fox 2011

Figure 4.1- The research took place at three locations on the Delmarva Peninsula within or near the Choptank Basin. Rfarm is indicated by a diamond and is located in the Little Choptank Basin, just south of the Choptank Basin, Mfarm (triangle) and EFAG (circle) are located in the upper Choptank Basin.

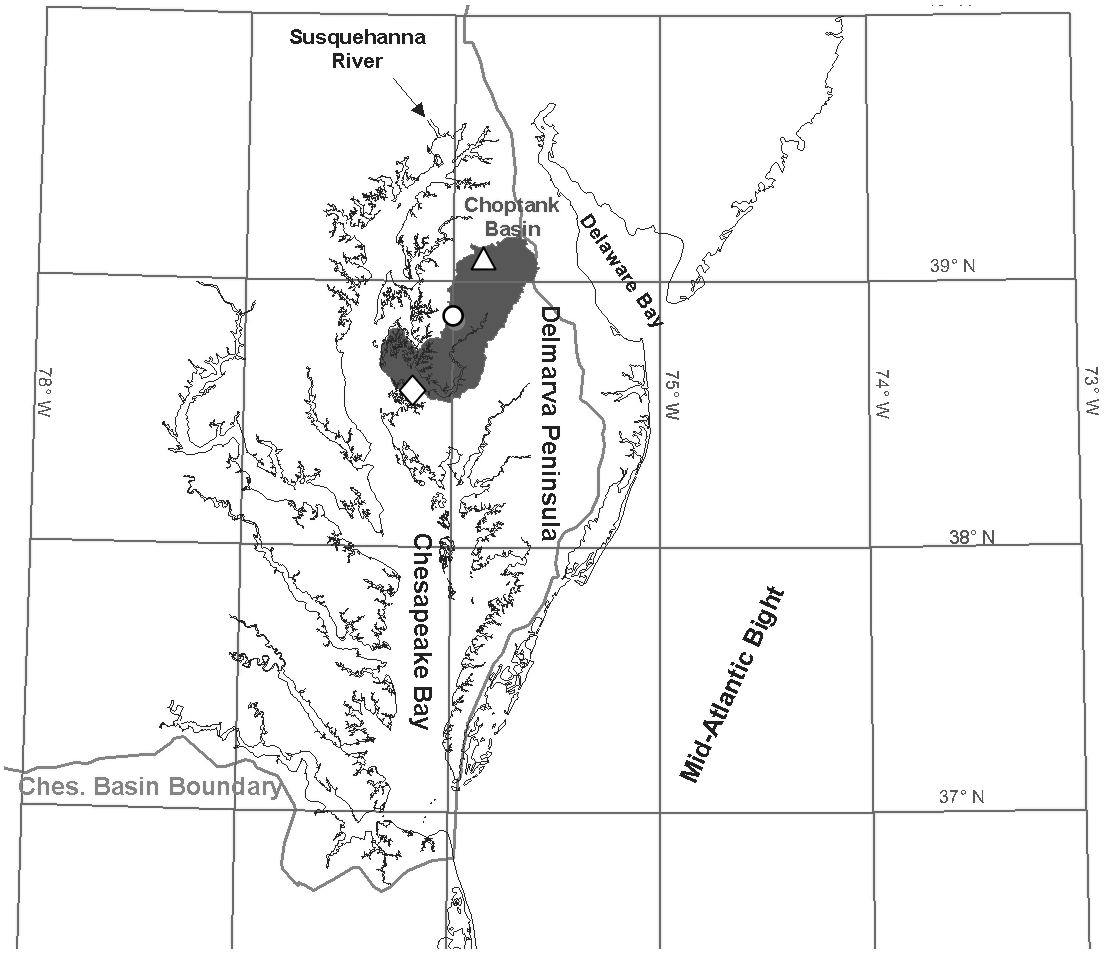

Figure 4.2 – An aerial view of the three study sites. **A)** Mfarm, a mature forested buffer. The horizontal distance between the piezometers is to scale, but reduced by a factor of 15. **B)** EFAG, a hydrologically restored wetland. The horizontal axis is to scale, but reduced by a factor of 45. **C)** Rfarm, a conservation reserve enhancement program (CREP) buffer. The horizontal scale is reduced by a factor of 12. In each site, the stars represent equilibration chambers, and the filled circles represent piezometers.

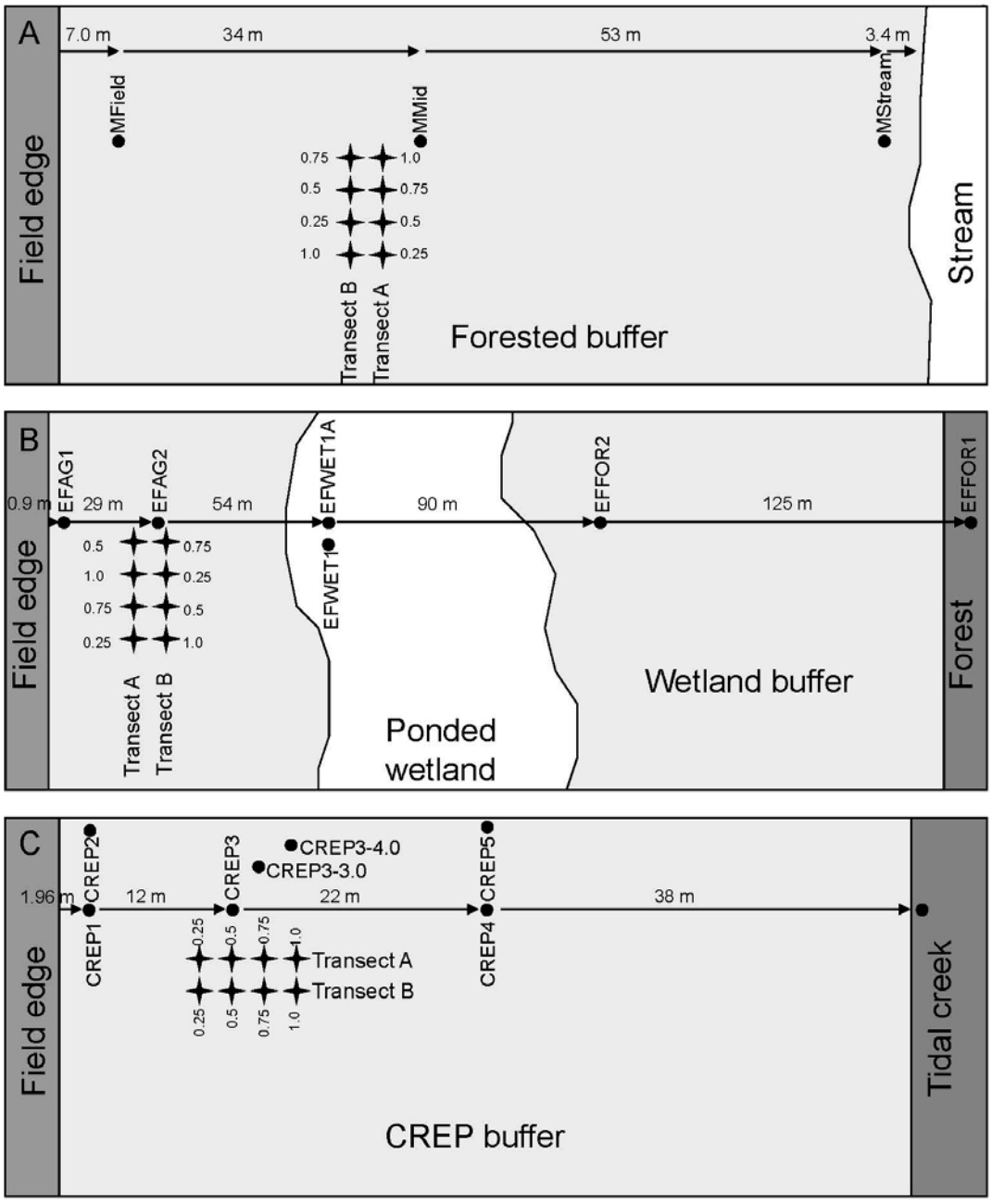
A
Field edge
7.0 m
34 m
53 m
3.4 m
MField
MMid
MStream
0.75
1.0
0.5
0.75
0.25
0.5
1.0
0.25
Transect B
Transect A
Forested buffer
Stream
B
Field edge
0.9 m
EFAG1
29 m
EFAG2
54 m
EFWET1A
90 m
EFFOR2
125 m
EFFOR1
EFWET1
0.5
0.75
1.0
0.25
0.75
0.5
0.25
1.0
Transect A
Transect B
Ponded
wetland
Wetland buffer
Forest
C
Field edge
1.96 m
CREP2
12 m
CREP3
CREP3-4.0
CREP3-3.0
22 m
CREP5
38 m
CREP1
0.25
0.5
0.75
1.0
Transect A
Transect B
CREP4
CREP buffer
Tidal creek

Figure 4.3- Examples of gas profiles from groundwater into the vadose zone at MFarm and EFAG on September 2nd 2010. Transects A (filled circles) and B (open circles) are represented separately and the gas concentrations are expressed in partial pressure units (mmHg) in order to compare gas dissolved in groundwater and gas in the vadose zone. The dotted line on the N_2O, CO_2, and CH_4 panels (**E,F**) represents the atmospheric concentrations of N_2O, CO_2 and CH_4

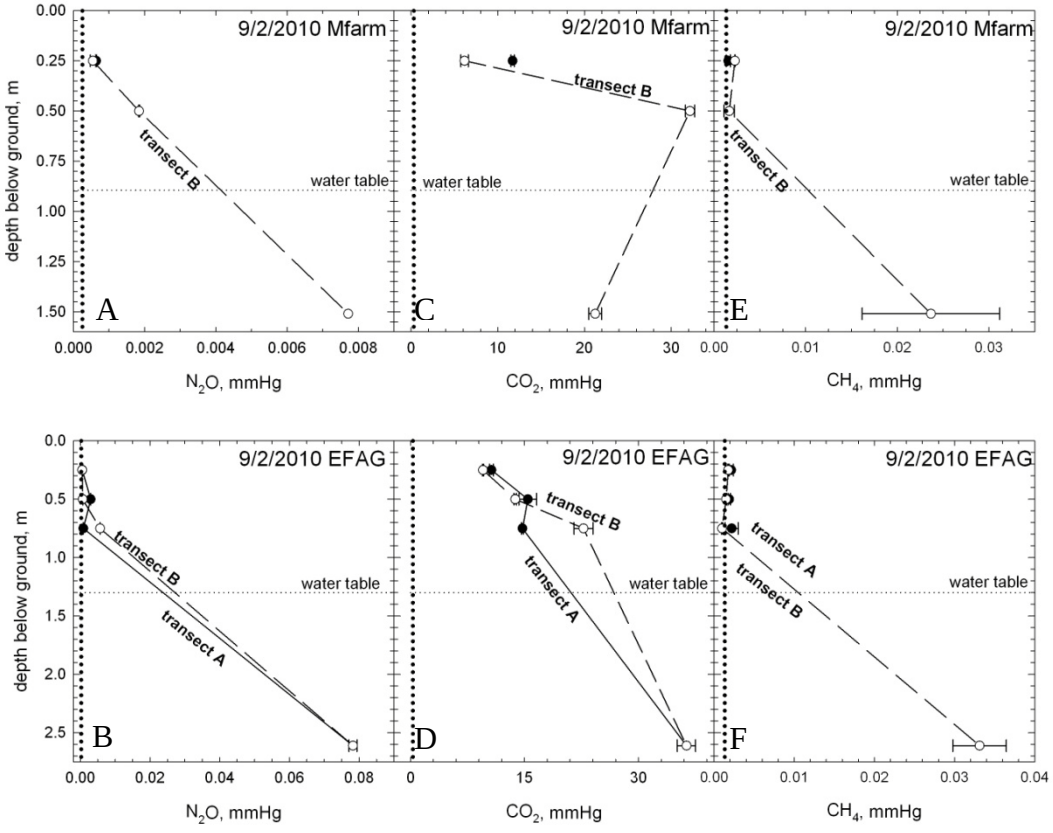

Figure 4.4- **A)** The precipitation record from 2009 acquired at the Horn Point Laboratory weather station. **B)** The barometric pressure record taken from a data logger at the Horn Point Laboratory expressed as a change in barometric pressure from 760 mmHg. The dashed line represents the average barometric pressure in 2009. Low pressure systems were defined as being in the 10th percentile of all of the yearly 2009 30 minute data and the high pressure systems were defined as being in the 90th percentile.

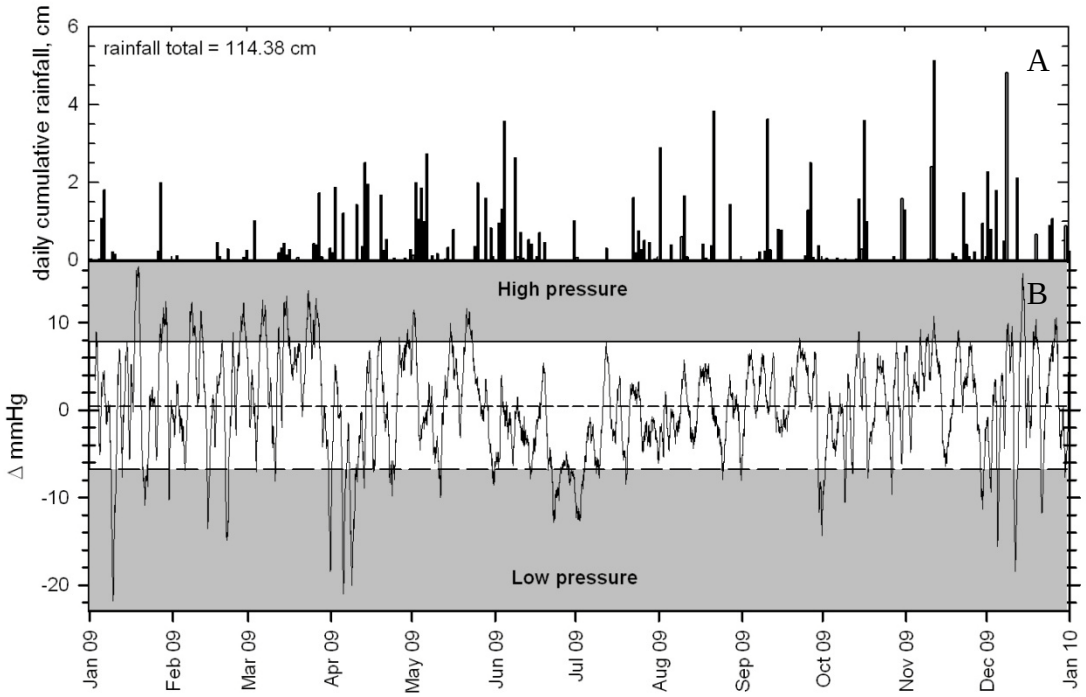

Figure 4.5- A frequency plot of the rain events measured at the Horn Point Laboratory weather station, Cambridge, MD (www.cbos.org).

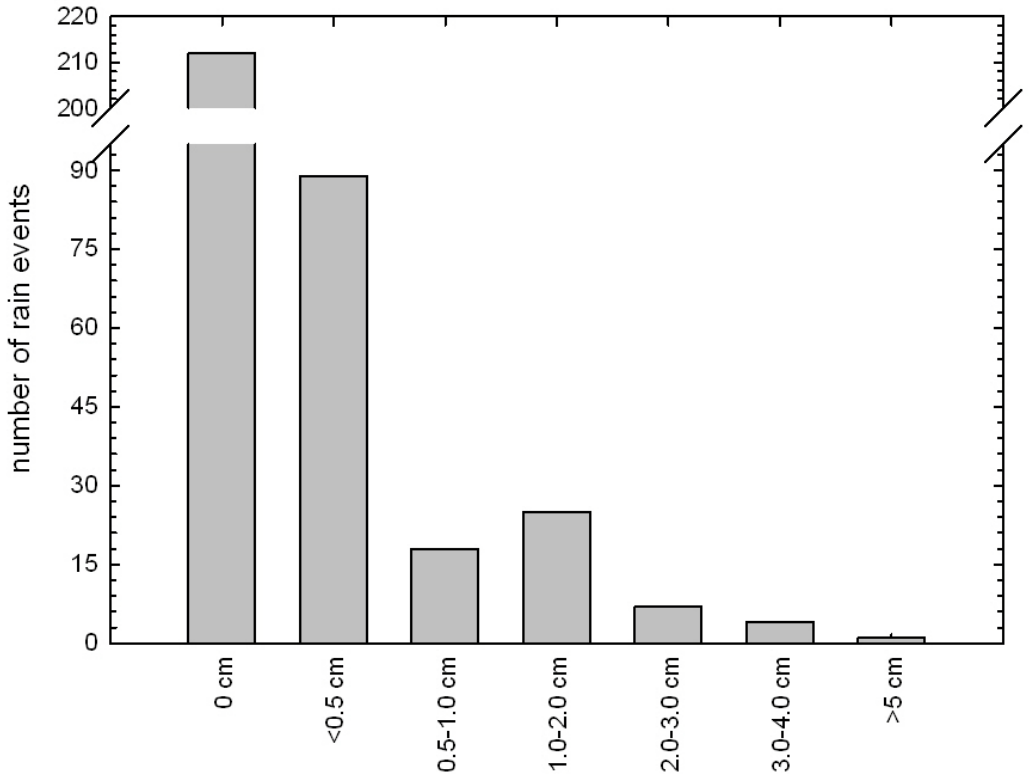

Figure 4.6 – The effects of a 5.84 cm rainfall event on the fractional water-filled pore space (**A**), the gas concentrations in the vadose zone (**B-G**), and the dissolved gas concentrations in groundwater (**H-J**) at Mfarm. Stars indicate statistically significant differences and NS indicates no statistically significant difference. The dotted lines on the N_2O and CH_4 panels indicate the atmospheric concentration of each gas. Transect A is the top three panels and transect B is the lower three panels.

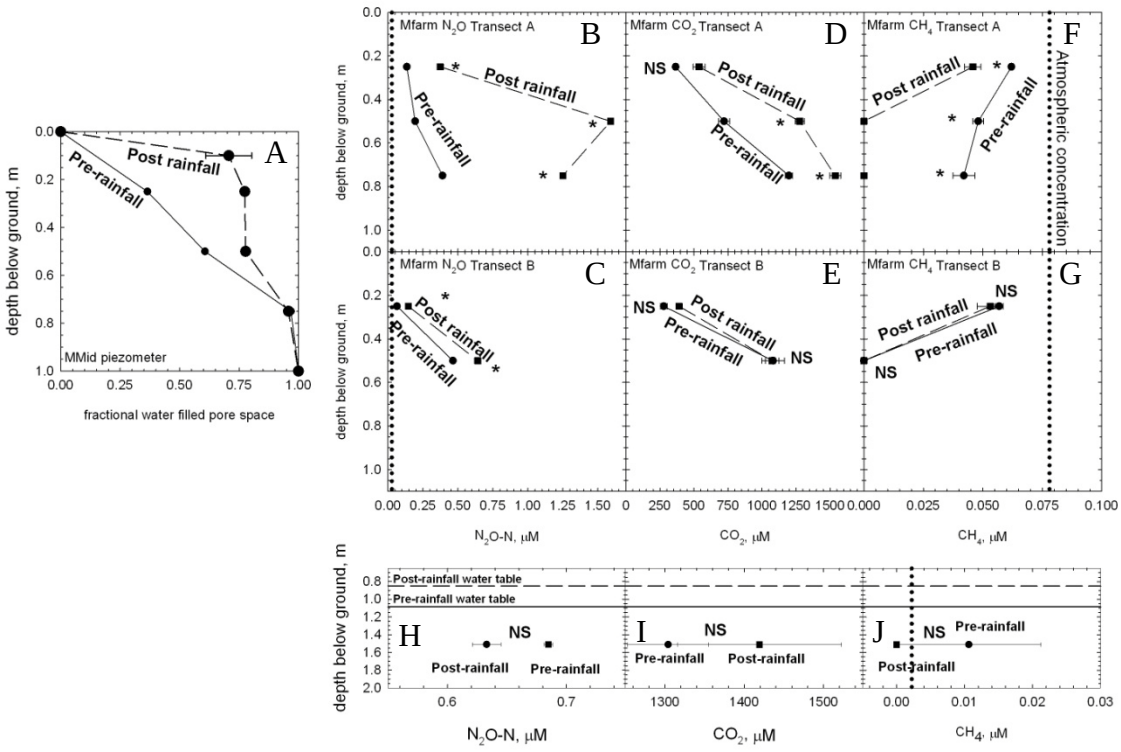

Figure 4.7 – The effects of a 5.84 cm rainfall event on the fractional water-filled pore space (**A**), the gas concentrations in the vadose zone (**B-G**), and the dissolved gas concentrations in groundwater (**H-J**) at EFAG. Stars indicate statistically significant differences and NS indicates no statistically significant difference. The dotted lines on the N_2O and CH_4 panels indicate the atmospheric concentration of each gas. Transect A is the top three panels and transect B is the lower three panels.

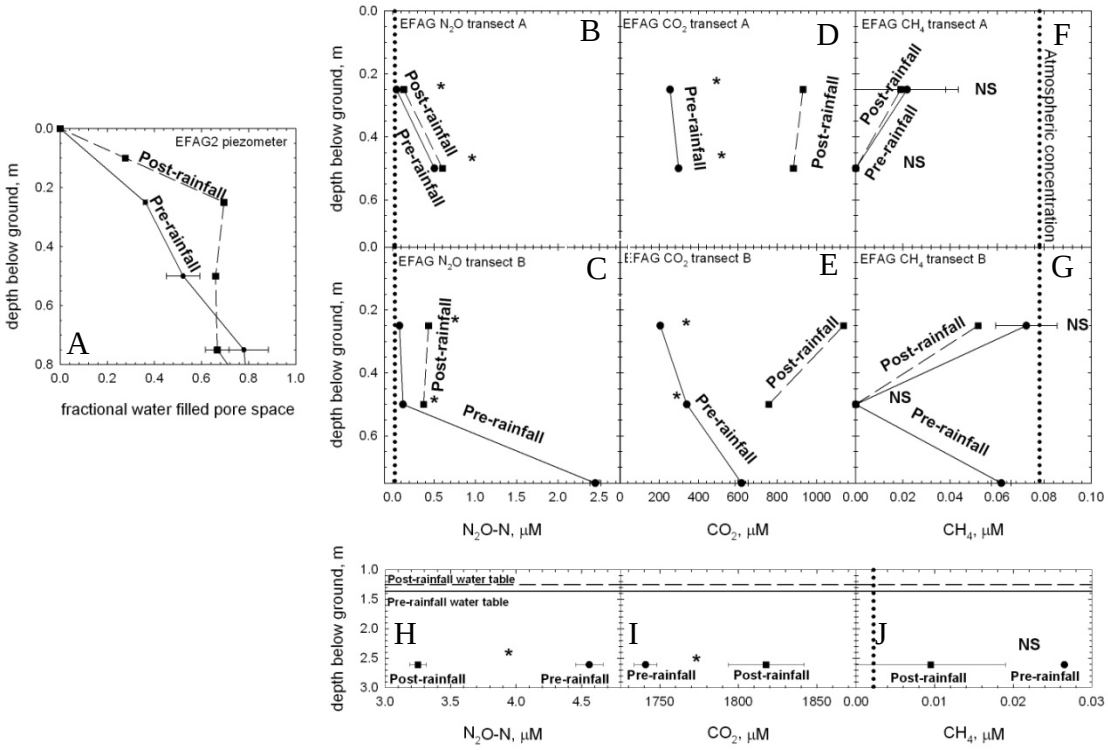

Figure 4.8 – The effects of a 6.88 cm rainfall event on the fractional water-filled pore space (**A**), the gas concentrations in the vadose zone (**B-G**), and the dissolved gas concentrations in groundwater (**H-J**) at Rfarm. Stars indicate statistically significant differences and NS indicates no statistically significant difference. The dotted lines on the N_2O and CH_4 panels indicate the atmospheric concentration of each gas. Transect A is the top three panels and transect B is the lower three panels.

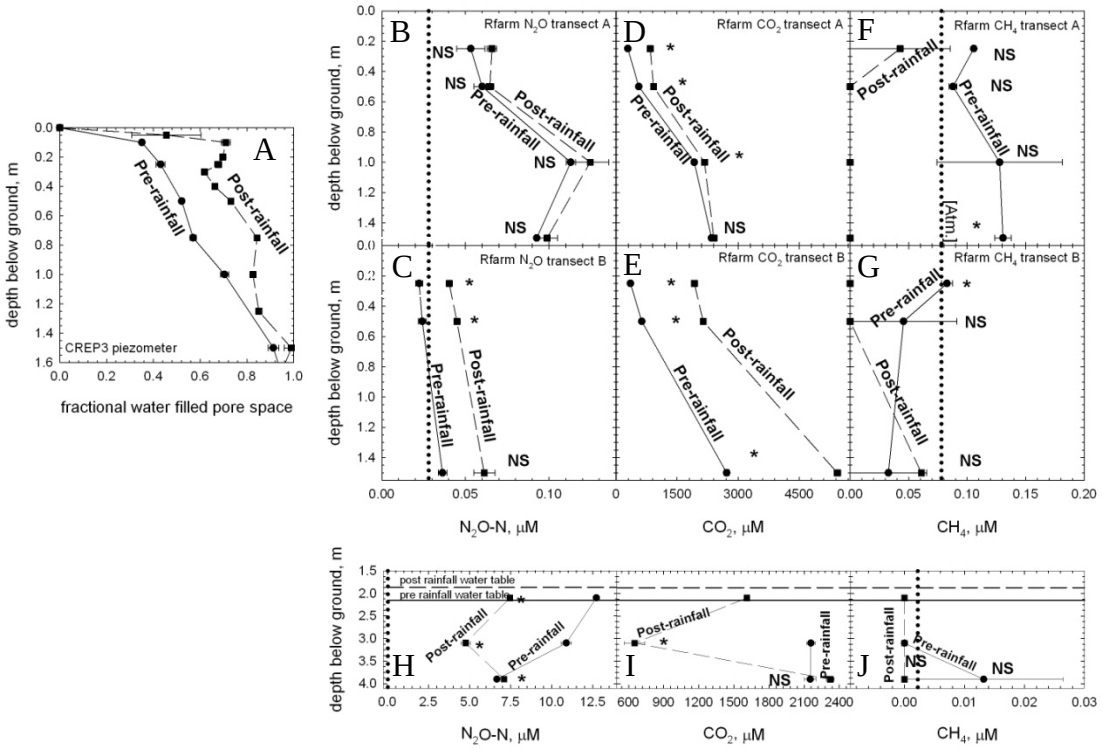

Figure 4.9 – A comparison of the O_2 deficit plus excess N_2 (electron acceptors) and excess CO_2 concentration (electron donors) for groundwater at selected sites in June 2008.

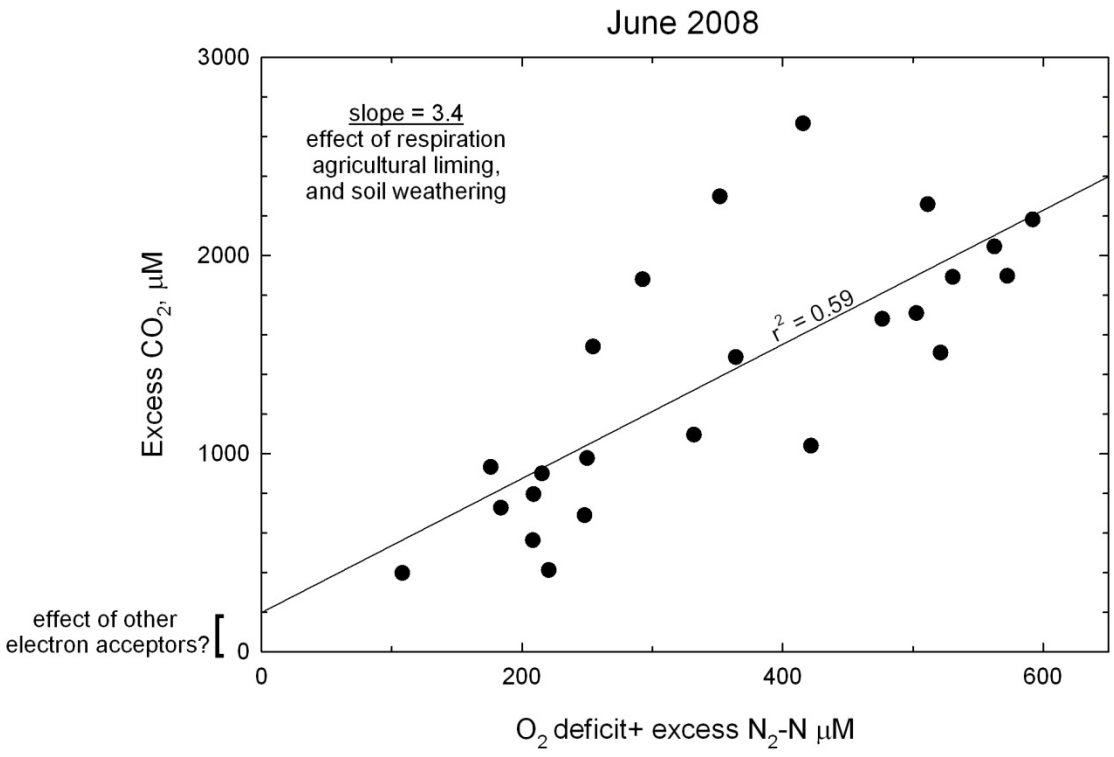

Figure 4.10 – A comparison of the median diffusional fluxes with the convective fluxes through barometric pressure changes and infiltration. The CH_4 diffusional flux is the maximum positive value as the median CH_4 diffusional flux was negative (into the soil).

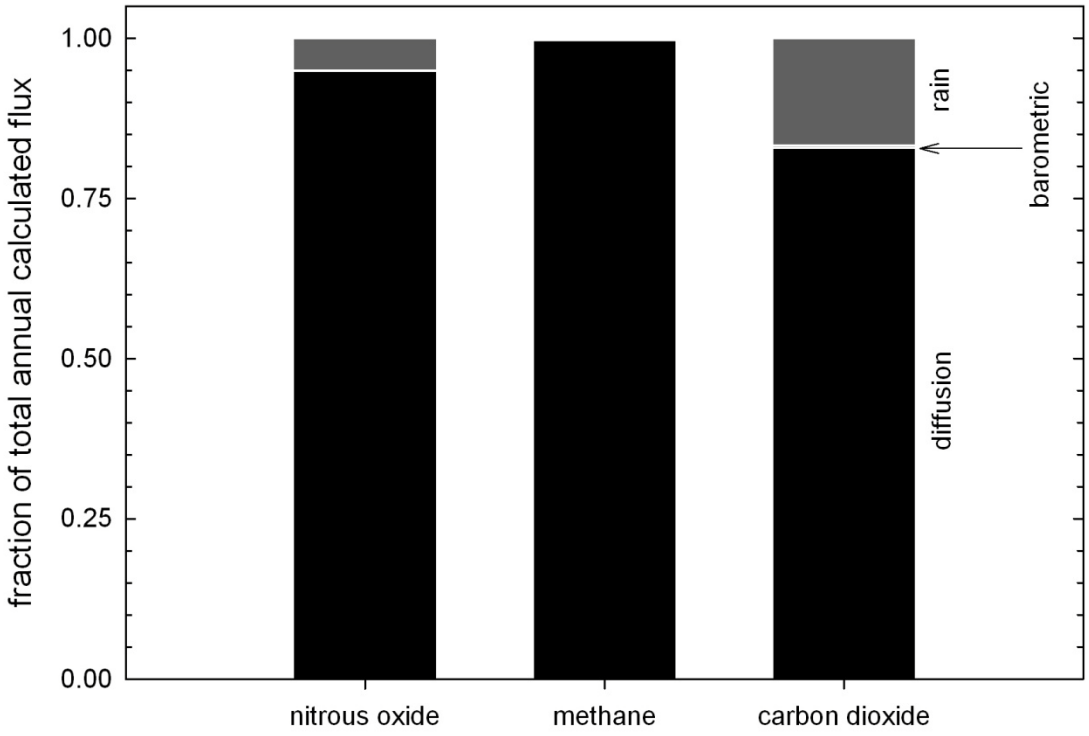

Figure 4.11 – A. The depth of the water table below the ground surface in 2009 (black) in comparison to 2010 (gray). B. The groundwater temperature in 2009 (black) and 2010 (gray).

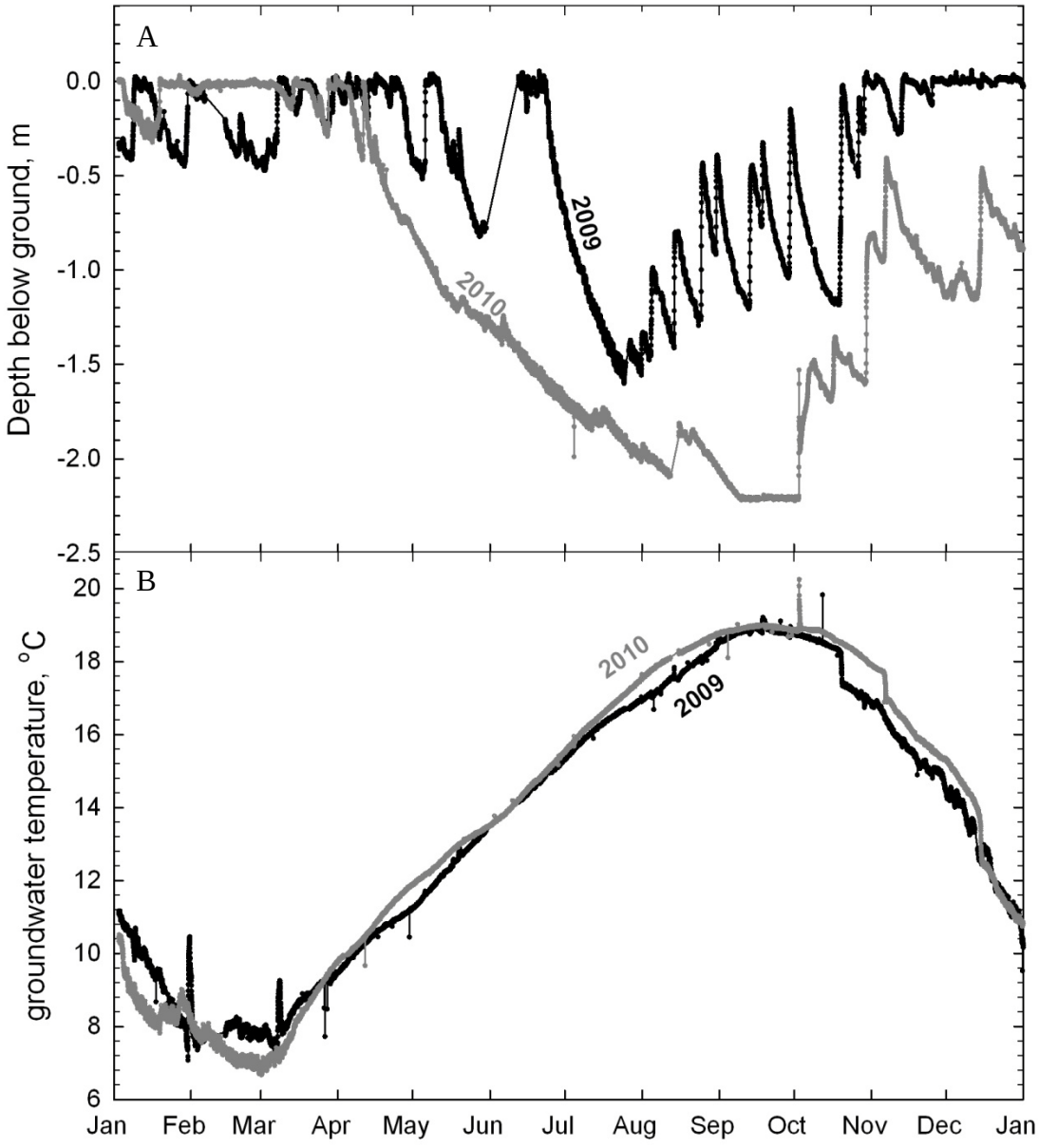

CHAPTER 5:

SYNTHESIS

Introduction

Two ongoing research projects inspired this thesis. The projects were focused on the "missing N" on a watershed scale, and on the evaluation of the abilities of wetlands to reduce N in agricultural settings. My research was intended to examine N_2O concentrations in groundwater in relation to the "missing nitrogen", and to investigate N_2O concentrations as a result of denitrification in wetlands intended to mitigate NO_3^- in agricultural settings. I was interested in N_2O because it is a by-product of denitrification, and denitrification has the potential to decrease the concentration of NO_3^- flowing downstream, which could improve water quality. Unfortunately, N_2O is a harmful greenhouse gas that has the ability to destroy stratospheric ozone (Crutzen 1981), and the concentration of N_2O has been increasing since pre-industrial times (IPCC 2007). CH_4 and CO_2 became part of the thesis because they are also produced in soils and groundwater and are greenhouse gases that are increasing in concentration in the atmosphere (IPCC 2007). Currently, the majority of the world has heard of the imminent progression of climate change, and reducing our greenhouse gas production is a high priority. Areas that are intended to reduce NO_3^- concentrations flowing downstream, such as restored wetlands, riparian buffers, and controlled drainage structures also have the ability to produce large concentrations of N_2O, CH_4, and CO_2 in groundwater and the vadose zone of soils.

Chapter 2

I examined the concentrations of the gases N_2O and CH_4 dissolved in the surface unconfined aquifer of 10 locations with 64 piezometers located throughout them. These

areas included natural wetlands, hydrologically restored wetlands, riparian areas, controlled drainage ditches, prior converted croplands (PCC) and the wet spots within PCC's. The piezometers were located as transects across the different study sites.

The primary limitation of this research was the hydrology of these locations. Hypothesis 1 and 2 required the assumption that the groundwater flowed from one side of the management practice to the other down the topographic gradient, connecting the piezometers within the transect. This assumption is typically made in groundwater piezometer studies. Unfortunately, evidence from analyses of major ion and hydraulic gradient data found that this assumption was invalid at many of the locations. Groundwater does not always flow down the topographic gradient, and even when it does, it often flows from a point of local recharge through a relatively confined flow path towards the groundwater outflow area without much interaction between individual flow paths. Concentration gradients may exist within single flow paths in these wetlands, but the gradients were difficult to determine based upon our single transect sampling scheme amid the complex hydrology.

The invalidation of this assumption also limited the assessment of the ability of these wetlands to remove agricultural N. The major ion and hydraulic gradient data showed that the piezometers were hydrologically connected at one of the 10 locations. Connections were not established at the other 9 locations because either the hydrology of the sites was too complex or the hydrology was not analyzed sufficiently to satisfactorily connect the piezometers and make claims on the ability of the areas to reduce NO_3^-. At the PCC Brfarm, a hydrologic connection was supported by the major ion and hydraulic gradient data, and the concentration of NO_3^- was significantly reduced after flowing

through a field wet spot (from 1mM to 16 µM NO_3^-), and the concentration of excess N_2 significantly increased from 24 to 308 µM N_2-N. Although NO_3^- was reduced, only moderate concentrations of N_2O (0.6 µM N_2O-N) and CH_4 (2 µM CH_4) were observed. N_2O typically was equivalent to 0.5 to 5% of the excess N_2.

Although concentration gradients and N reduction across most transects could not be satisfactorily determined, I was able to show that a large amount of the N_2O and CH_4 produced within individual piezometers occurred during hot moments. Hot moment peaks in concentration were observed in the time series data sets, and accounted for on average 39 and 49% of the total N_2O and CH_4 produced per piezometer but only occurred for ~ 10% of the time. As hot moments only last for short periods of time, they are difficult to sample without spending significant time and resources on a frequent sampling strategy. Catching these hot moments is important to estimate accurately the total N_2O or CH_4 concentration that accumulated at each piezometer. I did capture significant variation in N_2O and CH_4 concentrations with a one month sampling strategy, and more frequent sampling may not have produced that much more information relative to the amount of time required to acquire and process the samples.

Hot spot locations accumulated large concentrations of N_2O or CH_4, but not both. Three N_2O and four CH_4 hot spots were located in the 64 piezometer data set. N_2O and CH_4 hot spots had median concentrations greater than 5.5 µM N_2O-N and 17.5 µM CH_4. The N_2O hot spots were situated in riparian areas or hydrologically restored wetlands adjacent to agriculture which suggests that wetlands exposed to agricultural NO_3^- can produce large groundwater concentrations of N_2O. The CH_4 hot spots were located in natural wetlands or hydrologically restored wetlands away from the agricultural field or

within shallow ephemerally flooded soils which suggest that CH_4 production in agriculturally restored wetlands will only occur when there is not an agricultural N source in close proximity. Unfortunately, it is difficult to sample hot spot locations without sampling a large area, which requires time, money, and land owner permission, and missing these hotspots would create an illusion that an area was not producing large concentration of N_2O or CH_4 when it in fact was. The high temporal and spatial variability of the accumulation of these gases makes sampling for them difficult, but my sampling strategy captured areas of both unusually high and low CH_4 accumulation.

One of the most interesting observations from this thesis was the evidence of CH_4 ebullition within these shallow groundwater locations. CH_4 ebullition presents a problem when estimating denitrification because the CH_4 bubbles strip the dissolved concentrations of all gases including N_2 and Ar, making it nearly impossible to determine the denitrification history of a groundwater mass that has entered a high CH_4 production area. The CH_4 bubbles also transfer large concentrations of CH_4 from groundwater to the vadose zone, and these flux mechanisms likely outweigh diffusional fluxes, although the ebullition flux was not quantified here. Two locations had significant CH_4 ebullition and both were shallow piezometers (~0.5 m deep) in hydrologically restored ponded wetland areas (JLAG3a and EFWET1a). Other locations showed CH_4 ebullition less frequently in conjuncture with hot moments, while some locations had no evidence of CH_4 ebullition despite high hot moment CH_4 concentrations (e.g., 340 µM CH_4 at EFFOR2 in Dec 09). Evidence of ebullition was observed throughout the year, but these events occurred less frequently in January through April when groundwater levels are high and temperatures are cooler, and a peak in the number of events was observed in July. For future research,

it would be interesting to try to capture one of these events at the soil surface or within the vadose zone, although the timing of this would be difficult. I have presented evidence of CH_4 ebullition, but the amount of CH_4 transferred via this process to the vadose zone or soil surface is unknown. CH_4 ebullition might be transferring significant amounts of CH_4 to the atmosphere, and if so, quantifying this flux would create better CH_4 budgets. Before this research could take place, the threshold at which CH_4 ebullition occurs would have to be analyzed to be able to capture the event with the least amount of time and effort spent waiting for the ebullition to occur.

The accumulation of both N_2O and CH_4 was temporally and spatially variable. From a management perspective, it would be convenient to have an approximate idea of how much N_2O or CH_4 accumulation could be expected from a specific type of restoration or land use. There was a great deal of variability between the piezometers within categories, and the agriculturally affected wet locations, including riparian areas, ditch or buffer edges, and wet spots, had the highest concentrations of N_2O likely because of the close proximity to an agricultural N source. The natural wetlands had the largest accumulations of CH_4 because they lack an N source, and the redox potentials associated with these areas are often low. Large accumulations of N_2O and CH_4 were also observed at individual piezometers within the hydrologically restored wetlands. EFWET1A, a shallow piezometer in a hydrologically restored ponded wetland area adjacent to an agricultural field, had both the largest individual concentrations (hot moments) of N_2O (75 µM N_2O-N) and CH_4 (1014 µM).

In general, nitrification tends to occur under conditions of higher O_2 (Bremner and Blackmer, 1978). Nitrification also produces NO_3^- as an end product, whereas NO_3^- is

consumed in the process of denitrification under low concentrations of O_2, with N_2 typically being the dominant end product. Therefore, sites that have positive relationships between $\%O_2$ saturation and N_2O, and NO_3^- and N_2O could be inferred to be dominated by nitrification; likewise, sites that have negative relationships between NO_3^- and N_2O, and $\%O_2$ and N_2O, could be inferred to be dominated by denitrification. Visual inspection of the gas relationships in Figure 5.1 shows that the highest N_2O values were often measured with low NO_3^- and low O_2, which is indicative of denitrification. The excess N_2 to N_2O relationship showed that the highest N_2O concentrations had moderate concentrations of excess N_2-N (75-225 µM), and these high N_2O values could be due to inefficient denitrification. Overall, this suggests that the highest N_2O values were produced by denitrification, and that the lower values associated with higher NO_3^- and O_2 were produced through nitrification.

Although N_2O production sources can not be conclusively determined from these relationships, there was supporting evidence for both nitrification and denitrification as sources of N_2O. Denitrification removes N from agricultural systems, while nitrification transforms NH_4^+ to more mobile NO_3^-. N_2O produced through denitrification is produced as an intermediate step in the reduction of N within agricultural watersheds, which reduces the transport of N downstream. Nitrification mobilizes NO_3^-, which can decrease downstream water quality, while producing atmospherically harmful N_2O.

In general, large concentrations of N_2O and CH_4 were observed within the groundwater of these locations. These concentrations usually exceeded atmospheric concentrations by several orders of magnitude, indicating that groundwater is potentially

a significant source of these greenhouse gases. The importance of transport mechanisms across the vadose zone to the atmosphere is tested in chapters 3 and 4.

Chapter 3

A major limitation in denitrification research is the inability to measure denitrification directly as an increase in N_2 concentration in air. Part of this thesis was aimed at creating a new vadose zone method to measure directly the small increases in N_2 resulting from denitrification. This was not a minor task. The direct measurement of denitrification using excess N_2 in the gas phase has not occurred prior to this research because it is difficult to measure a small increase in N_2 from denitrification over the high background concentration of N_2 in air (78%). My thesis research, in collaboration with Todd Kana, resulted in a new method that measures with high precision (0.05 % CV) the N_2/Ar ratio in soil gas, with the aim of directly estimating an increase in N_2 from denitrification.

I had hoped to measure increases in N_2 directly in order to estimate denitrification in soils in relation to N_2O concentrations. The direct measurement of N_2O in air is easy because of the low background concentrations of N_2O and the high sensitivity of GC-ECDs for N_2O. High concentrations of excess N_2 and N_2O dissolved in groundwater have been observed all over the Delmarva Peninsula (Fisher et al. 2010), and I hypothesized that these high dissolved excess N_2 and N_2O concentrations would diffuse out of groundwater and into the vadose zone, potentially accounting for the missing N on the transect scale. The missing N on the transect scale was measured as the difference in N between two piezometers on the same hydraulic gradient. Once the excess N_2 diffused

out of groundwater, I hypothesized that I would be able to measure the diffused excess N_2 as a vertical profile in the vadose zone. The profile could then be used to estimate the diffusion gradient and diffusive flux of excess N_2 from the soil surface.

Significant differences in concentrations of N often occur in groundwater between piezometers on the same hydraulic gradient. For example, the sum of NO_3^-, NH_4^+, excess N_2, and N_2O often decrease along a hydraulic gradient from an agricultural field through a buffer. We have often assumed that the decrease in N occurred because excess N_2 and N_2O had diffused out of the groundwater and into the vadose zone due to the high concentrations dissolved in groundwater. My direct measurements and calculated diffusional fluxes did not support the hypothesis that all of the missing N on the transect scale was diffusing into the vadose zone because only between 0.1 and 0.5% of the missing N could be accounted for in calculations of diffusional flux from groundwater to the vadose zone. Potentially, the missing N was taken up by plants within the transect, could be caused by locally infiltrating water with low N content from the buffer, or was the result of sampling different groundwater flow paths.

Within the vadose zone, I was able to measure vertical profiles of partial pressures of excess N_2, N_2O, and CO_2. The excess N_2 and N_2O profiles showed high partial pressures dissolved in groundwater that decreased towards the soil surface. The CO_2 concentrations were always highest below 1.0 m, but the partial pressure was not always highest in groundwater. Production and consumption was inferred by concave or convex vadose zone profiles. Both positive and negative excess N_2 concentrations (below atmospheric N_2 concentrations) were observed in the vadose zone, and the negative excess N_2 values are thought to be a result of solubility differences driven by seasonal

temperature effects on both the concentrations of N_2 and Ar. The positive concentrations of excess N_2 could also be influenced by these physical processes and I plan to employ other noble gases (neon, xenon, and krypton) in future research to separate the biological processes from the physical processes.

Physical processes do not affect the estimation of N_2O and CO_2 in the vadose zone because absolute concentrations are measured, not ratios. The calculated N_2O and CO_2 fluxes from the soil surface were within range of other reported fluxes in the literature. The positive excess N_2 fluxes from the soil surface were on the high end of reported fluxes by other researchers (-607 to 881 mmoles N_2-N m^{-2} day^{-1}). The negative calculated fluxes appear to be a result of solubility-driven differences. Although this range of estimated fluxes from the soil surface includes values sufficient to explain the missing N on the watershed scale, we currently cannot determine the source affecting the N_2/Ar ratio in the vadose zone and therefore cannot assume that increases in excess N_2 in the vadose zone are due to biological denitrification. Temperature-driven changes in solubility could also produce N_2/Ar relationships that are similar to those associated with denitrification fluxes, and I hope to estimate the soil physical processes by adding additional noble gas measurements (e.g., neon, krypton, or xenon) to separate the biological and physical processes in the future. If I can account for the physical processes using noble gas measurements, this method could be used to estimate the flux of excess N_2 from the soil surface which would help find the "missing N" on the watershed scale. This method is an improvement on our current abilities to directly measure excess N_2 in the vadose zone because it sets limits on the range of values, although it cannot yet separate physical processes from biological ones.

Chapter 4

The previous two chapters documented the high concentrations of N_2O and CH_4 in groundwater in the Choptank Basin and the measureable concentrations of N_2O and CO_2 in the vadose zone at Rfarm. Once these gases are in the vadose zone, this chapter sought to determine which process, diffusion or convection, primarily caused the transport of the gases from the soil surface. Although there are four known convective gas transport processes (barometric pressure changes, infiltration from rainfall, temperature changes, and wind), this study only looked at the first two processes. In this chapter, I also hypothesized that the concentrations of N_2O, CO_2, and CH_4 in the vadose zone would increase after rainfall events.

It is widely believed that the dominant transport process moving gas from the soil to the atmosphere is diffusion. In fact, many studies only calculate diffusional flux, and ignore convective flux. I found that the diffusive fluxes of N_2O, CO_2, and CH_4 were in fact the primary transport processes moving the gases through the soil surface on a yearly time scale. Convective fluxes have the ability to affect the short term N_2O, CO_2, and CH_4 budget; however, the convective flux of CH_4 was minor due to the low concentrations that accumulated within the soils of the study locations. The median N_2O convective flux was also small, but did account for approximately 5% of the median total calculated yearly flux. The median calculated convective flux of CO_2 was detectable and significant, accounting for approximately 20% of the median annual total calculated flux from the soil surface. The high CO_2 vadose zone concentrations created the high CO_2 convective flux from the soil surface. In terms of the two convective flux mechanisms, infiltration from rainfall transported more gas to the atmosphere than barometric pressure

changes. For future studies where large concentrations of any gas build within the vadose zone, the convective fluxes of this high concentration gas should be calculated along with the diffusional fluxes.

The fluxes of N_2O, CH_4, and CO_2 have been shown to be temporally and spatially heterogeneous (e.g., Goodroad and Keeney 1985, Adrian et al. 1994, Goodroad et al. 1984, Breuer et al. 2000, Mathieu et al. 2006, Yao et al. 2010). Hot moments are a type of temporal variability and are defined as a short period of time with increased biogeochemical reaction rates compared to longer periods with much lower rates (McClain et al. 2003). Researchers have also shown increased fluxes of N_2O after rainfall events, both using soil cores (Ruser et al. 2006) and in the field (Dobbie and Smith 2003), and increased N_2O production has also been observed after soil thawing (Goodroad et al. 1984, Papen & Butterbach-Bahl 1999, Teppe et al. 2001, Koponen et al. 2004), and fertilizer additions (Dobbie & Smith, 2003, Meng et al 2005). Pulses of CO_2 have been observed after rainfall events (Morell et. al. 2010, Rochette et al. 1991) and after soil disturbance such as tillage (Morell et al. 2010). These flux measurements are often made within chambers, and therefore provide only the diffusional flux from the surface with little indication of what is occurring below ground. I hypothesized that higher concentrations of N_2O, CO_2, and CH_4 would occur in the vadose zone after rainfall events, which would cause a steeper concentration gradient towards the soil surface.

Increased concentrations of both CO_2 and N_2O were observed in the vadose zone after rainfall events at three locations, but CH_4 concentrations decreased after rainfall events. Most of the literature suggests that CH_4 oxidation would decrease under increased % water filled pore space (%WFPS) conditions, which contradicts my

observations. In the groundwater, concentrations of the three gases produced no consistent patterns after rainfall, likely due to the small sample size. As global climate change is inevitable, and many areas are predicted to have increased precipitation and longer dry periods, the increased production of N_2O and CO_2 after rainfall events is important to understand.

Overall conclusions

This research further establishes the high degree of spatial and temporal variability observed in both groundwater and soils. I have shown that large concentrations of N_2O, CH_4, and CO_2 accumulate in the groundwater of this coastal plain watershed in both natural and anthropogenically altered areas, and Fisher et al. (2010) showed large concurrent concentrations of excess N_2 at these locations. Large concentrations of these gases are produced during hot moments, or at hot spot locations. Once these high concentrations build within groundwater, the dissolved gases can be transported from groundwater to the vadose zone either via diffusion or convective processes such as CH_4 ebullition. However, in comparison to the missing N on the transect scale, the diffusive loss of excess N_2 and N_2O across the water table is minor. Concentration gradients in the vadose zone of excess N_2 can be measured, but the source producing the increase in the N_2/Ar ratio could be either biological or physical, and currently I cannot distinguish between the two. Once these gases are in the vadose zone, the primary mechanism that transports these gases across the soil surface is diffusion, but convective fluxes can account for a significant amount of the yearly flux if large concentrations of a gas persist in the vadose zone. Lastly, higher concentrations of N_2O

and CO_2 were observed in the vadose zone after rainfall events, but CH_4 concentrations either stayed the same or decreased.

Understanding the sources and surface N_2O and CH_4 flux locations is important in relation to climate change. In terms of nitrogen and carbon budgets, both gases are loss terms, but are minor components in comparison to their more dominant counterparts N_2 and CO_2, respectively. Calculated fluxes of N_2O and CH_4 from the soil surface were minor at my study locations, even though two of the three monitored locations had been chosen based on the consistently high N_2O groundwater concentrations measured prior. The flux of N_2O and CH_4 out of groundwater and into the vadose zone was more minor than expected; the large dissolved N_2O concentrations in groundwater presumably remained dissolved in groundwater or were further converted to N_2 before entering surface waters. The residence time of groundwater on the Delmarva Peninsula is >1 to 15 years, which can create an offset between production of N_2O and CH_4, and emergence in streams and rivers. Production today may not show up in streams and rivers for 15 years, and longer in other locations. As these gases can travel for long time periods in groundwater, reducing the amount of N_2O and CH_4 produced in groundwater today might not change stream and ditch surface N_2O and CH_4 flux for many years.

Groundwater residence time also affects cleanup efforts in the Chesapeake Bay and its tributaries. Degraded water quality will persist in the Choptank River until anthropogenic N loading is reduced. However, even if application of all agricultural N subsided today, high N groundwater would continue to flow into our ditches and streams for up to 15 years. Agricultural management practices have the potential to reduce agricultural N transport downstream by fostering denitrification, but creating locations

suitable for denitrification is difficult, and increased denitrification always has the potential to increase N_2O emissions. High groundwater N_2O concentrations were observed within many managed locations. Reducing N inputs to the watershed is the solution. Reduced N inputs would reduce the transport of N downstream and would eventually reduce the amount of NO_3 available for denitrification in soil and groundwater. Climate change is occurring; reducing the amount of N inputs within a watershed can both increase water quality and decrease N_2O emissions.

Increased rainfall intensity, longer duration between rainfall events, and increased surface temperatures are expected as a result of climate change. I have shown both N_2O and CO_2 concentration increases in the vadose zone after large precipitation events and the magnitude of these pulses would likely increase with larger events and longer spacing between these events as more substrate could accumulate between rainstorms. This more variable environment may not produce more N_2O and CO_2 on a yearly time scale, but the dynamics of the system are affected and the number of hot moments a year will likely increase.

Although N_2O is an important greenhouse gas, the flux of N_2O from a watershed is minor in comparison to the flux of N_2. Estimating N_2 flux on the watershed scale is difficult because denitrification is both temporally and spatially highly variable and directly measuring N_2 concentrations is extremely difficult. Large concentrations of N_2 build in groundwater under agricultural management practices and within water saturated areas of fields, but the majority of N_2 is likely lost from the vadose zone to the atmosphere after production in the vadose zone. I have made estimates of N_2 flux from the vadose zone on a yearly time scale, and my flux estimates can account for as much as

26% of the missing N. Currently, this new method to directly measure excess N_2 has many possible errors associated with its use including confounding physical effects that can potentially be resolved with additional noble gas tracers. An easy, direct way to measure denitrification is important to better standardize denitrification measurement techniques. Potential denitrification rates are also often reported, which is important, but actual denitrification rates are needed to understand the current denitrification rates of a system.

Another important finding of this collaborative research was the complexity of flow paths in areas with little surface topography. Studies often assume a hydrologic connection between close proximity piezometers, and the collaborative work of the CEAP wetlands project either found evidence to refute this common assumption or the flow paths were not adequately determined at 9 of the 10 locations. Initial research on the underlying groundwater hydrology should be undertaken before applying simple hydrologic concepts. The complexity of the hydrology made it difficult to assess the mitigating potential of wetlands adjacent to crop fields to capture NO_3^-. Future studies should consider installing a greater number of piezometer transects with nested piezometers that sample different depths within the unconfined aquifer. The use of major ion analysis and tracer studies (e.g., KBr) to evaluate flow paths would help confirm or reject assumptions concerning flow paths through a piezometer grid.

Choosing suitable management practice locations is difficult in locations with complex hydrology. Management practices only work to reduce N if the high N groundwater passes through the management area. Management practices should be constructed in locations through which the groundwater flows, which can be tentatively

determined by learning the dominant direction of the groundwater slope. Second, locations with a shallow depth to the confining unit will channel water through a thinner vertical distance in the wetland. If anaerobic conditions are reached within the wetland, areas with a shallow depth to the confining unit will have a higher ability to reduce more N throughout the entire soil column. Creating reduced conditions with sufficient carbon is difficult in itself to engineer, but the physical characteristics can be determined prior to installation of a management practice to ensure potential success. However, management practices would not be relied upon as heavily if we reduced N inputs within watersheds. Reducing N inputs would reduce the concentration of N flowing downstream, and would reduce N_2O emissions to the atmosphere thereby increasing water quality and reducing greenhouse gas emissions.

References

Adrian, N.R., J.A. Robinson, J.M. Suflita. 1994. Spatial variability in biodegradation rates as evidenced by methane production from an aquifer. Applied and Environmental Microbiology. 60(10):3632-3639.

Bremner, J.M., A.M. Blackmer. 1978. Nitrous oxide: emission from soils during nitrification of fertilizer nitrogen. Science. 199:295-296.

Breuer, L., H. Papen, K. Butterbach-Bahl. 2000. N_2O emission from tropical forest soils of Australia. Journal of Geophysical Research. 105(D21):26,353-26,357.

Crutzen, P.J., 1981. Atmospheric chemical processes of the oxides of nitrogen, including N_2O. In Delwiche,C.C.(ed.). Denitrification, Nitrification, and Atmospheric Nitrous Oxide. Wiley, New York, pp.17-44.

Dobbie, K.E., K.A. Smith. 2003. Nitrous oxide emission factors for agricultural soils in Great Britain: The impact of soil water-filled pore space and other controlling variables. Global Change Biology. 9:204-218.

Fisher, T.R., T.E. Jordan, K.W. Staver, A.B. Gustafson, A.I. Koskelo, R.J. Fox, A.J. Sutton, T. Kana, K.A. Beckert, J.P. Stone, G.W. McCarty, M.W. Lang. 2010. The Choptank Basin in transition intensifying agriculture, slow urbanization, and estuarine eutrophication. In Kennish M.J., Paerl H.W (ed.). Coastal Lagoons Critical Habitats of Environmental Change, CRC Press, pp 135-165.

Goodroad, L.L., D.R. Keeney, L.A. Peterson. 1984. Nitrous oxide emissions from agricultural soils in Wisconsin. Journal of Environmental Quality. 13(4):557-561.

Goodroad, L.L., D.R. Keeney. 1985. Site of nitrous oxide production in field soils. Biological fertility of soils. 1:3-7.

IPCC, (Intergovernmental Panel on Climate Change), 2007. Climate change 2007- The physical science basis. Contribution of working group I to the forth assessment report of the IPCC. Cambridge University Press, Cambridge.

Koponen, H.T., L.Flöjt, P.J. Martikainen. 2004. Nitrous oxide emissions from agricultural soils at low temperatures: A laboratory microcosm study. Soil Biology and Biochemistry. 36:757-766.

Mathieu, O., J. Lévêque, C. Hénault, M.-J. Milloux, F. Bizouard, F. Andreux. 2006. Emissions and spatial variability of N_2O, N_2 and nitrous oxide mole fraction at the field scale, revealed with ^{15}N isotopic techniques. Soil Biology and Biogeochemistry. 38(5):941-951.

McClain, M.E., E.W. Boyer, C.L. Dent, S.E. Gergel, N.B. Grimm, P.M. Groffman, S.C. Hart, J.W. Harvey, C.A. Johnston, E. Mayorga, W.H. McDowell, G. Pinay. 2003. Biogeochemical hot spots and hot moments at the interface of terrestrial and aquatic ecosystems. Ecosystems. 6:301-312.

Meng, L., W. Ding, Z. Cai. 2005. Long-term application of organic manure and nitrogen fertilizer on N_2O emissions, soil quality and crop production in a sandy loam soil. Soil Biology & Biochemistry. 37:2037-2045.

Morell, F.J., J. Álvaro-Fuentes, J. Lampurlanés, C. Cantero-Martínez. 2010. Soil CO_2 fluxes following tillage and rainfall events in a semiarid Mediterranean agroecosystems: Effects of tillage systems and nitrogen fertilization. Agriculture, Ecosystems and Environment. 139:167-173.

Papen, H., K. Butterbach-Bahl. 1999. A 3-year continuous record of nitrogen trace gas fluxes from untreated and limed soil of a N-saturated spruce and beech forest ecosystem in Germany, 1 N_2O emissions. Journal of Geophysical Research. 104(D15):18,487-18,503.

Rochette, P., R.L. Desjardins, E. Pattey. 1991. Spatial and temporal variability of soil respiration in agricultural field. Canadian Journal of Soil Science. 71:189-196.

Ruser, R., H. Flessa, R. Russow, G. Schmidt, F. Buegger, J.C. Munch. 2006. Emissions of N_2O, N_2 and CO_2 from soil fertilized with nitrate: Effect of compaction, soil moisture and rewetting. Soil Biology and Biochemistry. 38:263-274.

Teepe, R., R. Brumme, F. Beese. 2001. Nitrous oxide emissions from soil during freezing and thawing periods. Soil Biology and Biochemistry. 33:1269-1275.

Yao, Z., B. Wolf, W. Chen, K. Butterbach-Bahl, N. Brüggemann, M. Wiesmeier, M. Dannenmann, B. Blank, X. Zheng. 2010. Spatial variability of N_2O, CH_4 and CO_2 fluxes within the Xilin River catchment of Inner Mongolia, China: A soil core study. Plant Soil. 331:341-359. DOI 10.1007/s11104-009-0257-x.

Figure 5.1 - Relationships between $\%O_2$ and N_2O, NO_3^- and N_2O, and excess N_2 and N_2O in groundwater.

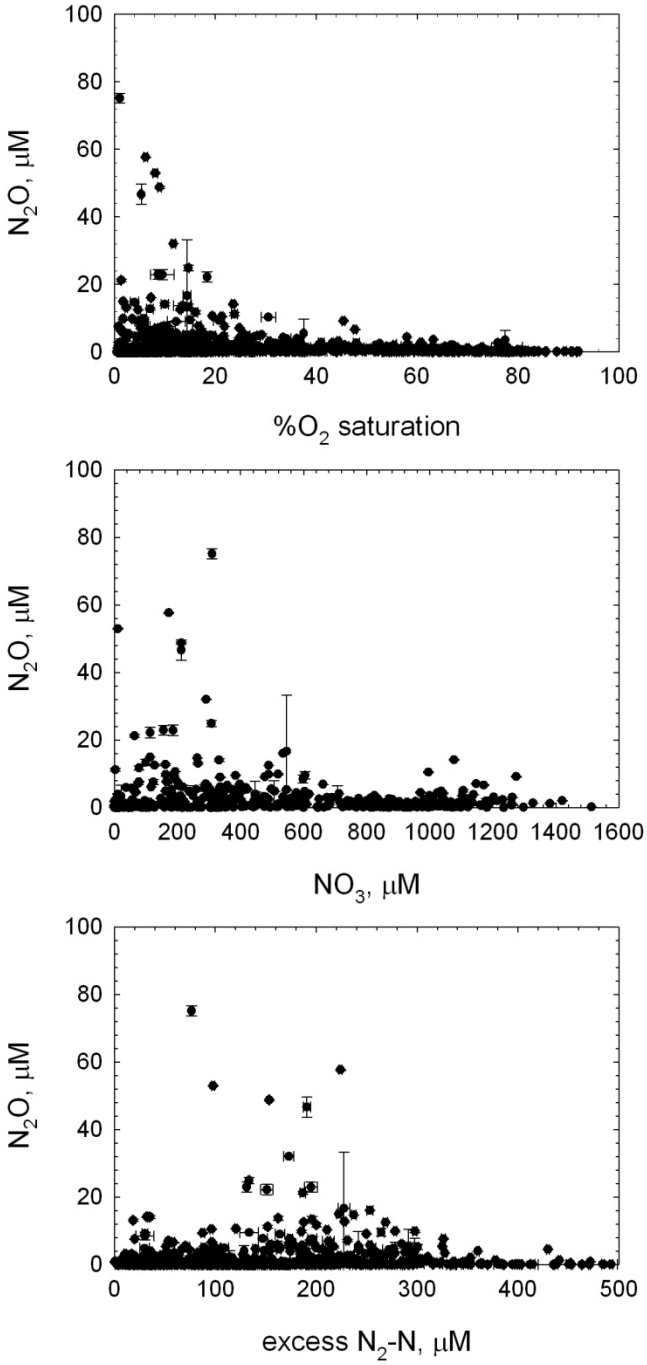

REFERENCES

Abbasi, M.K., W.A. Adams. 2000. Estimation of simultaneous nitrification and denitrification in grassland soil associated with urea-N using ^{15}N and nitrification inhibitor. Biology and Fertility of Soils. 31:38-44.

Adrian, D.D., J.B. Franzini. 1966. Impedance to infiltration by pressure build-up ahead of the wetting front. Journal of Geophysical Research. 71:5858-5862.

Adrian, N.R., J.A. Robinson, J.M. Suflita. 1994. Spatial variability in biodegradation rates as evidenced by methane production from an aquifer. Applied and Environmental Microbiology. 60(10):3632-3639.

Aeschbach-Hertig, W., F. Peeters, U. Beyerle, and R. Kipfer. 2000. Palaeotemperature reconstruction from noble gases in groundwater taking into account equilibration with entrapped air. Nature. 405:1040-1044.

Aeschbach-Hertig, W., H. El-Gamal, M. Wieser, L. Palcsu. 2008. Modeling excess air and degassing in groundwater by equilibrium partitioning with a gas phase. Water Resources Research. 44:1-12.

Ahrens, C.D. 2007. Meterology Today: An introduction to weather, climate, and the environment. 8th ed. Belmont, CA. Thomas Brooks/Cole.

Ambus, P. 1998. Nitrous oxide production by denitrification and nitrification in a temperate forest, grassland and agricultural soils. European Journal of Soil Science. 49(3):495-302.

Anderson, D.M., J.M. Burkholder, M.P. Cochlan, P.M. Glibert, C.J. Gobler, C.A. Heil, R.M. Kudela, M.L. Parsons, J.E.J. Rensel, D.W. Townsend, V.L.

Trainer, G.A. Vargo. 2008. Harmful algal blooms and eutrophication: Examining linkages from selected coastal regions of the United States. Harmful Algae. 8:39-53.

Anderson, D.M., P.M. Glibert, J.M. Burkholder. 2002. Harmful algal blooms and eutrophication: Nutrient sources, composition, and consequences. Estuaries 25(4B):704-726.

Andrews, J.N. 1991. Noble gases and radioelements in groundwater. In Downing R.A., Wilkinson W.B. (ed.). Applied Groundwater Hydrology, Oxford University Press, pp 243-265.

Azam, F., C. Muller, A.Weiske, G. Benckiser, J.C.G. Ottow. 2002. Nitrification and denitrification as sources of atmospheric nitrous oxide- role of oxidizable carbon and applied nitrogen. 35(1):54-61.

Bateman, E.J., E.M. Baggs. 2005. Contribution of nitrification and denitrification to N_2O emissions from soils at different water-filled pore space. Biology and Fertility of Soils. 41:379-388. DOI: 10.1007/s00374-005-0858-3.

Bekku, Y., H. Koizumi, T. Nakadai, H. Iwaki. 1995. Measurements of soil respiration using closed chamber methods: An IRGA technique. Ecological Research. 10:369-373.

Bell, W.H., Favero P. 2000. Moving water. A report to the Chesapeake Bay Cabinet by the Public Drainage Task Force. Contribution No. 2000-1. Center for the Environment and Society, Washington College. http://www.dnr.state.md.us/Bay/tribstrat/public_drainage_report.pdf.

Benitez, J.A., T.R. Fisher. 2004. Historical land-cover conversion (1665-1820) in the Choptank watershed, Eastern United States. Ecosystems. 7:219-232.

Benson, B.B., D. Krause, Jr. 1976. Empirical laws for dilute aqueous solutions of nonpolar gases. The Journal of Chemical Physics. 64(2):689-709.

Blackmer, A.M., J.M. Bremner, 1978. Inhibitory effect of nitrate on reduction of N_2O to N_2 by soil microorganisms. Soil Biology and Biogeochemistry. 10(3)187-191.

Blicher-Mathiesen, G., G.W. McCarty, L.P. Nielsen. 1998. Denitrification and degassing in groundwater estimated from dissolved dinitrogen and argon. Journal of Hydrology. 208:16-24.

Bohlke, J.K., J.M. Denver. 1995. Combined use of groundwater dating, chemical, and isotopic analyses to resolve the history and fate of nitrate contamination in two agricultural watersheds, Atlantic coastal plain, Maryland. Water Resources Research. 31(9):2319-2339.

Bowden, W.B., F.H. Bormann. 1986. Transport and loss of nitrous oxide in soil water after forest clear-cutting. Science. 233:867-869.

Boyer, E.W., C.L. Goodale, N.A. Jaworki, R.W. Howarth. 2002. Anthropogenic nitrogen sources and relationships to riverine nitrogen export in the northeastern U.S.A. Biogeochemistry. 57/58:137-169.

Boynton, W.R., W.M. Kemp, C.G. Osborne. 1980. Nutrient fluxes across the sediment-water interface in the turbid zone of a coastal plain estuary. Estuarine Perspectives. Academic Press, pp. 93-107.

Bradley, P.M., M. Fernandez, F.H. Chapelle. 1992. Carbon limitation of denitrification rates in an anaerobic groundwater system. Environmental Science and Technology. 26(12):2377-2381.

Brady, N.C., R.R. Weil. 2002. The nature and properties of soils. Upper Saddle River, NJ. Prentice Hall.

Bremner, J.M., A.M. Blackmer. 1978. Nitrous oxide: emission from soils during nitrification of fertilizer nitrogen. Science. 199:295-296.

Brettar, I., M.G. Höfle. 2002. Close correlation between the nitrate elimination rate by denitrification and the organic matter content in hardwood forest soils of the Upper Rhine floodplain (France). Wetlands. 22(2):214-224.

Breuer, L., H. Papen, K. Butterbach-Bahl. 2000. N_2O emission from tropical forest soils of Australia. Journal of Geophysical Research. 105(D21):26,353-26,357.

Bruland, G.W., C.J. Richardson, S.C. Whalen. 2006. Spatial variability of denitrification potential and related soil properties in created, restored, and paired natural wetlands. Wetlands. 26(4):1042-1056.

Burgin, A.J., S.K. Hamilton. 2007. Have we overemphasized the role of denitrification in aquatic ecosystems? A review of nitrate removal pathways. Frontiers in Ecology and the Environment. 5(2):89-96.

Cai, Y., D. Weixin, X. Zhang, H. Yu, L. Wang. 2010. Contribution of heterotrophic nitrification to nitrous oxide production in a long-term N-fertilized arable black soil. Communications in Soil Science and Plant Analysis. 41:2264-2278, DOI: 10.1080/00103624.2010.507833.

Castro, M.S., J.M. Melillo, P.A. Steudler, J.W. Chapman. 1994. Soil moisture as a predictor of methane uptake by temperate forest soils. Canadian Journal of Forestry Research. 24:1805-1810.

Choi, J.W., F.D. Tillman Jr., J.A. Smith. 2002. Relative importance of gas-phase diffusive and advective trichloroethene (TCE) fluxes in the unsaturated zone under natural conditions. Environmental Science and Technology. 36:3157-3164.

Christensen, S. 1985. Denitrification in a sandy loam as influenced by climatic and soil conditions. Tidsskr. Planteavl. 89:351-365.

Christiansen, J.R., J.F.J. Korhonen, R. Juszczak, M. Giebels, M. Pihlatie. 2011. Assessing the effects of chamber placement, manual sampling and headspace mixing on CH_4 fluxes in a laboratory experiment. Plant and Soil. 343:171-185. DOI: 10.1007/s11104-010-0701-y.

Clapp, R.B., G.M. Hornberger. 1978. Empirical equations for some soil hydraulic properties. Water Resources Research. 14(4):601-604.

Clough, T.J., R.R. Sherlock, D.E. Rolson. 2005. A review of the movement and fate of N_2O in the subsoil. Nutrient Cycling in Agroecosystems. 72:3-11.

Clough, T.J., S.C. Jarvis, E.R. Dixon, R.J. Stevens, R.J. Laughlin, D.J. Hatch. 1999. Carbon induced subsoil denitrification of ^{15}N-labelled nitrate in 1 m deep soil columns. Soil Biology and Biochemistry. 31:31-41.

Codispoti, L.A., 2010. Interesting times for marine N_2O. Science. 327:1339-1340.

Codispoti, L.A., J.P. Christensen. 1985. Nitrification, denitrification and nitrous oxide cycling in the eastern tropical South Pacific Ocean. Marine Chemistry. 16:277-300.

Colt, J. 1984. Computation of dissolved gas concentrations in water as functions of temperature, salinity, and pressure. Bethesda, MD: American Fisheries Society.

Conrad, R., F. Rothfuss. 1991. Methane oxidation in the soil surface layer of a flooded rice field and the effect of ammonium. Biology and Fertility of Soils. 12(1):28-32. DOI: 10.1007/BF00369384.

Crutzen, P.J., 1981. Atmospheric chemical processes of the oxides of nitrogen, including N_2O. In Delwiche, C.C.(ed.). Denitrification, Nitrification, and Atmospheric Nitrous Oxide. Wiley, New York, pp.17-44.

Davidson, E.A., K. Savage. L.V. Verchot, R. Navarro. 2002. Minimizing artifacts and biases in chamber-based measurements of soil respiration. Agricultural and Forest Meterology. 113:21-37.

De Klein, C.A.M., R.S.P. Van Logtestijn. 1996. Denitrification in grassland soils in the Netherlands in relation to irrigation, N-application rate, soil water content and soil temperature. Soil Biology & Biochemistry 28(2):231-237.

Denver, J.M., S.W. Ator. 2011. Nitrogen fate and transport through upland depressional wetlands along an alternation gradient in an agricultural landscape, upper Choptank Watershed, Maryland. In Prep.

Dlugokencky, E.J., L. Bruhwiler, W.C. White, L.K. Emmons, P.C. Novelli, S.A. Montzka, K.A. Masarie, P.M. Lang, A.M. Crotwell, J.B. Miller, L.V. Gatti.

2009. Observational constraints on recent increases in the atmospheric CH_4 burden. Geophysical Research Letters. 36, L18803. DOI:10.1029/2009GL039780.

Dlugokencky, E.J., S. Houweling, L. Bruhwiler, K.A. Masarie, P.M. Lang, J.B. Miller, P.P. Tans. 2003. Atmospheric methane levels off: Temporary pause or a new steady-state? Geophysical Research Letters, 30 (19). doi:10.1029/2003GL018126,2003.

Dobbie, K.E., K.A. Smith, A. Priemé, S. Christensen, A. Degorska, P. Orlanski. 1996A. Effect of land use on the rate of methane uptake by surface soils in northern Europe. Atmospheric Environment. 30(7):1005-1011.

Dobbie, K.E., K.A. Smith. 1996B. Comparison of CH_4 oxidation rates in woodland, arable and set aside soils. Soil biology & biochemistry. 28(10-11):1357-1365.

Dobbie, K.E., K.A. Smith. 2001. The effects of temperature, water-filled pore space and land use on N_2O emissions from an imperfectly drained gleysol. European Journal of Soil Science. 52:667-673.

Dobbie, K.E., K.A. Smith. 2003. Nitrous oxide emission factors for agricultural soils in Great Britain: The impact of soil water-filled pore space and other controlling variables. Global Change Biology. 9:204-218.

Dukes, M.D., R.O. Evans, J.W. Gilliam, S.H. Kunickis. 2003. Interactive effects of controlled drainage and riparian buffers on shallow groundwater quality. Journal of Irrigation and Drainage Engineering. 129(2):82-92. DOI: 10.1061/(ASCE)0733-9437(2003)129:2(82).

Dunfield, P.F., E. Topp, C. Archambault, R. Knowles. 1995. Effect of nitrogen fertilizers and moisture content on CH_4 and N_2O fluxes in a humisol: Measurements in the field and intact soil cores. Biogeochemistry. 29:199-222.

Eichner, M.J. 1990. Nitrous oxide emissions from fertilized soils: Summary of available data. Journal of Environmental Quality. 19:272-280.

Elberling, B., L. Askaer, C.J. Jørgensen, H.P. Joensen, M. Kühl, R.N. Glud, F.R. Lauritsen. 2011. Linking soil O_2, CO_2, and CH_4 concentrations in a wetland soil: Implications for CO_2 and CH_4 fluxes. 45:3393-3399. dx.doi.org/10.1021/es103540k.

Elmi, A.A., C. Madramootoo, C. Hamel, A. Liu. 2003. Denitrification and nitrous oxide to nitrous oxide plus dinitrogen ratios in the soil profile under three tillage systems. Biology and Fertility of Soils. 38(6):340-348.

Evans, R.O., J.W. Gilliam, R.W Skaggs. 1991. Controlled drainage management guidelines for improving drainage water quality. Cooperative Extension Service, North Carolina State University Publication No. AG-443: 16pp.

Faybishenko, B.A. 1995. Hydraulic behavior of quasi-saturated soils in the presence of entrapped air: Laboratory experiments. Water Resources Research. 31:2421-2435.

Fetter, C.W. 2001. Applied Hydrogeology. Upper Saddle River, NJ: Prentice-Hall, Inc.

Fisher, T.R., J.A. Benitez, K. Lee, A.J. Sutton. 2006. History of land cover change and biogeochemical impacts in the Choptank River basin in the mid-Atlantic

region of the US. International Journal of Remote Sensing. 27(17):3683-3703.

Fisher, T.R., R.J. Fox, A.B. Gustafson, T.E. Jordan, K.W. Staver, M. Fogel, M. Altabet, T. Kana. In prep. The search for the missing N.

Fisher, T.R., T.E. Jordan, K.W. Staver, A.B. Gustafson, A.I. Koskelo, R.J. Fox, A.J. Sutton, T. Kana, K.A. Beckert, J.P. Stone, G.W. McCarty, M.W. Lang. 2010. The Choptank Basin in transition intensifying agriculture, slow urbanization, and estuarine eutrophication. In Kennish M.J., Paerl H.W (ed.). Coastal Lagoons Critical Habitats of Environmental Change, CRC Press, pp 135-165.

Fortuin, N.P.M., A. Willemsen. 2005. Exsolution of nitrogen and argon by methanogenesis in Dutch ground water. Journal of Hydrology. 301:1-13.

Fulweiler, R.W., S.W. Nixon, B.A. Buckley, S.L. Granger. 2007. Reversal of the net dinitrogen gas flux in coastal marine sediments. Nature. 448:180-182.

Galloway, J.N., J.D. Aber, J.W. Erisman, S.P. Seitzinger, R.W. Howarth, E.B. Cowling, B.J. Cosby. 2005. The nitrogen cascade. Bioscience. 53(4):341-356.

Galloway, J.N., W.H. Schlesigner, H. Levy II, A. Michaels, J.L. Schnoor. 1995. Nitrogen fixation: Anthropogenic enhancement-environmental response. Global biogeochemical cycles. 9(2):235-252.

Goodroad, L.L., D.R. Keeney, L.A. Peterson. 1984. Nitrous oxide emissions from agricultural soils in Wisconsin. Journal of Environmental Quality. 13(4):557-561.

Goodroad, L.L., D.R. Keeney. 1985. Site of nitrous oxide production in field soils. Biological fertility of soils. 1:3-7.

Goreau, T.J., W.A. Kaplan, S.C. Wofsy, M.B. McElroy, F.W. Valois, S.W. Watson. 1980. Production of NO_2^- and N_2O by nitrifying bacteria at reduced concentrations of oxygen. Applied and Environmental Microbiology. 40(3):526-532.

Groffman, P.M., A.J. Gold, P. Jacinthe. 1998. Nitrous oxide production in riparian zones and groundwater. Nutrient Cycling in Agroecosystems. 52:179-186.

Groffman, P.M., K. Butterbach-Bahl, R.W. Fulweiler, A.J. Gold, J.L. Morse, E.K. Stander, C. Tague, C. Tonitto, P. Vidon. 2009. Challenges to incorporating spatially and temporally explicit phenomena (hotspots and hot moments) in denitrification models. Biogeochemistry. 93:49-77. DOI 10.1007/s10533-008-9277-5.

Groffman, P.M., M.A. Altabet, J.K. Bohlke, K. Butterbach-Bahl, M.B. David, M.K. Firestone, A.E. Giblin, T.M. Kana, L.P. Nielsen, M.A. Voytek. 2006. Methods for measuring denitrification: Diverse approaches to a difficult problem. Ecological Applications. 16(6):2091-2122.

Hamborg, E.S, P.W.J. Derks, S.R.A. Kersten, J.P.M. Niederer, G.F. Verstegg. 2008. Diffusion coefficients of N_2O in aqueous piperazine solutions using the Taylor Dispersion technique from (293 to 333) K and (0.3 to 1.4) $mol \cdot dm^{-3}$. Journal of Chemical Engineering Data. 53:1462-1466.

Hao, Y., Y. Wang, X. Mei, X. Cui. 2010. The response of ecosystem CO_2 exchange to small precipitation pulses over a temperate steppe. Plant Ecology. 209:335-347.

Harms, T. K., and N. B. Grimm. 2008. Hot spots and hot moments of carbon and nitrogen dynamics in a semiarid riparian zone. Journal of Geophysical Research. 113:1-14.

Heincke, M., M. Kaupenjohann. 1999. Effects of soil solution on the dynamics of N_2O emissions: A review. Nutrient Cycling in Agroecosystems. 55:133-157.

Houlton, B.Z., E. Bai. 2009. Imprint of denitrifying bacteria on the global terrestrial biosphere. Preceedings of the National Academy of Sciences. 106(51):21713-21716.

Howarth, R.W., G. Billen, D. Swaney, A. Townsend, N. Jaworski, K. Lajtha, J.A. Downing, R. Elmgren, N. Caraco, T. Jordan, F. Berendse, J. Freney, V. Kudeyardov, P. Murdoch, Z. Zhao-Liang. 1996. Regional nitrogen budgets and riverine N & P fluxes for the drainages to the North Atlantic Ocean: Natural and human influences. Biogeochemistry. 35(1):75-139.

Ingram, R.G.S., K.M. Hiscock, P.F. Dennis. 2007. Noble gas excess air applied to distinguish groundwater recharge conditions. Environmental Science Technology. 41:1949-1955.

IPCC (Intergovernmental Panel on Climate Change), 2007. Climate change 2007-The physical science basis. Contribution of working group I to the forth assessment report of the IPCC. Cambridge University Press, Cambridge.

Isermann, K., 1994. Agriculture's share in the emission of trace gases affecting the climate and some cause-oriented proposals for sufficiently reducing this share. Environmental Pollution. 83(1-2):95-111.

Jetten, M.S.M. 2001. New pathways for ammonia conversion in soil and aquatic systems. Plant and Soil. 230(1):9-19.

Jones W.J. 1991. Diversity and physiology of methanogens. In Rogers J.E., W.B. Whitman (ed). Microbial Production and consumption of greenhouse gases: Methane, nitrogen oxides, and halomethanes. American Society for Microbiology, pp.39-55.

Jordan, T.E., D. W. Weller. 1996. Human contributions to terrestrial nitrogen flux. BioScience 46(9):655-664.

Jordan, T.E., D.L. Correll, D.E. Weller. 1997. Effects of agriculture of discharges of nutrients from coastal plain watersheds of Chesapeake Bay. Journal of Environmental Quality. 26(3):836-848.

Jury, W.A., R. Horton. 2004. Soil Physics. 6th ed. Hoboken. Wiley.

Kana, T.M., C. Darkangelo, M.D. Hunt, J.B. Oldham, G.E. Bennett, J.C. Cornwell. 1994. Membrane inlet mass spectrometer for rapid high-precision determination of N_2, O_2 and Ar in environmental water samples. Analytical Chemistry. 66(23):4166-4170.

Kemp, W.M., R.R. Twilley, J.C. Stevenson, W.R. Boynton, J.C. Means. 1983. The decline of submerged vascular plants in upper Chesapeake Bay- summary of results concerning possible causes. Marine Technology Society Journal. 17(2):78-89.

Kemp, W.M., W.R. Boynton, J.E. Adolf, D.F. Boesch, W.C. Boicourt, G. Brush, J.C. Cornwell, T.R. Fisher, P.M. Glibert, J.D. Hagy, L.W. Harding, E.D. Houde, D.G. Kimmel, W.D. Miller, R.I.E. Newell, M.R. Roman, E.M. Smith, J.C.

Stevenson. 2005. Eutrophication of Chesapeake Bay: Historical trends and ecological interactions. Marine Ecology Progress Series. 303:1-29.

Khalil, M.I., A.B. Rosenani, O.Van Cleemput, C.I. Fauziah, J. Shamshuddin. 2002. Nitrous oxide emissions from the humid tropics under maize-groundnut rotation. Journal of Environmental Quality. 31(4):1071-1078.

Khalil, M.I., E.M. Baggs. 2005. CH_4 oxidation and N_2O emissions at varied soil water-filled pore spaces and headspace CH_4 concentrations. Soil Biology and Biochemistry. 37:1785-1794.

Kliewer, B.A., J.W. Gilliam. 1995. Water table management effects on denitrification and nitrous oxide evolution. Soil Science Society of America. 59(6):1694-1701.

Knowles, R. 1982. Denitrification. Microbiological Reviews. 46(1):43 -70

Koponen, H.T., L. Flöjt, P.J. Martikainen, 2004. Nitrous oxide emissions from agricultural soils at low temperatures: A laboratory microcosm study. Soil Biology and Biogeochemistry. 36(5):757-766.

Kutzbach, L., D. Wagner, E.M. Pfeiffer. 2004. Effects of micro relief and vegetation on methane emissions from wet polygonal tundra, Lena Delta, Northern Siberia. Biogeochemistry. 69:341-362.

Lange, N.A., 1961. Handbook of Chemistry and Physics. New York, NY. McGraw-Hill Book Company, Inc.

Le Mer, J., P. Roger. 2001. Production, oxidation, emission and consumption of methane by soils: A review. European Journal of soil Biology. 37:25-50.

Lee, K., T.R. Fisher, E. Rochelle-Newall. 2001. Modeling the hydrochemistry of the Choptank River basin using GWLF and Arc/Info: 2. Model validation and application. Biogeochemistry. 56:311-348.

Lee, X., H.J. Wu, J. Sigler, C. Oishi, T. Siccama. 2004. Rapid and transient responses of soil respiration to rain. Global Change Biology. 10:1017-1026.

Leffekaar, P.A. 1986. Dynamics of partial anaerobiosis in a model soil in respect to denitrification. Soil Science, 128, 110-120.

Lessard, R., P. Rochette, E.G. Gregorich, E. Pattey, R.L. Desjardins. 1996. Nitrous oxide fluxes from manure-amended soil under maize. Journal of Environmental Quality. 25(6):1371-1377.

Liebig, M.A., J.A. Morgan, J.D. Reeder, B.H. Ellert, H.T. Gollany, G.E. Schuman. 2005. Greenhouse gas contributions and mitigation potential of agricultural practices in northwestern USA and western Canada. Soil & Tillage Research. 83:25-52.

Lindau, C.W., W.H. Patrick Jr., R.D. Delaune, K.R. Reddy. 1990. Rate of accumulation and emission of N_2, N_2O and CH_4 from a flooded rice soil. Plant and Soil. 129:269-276.

Lowrance, R.R, L.S. Altier, J.D. Newbold, R.R. Schnabel, P.M. Groffman, J.M. Denver, D.L. Correll, J.W. Gilliam, J.L. Robinson, R.B. Brinsfield, K.W. Staver, W. Lucas, A.H. Todd. 1997. Water quality functions of riparian forest buffers in Chesapeake Bay watersheds. Environmental Management. 21(5):687-712.

Lowrance, R.R., R. Todd, J. Fail Jr., O. Hendrickson Jr., R. Leonard, L. Asmussen. 1984 b. Riparian forests as nutrient filters in agricultural watersheds. BioScience. 34(6):374-377.

Lowrance, R.R., R.L. Todd, L.E. Asmussen. 1984 a. Nutrient cycling in an agricultural watershed: I. Phreatic movement. Journal of Environmental Quality. 13(1):22-27.

Maharajh, D.M., J. Walkley. 1973. The temperature dependence of the diffusion coefficients of Ar, CO_2, CH_4, CH_3Cl, CH_3Br, and $CHCl_2F$ in water. Canadian Journal of Chemistry. 51:944-952.

Mander, Ü., K. Lõhmus, S. Teiter, V. Uri, J. Augustin. 2008. Gaseous nitrogen and carbon fluxes in riparian alder stands. Boreal Environment Research. 13:231-241.

Martikainen, P.J., W.De Boer. 1993. Nitrous oxide production and nitrification in acidic soil from a Dutch coniferous forest. Soil Biology and Biogeochemistry. 25(3):343-347.

Massman, J., D.F. Farrier. 1992. Effects of atmospheric pressures on gas transport in the vadose zone. Water Resources Research. 28(3):777-791.

Massman, W.J. 1998. A review of the molecular diffusivities of H_2O, CO_2, CH_4, O_3, SO_2, NH_3, N_2O, NO, and NO_2 in air, O_2 and N_2 near STP. Atmospheric Environment. 32(6):1111-1127.

Mathieu, O., J. Lévêque, C. Hénault, M.-J. Milloux, F. Bizouard, F. Andreux. 2006. Emissions and spatial variability of N_2O, N_2 and nitrous oxide mole fraction at

the field scale, revealed with ^{15}N isotopic techniques. Soil Biology and Biogeochemistry. 38(5):941-951.

McClain, M.E., E.W. Boyer, C.L. Dent, S.E. Gergel, N.B. Grimm, P.M. Groffman, S.C. Hart, J.W. Harvey, C.A. Johnston, E. Mayorga, W.H. McDowell, G. Pinay. 2003. Biogeochemical hot spots and hot moments at the interface of terrestrial and aquatic ecosystems. Ecosystems. 6:301-312.

Megonigal, J.P., M.E. Hines, P.T. Visscher. 2005. Anaerobic metabolism: Linkages to trace gases and aerobic processes. In Schlesinger W.H. (ed). Biogeochemistry. Elsevier, pp 317-424.

Meng, L., W. Ding, Z. Cai. 2005. Long-term application of organic manure and nitrogen fertilizer on N_2O emissions, soil quality and crop production in a sandy loam soil. Soil Biology & Biochemistry. 37:2037-2045.

Moldrup, P., T. Olesen, J. Gamst, P. Schjønning, T. Yamaguchi, D.E. Rolston. 2000 A. Predicting the gas diffusion coefficient in repacted soil: Water-induced linear reduction model. Soil Society of America Journal. 64:1588-1594.

Moldrup, P., T. Olesen, J. Gamst, P. Schjønning, T. Yamaguchi, D.E. Rolston. 2000 B. Predicting the gas diffusion coefficient in undistrubed soil from soil water characteristics. Soil Society of America Journal. 64:94-100.

Moldrup, P., T. Olesen, T. Yamaguchi, P. Schjonning, and D. Rolston. 1999. Modeling diffusion and reaction in soils: IX. The Buckingham-Burdine-Campbell equation for gas diffusivity in undisturbed soil. Soil Science. 164:542-551.

Mookherji, S., G.W. McCarty, J.T. Angier. 2003. Dissolved gas analysis for assessing the fate of nitrate in wetlands. Journal of the American Water Resources Association. 39(2):381-387.

Morell, F.J., J. Álvaro-Fuentes, J. Lampurlanés, C. Cantero-Martínez. 2010. Soil CO_2 fluxes following tillage and rainfall events in a semiarid Mediterranean agroecosystems: Effects of tillage systems and nitrogen fertilization. Agriculture, Ecosystems and Environment. 139:167-173.

Mosier, A.R., J.M. Duxbury, J.R. Freney, O. Heinemeyer, K. Minami, D.E. Johnson. 1998. Mitigating agricultural emissions of methane. Climate Change. 40(1):30-80.

Mulder, A., A.A. Vandergraaf, L.A. Robertson, J.G Kuenen. 1995. Anaerobic ammonium oxidation discovered in a denitrifying fluidized-bed reactor. FEMS Microbiology Ecology 16(3):177-183.

Mulholland, P.J., A.M. Helton, G.C. Poole, R.O. Hall Jr, S.K. Hamilton, B.J. Peterson, J.L. Tank, L.R. Ashkenas, L.W. Cooper, C.N. Dahm, W.K. Dodds, S.E.G. Findlay, S.V. Gregory, N.B. Grimm, S.L. Johnson, W.H. McDowell, J.L. Meyer, H.M. Valett, J.R. Webster, C.P. Arango, J.J. Beaulieu, M.J. Bernot, A.J. Burgin, C.L. Crenshaw, L.T. Johnson, B.R. Niederlehner, J.M. O'Brien, J.D. Potter, R.W. Sheibley, D.J. Sobota, S.M. Thomas. 2008. Stream denitrification across biomes and its response to anthropogenic nitrate loading. Nature. 452(7184): 202-205.

Munoz, C., L. Paulino, C. Monreal, E. Zagal. 2010. Greenhouse gas (CO_2 and N_2O) emissions from soils: A review. Chilean Journal of Agricultural Research. 70(3):485-497.

Ohashi, M., L. Finer, T. Domisch, A.C. Risch, M.F. Jurgensen, P. Niemela. 2006. Seasonal and diurnal CO_2 efflux from red wood ant (*Formica aquilonia*) mounds in boreal coniferous forests. Soil Biology and Biogeochemistry. 39(7):1504-1511. DOI:10.1016/j.soilbio.2006.12.034 .

Orr, C.H., E.H. Stanley, K.A. Wilson, J.C. Finlay. 2007. Effects of restoration and reflooding on soil denitrification in a leveed Midwestern floodplain. Ecological Applications. 17(8):2365-2376.

Otte, S., N.G. Grobben, L.A. Robertson, M.S.M Jetten, J.G. Kuenen. 1996. Nitrous oxide production by *Alcaligenes faecalis* under transient and dynamic aerobic and anaerobic conditions. Applied and Environmental Microbiology. 62(7):2421-2426.

Owens, J.P., and C.S. Denny. 1979. Upper Cenozoic deposits of the central Delmarva Peninsula, Maryland and Delaware. US Geological Survey Professional Paper 1067-A.

Pacific, V.J., B.L. McGlynn, D.A. Riveros-Iregui, D.L. Welsch, H.E. Epstein. 2008. Variability in soil respiration across riparian-hillslope transitions. Biogeochemistry. 91:51-70.

Papen, H., K. Butterbach-Bahl. 1999. A 3-year continuous record of nitrogen trace gas fluxes from untreated and limed soil of a N-saturated spruce and beech

forest ecosystem in Germany, 1 N_2O emissions. Journal of Geophysical Research. 104(D15):18,487-18,503.

Parkin, T.B. 1987. Soil microsites as a source of denitrification variability. Soil Science Society of America Journal. 51(5):1194-1199.

Paul, E.A. (ed.). 2007. Soil Microbiology, Ecology, and Biochemistry, Academic Press, pp. 532.

Peralta, A.L., J.W. Matthews, A.D. Kent. 2010. Microbial community structure and denitrification in a wetland mitigation bank. Applied and Environmental Microbiology. 76(13):4207-4215. DOI: 10.1128/AEM.02977-09.

Peterjohn, W.T., D.L. Correll. 1984. Nutrient dynamics in an agricultural watershed: Observations on the role of a riparian forest. Ecology. 65(5):1466-1475.

Peterson, B.J., W.M. Wollheim, P.J. Mulholland, J.R. Webster, J.L. Meyer, J.L. Tank, E. Marti, W.B. Bowden. H.M. Valett, A.E. Hershey, W.H. McDowell, W.K. Dodds, S.K. Hamilton, S. Gregory, D.D. Morrall. 2001. Control of nitrogen export from watersheds by headwater streams. Science. 292(5514):86-90.

Pinay, G., L. Roques, A. Fabre. 1993. Spatial and temporal patterns of denitrification in a riparian forest. The Journal of Applied Ecology. 30(4):581-591.

Popovičová, J., M.L. Brusseau. 1997. Dispersion and transport of gas-phase contaminants in dry porous media: Effects of heterogeneity and gas velocity. Journal of Contaminant Hydrology. 28:157-169.

Poth, M., D.D. Focht. 1985. ^{15}N kinetic analysis of N_2O production by *Nitrosomonas europaea* and examination of nitrifier denitrification. 1985. Applied and Environmental Microbiology. 49(5):1134-1141.

Powlson, D.S., K.W.T. Goulding, T.W. Willison, C.P. Webster, B.W. Hütsch. 1997. The effect of agriculture on methane oxidation in soils. Nutrient cycling in agroecosystems. 49:59-70.

Prescott, L.M., J.P Harley, D.A. Klein. 2002. Microbiology. 5th ed. New York. McGraw-Hill.

Priemé, A., S. Christensen. 2001. Natural pertubations, drying-wetting and freezing-thawing cycles, and the emission of nitrous oxide, carbon dioxide and methane from farmed organic soils. Soil Biology and Biochemistry. 33:2083-2091.

Quinn, G.P., M.J. Keough. 2002. Experimental design and data analysis for biologists. Cambridge University Press. Cambridge, U.K.

Raghoebarsing, A.A., A. Pol, K.T. Van de Pas-Schoonen, A.J.P. Smolders, K.F. Ettwig, W.I.C. Rijpstra, S. Schouten, J.S.S. Damste, H.M.M. Op den Camp, M.S.M. Jetten, M. Strous. 2006. A microbial consortium couples anaerobic methane oxidation to denitrification. Nature. 440:918-921. DOI:10.1038/nature04617.

Rigby, M., R.G. Prinn, P.J. Frazer, P.G. Simmonds, R.L. Langenfeld, J. Huang, D.M. Cunnold, L.P. Steele, P.B. Krummel, R.F. Weiss, S. O'Doherty, P.K. Salameh, H.J. Wang, C.M. Harth, J. Mühle, L.W. Porter. 2008. Renewed growth of atmospheric methane. Geophysical Research Letters. 35, L22805. DOI:10.1029/2008GL036037.

Rochette, P., R.L. Desjardins, E. Pattey. 1991. Spatial and temporal variability of soil respiration in agricultural field. Canadian Journal of Soil Science. 71:189-196.

Rolston, D.E., M. Fried, D.A. Goldhamer. 1976. Denitrification measured directly from nitrogen and nitrous oxide gas fluxes. Soil Science Society of America. 40: 259-266.

Romell, L.G. 1922. Luftväxlingen I marken som ekologisk factor. Medd. Statens Skogsfarsoks-anstalt 19:2.

Ruser, R., H. Flessa, R. Russow, G. Schmidt, F. Buegger, J.C. Munch. 2006. Emissions of N_2O, N_2 and CO_2 from soil fertilized with nitrate: Effect of compaction, soil moisture and rewetting. Soil Biology and Biochemistry. 38:263-274.

Saari, A., J. Heiskanen, P.J. Martikainen. 1998. Effect of the organic horizon on methane oxidation and uptake in soil of a boreal Scots pine forest. FEMS Microbiology Ecology. 26:245-255.

Sander, R. 1999. Compilation of Henry's Law constants for inorganic and organic species of potential importance in environmental chemistry (Version 3) http://www.henrys-law.org

Schaefer, S. C. and M. Alber. 2007. Temperature controls a latitudinal gradient in the proportion of watershed nitrogen exported to coastal ecosystems. Biogeochemistry. 85:333-346.

Sehy, U., R. Ruser, J.C. Munch. 2003. Nitrous oxide fluxes from maize fields: Relationship to yield, site-specific fertilization, and soil conditions. Agricultural, Ecosystems and the Enviornment. 99:97-111.

Seitzinger, S., J.A. Harrison, J.K. Bohlke, A.G. Bouwman, R. Lowrance, B. Peterson, C. Tobias, G. Van Drecht. 2006. Denitrification across landscapes and waterscapes: A synthesis. Ecological Applications. 16(6):2064-2090.

Shao, M, T. Zhang, H.H. Fang. 2010. Sulfur-driven autotrophic denitrification: Diversity, biochemistry, and engineering applications. Applied Microbiology and Biotechnology. 88:1027-1042, DOI:10.1007/s00253-010-2847-1.

Silver, W.L., A.E. Lugo, M. Keller. 1999. Soil oxygen availability and biogeochemistry along rainfall and topographic gradients in upland wet tropical forest soils. Biogeochemistry. 44: 301-328.

Soil Survey Staff, Natural Resources Conservation Service, United States Department of Agriculture. Web Soil Survey. Available online at http://websoilsurvey.nrcs.usda.gov/ accessed [07/01/2011].

Stainton, M.P. 1973. A syringe gas-stripping procedure for gas-chromatographic determination of dissolved inorganic and organic carbon in fresh water and carbonates in sediments. Journal of Fisheries Research Board of Canada. 30:1441-1445.

Staver, K.W., R.B. Brinsfield. 2001. Agriculture and water quality on the Maryland eastern shore: Where do we go from here? Bioscience 51:859-868.

Staver, K.W., R.B. Brinsfield. 1998. Using cereal grain winter cover crops to reduce groundwater nitrate contamination in the Mid-Atlantic coastal plain. The Journal of Soil and Water Conservation. 53(3):230-240.

Sutton, A.J., T.R. Fisher, A.B. Gustafson. 2010. Effects of restored stream buffers on water quality in non-tidal streams in the Choptank River basin. Water Air and Soil Pollution. 208(1-4):101-118. DOI: 10.1007/s11270-009-0152-3.

Teepe, R., R. Brumme, F. Beese, 2001. Nitrous oxide emissions from soil during freezing and thawing periods. Soil Biology and Biogeochemistry 33(9):1269-1275.

Ueda, S., N. Ogura, T. Yoshinari. 1993. Accumulation of nitrous oxide in aerobic groundwaters. Water Research. 27(12):1787-1792.

United States Environmental Protection Agency. 2011. Clean water act, section 404. Retrieved: July 15th, 2011 from http://water.epa.gov/lawsregs/guidance/wetlands/sec404.cfm.

Van Breemen, N., E.W. Boyer, C.L. Goodale, N.A. Jaworki, K. Paustian, S.P. Seitzinger, K. Lajtha, B. Mayer, D. Van Dam, R.W. Howarth, K.J. Nadelhoffer, M. Eve, G. Billen. 2002. Where did all the nitrogen go? Fate of nitrogen inputs to large watersheds in the northeastern U.S.A. Biogeochemistry. 57/57:267-293.

Van den Pol-van Dasselaar, A., M.L. van Beusichem, O. Oenema. 1998. Effects of soil moisture content and temperature on methane uptake by grasslands on sandy soils. Plant and Soil. 204:213-222.

Wang, Z., J. Feyen, M.T. Van Genuchten, D.R. Nielsen. 1998. Air entrapment effects on infiltration rates and flow instability. Water Resources Research. 34(2):213-222.

Weier, K.L., J.W. Doran, J.F. Power, D.T. Walters. 1993. Denitrification and the dinitrogen/nitrous oxide ratio as affected by soil water, available carbon, and nitrate. Soil Science Society of America Journal 57(1):66-72.

Weiss, R.F. 1970. The solubility of nitrogen, oxygen and argon in water and seawater. Deep Sea Research and Oceanographic Abstracts. 17(4):721-735.

Weiss, R.F., B.A. Price. 1980. Nitrous oxide solubility in water and seawater. Marine Chemistry. 8:347-359.

Wilson, G.B., G.W. McNeill. 1997. Noble gas recharge temperatures and the excess air component. Applied Geochemistry. 12:747-762.

Wise, D.L., G. Houghton. 1966. The diffusion coefficients of ten slightly soluble gases in water at 10-60^{o}C. Chemical Engineering Science. 21:999-1010.

Woli, K.P., M.B. David, R.A. Cooke, G.F. McIsaac, C.A. Mitchell. 2010. Nitrogen balance in and export from agricultural fields associated with controlled drainage systems and denitrifying bioreactors. Ecological Engineering. 36:1558-1566. DOI:10.1016/j.ecoleng.2010.04.024.

Woltemade, C.J., J. Woodward. 2008. Nitrate removal in a restored spring-fed wetland, Pennsylvania, USA. Journal of the American Water Resources Association. 44(1):222-234. DOI: 10.1111/j.1752-1688.2007.00149.x.

Wrage, N., G.L. Velthof, M.L. van Beusichem, O. Oenema. 2001. Role of nitrifier denitrification in the production of nitrous oxide. Soil Biology and Biochemistry. 33(12-13):1723-1732.

Xiong, Z., Y. Xie, G. Xing, Z.Zhu, C. Butenhoff. 2006. Measurements of nitrous oxide emissions from vegetable production in China. Atmospheric Environment. 40(12):2225-2234.

Yao, Z., B. Wolf, W. Chen, K. Butterbach-Bahl, N. Brüggemann, M. Wiesmeier, M. Dannenmann, B. Blank, X. Zheng. 2010. Spatial variability of N_2O, CH_4 and CO_2 fluxes within the Xilin River catchment of Inner Mongolia, China: A soil core study. Plant Soil. 331:341-359. DOI: 10.1007/s11104-009-0257-x.